IL NUOVO CIMENTO

ORGANO DELLA SOCIETÀ ITALIANA DI FISICA

SOTTO GLI AUSPICI DEL CONSIGLIO NAZIONALE DELLE RICERCHE

VOLUME XIV

Serie decima

Anno centesimoquinto

1959

PRINTED IN ITALY

NICOLA ZANICHELLI EDITORE
BOLOGNA

IL
NUOVO CIMENTO
ORGANO DELLA SOCIETÀ ITALIANA DI FISICA
SOTTO GLI AUSPICI DEL CONSIGLIO NAZIONALE DELLE RICERCHE

VOL. XIV, N. 1 *Serie decima* 1° Ottobre 1959

High Energy Nuclear Disintegrations.

E. TAMAI (*)
Department of Physics, Rikkyo (St. Paul's) University - Tokyo

(ricevuto il 9 Dicembre 1958)

Summary. — The disintegrations of heavy nuclei (Ag or Br) in emulsion were examined. These disintegrations were produced by the proton beam (6.2 GeV) of the Bevatron. The probabilities of emission of protons, α-particles, Li, Be, B, and C fragments from stars at given excitation energies were investigated, and these experimental results were compared with those calculated by the evaporation theory.

1. – Introduction.

It has been noted by many workers [1-15] in the study of the stars produced by cosmic rays or accelerator beams in nuclear emulsions that relatively slow

(*) Now at School of Physics, University of Minnesota.

(1) M. BLAU and H. WAMBACHER: *S. B. Akad. Wiss. Wien*, **146**, 623 (1937).

(2) G. ORTNER: *S. B. Akad. Wiss. Wien*, **149**, 259 (1940).

(3) J. B. HARDING, S. LATTIMORE and D. H. PERKINS: *Proc. Roy. Soc.*, A **196**, 325 (1949).

(4) N. PAGE: *Proc. Phys. Soc.*, A **63**, 250 (1950).

(5) D. H. PERKINS: *Phil. Mag.*, **41**, 138 (1950).

(6) G. BERNARDINI, G. CORTINI and A. MANFREDINI: *Phys. Rev.*, **79**, 952 (1950).

(7) P. E. HODGSON: *Phil. Mag.*, **43**, 190 (1952).

(8) S. NAKAGAWA, E. TAMAI, H. HUZITA and K. OKUDAIRA: *Journ. Phys. Soc. Japan*, **11**, 191 (1956).

(9) E. L. GRIGOR'EV and L. P. SOLOV'EVA: *Sov. Phys. Journ. Exp. Theor. Phys.*, **4**, 801 (1957).

(10) V. I. OSTROUMOV: *Sov. Phys. Journ. Exp. Theor. Phys.*, **5**, 12 (1957).

(11) V. WEISSKOPF: *Phys. Rev.*, **52**, 295 (1937).

(12) E. BAGGE: *Ann. d. Phys.*, **39**, 512 (1941).

(13) K. J. LE COUTEUR: *Proc. Phys. Soc.*, A **63**, 259 (1950).

(14) Y. FUJIMOTO and Y. YAMAGUCHI: *Progr. Theor. Phys.*, **5**, 787 (1950).

(15) R. HAGEDORN and W. MACKE: *Kosmische Strahlung* (Berlin, 1953), p. 201.

particles (mainly protons or α-particles) are emitted from nuclear stars (Ag, Br) in the evaporation process. Some of these workers ([3-6]) examined also the ratio of doubly to singly charged particles emitted from stars. Their results were compared with the values obtained by LE COUTEUR ([13]), and there was good agreement with the theory. The study of nuclear disintegration with emission of particles with charge $Z \geqslant 3$ has been carried out in our laboratory. As stated in our previous reports ([16]), the emission process of slow fragments ($Z \geqslant 3$) seemed to be attributable to that of evaporation. In order to obtain more detailed information about the emission mechanism of fragments and the formation of fragments inside the nucleus, the author observed protons, α-particles, Li, Be, B and C fragments evaporated from large stars which were produced by the Bevatron beam, and examined the probabilities of emission of these various types of particles at given nuclear temperatures (or excitation energies). Our values were then compared with those obtained from the theory ([11,13-15]).

2. – Experimental details.

The experiments were carried out on the stacks of G-5 pellicle emulsions, 600 μm thick (3 in.$\times$3 in.), irradiated by protons with energy of 6.2 GeV from the Bevatron at Berkeley, as was described in a previous paper ([17]). In order to test the stars due to Ag and Br, those which had more than 8 prongs (grey tracks+black tracks) were selected.

Using the following criteria ([18]), the tracks of particles emitted from these stars were divided into three groups according to their grain density as compared with minimum grain density $g_{\min}$:

(i) « Thin » tracks, $g_{\min} \leqslant g \leqslant 1.4\, g_{\min}$ (shower particles);

(ii) « Grey » tracks, $1.4\, g_{\min} < g < 6.8\, g_{\min}$;

(iii) « Black » tracks, $g > 6.8\, g_{\min}$.

In our plates, the average value of $g_{\min}$ was about 18.7 grains per 100 μm. The black track is usually considered to be that of the evaporated particle. The number of « black » tracks from a star is represented by the symbol N_b, and the stars due to Ag or Br were classified by the magnitude of N_b.

As was described in previous papers ([8,16,17]), the charges of various par-

---

([16]) S. NAKAGAWA, E. TAMAI, H. HUZITA and K. OKUDAIRA: *Journ. Phys. Soc. Japan*, **12**, 747 (1957).

([17]) S. NAKAGAWA, E. TAMAI and S. NOMOTO: *Nuovo Cimento*, in print.

([18]) J. G. WILSON: *Progress in Cosmic Ray Physics*, vol. **1** (Amsterdam, 1952), p. 6.

ticles were determined by measuring the mean width of the end portion of their tracks with dip angles less than 12.5° before processing the emulsions. Fig. 1 shows the distribution of the track width, and from this figure it can be seen that the separation of each group is good enough to identify the charge

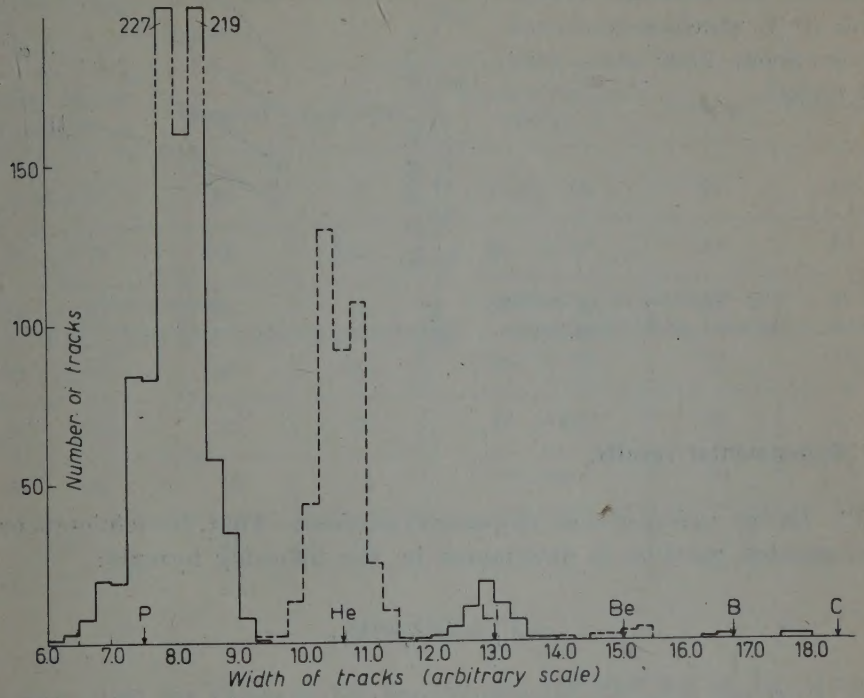

Fig. 1. – Distribution of track widths. The arrows show the estimated width of each group by assuming the proportionality of the width of $\sqrt{Z}$ (Z: charge). In the case of He the tracks from radio-thorium stars in the emulsion were analysed.

of the particle. In order to check our method of charge determination, some tracks which had already been measured by the above method were examined by the method of « gap density measurement » ([19]). Examples of such observations taken by this method are given in Fig. 2, where three cases of π-mesons, eighteen cases of protons, eleven cases of α-particles and four cases of Li fragments are plotted together. Each point represents the number of gaps (per 100 μm) greater than about 0.7 μm in length. From Fig. 2, it seems that there is good discrimination between the various particles.

([19]) F. T. Gardner and R. D. Hill: *Nuovo Cimento*, **2**, 820 (1955).

In this experiment, 328 stars (with > 8 prongs) were examined, and 1406 measurable particles (charge $Z = 1, 2, 3, 4, 5$ and 6) ejected from these stars were observed. In addition to this, 225 fragments ($Z \geqslant 3$) had been already analysed in our previous experiments ([16,17]) which were carried out on about 2300 stars with > 8 prongs.

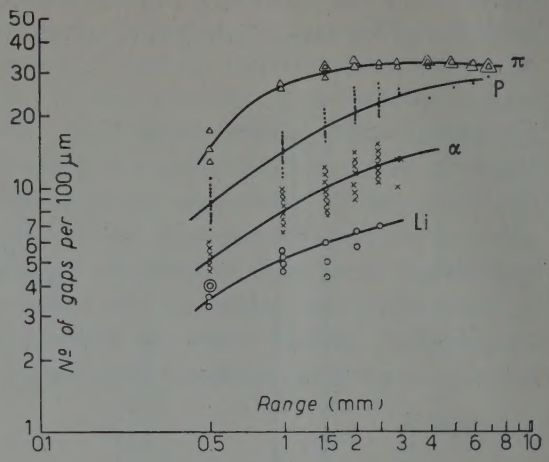

Fig. 2. – Gap densities of π-mesons, protons, α-particles, and Li-fragments.

3. – Experimental results.

3·1. *Energy regions of slow (evaporated) particles.* – First, the minimum energy of evaporated particles is determined by the following formula:

$$V_j' = (ZZ_j e^2/R),$$

where V_j' is the mean Coulomb potential barrier height for a j-particle with the charge Z_j during the evaporation process, and Z is the charge of the parent nucleus. Table I gives the potential barrier heights for various particles. Next, we must define the maximum energy of the evaporated particles. Table II shows the ratios of the number of observed forward emitted protons and α-particles to those backward emitted with respect to the incident proton beam for several energy regions. As is well known, the angular distribution of evaporated particles is isotropic, so in the above cases the maximum

TABLE I.

Particle	Proton	α-particle	Li	Be	B	C
barrier height (Mev)	6.55	11.5	16.0	21.0	24.2	27.4

energies of protons and α-particles seem to be 40 and 70 MeV (*), respectively. On the other hand, the maximum energies of the particles with charge $Z \geqslant 3$ were examined in the previous experiment ([17]). On the basis of those results,

TABLE II.

a: Proton			*b*: α-particle		
Energy region (MeV)	Forward	Backward	Energy region (MeV)	Forward	Backward
6.55÷10	61	57	11.5÷ 20	67	53
10 ÷20	160	132	20 ÷ 30	38	25
20 ÷30	84	73	30 ÷ 50	36	23
30 ÷40	47	50	50 ÷ 70	17	18
40 ÷50	33	12	70 ÷100	22	11
50 ÷60	19	6	> 100	20	5
> 60	21	11			

the author used the values of 60, 80, 100 and 120 MeV for Li, Be, B and C fragments, respectively.

The energies of these particles in this experiment were obtained by measuring the ranges of their tracks in emulsion.

3·2. *Emission rates of various particles.* – From the above defined energy range, 975 particles emitted from 306 stars were selected. Table III gives the emission frequencies of the various particles from several groups of stars. In Table III-*a*, the emission frequencies of Be, B and C fragments were extrapolated from the values of Table III-*b*, which were obtained in the previous experiments ([16,17]). These frequencies of the various particles were corrected for restriction in dip angle $\theta \leqslant 12°.5$.

(*) This value is thought to be too high. However, the observed frequency of those particles is relatively small, and so it is not so important whether this value is used or not.

TABLE III-*a*.

N_b	No. of star	Proton	α-particle	Li	Be	B	C
6, 7, 8	69	111	41	6	1.03	0.83	—
corrected		358	132	19.3	3.32	2.67	—
emission rate/star		5.18	1.92	0.28	0.048	0.038	—
9, 10, 11	82	157	69	11	4,35	0.51	0.51
corrected		505	222	35.4	14.0	1.64	1.64
emission rate/star		6.18	2.71	0.43	0.17	0.02	0.02
12, 13, 14	87	194	89	15	6,37	3,64	0.91
corrected		625	287	48.4	20.5	11.7	2.93
emission rate/star		7.18	3.30	0.556	0.236	0.134	0.034
15, 16, 17	42	110	44	7	2.57	1.40	0.234
corrected		354	142	22.5	8.27	4.51	0.754
emission rate/star		8.45	3.38	0.537	0.197	0.107	0.018
$\geqslant 18$	26	79	24	4	3	1	1
corrected		254	77.3	12.9	9.66	3.22	3.22
emission rate/star		9.77	2.97	0.49	0.37	0.124	0.124

TABLE III-*b*.

N_b	Li	Be	B	C
6, 7, 8	29	5	4	0
9, 10, 11	43	17	2	2
12, 13, 14	33	14	8	2
15, 16, 17	30	11	6	1
$\geqslant 18$	8	6	2	2

3·3. *Probabilities of emission of various particles.* – Since a relationship between prong number N_b and thermal excitation energy is very useful in the interpretation of nuclear disintegration, all stars observed were classified into five groups by N_b, as shown in Table III-*a*. This relationship was investigated by PERKINS [5] and LE COUTEUR [20], and there appeared to be good agreement between experimental and theoretical data, which are well approximated by the relation $U = (40 + 42\,N_b)$ MeV. Moreover, the initial nuc-

[20] K. J. LE COUTEUR: *Proc. Phys. Soc.*, **63**, 498 (1950).

lear temperature T with excitation energy U can be estimated by using the following relation ([21]):

$$U = aT^2 , \qquad a = \text{const.} ,$$

assuming the Fermi gas model. In Table IV, the values of the second column are those calculated by the above formulas.

TABLE IV.

N_b	(MeV) Temperature	Proton	α-particle	Li	Be	B	C
9, 10, 11	≈ 7	1.00±0.38	0.79±0.24	0.15±0.03	0.12 ±0.05	—	—
12, 13, 14	≈ 8	1.00±0.39	0.59±0.26	0.12±0.10	0.065±0.069	0.114±0.042	0.013±0.025
15, 16, 17	≈ 9	1.27±0.53	0.08±0.34	—	—	—	—
⩾18	⩾10	1.32±0.75	—	—	—	—	—

Since the intention was to compare directly the experimental data with those of the evaporation theory, the emission probabilities of the various particles at a given nuclear temperature were necessary. The emission probabilities in Table IV give the values of the differences between every two emission rates of the adjacent groups in Table III-*a*. From Table IV, it seems that the emission probabilities of the various particles show maximum values at nuclear temperature 7 MeV, although the statistical errors are considerably large.

4. – Comparison with the theory and discussion.

The probabilities of emission of the various types of particles can be calculated from the formula of Weisskopf ([11]), and many investigators ([13-15]) have made such calculations.

According to WEISSKOPF ([11]), the total width $\Gamma_j(W)$ of emission of a j particle is calculated by the integration,

$$\Gamma_j = \hbar \int_{B_j + V_j'}^{W} P_j(E, W)\, \mathrm{d}E \approx \frac{g_j M_j \sigma T^2}{\pi^2 \hbar^2} \exp\left[-\frac{a_j}{10} T - \frac{B_j + V_j'}{T} \right]$$

([21]) J. M. BLATT and V. F. WEISSKOPF: *Theoretical Nuclear Physics* (New York, 1952), p. 371.

where P_j is the probability per unit time that the nucleus (N, Z) with excitation energy W evaporates a j-particle with the energy E, $E+dE$; and $M_j = a_j m$, g_j, B_j and V_j' are mass, spin statistical weight, binding energy of the j-particle and Coulomb barrier height for the j-particle, respectively. m means nucleon mass. The cross-section σ is replaced by the simple form, $\sigma = \pi R^2$ $(R = r_0 A^{\frac{1}{3}})$.

Thus the above formula can be rewritten as follows:

$$\Gamma_j \approx \frac{g_j a_j}{2\pi} \frac{A^{\frac{2}{3}}}{11} T^2 \exp\left[-\frac{a_j}{10} \cdot T - \frac{B_j + V_j'}{T}\right]$$

Table V gives the calculated values of a_j, $g_j = 2S_j+1$ (S : spin of the j-particle), B_j and V_j of many isotopes. Γ_j can be calculated by using these values. Furthermore, in order to compare Γ_j with the experimental data, it

TABLE V.

Group	Isotope	a_j	$g_j = 2S_j+1$	B_j	V_j
Proton group	H	1	2	8.6	6.55
	d	2	3	15.0	6.55
	T	3	2	17.5	6.55
α-group	^{3}He	3	2	18.2	11.5
	α	4	1	6.3	11.5
Li-group	^{6}Li	6	3	19.8	16.0
	^{7}Li	7	4	21.2	16.0
	^{8}Li	8	1	27.9	16.0
Be-group	^{8}Be	8	1	12.6	21.0
	^{9}Be	9	4	19.6	21.0
B-group	^{10}B	10	3	21.6	24.2
	^{11}B	11	4	18.4	24.2
C-group	^{12}C	12	1	11.6	27.4
	^{13}C	13	2	15.3	27.4

is necessary to put each isotope into its proper group. Table VI shows the value of Γ_j normalized by the proton group at a given nuclear temperature.

From Table VI, it is apparent that the experimental data are significantly larger in value than those of the theory, although the statistical errors are considerably large. This difference between the experimental data and the

theory is so large that it could not be explained, even though, in an attempt to do so, Γ_j were calculated without considering the nuclear barrier height for j-particles.

TABLE VI.

	Temperature (MeV)	Proton	α-particle	Li	Be	B	C
Theor.	6	1	0.11	0.0098	0.0019	0.00039	0.000092
Exper.	≈ 6	—	—	—	—	—	—
Theor.	7	1	0.14	0.013	0.0023	0.00046	0.000084
Exper.	≈ 7	1.00	0.79	0.15	0.12	—	—
Theor.	8	1	0.13	0.013	0.0018	0.00031	0.000073
Exper.	≈ 8	1.00	0.59	0.12	0.065	0.114	0.013
Theor.	9	1	0.12	0.012	0.0015	0.00019	0.000027
Theor.	9	1.27	0.16	0.015	0.0019	0.00025	0.000034
Exper.	≈ 9	1.27	0.080	—	—	—	—
Theor.	10	1	0.095	0.0089	0.00097	0.00013	0.000017
Theor.	10	1.32	0.126	0.011	0.0012	0.00017	0.000022
Exper.	⩾ 10	1.32	—	—	—	—	—

It has been pointed out by LE COUTEUR [13] that in Weisskopf's formula [11] there are no explicit factors representing the probability of the existence of heavy particles inside the nucleus. Also he has suggested that it would not have been possible to obtain agreement with the experimental data if additional factors representing small probabilities of existence had been introduced into the emission formula.

However, on the basis of our experimental results, it seems to be necessary to introduce some factor to represent the considerably large probability of existence or of formation of fragments inside the nucleus in the highly excited state.

If the above hypothesis is true, the probability of existence of individual nucleons inside the nucleus at such an energy state may be decreased. These conditions seem to be suitable for interpreting our results.

The fact that the emission probabilities of observed heavy particles ($Z \geqslant 2$) give maximum values at nuclear temperature 7 MeV and decrease gradually with an increase in nuclear temperature seems to indicate that there is an

optimum condition for the agglomeration of nucleons at 7 MeV, and then the cluster is broken up at > 7 MeV.

The present experimental data are not sufficient to discuss at length the above questions. For a more satisfactory explanation, further investigations are required.

* * *

The author would like to express his sincere thanks to Professor E. J. LOFGREN and the members of the Radiation Laboratory at Berkeley, California, who made the exposure of the nuclear plates possible. Also, the author is grateful to Professor S. NAKAGAWA for his useful suggestions and continued interest in this work; and to Mr. N. ODA for helpful discussions. The assistance of Miss N. KUROKI is also greatly appreciated. This work was partially financed by the Scientific Research Fund of the Ministry of Education.

RIASSUNTO (*)

Sono state esaminate in emulsione le disintegrazioni di nuclei pesanti (Ag o Br). Tali disintegrazioni sono state prodotte dal fascio protonico (6.2 GeV) del Bevatrone. Sono state investigate le probabilità di emissione di protoni, di particelle α, di frammenti di Li, Be, B e C da parte di stelle di date energie di eccitazione, e sono stati confrontati tali risultati sperimentali con quelli calcolati dalla teoria dell'evaporazione.

(*) *Traduzione a cura della Redazione.*

IL NUOVO CIMENTO Vol. XIV, N. 1 1° Ottobre 1959

On the Beta Decay of Uranium X2 (*).

H. Schneider (**), P. W. de Lange (***) and J. W. L. de Villiers (***)

National Physical Research Laboratory
South African Council for Scientific and Industrial Research
Pretoria

(ricevuto il 20 Dicembre 1958)

Summary. — The β- and γ-ray spectra observed in the decay of UX2 (1.175 min half-life in ^{234}Pa) are investigated. β-γ-coincidences, obtained in a β-ray spectrometer, as well as γ-γ-coincidence measurements with selected energies are described. In the β-spectrum 11 partial spectra, leading to different states in the daughter nucleus ^{234}U, are resolved and their log *ft* values are given. The high energy part of this spectrum, which was always assumed to go to the ground state, is shown to be highly complex containing 5 partial spectra. The log *ft* value of the ground state transition is found to be 6.9, indicating the same degree of forbiddenness as observed for the transition ^{234}Th-^{234}Pa. Spin assignment is made to UX2 and some excited states in ^{234}U. A decay scheme is presented.

1. — Introduction.

According to Hahn (1) the β-decay of ^{234}Th (UX1) with a half-life of 24.1 days leads to two daughters in ^{234}Pa with measurable life times, which are called UX2 (1.175 min) and UZ (6.7 hours). The common end product of this isomeric pair is ^{234}U(U2), which decays by α-emission. In all three β-transitions γ-rays are also observed. The complex has been studied by many

(*) This work forms part of a D.Sc. thesis submitted to the University of Pretoria by P. W. de Lange. The investigation of the UX-complex was partially sponsored by the South African Atomic Energy Board.

(**) Present address: Physic Institut der Universität Fribourg.

(***) Present address: Atomic Energy Board, Private bag 59, Pretoria.

(1) O. Hahn: *Ber. dtsch. chem. Ges.*, **54**, I, 1131 (1921); *Zeits. f. phys. Chemie*, **103**, 461 (1922).

authors ([2-9]). Different β-spectra, some γ-quanta and a great number of conversion lines were found. The main results are summarized in Table I in the work of DE HAAN *et al.* ([5]). Coincidence experiments are also described ([4,5,8]) giving information on the relationship between different γ-rays as well as between β- and γ-rays.

However, with the data available three problems remain unsolved:

1) Spin and parity assignment of UX2 exhibits a serious inconsistency. As FEATHER and RICHARDSON ([10,11]) first pointed out, the main difficulty arises from the fact that the β-transition leading from UX1 to UX2 is first forbidden whereas the β-spectrum of UX2 going to the ground state in U2 is allowed. UX1 and U2 are even-even nuclei and should therefore be 0^+.

2) The knowledge on the excited states in U2 is rather vague. Especially in the low energy region it is not yet understood which role the rotational states (43.3 keV, 143.3 keV and 296.4 keV) known from the α-decay of ^{238}Pu ([15]) play in the β-decay of UX2 and or UZ.

3) The relative position of the isomeric pair UX2 and UZ is not yet determined. Whereas in the earlier works BRADT and SCHERRER ([4]) came to the conclusion that UZ must be the ground state, the coincidence experiments of JOHANSSON ([8]) indicate that UZ should have an energy slightly higher than that of UX2.

The main difficulties in solving these problems are the following: Since chemical separation and spectroscopic measurements require periods longer than the half-life of UX2 (1.1 min) this activity can only be investigated in the presence of its parent UX1 (24. 1 days). UZ (6.7 hours) is therefore always present, and every spectrum contains the complex radiation of three decaying nuclei. It must be admitted that the ratio of UZ to the total activity is very small (0.63 %) ([12]) and one should expect that in the spectrum of the complex the radiation due to UZ can hardly be detected. This is cer-

---

([2]) L. MEITNER: *Zeits. f. Phys.*, **17**, 54 (1923).
([3]) H. BRADT and P. SCHERRER: *Helv. Phys. Acta*, **19**, 305 (1946).
([4]) H. BRADT, H. G. HEINE and P. SCHERRER: *Helv. Phys. Acta*, **16**, 455 (1943).
([5]) E. F. DE HAAN, G. J. SIZOO and P. KRAMER: *Physica*, **21**, 803 (1955).
([6]) M. HEERSCHAP: *Thesis*, Amsterdam Vrije Universiteit (1951).
([7]) P. H. STOKER, M. HEERSCHAP and ONG PING HOK: *Physica*, **19**, 433 (1953).
([8]) SVEN A. E. JOHANSSON: *Phys. Rev.*, **96**, 1075 (1954).
([9]) ONG PING HOK, J. TH. VERSCHOOR and P. BORN: *Physica*, **22**, 465 (1956).
([10]) N. FEATHER and H. O. W. RICHARDSON: *Proc. Phys. Soc.*, **61**, 452 (1948).
([11]) N. FEATHER: K. SIEGBAHN, *Beta and Gamma-ray Spectroscopy* (Amsterdam, 1955).
([12]) W. L. ZIJP, sj. TOM and G. J. SIZOO: *Physica*, **20**, 727 (1954).

tainly true and simplifies matters at least at higher energies. In coincidence work the interference of UZ in the experiments with the complex also seems to be negligible as can be shown by simple estimates. But if coincidence rates are investigated (ratio of coincidences to single counts) the single counts are involved and at least at low energies the presence of the UX1 spectrum creates considerable difficulties in the interpretation. Especially the search for transitions common to UX2 and UZ by means of coincidence work, and there must be such transitions at low energy, exhibits complications not yet overcome.

Concerning the relative position of the two isomers it seems that there is little hope to find a γ-transition (converted or not) or a branch of the β-spectrum of such low intensity (0.6%), and furthermore to prove experimentally that it is the link between UZ and its parent. The most reasonable way therefore is to come to a better knowledge of both decay schemes first and to construct the position of the isomers beginning with the U2 ground state. In the present article we are only dealing with UX2.

2. — Experiments.

2·1. *The source.* – As the goal of the present investigation was mainly a careful study of the β-spectrum of UX2 especially near the maximum energy, it was evident that much stronger sources had to be prepared than those used by previous authors. We therefore started with 60 kg U_3O_8 (*).

The chemical separation of the thorium for the UX1 sources and the protoactinium for the UZ sources were carried out by the radiochemical group. The details have been published elsewhere ([13]). The thorium was isolated from the uranium by means of a cation exchange procedure and the protoactinium was milked off periodically from the purified UX1. This latter separation was carried out with an anion exchanger in hydrochloric acid medium. The UZ was eluted from the column with a small volume of 3M HCl and the eluate evaporated to about one drop. This was then transferred to the source holder consisting of a polyvinylchloride film (0.0002 inches thick) and taken to dryness. UX1 sources were prepared similarly by evaporating drops of the solution to dryness. The activity covered a round spot of 2 mm diameter on the foil. In the UZ-spectrum no contamination whatsoever of UX1 and UX2 could be found. The maximum activity achieved for the UZ-sources was 73 μC. For the UX2 measurements sources of about 250 μC were used.

(*) We are deeply indebted to Messrs. Calcined Products, Johannesburg, who with permission of the S. A. Atomic Energy Board placed 100 kg U_3O_8 at our disposal.

([13]) J. van R. Smit, M. Peisach and F. W. E. Strelow: *Second Itern. Conf. on the Peaceful Uses of Atomic Energy.* A/Conf. 15/P/1119 (1958).

2·2. *The β-spectrum of the complex.* – An intermediate image β-ray spectrometer (LBK 3024 Siegbahn-Slätis) was used. The alterations of the apparatus made in connection with the coincidence setup permit the choice of different G.M. tubes or scintillation counters according to the experiment. For the β-spectrum in question a halogen G.M. counter (DR 3 Nuclear Instruments) with 3.5 mg/cm² mica window was used and the spectrometer was set at 2.5% resolution. After the very first runs it turned out that the high energy part was complex and that for a detailed study much finer steps had to be taken as was permitted by the usual millivoltmeter-reading. Therefore a compensation circuit parallel to the mV-meter containing a battery, Helipot

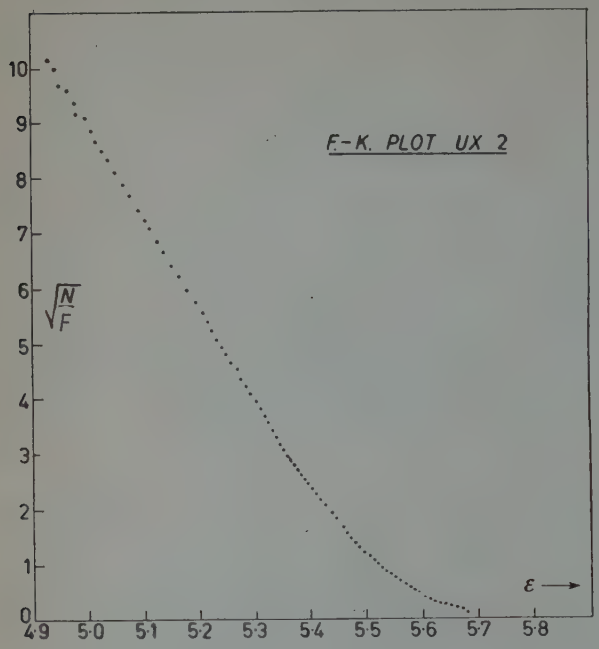

Fig. 1. – F-K plot of the β-spectrum of UX2; high energy part.

TABLE I. – *Results of the* F-K *analysis of the β-spectrum of* UX2. *The calibration of the spectrometer is based on the conversion-line of* ^{137}Cs *and different lines in* Th(B+C+C″) (14).

No.	E_0	%	log *ft*
1	2404.5 ± 3	5.4	6.9
2	2356 ± 5	5.3	6.9
3	2328 ± 5	12.7	6.5
4	2290 ± 5	26.4	6.1
5	2234 ± 5	28.4	6.1
6	1535 ± 50	5.9	6.1
7	1277 ± 40	3.8	6.0
8	982 ± 25	5.8	5.3
9	576 ± 20	1.4	5.1
10	352 ± 20	2.2	4.4
11	228 ± 20	2.7	3.6
12	150 ?	(UX1 ?)	—

(14) K. SIEGBAHN: *Beta and Gamma-ray Spectroscopy* (Amsterdam, 1955).

potentiometer and a galvanometer as zero reading instrument was used to set the spectrometer. This arrangement was carefully calibrated and checked with respect to reproducibility and stability.

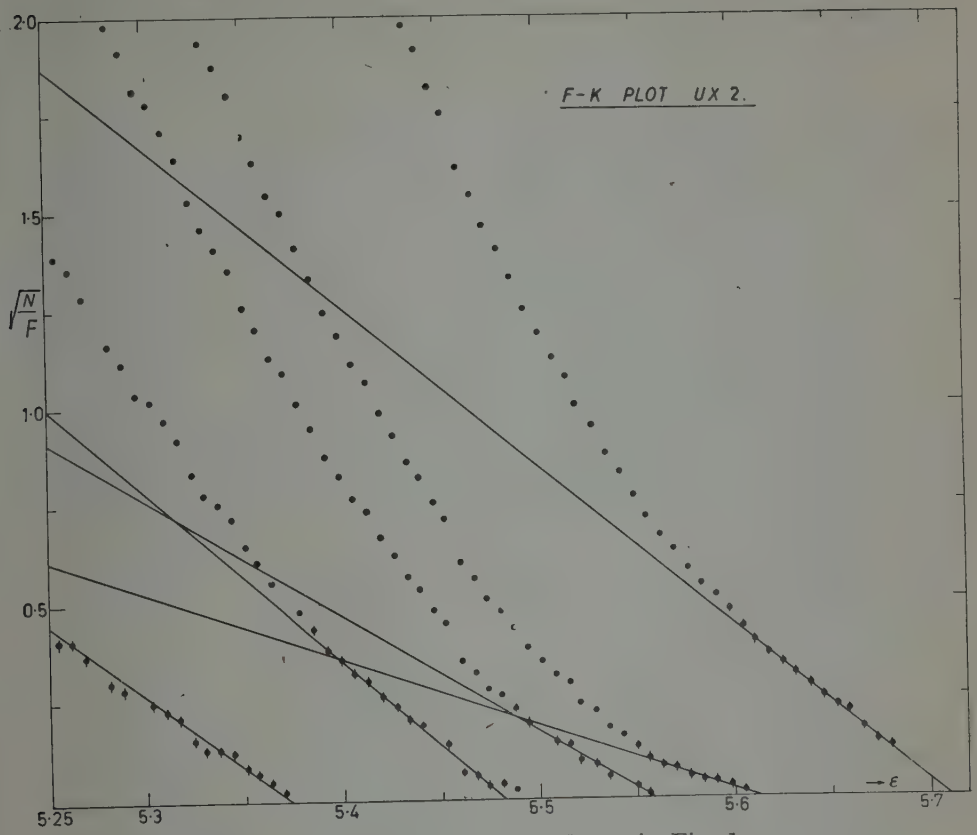

Fig. 2. – Analysis of F-K plot shown in Fig. 1.

In Fig. 1 the upper part of the Fermi-Kurie plot is shown and the deviation from a straight line is obvious. The interpretation of this part is given in Fig. 2, where the different partial spectra are subtracted. The results of the total analysis are given in Table I.

No special attention has been given to the transitions from UX1 and the last values from STOKER [7] and ONG [9] were accepted. But it should be noted, that according to our F-K plot the 193 keV branch [7,9] appears at 178 keV. However this discrepancy has no influence on our investigation of the UX2-decay. Another striking detail is the observation of a 150 keV transition, which is hidden in the UX1 decay. According to intensity considerations, this transition is most probably not the 150 keV spectrum observed in the UZ-decay [9] but belongs to UX1.

2·3. The γ-*spectrum*. – The γ-spectrum was measured using a single channel analyser. (NaI crystal: $1\frac{3}{4}$ inches in diameter and 2 inches long. Photomultiplier tube: Dumont 6292). The line widths of the ^{60}Co lines were 7%. For the higher energies absorbers were used to shield off the strong β-radiation. In general our spectrum is in agreement with the measuremets of ONG *et*

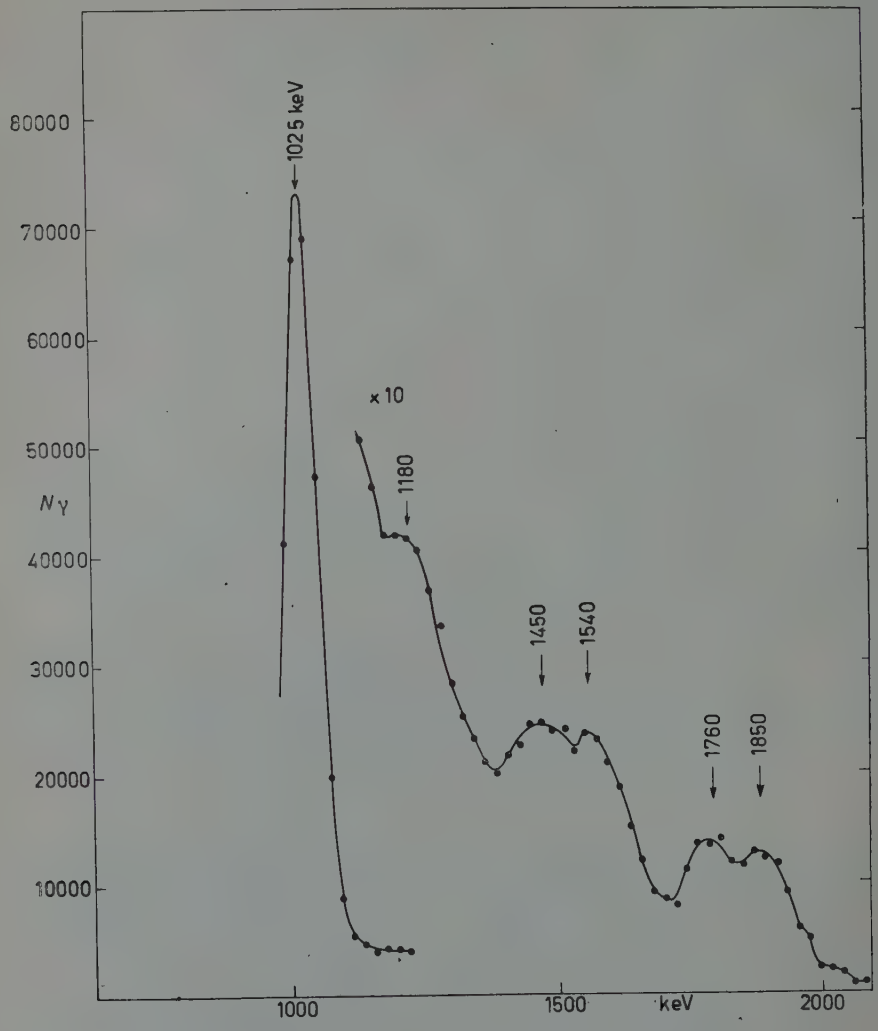

Fig. 3. – High energy part of the γ-spectrum of the complex.

al. (9), and only in the high energy part some deviations are observed. As is shown in Fig. 3 an indication was found of the following energies: 1850, 1760, 1540, 1450 and 1180 keV (each $\pm$ 20 keV). Our 1450 and 1850 keV lines

most probably correspond respectively to the 1440 and 1830 keV found by other authors (9). No peaks could be detected at 1690 and 1240 keV listed in reference (9). In the medium and low energy part of the spectrum many more lines seem to be present as were known hitherto, but this conclusion is drawn from the results of coincidence work and will be shown in the following chapters.

2·4. *Beta-gamma coincidence work.* – In the γ-spectrum at higher energy two striking photopeaks are known (JOHANSSON (8): 750 keV and 1000 keV; ONG (9): 770 keV and 1010 keV, etc.). In our experiments these peaks were found at (770 ± 20) keV and (1025 ± 20) keV, respectively. These two are not in coincidence (8) but the 750 keV was found to be in coincidence with a 250 keV line and therefore JOHANSSON concluded that the 1000 keV is the crossover of a (750 ÷ 250) keV cascade. This was further supported by γ-β coincidences, showing that both are in coincidence with the same β-ray of 1350 keV. In our F-K plot no β-ray of this energy was found and it was therefore decided to repeat this experiment with improved techniques. The β-γ coincidence spectrum was measured using the β-ray spectrometer. The γ-rays

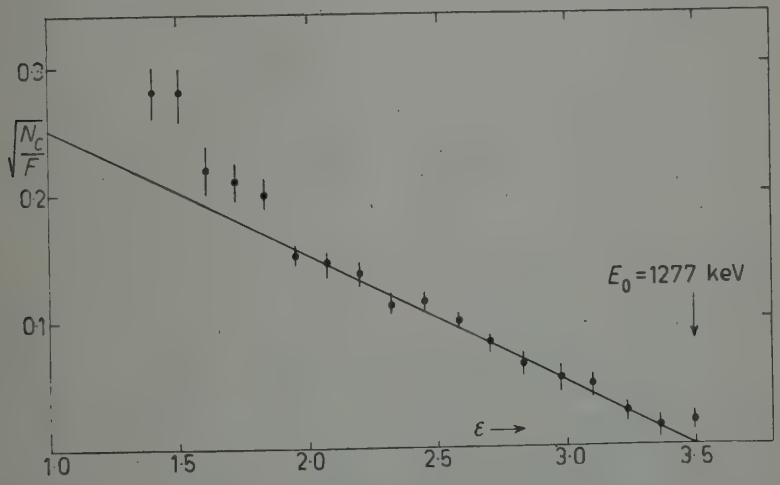

Fig. 4. – F-K plot of the β-γ coincidence spectrum with the γ channel set on the 770 keV photopeak.

were detected with a NaI crystal (1¾ inches diameter and 2 inches long) about 3 cm « behind » the source on the axis of the spectrometer. A single pulse-height analyser was used to select the photopeak of the γ-line and the coinci-

dences between these pulses and those from the β-particles on the β-ray spectrometer were taken to draw the F-K plot. Fig. 4 shows this plot of the coincidences between the 770 keV γ-line and the β-spectrum.

The same experiment with the γ-ray analyser set on the photopeak of the 1025 keV line gives the result shown in Fig. 5 and we must conclude, that both transitions, the 1025 keV as well as the cascade, have their origin at the 1135 keV level in ^{234}U within the experimental errors. (See decay scheme Fig. 11). Nevertheless they can still lead to different final states as will be shown later.

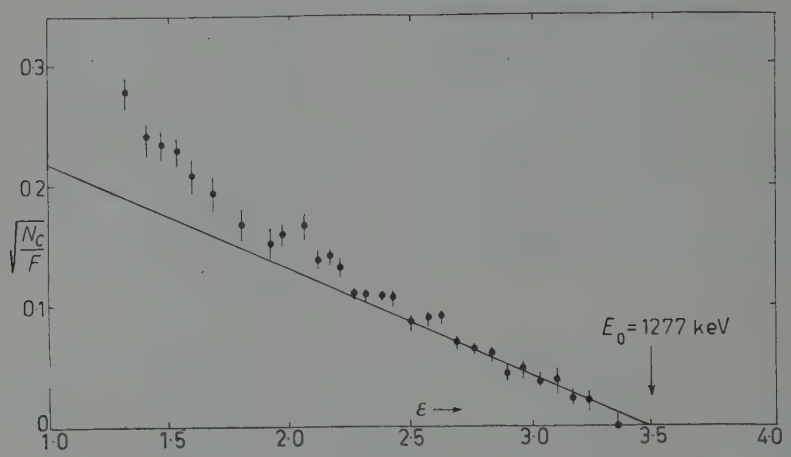

Fig. 5. – F-K plot of the β-γ coincidence spectrum with the γ channel set on the 1025 keV photopeak.

Another striking feature in the decay is the occurrence of some strong conversion lines at 690 keV and 780 keV. These lines are reported by several authors and were ascribed to a transition of 805 keV ([5]) which is totally converted and is therefore, most probably, a 0-0 transition ([8]). To obtain the coincidences between these conversion electrons and the γ-spectrum the β-spectrometer was set on the peak of the *K*-line and the γ-channel window was shifted over the spectrum. A second run was made with the β-spectrometer off the line on the β-spectrum. These two runs are shown in Fig. 6. The most remarkable results are: A strong coincidence peak at 75 keV and no coincidences with the 1025 keV γ-line. Furthermore there is a weak indication of coincidences with γ-energies of 200, 300 and 770 keV. The latter seems to be in contradiction with the assumption that the 1025 keV and the 770 keV are in a parallel position. From intensity considerations however it can be shown that there are no coincidences with the intense 770 keV line.

These coincidences are due to another but weaker line of similar energy hidden in the 770 keV photopeak. Two further arguments support this assumption:

1) The shape of the 770 keV photopeak in the γ-spectrum indicates that there are at least two components.

2) The γ-γ coincidence spectrum shows coincidences between the 770 keV and a γ-ray of about the same energy.

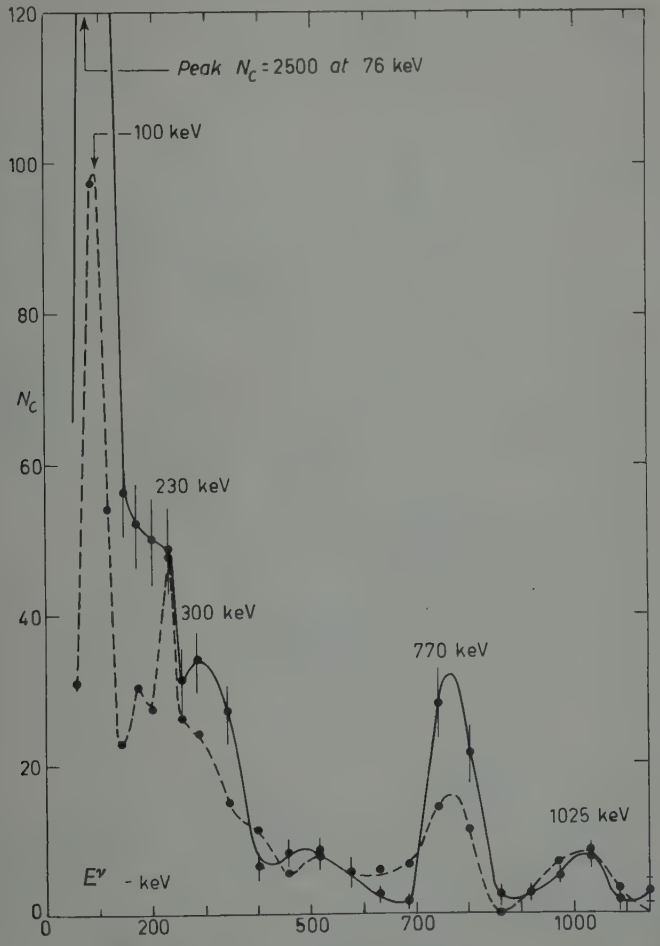

Fig. 6. – Coincidence between the 805 keV conversion electrons and the γ spectrum. Solid line: coincidence with the β spectrometer on the K-line; Dotted line: coincidences with the β spectrometer off the line.

2·5. *γ-γ coincidence work.* – In these experiments two identical single channel pulse height analysers with NaI crystals were used. One channel was set on the desired energy with a suitable window and the other channel was used to

scan the spectrum. Records were taken automatically by means of a typewriting equipment because each point had to be measured for one or two hours and many runs were taken with different window widths. The 770 keV line was found to be in coincidence with at least 17 other energies. Fig. 7 and Fig. 8 show the result at lower and higher energies. At about 790 keV

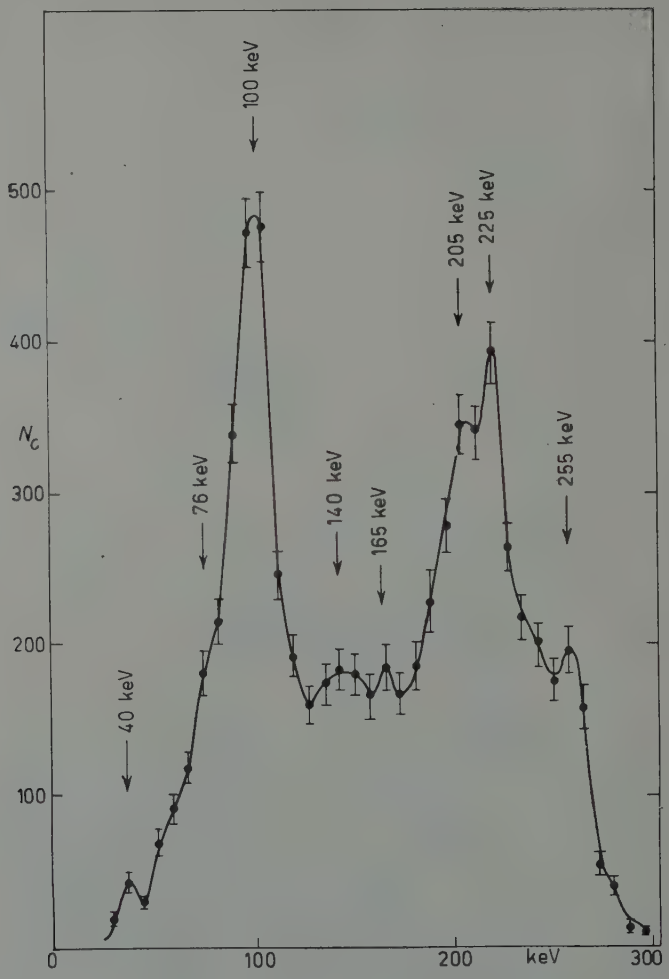

Fig. 7. – γ-γ coincidence with 770 keV; low energy region.

there is a clear indication of coincidences with the 780 keV line, which explains the weak coincidence rate found in the β-γ work with the conversion lines of the 805 keV transition.

At an energy below 280 keV (Fig. 7) the number of coincidences increases

by a factor of about 10. The coincidence rate proves that this is not due to the increasing efficiency of the crystal. This coincidence rate permits an estimate of the relative number of coincidence partners and confirms the results of the β-γ coincidence work *i.e.* the branching at 1135 keV.

The same investigation was made with the 1025 keV line. As was already shown by JOHANSSON ([8]) this line is not in coincidence with the 250 keV group, a very striking effect, which could be confirmed immediately. In the

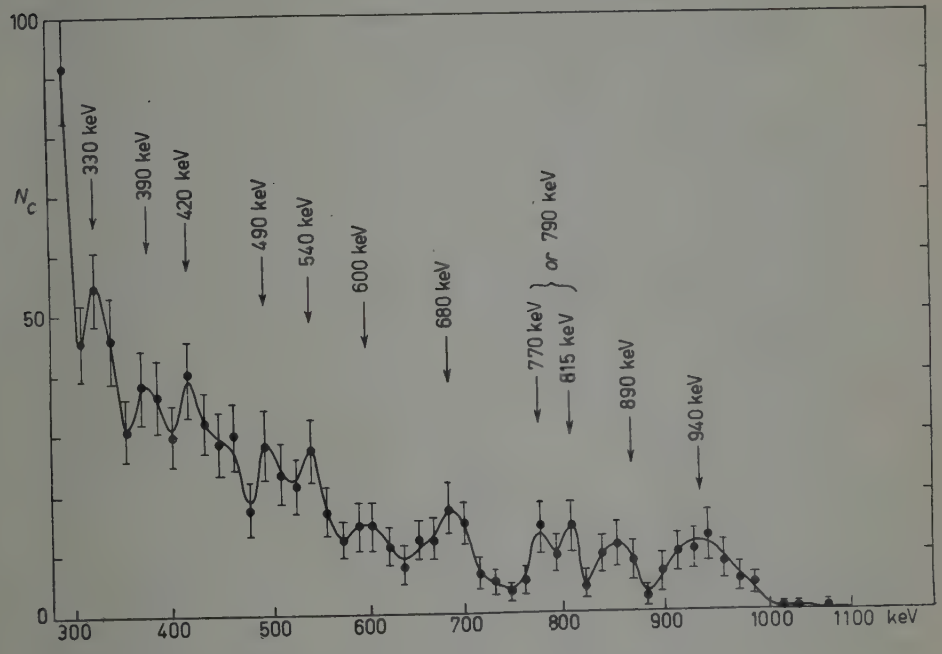

Fig. 8. – γ-γ coincidence with 770 keV; high energy region.

first runs the lower energy part seemed to be very similar to that obtained in the experiment with the 770 keV line, whereas at high energy the coincidence spectrum seemed to be slightly different. This caused great difficulty in the interpretation until it turned out that the spectrum obtained in this experiment also contains the coincidences with the 940 keV line which is again in coincidence with the 770 keV. The two lines 940 keV and 1025 keV cannot be separated properly unless the window is made very narrow and the results become poor. The comparison of the coincidence rates taken at 100 keV (Fig. 7) also showed a suspicious discrepancy between the experiment with the 770 keV and that with the 1025 keV line. To overcome this difficulty, the fixed channel was set on each of the low energy lines in question and the

scanning channel was shifted through the spectrum covering the two lines 770 keV and 1025 keV. Fig. 9 shows the run where the coincidences between 95 to 125 keV γ-energies and the spectrum are given. In this way it was found, that the two lines have different coincidence partners in the low energy region. In particular the 1025 keV line is not in coincidence with the 100 keV line as it is the case for the 770 keV transition.

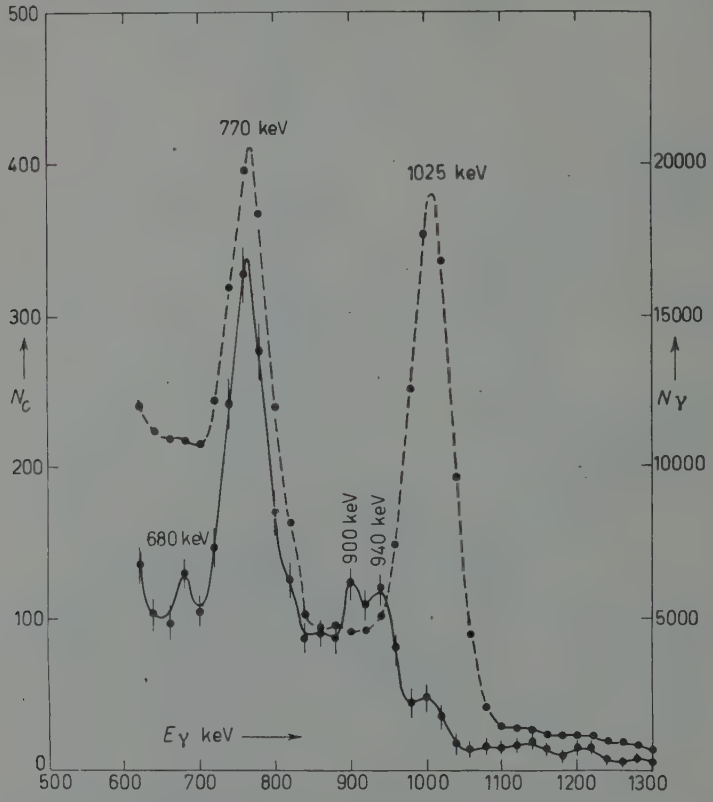

Fig. 9. – γ-γ coincidence with 100 keV. Dotted line: single counts.

Besides this the spectrum shown in Fig. 7 proves that the 250 keV group is complex and consists of peaks at 205, 225 and 255 keV. The conclusion is that the 770 keV decay leads via these lines to different states. The most interesting question seems to be where the 100 keV transition—a very pronounced peak—fits into the decay scheme. The conversion of this transition must be low, but unfortunately it overlaps with the known 93 keV in ^{234}Pa ([5]). The coincidence spectrum taken with the 30 keV line in the low energy region

TABLE II. – *List of γ-energies and their coincidences.*

I	II	III	IV	V	VI	
No.	keV	keV	± keV	keV	keV	keV
1		33	3 weak (*)	34 strong		
2		34	3	33 strong	76 weak	
3	43	43	4	770 weak	1025 weak	
4		63	5	30 strong (**)		
5		66	5 strong	770 weak		
6		76	5	770 weak	805 strong	34 weak
7	91.4	(**)				
8		100	5 strong	770 strong	1025 no	
9	152	140	10 weak	770 weak		
10		165	5	770 weak	205?	
11		205	10	770 weak?		
12	230	225	10 ?	770 strong	1025 no	
13	255	255	10	770 strong	1025 no	
14		295	10	770 weak	1025 weak	805 weak
15		330	10	770 weak	940 weak?	
16		360	10	770 weak		
17		420	20	770 ?		
18	(500)	490	20 weak	770 weak	1025 weak	
19		540	20	770 weak		
20		600	20	770 weak	1025 weak	
21		680	20 weak	770 weak	1025 weak	100 weak
22	770	770	20 strong	780 weak	100 strong	
23		780	20	770 weak	805 weak	
24	807	805	5	780 weak	1025 no	76 strong
25		815	20	770 weak		
26		870	20	770 weak		
27		900	20	770 weak	100 weak	
28		940	20	770 weak	100 weak	
29	1010	1025	20 strong	770 no	100 no	
30		1180	20 weak			
31	1440	1450	20 weak			
32		1540	20 weak			
33		1760	20 weak			
34	1830	1850	20 weak			

(*) partly UX-1.
(**) UX-1.

Legend: Column I Number.
II γ-transitions according to reference (*).
III γ-transitions according to our investigation.
IV Estimated error.
V Indication of line intensity in single spectrum.
VI Coincidence partners.

(Fig. 10) shows that there are two lines at about 30 keV in coincidence, which we call the 33 and the 34 keV lines, to distinguish between them. Here the coincidences between the 30 keV and 63 keV in ^{234}Pa, described by JOHANSSON ([8]), are also present. A weak indication of coincidences with a 76 keV line confirms the β-γ coincidence experiment with the conversion electrons of the 805 keV transition, where the existence of this 76 keV line was proved.

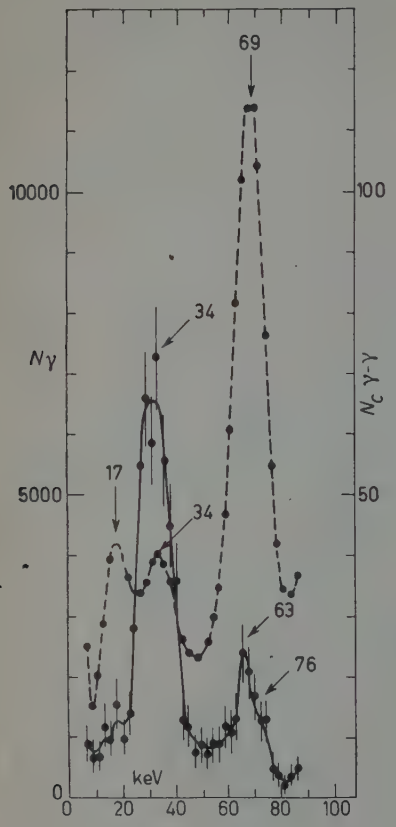

Fig. 10. – γ-γ coincidences with 30 keV. Dotted line: single counts.

In this way many lines were found, which are listed in column III of Table II. In column IV (Table II) estimated errors are given and in column V it is stated whether the respective line appears in the γ-spectrum. In column VI the γ-energies are given with which the respective lines are found to be in coincidence. The statement « weak » or « strong » in Table II has very little to do with the real intensities and describes only whether we were able to produce a strong effect as *e.g.* the coincidence peak at 30 keV in Fig. 10 or only a weak indication as *e.g.* the coincidence peaks in Fig. 8. At the first glance it seems astonishing that the 770 keV γ-ray is in coincidence with nearly everything. However, regarding the fact that there are two transitions with nearly the same energy at 770 keV (one may be 780 keV) which are in coincidence, it is clear that the coincidences with this 770 keV group give the best information about all γ-energies. Nevertheless the assignment in the decay scheme becomes extremely difficult. Regarding the intensities of the γ-transitions 770 keV and 1025 keV, a rough analysis of the spectrum was made which indicated that each line represents about 10% of the total γ-ray intensity. No attempt was made to estimate the intensity of the other 32 lines listed in Table II.

3. — Decay scheme and spin assignment.

Our decay scheme is based in the first instance on the information from the β-ray analysis. The first problem, mentioned in the introduction, is solved

because the transition to the ground state is found to be first forbidden (Table I, No. 1). The same degree of forbiddenness has been found by other authors ([6,7]) for the transition ^{234}Th(UX1) $\rightarrow$ ^{234}Pa(UX2). ^{234}Th and ^{234}U are even-even nuclei and therefore 0^+ in the ground state. Hence UX2 could be 0^- or 1^-. The next β-transition (No. 2) leads to the first excited state in ^{234}U of (49 ± 8) keV and there is no doubt that this corresponds to the value 43.5 keV found from the α-decay of ^{238}Pu ([15]). The 43 keV transition has been proved to be $E2$ ([16]) and the first excited state is 2^+ as expected ([15]). The log *ft* value 6.9 for the β-spectrum leading to this state (No. 2) excludes 0^- for UX2. $\Delta I = 2$, yes, is not possible following the classification of unique forbidden transitions ([17]). The only possibility remaining is 1^-.

Additional support for this assignment can be obtained from the decay of ^{234}Th. Unfortunately these arguments involve the multipolarity of some low energy γ-rays not yet known with certainty as well as the possible existence of another β-transition listed in Table I (No. 12) which, according to intensity considerations, should belong to this decay. So the only thing that can be said at this stage is, that the assignment 1^- for UX2 is not in disagreement with experimental data concerning the decay of ^{234}Th. In particular the *ft* value for the β-transition to the ground state (UX2) is not affected by the existence of another β-transition.

Once the value 1^- is accepted for UX2, spin and parity assignments can be made to the excited states in ^{234}U according to the log *ft* values listed in Table I. In some cases additional information is obtained from γ-decay and the most probable value is proposed. Many of the γ-rays fit in the levels obtained by β-decay within experimental errors. But in two rather important cases levels seem to be involved which are not populated by β-decay directly. The first is the 4^+ (rotational) state at 143 keV known from the α-decay of ^{238}Pu ([15]). Whereas the β-transition to the 2^+ (rotational) state at 43 keV was found, it is clear that the corresponding transition to the 4^+ state should be highly forbidden and in fact none of the β-rays could be ascribed to this transition, not only for energy reasons, but also for reasons of forbiddenness. The point is that an excitation of this state causes an $E2$ radiation of 99.8 keV ([15]). This energy of course appears in our experiments as 100 keV. The conversion of an $E2$ at 100 keV is not too high and in fact strong coincidences are found in the γ-γ coincidence experiments with the 770 keV line. On the other hand it must be noted that between the other excited states at low energy, giving rise to the cascade 43, 33, 34 and 57 keV, some crossover

---

([15]) J. O. Newton, B. Rose and J. Milsted: *Phil. Mag.*, **1**, 981 (1956).
([16]) F. Asaro and I. Perlmann: *Phys. Rev.*, **94**, 381 (1954).
([17]) E. Feenberg: *Shell Theory of the Nucleus* (Princeton, 1955).

transitions might be possible, which eventually could be mixed up with the 100 keV line in question. This possibility was checked carefully. A 124 keV line has been found by other authors *e.g.* in reference (9) where it has been ascribed to UZ; in the complex it is completely masked by the UX1 decay. We propose to place the 124 keV line between the 165 keV and the 43 keV levels in agreement with the fact that the 57 keV is extremely weak. A 110 keV transition to the ground state must be regarded as a 0-0 transition and therefore completely converted. For this we have different arguments:

a) In the γ-spectrum the complex peak at (90÷100) keV consists of different components: The 93 keV transition in ^{234}Pa, X-rays in ^{234}Pa and ^{234}U and the 100 (99) keV transition in ^{234}U. The γ-γ coincidence measurements with different parts of the spectrum exhibit this complex structure, but no indication for a 110 keV γ-energy was found.

b) The 1025 keV transition which, according to energy consideration, β-γ coincidence and β-ray analysis, leads from the 1135 keV to the 110 keV level, shows no γ-γ coincidences with partners between 95 and 125 keV (Fig. 9).

c) The 805 keV transition according to energy consideration, β-γ coincidences and β-ray analysis, fits only in between the 110 keV and the 915 keV level. In particular there seems to be no possibility at all that the 805 keV transition leads to the ground state directly. There can be no doubt that it is a 0-0 transition. So there must be another level with angular momentum 0 and perhaps another 0-0 transition. Therefore 0^+ is assigned to the 110 keV level. This is also in agreement with the log *ft* value of β-transition No. 4. No indication could be found for a 90 keV crossover. In any case it seems clear that the coincidences at 100 keV cannot be explained by any of these transitions and the conclusion therefore is that the 770 keV leads partly to the rotational state (4^+) at 143 keV and partly to the cascade following the 165 keV level. A direct consequence of these assignments is the existence of the second state not populated by β-decay namely the 3^- at 370 keV.

We regard this 100 keV transition as identical with the strong 99.8 keV in UZ described by ONG (9) and this line is therefore common to UZ and UX2. The search for these crossovers in the low energy region is of special importance, because the decay scheme must be in agreement with the fact that the intensity of the 43 keV transition is of the order of about 5% (9). From β-decay alone (Table I, No. 2) this state is populated with about 5%, and therefore most of the de-excitation of the high energy states must take place via crossover. It is very likely that the 76 keV crossover plays the most important role regarding intensity considerations, but no quantitative information can be given at this stage.

4. — Discussion.

It must be noted that all γ-ray energies in the decay scheme (Fig. 11) must be taken with their experimental error given in column IV of Table II. No corrections were made using the knowledge of conversion lines. The expe-

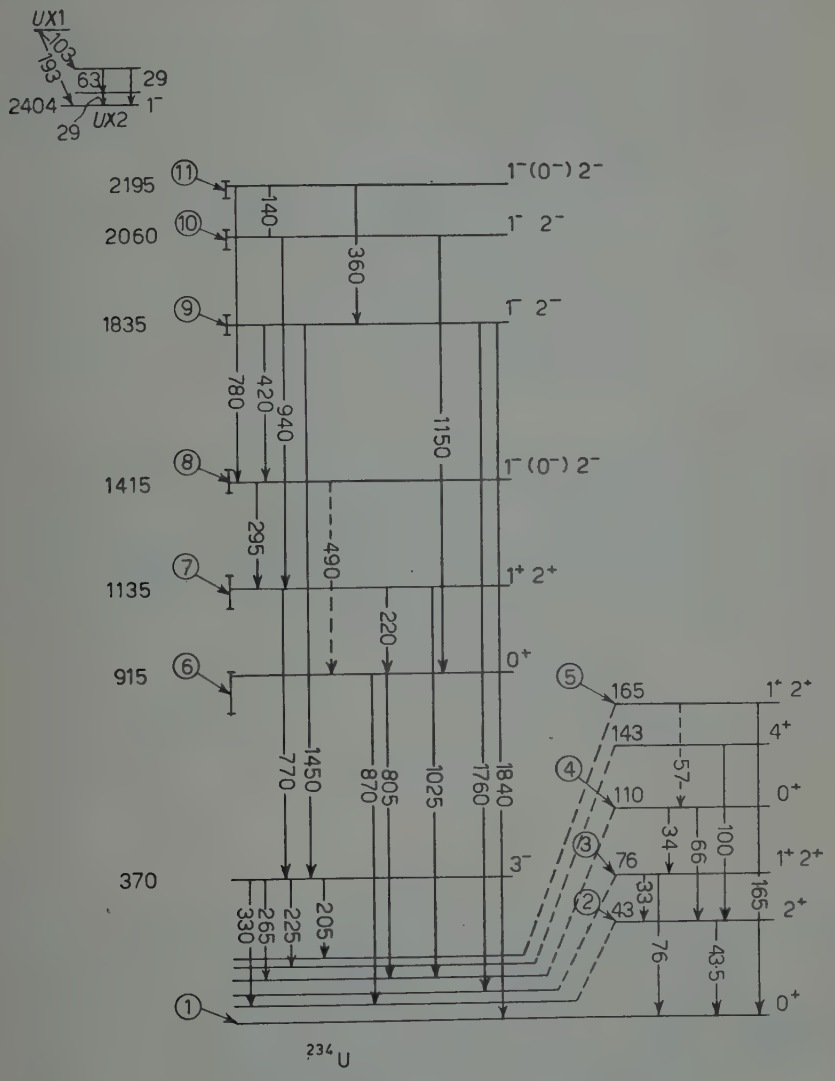

Fig. 11. – Decay scheme of UX2.

rimental errors of the β-ray-analysis are indicated on the left side of the level line. Only 27 of the 34 γ-rays listed in Table II are inserted in the decay scheme. Three of these (1840, 1760 and 1150 keV) have no support from

coincidence measurements, but there seems to be no other place for them in the scheme according to energy considerations. The other lines are inserted following the information of at least one coincidence experiment. Most of them are confirmed by different experiments. No attempt has been made to remeasure the conversion lines, although this should confirm many of the listed γ-energies and increase the accuracy of these transitions considerably. The reason for this is the following: the γ-spectrum is much more complicated than expected and in fact about 35 conversion lines were found below 200 keV but no proper resolution could be achieved mainly because of energy loss in the source. Although the sources were carrier-free, they were all visible and apparently not free from some salts that passed the ion exchange column. Some experiments were made with electrolysis following the procedure described by ERBACHER ([18]) but, similar to the results of ATEN and BARENDREGT ([19]) they were not successful. It seems that considerable experimental difficulties must be overcome before really thin and strong sources are available so that further work can be done on the conversion lines especially at lower energies. Therefore the relative intensities and multipolarities of the transitions are also still unknown.

* * *

The authors would like to thank the South African Council for Scientific and Industrial Research and the South African Atomic Energy Board for permission to publish this paper. We would also like to thank Dr. J. VAN R. SMIT and the radiochemical group for the chemical separations. One of us (J.W.L.) is indebted to the South African Atomic Energy Board for a research fellowship.

([18]) O. ERBACHER: *Zeits. anorg. allg. Chem.*, **252**, 282 (1944).
([19]) J. B. TH. ATEN and F. BARENDREGT: *Physica*, **16**, 760 (1950).

RIASSUNTO (*)

Si studiano gli spettri γ e β osservati nel decadimento dell'UX2 (vita media 1.175 min nel ^{234}Pa). Si descrivono le coincidenze β-γ ottenute in uno spettrometro a raggi β, come pure le misure di coincidenza γ-γ con energie selezionate. Nello spettro β si risolvono 11 spettri parziali che conducono a stati differenti nel nucleo derivato ^{234}U e si danno i valori dei loro log *ft*. Si dimostra che la porzione di alta energia di questo spettro, che si è sempre ritenuto si riducesse allo stato fondamentale, è assai complessa, contenendo 5 spettri parziali. Il valore del log *ft* della transizione allo stato fondamentale risulta 6.9, indicando lo stesso grado di proibizione osservato per la transizione ^{234}Th-^{234}Pa. Si assegnano gli spin dell'UX2 e di alcuni stati eccitati del ^{234}U. Si presenta uno schema di decadimento.

(*) *Traduzione a cura della Redazione.*

IL NUOVO CIMENTO Vol. XIV, N. 1 1° Ottobre 1959

Use of an Electronic Computer for the Construction of Exact Eigenfunctions of Orbital Angular Momentum in L-S Coupling.

E. Abate (*) and E. Fabri (**)

Centro Studi Calcolatrici Elettroniche dell'Università - Pisa

(ricevuto il 18 Febbraio 1959)

Summary. — The application of a digital electronic computer to the evaluation of exact eigenfunctions of total orbital angular momentum for many-electrons systems is studied. Some unusual features presented by such problem, as compared with ordinary applications of electronic computers, are discussed. Computations have been carried out following the projection operator tecnique, and results are given for 3 and 4 electrons in d- and f-states, and for 5 electrons in d-states only. Because of the relative smallness of the computer used, results are not complete; the way followed, however, appears to be quite promising for future extensions of the computation with a bigger machine.

Introduction.

Functions having particular symmetry properties which are connected with the angular momentum operators are often useful in many atomic and molecular problems. In this connection, one problem of a very frequent occurrence is the composition of angular momenta, *i.e.* the research of the eigenfunctions of the sum of two or more angular momentum operators, belonging

(*) On leave of absence from the Milan Section of the Istituto Nazionale di Fisica Nucleare.

(**) Now at the Pisa Section of the Istituto Nazionale di Fisica Nucleare.

to different parts of the same system—or else to different degrees of freedom—the eigenfunctions of each individual operator being known in advance.

From a group-theoretical point of view, the problem is to find the irreducible representations the product of two or more irreducible representations of the orthogonal group can be decomposed into; the question is a classical one and has been solved since a long time. Nevertheless, for practical applications to atomic and molecular systems, a theoretical solution is not enough: it must be integrated by computational techniques, giving the theory a form suitable for problems that actually arise.

But when such a technique is made available, we are still faced with further difficulties as soon as we try to deal with rather complex systems: the time required for calculations becomes rapidly prohibitive, while the probability of errors grows still faster. It is thereafter a quite natural idea to make use of an automatic computer in order to overcome the difficulty, and this is what we have done. We do not know, however, that electronic computers have been used before for such kind of problems: if it is true, there should be no surprise, since electronic computers have been mainly intended as an aid for pure computational work. Of course we do not think that this is the only work wherein electronic computers have been used all over the world; we only claim that it has been their main use, and among physicists perhaps the only one. This is the reason why we found interesting to study the programming of the construction of eigenfunctions of total orbital angular momentum by an electronic computer. In the following the procedure adopted is outlined, and the main points and the results are reported and criticized.

In Section **1** some basic notations are stated.

In Section **2** the projection operator method, whereon our work is founded, is outlined.

Section **3** is devoted to an exposition of the detailed formulation of the calculation, in terms of recursive formulae.

In Section **4** the flow diagram of the program is given and discussed.

In Section **5** an account is given of the main arithmetical difficulties encountered, together with the solution adopted.

In Section **6** the results of the calculation are given, and some concluding remarks about the experience gained in this work are made.

1. – Notations.

In this paper we are concerned with the case of many-electrons atoms in Russel-Saunders coupling scheme: our problem is to build eigenfunctions of the orbital angular momentum of the system, starting from eigenfunctions of the orbital angular momenta of the individual electrons.

Let us introduce here some notations:

$\boldsymbol{l}(i)$	for the one-electron orbital angular momentum;
$l_x(i)$, $l_y(i)$, $l_z(i)$	for its components;
$l^2(i)$	for its modulus squared;
$\mathrm{l}_i(\mathrm{l}_i+1)$, m_i	for the eigenvalues of $l^2(i)$ and $l_z(i)$ (in units of $\hbar$);
$l_+(i) = l_x(i) + il_y(i)$	for the one-electron step-up operator;
$l_-(i) = l_x(i) - il_y(i)$	for the one-electron step-down operator.

Besides we will denote by $(\mathrm{l}_i, \mathrm{m}_i)$ an eigenfunction of $l^2(i)$ and $l_z(i)$ with the eigenvalues $\mathrm{l}_i(\mathrm{l}_i+1)$ and m_i.

Accordingly, for the many-electrons system the notations will be: $\mathcal{L} = \sum \boldsymbol{l}(i)$ for the orbital angular momentum operator; $\mathcal{L}_x$, $\mathcal{L}_y$, $\mathcal{L}_z$ and $\mathcal{L}^2$ for its components and modulus squared; $L(L+1)$ and M for the eigenvalues of $\mathcal{L}^2$ and $\mathcal{L}_z$;

$\mathcal{L}_+ = \mathcal{L}_x + i\mathcal{L}_y = \sum l_+(i)$	for the step-up operator,
$\mathcal{L}_- = \mathcal{L}_x - i\mathcal{L}_y = \sum l_-(i)$	for the step-down operator,
(L, M)	for the eigenfunctions.

Coming back to our subject, now let us point out that, by building an antisymmetrized product of the $(\mathrm{l}_i, \mathrm{m}_i)$ we get an eigenfunction belonging to the eigenvalue $M = \sum \mathrm{m}_i$ of $\mathcal{L}_z$. Let us design such antisymmetrized product by

$$(\mathrm{l}_1\mathrm{m}_1, \mathrm{l}_2\mathrm{m}_2, \ldots, \mathrm{l}_p\mathrm{m}_p \,|\, \mathrm{l}_{p+1}\mathrm{m}_{p+1}, \ldots, \mathrm{l}_n\mathrm{m}_n) ,$$

where the stroke means that the first p electrons are in a spin state belonging to the eigenvalue $\frac{1}{2}$ of s_z and the others in a state belonging to the eigenvalue $-\frac{1}{2}$.

If the n electrons are equivalent, what implies that $\mathrm{l}_1 = \mathrm{l}_2 = \ldots = \mathrm{l}_n = \mathrm{l}$ (this is the case we will consider), we can design the product function simply by

$$(\mathrm{m}_1\, \mathrm{m}_2 \ldots \mathrm{m}_p \,|\, \mathrm{m}_{p+1} \ldots \mathrm{m}_n) .$$

As we have already pointed out, a function of this kind, which we will call a « configuration », is an eigenfunction of $\mathcal{L}_z$ with the eigenvalue $M = \sum \mathrm{m}_i$, but generally it is not an eigenfunction of $\mathcal{L}^2$. A configuration is a mixture of eigenfunctions of $\mathcal{L}^2$ belonging to different L's (always $\geqslant M$) and vice-versa an eigenfunction of $\mathcal{L}^2$ and $\mathcal{L}_z$ is a linear combination of different con-

figurations referring to the same M. Our problem is just to find such linear combination, starting from a certain configuration; or else to find out the component belonging to a particular eigenvalue L from the mixture the starting configuration consists of: this can be done by the projection operator formalism which we will shortly recall here.

2. – The projection operator method [1].

Consider a system of n equivalent electrons, p having their spin up and the remaining down; and take into account the space $S^{(M)}$ spanned by the eigenvectors of $\mathcal{L}_z$ belonging to a given eigenvalue M. Among these, the eigenvectors of $\mathcal{L}^2$ belonging to a given L will form a subspace $S_L^{(M)}$ of $S^{(M)}$. A configuration will generally be a vector of $S^{(M)}$, not lying on $S_L^{(M)}$; what we need is to project such vector onto $S_L^{(M)}$. This can readily be done, if a suitable projection operator is known, simply by applying such operator to the given configuration. It should be noted that the result of the projection will not be generally independent from the starting configuration, as $S_L^{(M)}$ may have more than one dimension, *i.e.* several independent eigenvectors (L, M) can exist.

Now the problem is to find the form of the projection operator. Let us consider the following product of commuting factors:

$$\prod_{L' \neq L} \frac{\mathcal{L}^2 - L'(L'+1)}{L(L+1) - L'(L'+1)}, \tag{1}$$

where L' ranges from M to K (the greatest L allowed by the given assignment of l and the spins), with the only exception of the wanted L. It is easily shown that (1), when working on an arbitrary vector, and in particular on a configuration, annihilates all components belonging to quantum numbers $L' \neq L$. Besides, the denominator has been so chosen that the operator lets unchanged the component belonging to L. Hence (1) is just the projection operator we were looking for.

We will stress here that the eigenvector obtained by this operator is not normalized, since it is a component of a normalized configuration.

We will observe that by an analogous procedure we can also project an arbitrary vector from the whole Hilbert space into the subspace spanned by

---

[1] For a thorough exposition of the method, first developed by P. O. Löwdin, see R. Fieschi and P. O. Löwdin: *Atomic state wave functions generated by projection operators* (Istituto Nazionale di Fisica Nucleare, Sezione di Milano, 1957 and Quantum Chemistry Group, Uppsala University, 1957), after referred to as FL.

the eigenfunctions of $\mathcal{L}_z$ belonging to a particular M; but, as we already discussed above, in our case we do not need this since a different and easier procedure to build eigenfunctions of $\mathcal{L}_z$ is available.

Moreover, we will point here that what we said above is still worth when the problem is to build eigenfunctions of a general angular momentum operator: so the projection operator formalism can be helpful, for instance, in nuclear problems, in which it is usual the j-j coupling scheme and eigenfunctions of J^2 and J_z are wanted.

From (1) we can derive for the projection operator the two forms we quote here

$$O_{LL} = (2L+1)! \sum_{\nu=0}^{K-L} (-1)^{\nu} \frac{\mathcal{L}_-^{\nu} \mathcal{L}_+^{\nu}}{\nu!\,(\nu+2L+1)!}, \tag{2}$$

$$O_{LL} = \prod_{L'=L+1}^{K} \left\{ \frac{\mathcal{L}_- \mathcal{L}_+}{(L-L')(L+L'+1)} + 1 \right\}. \tag{3}$$

Such simpler formulae are valid only in the « principal case » $L = M$, while the general case $L \geqslant M$ would lead us to more complicated formulae; however this is not a trouble, since we can easily obtain any (L, M), with $M < L$, from (L, L) simply by applying the step-down operator $L - M$ times.

Since the calculation was carried out with the help of an electronic digital computer, (3) was found more suitable than (2), which, on the contrary, is more convenient for hand-calculations.

As far as we are concerned, there remains only to find how an electronic computer can be instructed to apply O_{LL} to a suitable starting configuration. Of course this is not the whole story: before applying O_{LL} we need to know how many independent (L, L) exist for a given L, and how to choose starting configurations in order to be sure of getting independent final results. However, we did not require this too from the computer, but preferred to do ourselves such preliminary work. For this reason, we need not dwell upon such subject, and refer to FL for discussion.

3. – Recursive formulation of the method.

In view of programming the calculation on an electronic computer we must analyse the process of applying O_{LL} to a configuration into a succession of simpler steps, each expressed in a form easily translatable into a computer language. For that, we first must find a recursive expansion for our basic formula (3). We begin by writing:

$$O_{LL} = \prod_{L'=L+1}^{K} \mathcal{O}_{L'}^{(L)}, \tag{4}$$

with

$$\mathcal{C}_{L'}^{(L)} = \frac{\mathcal{L}_- \mathcal{L}_+}{(L-L')(L+L'+1)} + 1 .$$

From the definition of $\mathcal{L}_+$ and $\mathcal{L}_-$ it follows that by applying an operator $\mathcal{C}_{L'}^{(L)}$ to a particular configuration with $M = L$ a linear combination of configurations belonging to the same M obtains. In formulae:

$$\mathcal{C}_{L'}^{(L)} \boldsymbol{u}_i = \sum_{j=1}^{N} (\mathcal{C}_{L'}^{(L)})_{ij} \boldsymbol{u}_j \qquad (i = 1, ..., N), \tag{5}$$

where each $\boldsymbol{u}_i$ represents a configuration. Coefficients $(\mathcal{C}_{L'}^{(L)})_{ij}$ may be thought of as matrix elements in the basis $\boldsymbol{u}_i$.

When an operator $\mathcal{C}_{L'}^{(L)}$ works on a vector of $S^{(L)}$:

$$\Psi = \sum_i c_i \boldsymbol{u}_i$$

it gives rise to a vector of the same space

$$\mathcal{C}_{L'}^{(L)} \Psi = \sum_i c_i \mathcal{C}_{L'}^{(L)} \boldsymbol{u}_i = \sum_{ij} c_i (\mathcal{C}_{L'}^{(L)})_{ij} \boldsymbol{u}_j .$$

Now, as (4) shows, the calculation is to be carried out through $K - L$ steps, each step being characterized by a different operator $\mathcal{C}_{L'}^{(L)}$. At each step an operator works on the vector obtained by the preceding step. The vector, the first $\mathcal{C}_{L'}^{(L)}$ works on, is the starting configuration; the one obtained after last step is (L, L).

So, if $\Psi^{(L'-1)} = \sum_i c_i^{(L'-1)} \boldsymbol{u}_i$ is the function we have got after the step $L'-1$, then

$$\Psi^{(L')} = \mathcal{C}_{L'}^{(L)} \Psi^{(L'-1)} = \sum_i c_i^{(L'-1)} \mathcal{C}_{L'}^{(L)} \boldsymbol{u}_i = \sum_{ij} c_i^{(L'-1)} (\mathcal{C}_{L'}^{(L)})_{ij} \boldsymbol{u}_j = \sum_j \Big\{ \sum_i c_i^{(L'-1)} (\mathcal{C}_{L'}^{(L)})_{ij} \Big\} \boldsymbol{u}_j .$$

The components of the vector obtained after the step L' are therefore

$$c_j^{(L')} = \sum_{i=1}^{N} c_i^{(L'-1)} (\mathcal{C}_{L'}^{(L)})_{ij} \qquad (j = 1, ..., N) \tag{6}$$

The $c^{(L)}$'s are all zero but one which is 1, since $\Psi^{(L)}$ is the starting configuration; the $c^{(K)}$'s are just the amplitudes corresponding to the different configurations in (L, L).

Our problem is now reduced to evaluating the amplitudes $c^{(K)}$ by means of the recursive formula (6); by this formula we can calculate the $c^{(L')}$'s step-by-step from $c^{(L)}$ to $c^{(K)}$.

At this point it must be noted that in this section we have labelled the configurations by one index ranging from 1 to N, while in Section **1** we introduced the notation $(m_1 \dots m_p | m_{p+1} \dots m_n)$, where n labels are used. In order to put a relation between our last formulae and the preceeding ones—in particular to give an explicit expression of $(\mathcal{C}^{(L)}_{L'})_{ij}$—it is necessary to establish a correspondence between the two notations. As long as we are interested in hand calculations, this is a question of a formal kind; but it becomes a practical one when a computer is taken into account.

The required correspondence amounts to assigning an integral number to every set of m's whereby a configuration can be labelled. In fact we have to single out orderly all sets of n integers m_i fulfilling the following conditions:

1) $-1 \leqslant m_i \leqslant 1$;

2) $\sum m_i = M = L$;

3) $m_1 < m_2 < \dots < m_p$; $m_{p+1} < \dots < m_n$.

This may be done in a way we shall describe further. As soon as a set of m's fulfilling the conditions above is found, it is noted and labelled with an increasing index i. So all configurations are ordered and we are able to apply (6). About the procedure to order the sets of m's, we describe here the one we have followed.

The i-th set be known: in order to find the following one, m_{n-1} should be increased and m_n decreased by 1. In this way condition 2) is certainly kept, while 1) and 3) are to be verified. If all is right, we have found the $(i+1)$-th set; otherwise we try to increase m_{n-2}, giving m_{n-1} the lowest value permitted by 1) and 3), and choosing, m_n to satisfy 2). If such m^n satisfies 1) and 3) too, we have succeeded in finding the new set; if not, we must try to increase m_{n-3}, and so on. This process will end in one of the two following ways:

a) one is able to find the $(i+1)$-th set; then the $(i+2)$-th one is to be looked for in the same way:

b) one cannot find the $(i+1)$-th set, because in trying to increase an m, the first one, m_1, is unsuccessfully tried; then $i = N$, *i.e.* we had found last set. Anyhow the number of sets one can find is finite, since there is an upper bound for each m.

As to the set to start with, it must obviously be:

$$(-1, -1+1, \dots, -1+p-1 | -1, \dots, -1+n-p-2, \overline{m}_n) .$$

with $\overline{m}_n$ chosen so that 2) is satisfied. One cannot be sure that this is a good

set: conditions 1) and 3), indeed, will hardly be satisfied by $\overline{m}_n$. But it is, however, the first we must look at.

If the calculation is carried out by an electronic computer, an ordering subroutine is needed which execute such procedure.

4. – Flow diagram.

In order to describe how actually the program works we quote here some rough flow-diagrams with some explanatory notes

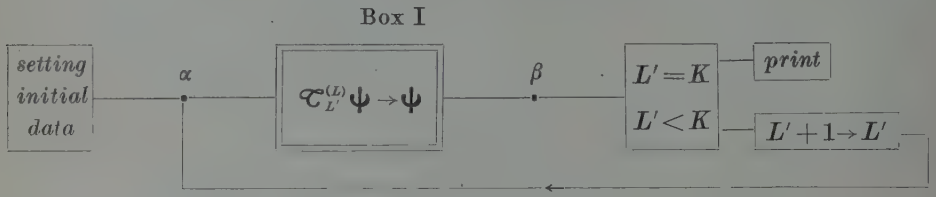

Diagram 1.

In diagram 1 the main cycle of the program is shown, in the course of which the successive steps are executed. Box I represents and individual step. $\mathcal{C}_{L'}^{(L)}\psi \to \psi$ means that the new vector $\mathcal{C}_{L'}^{(L)}\psi$ obtained after each step becomes the starting vector for the new step. This actually is made in the electronic computer by storing $\mathcal{C}_{L'}^{(L)}\psi$ in the same cells before occupied by ψ. The structure of box I is analyzed with more details in diagram 2.

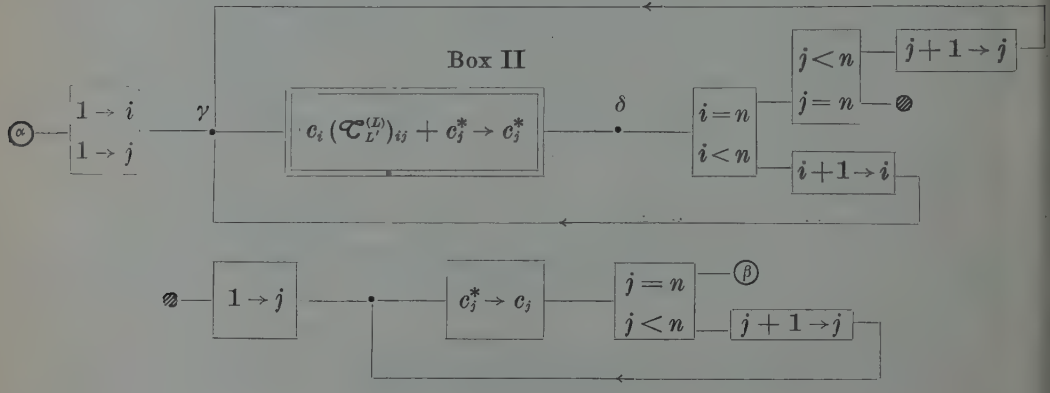

Diagram 2.

The most important feature shown by this diagram is the occurrence of a double cycle. From this the necessity comes of defining auxiliary variables c^*,

which are needed at the same time with the c's; at the end of both cycles the final c^*'s become the new c's. In the computer, this means storing the c^*'s in a separate place during the cycles, and substituting them for the c's at the end.

The contents of box II is furtherly specified by diagram 3.

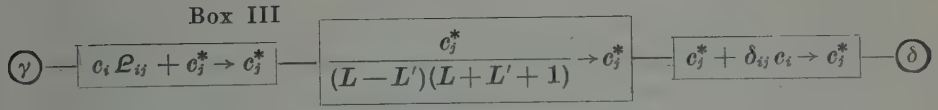

Diagram 3.

according to

$$(\mathcal{C}_{L'}^{(L)})_{ij} = \frac{\mathcal{L}_{ij}}{(L-L')(L+L'+1)} + \delta_{ij} ,$$

$\mathcal{L}_{ij}$ being the matrix element of $\mathcal{L}_- \mathcal{L}_+$.

To carry out the calculation described in box III we need the ordering subroutine twice: a first time to find the m's corresponding to a given i; a second time to decide whether for a particular j the matrix elements $\mathcal{L}_{ij}$ is different from zero and, in such case, to find its value.

To complete our brief description, we must say that in our program the ordering subroutine is needed twice more: at the beginning and when printing the results. That is due to starting configuration being given by means of its m's, while the computer is wanted to print the final results labelled by the corresponding sets of m's; both facts contrasting with the one-index representation used throughout the calculation.

5. – Arithmetical features of the program.

The first fact we must point out in this connection, is that surd numbers are to be worked upon through the calculation. This fact does not make any trouble for hand-calculations, but is complicates programming. Owing to the group-theoretical character of the problem it is desirable to carry out the calculation with an absolute accuracy, since it is possible by principle.

It is not so obvious that the numbers we are concerned with must be surds. But it is easily seen that the matrix elements $\mathcal{L}_{ij}$ are of the form $a\sqrt{b}$ (a, b integers) and may be shown that no more complicated number, like $\sqrt{m} + \sqrt{n}$, arises throughout the calculation in spite of the occurrence of additions.

In such particular situation, it is possible and worthwhile to use for these numbe a representation which permits an absolute accuracy. Such a representation can be obtained only using more than one integer for each number. We can choose, for instance, one of the following two representations:

1) the couple of integers $(a, \pm b)$, prime with respect to each other to represent the irrational number $\pm\sqrt{a/b}$;

2) the three integers $(\pm a, b, c)$ to represent the number $\pm a\sqrt{b}/c$. In the latter representation b will always be reduced to a product of prime factors all different from one another, while a and c are still prime with respect to each other.

Adopting such representations implies a good deal of multiplications to carry out the additions; thus as intermediate results one often gets quite large numbers, even if the final results may be represented by relatively small integers. Since in a computer the bits available to represent an individual integer are finite in number, the calculation will easily lead to overflows.

This puts an upper bound to the complexity of the eigenfunctions the program can give out. This bound will obviously depend upon the word-length of the particular computer we make use of. Another bound is put by a different feature of the computer, namely the size of the memory. In fact we have to store both the c's and the c^*'s, so a working storage is needed, whose size depends upon N, *i.e.* the number of configurations to be taken into account in the calculation.

In the computer we used (a reduced model of the machine being built at Pisa University), the two bounds we pointed above were rather narrow. The words were 18 bits long, so overflows were very frequent. In order to avoid them as far as possible, we chose the representation $(\pm a, b, c)$. We represented the three integers by means of 3 different words: $\pm a$ and c were represented in the usual binary representation, while for b a different representation was used. Since b occurs, during the calculation, only as a multiplying factor, it seemed convenient to represent it by its prime factors.

This was made by decomposing a word into six groups of three bits each; the groups represented orderly the exponents (all $\leqslant 7$) of 2, 3, 5, 7, 11, 13 arising from decomposing b into its prime factors. Of course it was assumed that no greater factor could arise, which was made sure by an analysis of the origin of each factor. The use of only six prime factors was possible until electrons with $l \leqslant 6$ were considered.

A major disadvantage of this kind of number representation is that arithmetic operation may no longer be executed by simple machine instructions, but require *ad hoc* subroutines. Besides, the results of arithmetic operations are generally not in the standard form (this accounts for our having allowed exponents in the representation of b to grow till 7, while in standard form only 0 and 1 may occur).

In order to avoid an overgrowth of numbers causing overflows, reduction to standard form must be accomplished after every operation, which together with the need of frequently calling the arithmetic subroutines considerably increases computing time.

6. – Discussion of the results.

The calculation actually carried out concerned the following cases: 3, 4, 5 d-electrons and 3, 4 f-electrons. The results for d-electrons could be compared with previous hand-calculations by FL, while f-electrons results are given here for the first time. Apart from exceptions we will explain later, our results agree with FL's as far as a check is possible; for f-electrons, no comparison term being available, special checks would have been advisable.

We did not do that for two kinds of reasons. First, the agreement found for d-case assures us that the program was errorless and at the same time gives us a good assurance against the occurrence of machine faults; on the other side, it may be assumed as a very improbable event that a machine error results in giving out quite reasonable numbers. Secondly, as it will be seen later, our results are not complete; thus it would have been of little use to undertake a check at such a stage of work.

The Table below summarizes our final results. In column 1 the spectroscopic notation for a term is found. We must note here that no account was taken of spin in our looking for eigenvectors; thus the labelling of terms with a doublet, triplet, etc. symbol is rather arbitrary. One should expect, indeed, that the eigenvectors we give are still a superposition of the different spin eigenvectors belonging to the same L.

In column 2 the starting configuration is given, while in column 3 and 4 the final eigenfunction is represented by writing the coefficient (in column 4) for every component configuration (column 3).

Column 5 contains some conventional symbols, with the following meaning:

FL means that the given eigenfunction checks with FL's.

(FL) means that the given eigenfunction is right, though it does not check with FL's because the latter is a spin eigenfunction, while the first is not.

Ov. corresponding to empty spaces in columns 3, 4, 5 means that the computer was not able to evaluate that function, because of overflows.

Empty space in column 5 means that no check was available for that case.

As a further comment to the Table hereupon we will only observe that it is far from being complete in two respects: because of computer's unability to deal with the most complicated cases; but also because of limits purposely imposed by us. We already said that no spin projection operator was used, so that final eigenfunctions are not eigenfunctions of spin, but only of orbital angular momentum. Moreover, even the number of independent eigenfunctions we give is smaller than it should be for a complete description of each $S_L^{(L)}$. One can see, for instance, that for a doublet term one only function is given,

TABLE I.

3 d-electrons					4 d-electrons				
^{2}H	$(2\vert12)$	$(2\vert12)$	1	FL	^{1}I	$(12\vert12)$	$(12\vert12)$	1	FL
^{2}G	$(2\vert02)$	$(1\vert12)$	$-\frac{1}{5}\sqrt{6}$	FL	^{3}H	$(2\vert012)$	$(2\vert012)$	1	FL
		$(2\vert02)$	$\frac{2}{5}$		^{3}G	$(2\vert\bar{1}12)$	$(1\vert012)$	$-\frac{1}{5}\sqrt{6}$	FL
^{4}F	(012)	(012)	1	FL			$(2\vert\bar{1}12)$	$\frac{2}{5}$	
^{2}F	$(2\vert\bar{1}2)$	$(0\vert12)$	$\frac{1}{12}\sqrt{6}$	FL	^{1}G	$(02\vert02)$	$(\bar{1}2\vert12)$	$-\frac{3}{11}$	FL
		$(1\vert02)$	$-\frac{1}{12}\sqrt{6}$				$(01\vert12)$	$-\frac{1}{11}\sqrt{6}$	
		$(2\vert\bar{1}2)$	$\frac{1}{2}$				$(02\vert02)$	$\frac{5}{11}$	
		$(2\vert01)$	$-\frac{1}{6}\sqrt{6}$				$(12\vert\bar{1}2)$	$-\frac{3}{11}$	
^{2}D	$(2\vert\bar{2}2)$	$(\bar{1}\vert12)$	$-\frac{1}{14}$	FL			$(12\vert01)$	$-\frac{1}{11}\sqrt{6}$	
		$(0\vert02)$	$\frac{1}{14}$		^{1}G	$(12\vert\bar{1}2)$	$(\bar{1}2\vert12)$	$\frac{9}{55}$	(FL)
		$(1\vert\bar{1}2)$	$-\frac{13}{42}$				$(01\vert12)$	$\frac{3}{55}\sqrt{6}$	
		$(1\vert01)$	$\frac{5}{42}\sqrt{6}$				$(02\vert02)$	$-\frac{3}{11}$	
		$(2\vert\bar{2}2)$	$\frac{23}{42}$				$(12\vert\bar{1}2)$	$\frac{31}{55}$	
		$(2\vert\bar{1}1)$	$-\frac{5}{21}$				$(12\vert01)$	$-\frac{8}{55}\sqrt{6}$	
^{2}D	$(0\vert02)$	$(\bar{1}\vert12)$	$-\frac{5}{14}$	FL	^{3}F	$(2\vert\bar{2}12)$	$(0\vert012)$	$\frac{1}{6}$	FL
		$(0\vert02)$	$\frac{5}{14}$				$(1\vert\bar{1}12)$	$-\frac{1}{6}$	
		$(1\vert\bar{1}2)$	$-\frac{3}{14}$				$(2\vert\bar{2}12)$	$\frac{2}{3}$	
		$(1\vert01)$	$-\frac{1}{14}\sqrt{6}$				$(2\vert\bar{1}02)$	$-\frac{1}{6}\sqrt{6}$	
		$(2\vert\bar{2}2)$	$\frac{1}{14}$		^{3}F	$(2\vert\bar{1}02)$	$(0\vert012)$	$\frac{1}{12}\sqrt{6}$	FL
		$(2\vert\bar{1}1)$	$\frac{1}{7}$				$(1\vert\bar{1}12)$	$-\frac{1}{12}\sqrt{6}$	
^{4}P	$(\bar{2}12)$	$(\bar{2}12)$	$\frac{3}{5}$	FL			$(2\vert\bar{2}12)$	$-\frac{1}{6}\sqrt{6}$	
		$(\bar{1}02)$	$-\frac{1}{5}\sqrt{6}$				$(2\vert\bar{1}02)$	$\frac{1}{2}$	
^{2}P	$(1\vert\bar{1}1)$	$(\bar{2}\vert12)$	$-\frac{6}{35}$	FL	^{1}F	$(12\vert\bar{2}2)$	$(\bar{2}2\vert12)$	$-\frac{1}{30}$	(FL)
		$(\bar{1}\vert02)$	$\frac{2}{35}\sqrt{6}$				$(\bar{1}1\vert12)$	$-\frac{1}{15}$	
		$(0\vert\bar{1}2)$	$-\frac{1}{70}\sqrt{6}$				$(\bar{1}2\vert02)$	$\frac{1}{30}\sqrt{6}$	
		$(0\vert01)$	$-\frac{9}{70}$				$(01\vert02)$	$\frac{1}{15}$	
		$(1\vert\bar{2}2)$	$-\frac{3}{35}$				$(02\vert\bar{1}2)$	$-\frac{2}{15}\sqrt{6}$	
		$(1\vert\bar{1}1)$	$\frac{9}{70}$				$(02\vert01)$	$\frac{7}{30}$	
		$(2\vert\bar{2}1)$	$\frac{3}{35}$				$(12\vert\bar{2}2)$	$\frac{19}{30}$	
		$(2\vert\bar{1}0)$	$-\frac{1}{14}\sqrt{6}$				$(12\vert\bar{1}1)$	$-\frac{7}{30}$	

TABLE I (*continued*).

		4 *d*-electrons		
^5D	$(\bar{1}012)$	$(\bar{1}012)$	1	FL
^3D	$(2\|\bar{2}02)$	$(\bar{1}\|012)$	$-\frac{1}{7}$	FL
		$(0\|\bar{1}12)$	$\frac{1}{7}$	
		$(1\|\bar{2}12)$	$-\frac{2}{21}\sqrt{6}$	
		$(1\|\bar{1}02)$	$\frac{1}{21}$	
		$(2\|\bar{2}02)$	$\frac{4}{21}$	
		$(2\|\bar{1}01)$	$-\frac{5}{21}$	
^1D	$(01\|01)$	$(\bar{1}0\|12)$	$\frac{1}{21}\sqrt{6}$	FL
		$(\bar{1}1\|02)$	$-\frac{1}{21}\sqrt{6}$	
		$(\bar{1}2\|\bar{1}2)$	$\frac{2}{7}$	
		$(\bar{1}2\|01)$	$-\frac{2}{21}\sqrt{6}$	
		$(01\|\bar{1}2)$	$-\frac{2}{21}\sqrt{6}$	
		$(01\|01)$	$\frac{3}{7}$	
		$(02\|\bar{1}1)$	$-\frac{1}{21}\sqrt{6}$	
		$(12\|\bar{1}0)$	$\frac{1}{21}\sqrt{6}$	
^1D	$(\bar{1}2\|\bar{1}2)$	$(\bar{2}1\|12)$	$\frac{1}{7}$	
		$(\bar{2}2\|02)$	$-\frac{1}{21}\sqrt{6}$	
		$(\bar{1}1\|02)$	$-\frac{1}{21}\sqrt{6}$	
		$(\bar{1}2\|\bar{1}2)$	$\frac{2}{7}$	
		$(\bar{1}2\|01)$	$-\frac{1}{21}\sqrt{6}$	
		$(01\|\bar{1}2)$	$-\frac{1}{21}\sqrt{6}$	
		$(01\|01)$	$\frac{2}{7}$	
		$(02\|\bar{2}2)$	$-\frac{1}{21}\sqrt{6}$	
		$(02\|\bar{1}1)$	$-\frac{1}{21}\sqrt{6}$	
		$(12\|\bar{2}1)$	$\frac{1}{7}$	
^3P	$(1\|\bar{1}01)$	$(\bar{2}\|012)$	$-\frac{3}{35}$	FL
		$(\bar{1}\|\bar{1}12)$	$\frac{1}{35}\sqrt{6}$	
		$(0\|\bar{2}12)$	$\frac{3}{35}$	
		$(0\|\bar{1}02)$	$-\frac{2}{35}\sqrt{6}$	
		$(1\|\bar{2}02)$	$-\frac{3}{35}$	
		$(1\|\bar{1}01)$	$\frac{9}{35}$	
		$(2\|\bar{2}\bar{1}2)$	$\frac{4}{35}\sqrt{6}$	
		$(2\|\bar{2}01)$	$-\frac{9}{35}$	
^3P	$(\bar{1}\|\bar{1}12)$	$(\bar{2}\|012)$	$-\frac{1}{7}\sqrt{6}$	FL
		$(\bar{1}\|\bar{1}12)$	$\frac{2}{7}$	
		$(0\|\bar{2}12)$	$-\frac{2}{35}\sqrt{6}$	
		$(0\|\bar{1}02)$	$-\frac{6}{35}$	
		$(1\|\bar{2}02)$	$\frac{2}{35}\sqrt{6}$	
		$(1\|\bar{1}01)$	$\frac{1}{35}\sqrt{6}$	
		$(2\|\bar{2}\bar{1}2)$	$-\frac{2}{35}$	
		$(2\|\bar{2}01)$	$-\frac{1}{35}\sqrt{6}$	
^1S	$(\bar{2}2\|\bar{2}2)$			Ov.
^1S	$(\bar{1}1\|\bar{1}1)$			Ov.
		5 *d*-electrons		
^2I	$(12\|012)$	$(12\|012)$	1	FL
^2H	$(12\|\bar{1}12)$	$(02\|012)$	$-\frac{1}{2}$	FL
		$(12\|\bar{1}12)$	$\frac{1}{2}$	
^4G	$(2\|\bar{1}012)$	$(2\|\bar{1}012)$	1	FL
^2G	$(01\|012)$	$(\bar{1}2\|012)$	$-\frac{8}{55}\sqrt{6}$	FL
		$(01\|012)$	$\frac{39}{55}$	
		$(02\|\bar{1}12)$	$-\frac{1}{11}\sqrt{6}$	
		$(12\|\bar{2}12)$	$\frac{6}{55}$	
		$(12\|\bar{1}02)$	$\frac{3}{55}\sqrt{6}$	
^2G	$(12\|\bar{2}12)$	$(\bar{1}2\|012)$	$\frac{3}{55}\sqrt{6}$	FL
		$(01\|012)$	$\frac{6}{55}$	
		$(02\|\bar{1}12)$	$-\frac{1}{11}\sqrt{6}$	
		$(12\|\bar{2}12)$	$\frac{39}{55}$	
		$(12\|\bar{1}02)$	$-\frac{8}{55}\sqrt{6}$	
^4F	$(1\|\bar{1}012)$	$(1\|\bar{1}012)$	$\frac{1}{2}$	FL
		$(2\|\bar{2}012)$	$-\frac{1}{2}$	
^2F	$(\bar{1}2\|\bar{1}12)$	$(\bar{2}2\|012)$	$-\frac{2}{15}\sqrt{6}$	FL
		$(\bar{1}1\|012)$	$-\frac{1}{60}\sqrt{6}$	

TABLE I (*continued*).

		5 *d*-electrons		
^2F	$(\bar{1}2\,\vert\,\bar{1}\bar{1}2)$	$(\bar{1}2\,\vert\,\bar{1}\bar{1}2)$	$\frac{3}{10}$	FL
		$(01\,\vert\,\bar{1}\bar{1}2)$	$\frac{1}{60}\sqrt{6}$	
		$(02\,\vert\,\bar{2}\bar{1}2)$	$-\frac{1}{15}\sqrt{6}$	
		$(02\,\vert\,\bar{1}02)$	$-\frac{1}{5}$	
		$(12\,\vert\,\bar{2}02)$	$\frac{1}{15}\sqrt{6}$	
		$(12\,\vert\,\bar{1}01)$	$\frac{1}{30}\sqrt{6}$	
^2F	$(02\,\vert\,\bar{1}02)$	$(\bar{2}2\,\vert\,012)$	$\frac{1}{30}\sqrt{6}$	FL
		$(\bar{1}1\,\vert\,012)$	$\frac{1}{15}\sqrt{6}$	
		$(\bar{1}2\,\vert\,\bar{1}\bar{1}2)$	$-\frac{1}{5}$	
		$(01\,\vert\,\bar{1}\bar{1}2)$	$-\frac{1}{15}\sqrt{6}$	
		$(02\,\vert\,\bar{2}\bar{1}2)$	$\frac{1}{60}\sqrt{6}$	
		$(02\,\vert\,\bar{1}02)$	$\frac{3}{10}$	
		$(12\,\vert\,\bar{2}02)$	$-\frac{1}{60}\sqrt{6}$	
		$(12\,\vert\,\bar{1}01)$	$-\frac{2}{15}\sqrt{6}$	
^4D	$(2\,\vert\,\bar{2}\bar{1}\bar{1}2)$	$(0\,\vert\,\bar{1}012)$	$\frac{2}{7}$	FL
		$(1\,\vert\,\bar{2}012)$	$-\frac{1}{7}\sqrt{6}$	
		$(2\,\vert\,\bar{2}\bar{1}\bar{1}2)$	$\frac{2}{7}$	
^2D	$(02\,\vert\,\bar{2}02)$	$(\bar{2}1\,\vert\,012)$	$-\frac{1}{21}\sqrt{6}$	FL
		$(\bar{2}2\,\vert\,\bar{1}\bar{1}2)$	$\frac{2}{21}$	
		$(\bar{1}0\,\vert\,012)$	$-\frac{2}{21}$	
		$(\bar{1}1\,\vert\,\bar{1}\bar{1}2)$	$\frac{4}{21}$	
		$(\bar{1}2\,\vert\,\bar{2}\bar{1}2)$	$-\frac{1}{7}$	
		$(\bar{1}2\,\vert\,\bar{1}02)$	$-\frac{1}{21}\sqrt{6}$	
		$(01\,\vert\,\bar{2}\bar{1}2)$	$-\frac{1}{21}\sqrt{6}$	
		$(01\,\vert\,\bar{1}02)$	$-\frac{2}{21}$	
		$(02\,\vert\,\bar{2}02)$	$\frac{5}{21}$	
		$(12\,\vert\,\bar{2}\bar{1}\bar{1}2)$	$-\frac{5}{21}$	
^2D	$(\bar{1}2\,\vert\,\bar{1}02)$	$(\bar{2}1\,\vert\,012)$	$\frac{1}{7}$	FL
		$(\bar{2}2\,\vert\,\bar{1}\bar{1}2)$	$-\frac{1}{21}\sqrt{6}$	
		$(\bar{1}1\,\vert\,\bar{1}\bar{1}2)$	$-\frac{1}{21}\sqrt{6}$	
		$(\bar{1}2\,\vert\,\bar{2}\bar{1}\bar{1}2)$	$-\frac{1}{21}\sqrt{6}$	
		$(\bar{1}2\,\vert\,\bar{1}02)$	$\frac{2}{7}$	
		$(01\,\vert\,\bar{2}\bar{1}\bar{1}2)$	$\frac{2}{7}$	
		$(01\,\vert\,\bar{1}02)$	$-\frac{1}{21}\sqrt{6}$	
^2D	$(\bar{1}2\,\vert\,\bar{1}02)$	$(02\,\vert\,\bar{2}02)$	$-\frac{1}{21}\sqrt{6}$	
		$(02\,\vert\,\bar{1}01)$	$-\frac{1}{21}\sqrt{6}$	
		$(12\,\vert\,\bar{2}01)$	$\frac{1}{7}$	
^2D	$(\bar{1}1\,\vert\,\bar{1}\bar{1}2)$	$(\bar{1}0\,\vert\,012)$	$-\frac{5}{21}$	FL
		$(\bar{1}1\,\vert\,\bar{1}\bar{1}2)$	$\frac{5}{21}$	
		$(\bar{1}2\,\vert\,\bar{2}\bar{1}\bar{1}2)$	$-\frac{2}{21}$	
		$(\bar{1}2\,\vert\,\bar{1}02)$	$-\frac{1}{21}\sqrt{6}$	
		$(01\,\vert\,\bar{2}\bar{1}\bar{1}2)$	$-\frac{1}{21}\sqrt{6}$	
		$(01\,\vert\,\bar{1}02)$	$-\frac{1}{7}$	
		$(02\,\vert\,\bar{2}02)$	$\frac{4}{21}$	
		$(02\,\vert\,\bar{1}01)$	$\frac{2}{21}$	
		$(12\,\vert\,\bar{2}\bar{1}\bar{1}2)$	$-\frac{2}{21}$	
		$(12\,\vert\,\bar{2}01)$	$\frac{1}{21}\sqrt{6}$	
^4P	$(\bar{1}\,\vert\,\bar{1}012)$	$(\bar{1}\,\vert\,\bar{1}012)$	$-\frac{1}{5}$	FL
		$(0\,\vert\,\bar{2}012)$	$\frac{1}{10}\sqrt{6}$	
		$(1\,\vert\,\bar{2}\bar{1}\bar{1}2)$	$-\frac{1}{10}\sqrt{6}$	
		$(2\,\vert\,\bar{2}\bar{1}02)$	$\frac{1}{5}$	
^2P	$(\bar{2}2\,\vert\,\bar{2}\bar{1}2)$	$(\bar{2}0\,\vert\,012)$	$\frac{3}{70}$	FL
		$(\bar{2}1\,\vert\,\bar{1}\bar{1}2)$	$-\frac{3}{70}$	
		$(\bar{2}2\,\vert\,\bar{2}\bar{1}2)$	$\frac{9}{35}$	
		$(\bar{2}2\,\vert\,\bar{1}02)$	$-\frac{1}{14}\sqrt{6}$	
		$(\bar{1}0\,\vert\,\bar{1}\bar{1}2)$	$-\frac{1}{70}\sqrt{6}$	
		$(\bar{1}1\,\vert\,\bar{2}\bar{1}2)$	$-\frac{3}{35}$	
		$(\bar{1}1\,\vert\,\bar{1}02)$	$\frac{2}{35}\sqrt{6}$	
		$(\bar{1}2\,\vert\,\bar{2}02)$	$-\frac{2}{35}\sqrt{6}$	
		$(\bar{1}2\,\vert\,\bar{1}01)$	$\frac{1}{14}\sqrt{6}$	
		$(01\,\vert\,\bar{2}02)$	$\frac{3}{35}$	
		$(01\,\vert\,\bar{1}01)$	$-\frac{9}{35}$	
		$(02\,\vert\,\bar{2}\bar{1}2)$	$\frac{1}{70}\sqrt{6}$	
		$(02\,\vert\,\bar{2}01)$	$\frac{3}{70}$	
		$(12\,\vert\,\bar{2}\bar{1}1)$	$-\frac{3}{70}$	
^6S	$(\bar{2}\bar{1}012)$	$(\bar{2}\bar{1}012)$	1	FL
^2S	$(\bar{2}2\,\vert\,\bar{2}02)$			Ov.

TABLE I (*continued*).

3 f-electrons

^{2}L	$(3\|23)$	$(3\|23)$	1
^{2}K	$(3\|13)$	$(2\|23)$	$-\frac{1}{8}\sqrt{15}$
		$(3\|13)$	$\frac{3}{8}$
^{4}I	(123)	(123)	1
^{2}I	$(1\|23)$	$(1\|23)$	$\frac{3}{7}$
		$(2\|13)$	$-\frac{3}{7}$
		$(3\|03)$	$\frac{1}{7}\sqrt{2}$
		$(3\|12)$	$\frac{1}{7}$
^{2}H	$(3\|\bar{1}3)$	$(0\|23)$	$-\frac{5}{91}\sqrt{2}$
		$(1\|13)$	$\frac{2}{91}\sqrt{15}$
		$(2\|03)$	$-\frac{37}{182}\sqrt{2}$
		$(2\|12)$	$\frac{27}{91}$
		$(3\|\bar{1}3)$	$\frac{32}{91}$
		$(3\|02)$	$-\frac{27}{182}\sqrt{2}$
^{2}H	$(0\|23)$	$(0\|23)$	$\frac{30}{91}$
		$(1\|13)$	$-\frac{6}{91}\sqrt{30}$
		$(2\|03)$	$\frac{20}{91}$
		$(2\|12)$	$\frac{10}{91}\sqrt{2}$
		$(3\|\bar{1}3)$	$-\frac{5}{91}\sqrt{2}$
		$(3\|02)$	$-\frac{10}{91}$
^{4}G	$(\bar{1}23)$	$(\bar{1}23)$	$\frac{5}{11}$
		(013)	$-\frac{1}{11}\sqrt{30}$
^{2}G	$(\bar{1}\|23)$	$(\bar{1}\|23)$	$\frac{42}{143}$
		$(0\|13)$	$-\frac{42}{715}\sqrt{30}$
		$(1\|03)$	$\frac{28}{715}\sqrt{30}$
		$(1\|12)$	$\frac{28}{715}\sqrt{15}$
		$(2\|\bar{1}3)$	$-\frac{14}{143}$
		$(2\|02)$	$-\frac{14}{143}\sqrt{3}$
		$(3\|\bar{2}3)$	$\frac{1}{143}\sqrt{15}$
		$(3\|\bar{1}2)$	$\frac{9}{143}$
		$(3\|01)$	$\frac{1}{143}\sqrt{30}$
^{2}G	$(3\|\bar{2}3)$	$(\bar{1}\|23)$	$\frac{1}{143}\sqrt{15}$
		$(0\|13)$	$-\frac{3}{143}\sqrt{2}$
		$(1\|03)$	$\frac{15}{143}\sqrt{2}$
		$(1\|12)$	$-\frac{24}{143}$
		$(2\|\bar{1}3)$	$-\frac{9}{143}\sqrt{15}$
		$(2\|02)$	$\frac{4}{143}\sqrt{30}$
		$(3\|\bar{2}3)$	$\frac{57}{143}$
		$(3\|\bar{1}2)$	$-\frac{10}{143}\sqrt{15}$
		$(3\|01)$	$\frac{18}{143}\sqrt{2}$
^{4}F	$(\bar{2}23)$	$(\bar{2}23)$	$\frac{1}{4}$
		$(\bar{1}13)$	$-\frac{1}{4}$
		(012)	$\frac{1}{4}\sqrt{2}$
^{2}F	$(3\|\bar{3}3)$	$(\bar{2}\|23)$	$-\frac{1}{132}$
		$(\bar{1}\|13)$	$\frac{1}{132}$
		$(0\|03)$	$-\frac{2}{33}$
		$(0\|12)$	$\frac{7}{132}\sqrt{2}$
		$(1\|\bar{1}3)$	$\frac{5}{44}$
		$(1\|02)$	$-\frac{7}{132}\sqrt{2}$
		$(2\|\bar{2}3)$	$\frac{3}{11}$
		$(2\|\bar{1}2)$	$\frac{7}{132}\sqrt{15}$
		$(2\|01)$	$-\frac{7}{66}\sqrt{2}$
		$(3\|\bar{3}3)$	$\frac{71}{132}$
		$(3\|\bar{2}2)$	$-\frac{35}{132}$
		$(3\|\bar{1}1)$	$\frac{7}{66}$
^{2}F	$(\bar{2}\|23)$	$(\bar{2}\|23)$	$\frac{7}{22}$
		$(\bar{1}\|13)$	$-\frac{7}{22}$
		$(0\|03)$	$\frac{7}{33}$
		$(0\|12)$	$\frac{7}{66}\sqrt{2}$
		$(1\|\bar{1}3)$	$-\frac{7}{66}$
		$(1\|02)$	$-\frac{7}{66}\sqrt{2}$
		$(2\|\bar{2}3)$	$\frac{5}{132}$
		$(2\|\bar{1}2)$	$\frac{1}{44}\sqrt{15}$
		$(2\|01)$	$\frac{5}{132}\sqrt{2}$
		$(3\|\bar{3}3)$	$-\frac{1}{132}$
		$(3\|\bar{2}2)$	$-\frac{1}{33}$
		$(3\|\bar{1}1)$	$-\frac{5}{132}$

TABLE I (*continued*).

		3 *f*-electrons	
^4D	$(\bar{3}23)$	$(\bar{3}23)$	$\frac{10}{21}$
		$(\bar{2}13)$	$-\frac{2}{21}\sqrt{15}$
		$(\bar{1}03)$	$\frac{5}{21}\sqrt{2}$
^2D	$(\bar{3}\|23)$	$(\bar{3}\|23)$	$\frac{5}{11}$
		$(\bar{2}\|13)$	$-\frac{1}{11}\sqrt{15}$
		$(\bar{1}\|03)$	$\frac{5}{33}\sqrt{2}$
		$(\bar{1}\|12)$	$\frac{5}{33}$
		$(0\|\bar{1}3)$	$-\frac{5}{66}\sqrt{2}$
		$(0\|02)$	$-\frac{5}{33}$
		$(1\|\bar{2}3)$	$\frac{5}{462}\sqrt{15}$
		$(1\|\bar{1}2)$	$\frac{15}{154}$
		$(1\|01)$	$\frac{5}{462}\sqrt{30}$
		$(2\|\bar{3}3)$	$-\frac{5}{462}$
		$(2\|\bar{2}2)$	$-\frac{10}{231}$
		$(2\|\bar{1}1)$	$-\frac{25}{462}$
		$(3\|\bar{3}2)$	$\frac{5}{462}$
		$(3\|\bar{2}1)$	$\frac{1}{154}\sqrt{15}$
		$(3\|\bar{1}0)$	$\frac{5}{462}\sqrt{2}$
^2D	$(2\|\bar{2}2)$		Ov.
^2P	$(\bar{2}\|03)$	$(\bar{2}\|03)$	$\frac{1}{28}$
		$(\bar{2}\|12)$	$-\frac{1}{28}\sqrt{2}$
		$(\bar{1}\|\bar{1}3)$	$-\frac{1}{84}\sqrt{30}$
		$(\bar{1}\|02)$	$\frac{1}{84}\sqrt{15}$
		$(0\|\bar{2}3)$	$\frac{1}{14}$
		$(0\|01)$	$-\frac{1}{28}\sqrt{2}$
		$(1\|\bar{3}3)$	$-\frac{1}{28}\sqrt{2}$
		$(1\|\bar{2}2)$	$-\frac{1}{28}\sqrt{2}$
		$(1\|\bar{1}1)$	$\frac{1}{28}\sqrt{2}$
		$(2\|\bar{3}2)$	$\frac{1}{84}\sqrt{30}$
		$(2\|\bar{1}0)$	$-\frac{1}{84}\sqrt{15}$
		$(3\|\bar{3}1)$	$-\frac{1}{28}\sqrt{2}$
		$(3\|\bar{2}0)$	$\frac{1}{28}$
^4S	$(\bar{3}03)$	$(\bar{3}03)$	$\frac{1}{7}$
		$(\bar{3}12)$	$-\frac{1}{7}\sqrt{2}$
^4S	$(\bar{3}03)$	$(\bar{2}\bar{1}3)$	$-\frac{1}{7}\sqrt{2}$
		$(\bar{2}02)$	$\frac{1}{7}$
		$(\bar{1}01)$	$-\frac{1}{7}$
		4 *f*-electrons	
^1N	$(23\|23)$	$(23\|23)$	1
^3M	$(3\|123)$	$(3\|123)$	1
^3L	$(3\|023)$	$(2\|123)$	$-\frac{1}{3}\sqrt{2}$
		$(3\|023)$	$\frac{1}{3}$
^1L	$(03\|23)$	$(03\|23)$	$\frac{29}{57}$
		$(12\|23)$	$-\frac{14}{57}\sqrt{2}$
		$(13\|13)$	$-\frac{1}{19}\sqrt{30}$
		$(23\|03)$	$\frac{10}{57}$
		$(23\|12)$	$\frac{5}{57}\sqrt{2}$
^1L	$(12\|23)$	$(03\|23)$	$-\frac{14}{57}\sqrt{2}$
		$(12\|23)$	$\frac{43}{57}$
		$(13\|13)$	$-\frac{1}{19}\sqrt{15}$
		$(23\|03)$	$\frac{5}{57}\sqrt{2}$
		$(23\|12)$	$\frac{5}{57}$
^3K	$(3\|\bar{1}23)$	$(1\|123)$	$\frac{3}{68}\sqrt{15}$
		$(2\|023)$	$-\frac{15}{136}\sqrt{2}$
		$(3\|\bar{1}23)$	$\frac{35}{68}$
		$(3\|013)$	$-\frac{11}{136}\sqrt{30}$
^3K	$(3\|013)$	$(1\|123)$	$\frac{15}{136}\sqrt{2}$
		$(2\|023)$	$-\frac{5}{136}\sqrt{15}$
		$(3\|\bar{1}23)$	$-\frac{11}{136}\sqrt{30}$
		$(3\|013)$	$\frac{81}{136}$
^1K	$(\bar{1}3\|23)$	$(\bar{1}3\|23)$	$\frac{95}{204}$
		$(02\|23)$	$-\frac{65}{408}\sqrt{2}$
		$(03\|13)$	$-\frac{25}{408}\sqrt{30}$
		$(12\|13)$	$\frac{13}{204}\sqrt{15}$

TABLE I (*continued*).

4 *f*-electrons

^{1}K	$(\bar{1}3\,\vert\,23)$	$(13\,\vert\,03)$	$\frac{1}{51}\sqrt{30}$
		$(13\,\vert\,12)$	$\frac{1}{51}\sqrt{15}$
		$(23\,\vert\,\bar{1}3)$	$-\frac{5}{102}$
		$(23\,\vert\,02)$	$-\frac{5}{102}\sqrt{2}$
^{5}I	(0123)	(0123)	1
^{3}I	$(3\,\vert\,\bar{1}13)$	$(0\,\vert\,123)$	$-\frac{1}{14}\sqrt{2}$
		$(1\,\vert\,023)$	$\frac{1}{14}\sqrt{2}$
		$(2\,\vert\,013)$	$-\frac{1}{14}\sqrt{2}$
		$(3\,\vert\,\bar{2}23)$	$-\frac{2}{7}$
		$(3\,\vert\,\bar{1}13)$	$\frac{2}{7}$
		$(3\,\vert\,012)$	$-\frac{3}{14}\sqrt{2}$
^{3}I	$(3\,\vert\,\bar{2}23)$	$(0\,\vert\,123)$	$-\frac{1}{28}\sqrt{2}$
		$(1\,\vert\,023)$	$\frac{1}{28}\sqrt{2}$
		$(2\,\vert\,\bar{1}23)$	$-\frac{1}{14}\sqrt{15}$
		$(2\,\vert\,013)$	$\frac{5}{28}\sqrt{2}$
		$(3\,\vert\,\bar{2}23)$	$\frac{1}{2}$
		$(3\,\vert\,\bar{1}13)$	$-\frac{2}{7}$
		$(3\,\vert\,012)$	$\frac{3}{28}\sqrt{2}$
^{1}I	$(\bar{1}3\,\vert\,13)$	$(\bar{2}3\,\vert\,23)$	$-\frac{75}{238}$
		$(\bar{1}2\,\vert\,23)$	$-\frac{3}{170}\sqrt{15}$
		$(\bar{1}3\,\vert\,13)$	$\frac{219}{595}$
		$(01\,\vert\,23)$	$\frac{27}{238}\sqrt{2}$
		$(02\,\vert\,13)$	$-\frac{36}{595}\sqrt{2}$
		$(03\,\vert\,03)$	$-\frac{122}{595}$
		$(03\,\vert\,12)$	$-\frac{61}{595}\sqrt{2}$
		$(12\,\vert\,03)$	$\frac{24}{595}\sqrt{2}$
		$(12\,\vert\,12)$	$\frac{24}{595}$
		$(13\,\vert\,\bar{1}3)$	$\frac{7}{85}$
		$(13\,\vert\,02)$	$\frac{7}{85}\sqrt{2}$
		$(23\,\vert\,\bar{2}3)$	$-\frac{1}{34}$
		$(23\,\vert\,\bar{1}2)$	$-\frac{3}{170}\sqrt{15}$
		$(23\,\vert\,01)$	$-\frac{1}{34}\sqrt{2}$
^{1}I	$(\bar{2}3\,\vert\,23)$	$(\bar{2}3\,\vert\,23)$	$\frac{243}{476}$
^{1}I	$(\bar{2}3\,\vert\,23)$	$(\bar{1}2\,\vert\,23)$	$-\frac{31}{476}\sqrt{15}$
		$(\bar{1}3\,\vert\,13)$	$-\frac{75}{238}$
		$(01\,\vert\,23)$	$\frac{39}{476}\sqrt{2}$
		$(02\,\vert\,13)$	$\frac{27}{238}\sqrt{2}$
		$(03\,\vert\,03)$	$\frac{16}{119}$
		$(03\,\vert\,12)$	$\frac{8}{119}\sqrt{2}$
		$(12\,\vert\,03)$	$-\frac{9}{119}\sqrt{2}$
		$(12\,\vert\,12)$	$-\frac{9}{119}$
		$(13\,\vert\,\bar{1}3)$	$-\frac{1}{34}$
		$(13\,\vert\,02)$	$-\frac{1}{34}\sqrt{2}$
		$(23\,\vert\,\bar{2}3)$	$\frac{5}{476}$
		$(23\,\vert\,\bar{1}2)$	$\frac{3}{476}\sqrt{15}$
		$(23\,\vert\,01)$	$\frac{5}{476}\sqrt{2}$
^{1}I	$(23\,\vert\,\bar{2}3)$	$(\bar{2}3\,\vert\,23)$	$\frac{5}{476}$
		$(\bar{1}2\,\vert\,23)$	$\frac{3}{476}\sqrt{15}$
		$(\bar{1}3\,\vert\,13)$	$-\frac{1}{34}$
		$(01\,\vert\,23)$	$\frac{5}{476}\sqrt{2}$
		$(02\,\vert\,13)$	$-\frac{1}{34}\sqrt{2}$
		$(03\,\vert\,03)$	$\frac{5}{476}$
		$(03\,\vert\,12)$	$-\frac{9}{119}\sqrt{2}$
		$(12\,\vert\,03)$	$\frac{8}{119}\sqrt{2}$
		$(12\,\vert\,12)$	$-\frac{9}{119}$
		$(13\,\vert\,\bar{1}3)$	$-\frac{75}{238}$
		$(13\,\vert\,02)$	$\frac{27}{238}\sqrt{2}$
		$(23\,\vert\,\bar{2}3)$	$\frac{243}{476}$
		$(23\,\vert\,\bar{1}2)$	$-\frac{31}{476}\sqrt{15}$
		$(23\,\vert\,01)$	$\frac{39}{476}\sqrt{2}$
^{3}H	$(3\,\vert\,\bar{2}23)$	$(\bar{1}\,\vert\,123)$	$\frac{1}{91}$
		$(0\,\vert\,023)$	$-\frac{1}{91}$
		$(1\,\vert\,\bar{1}23)$	$\frac{17}{182}$
		$(1\,\vert\,013)$	$-\frac{3}{182}\sqrt{30}$
		$(2\,\vert\,\bar{2}23)$	$-\frac{43}{182}$
		$(2\,\vert\,\bar{1}13)$	$\frac{1}{7}$
		$(2\,\vert\,012)$	$-\frac{11}{182}\sqrt{2}$
		$(3\,\vert\,\bar{3}23)$	$\frac{59}{91}$
		$(3\,\vert\,\bar{2}13)$	$-\frac{15}{182}\sqrt{15}$
		$(3\,\vert\,\bar{1}03)$	$\frac{19}{182}\sqrt{2}$
		$(3\,\vert\,\bar{1}12)$	$\frac{11}{182}$

TABLE I (*continued*).

	4 *f*-electrons		
^3H	$(\bar{1}\|123)$	$(\bar{1}\|123)$	$\frac{33}{91}$
		$(0\|023)$	$-\frac{33}{91}$
		$(1\|\bar{1}23)$	$\frac{18}{91}$
		$(1\|013)$	$\frac{3}{91}\sqrt{30}$
		$(2\|\bar{2}23)$	$-\frac{6}{91}$
		$(2\|\bar{1}13)$	$-\frac{12}{91}$
		$(2\|012)$	$-\frac{3}{91}\sqrt{2}$
		$(3\|\bar{3}23)$	$\frac{1}{91}$
		$(3\|\bar{2}13)$	$\frac{1}{91}\sqrt{15}$
		$(3\|\bar{1}03)$	$\frac{2}{91}\sqrt{2}$
		$(3\|\bar{1}12)$	$\frac{3}{91}$
^3H	$(2\|012)$	$(\bar{1}\|123)$	$-\frac{3}{91}\sqrt{2}$
		$(0\|023)$	$\frac{3}{91}\sqrt{2}$
		$(1\|\bar{1}23)$	$\frac{19}{182}\sqrt{2}$
		$(1\|013)$	$-\frac{5}{91}\sqrt{15}$
		$(2\|\bar{2}23)$	$-\frac{2}{91}\sqrt{2}$
		$(2\|\bar{1}13)$	$-\frac{15}{182}\sqrt{2}$
		$(2\|012)$	$\frac{40}{91}$
^3H	$(2\|012)$	$(3\|\bar{3}23)$	$-\frac{11}{182}\sqrt{2}$
		$(3\|\bar{2}13)$	$\frac{3}{182}\sqrt{30}$
		$(3\|\bar{1}03)$	$\frac{20}{91}$
		$(3\|\bar{1}12)$	$-\frac{20}{91}\sqrt{2}$
^3H	$(3\|\bar{1}03)$	$(\bar{1}\|123)$	$\frac{2}{91}\sqrt{2}$
		$(0\|023)$	$-\frac{2}{91}\sqrt{2}$
		$(1\|\bar{1}23)$	$-\frac{1}{182}\sqrt{2}$
		$(1\|013)$	$\frac{1}{91}\sqrt{15}$
		$(2\|\bar{2}23)$	$\frac{1}{7}\sqrt{2}$
		$(2\|\bar{1}13)$	$-\frac{25}{182}\sqrt{2}$
		$(2\|012)$	$\frac{20}{91}$
		$(3\|\bar{3}23)$	$\frac{19}{182}\sqrt{2}$
		$(3\|\bar{2}13)$	$-\frac{9}{182}\sqrt{30}$
		$(3\|\bar{1}03)$	$\frac{45}{91}$
		$(3\|\bar{1}12)$	$-\frac{10}{91}\sqrt{2}$
^1H	$(\bar{3}3\|23)$		Ov.
^1H	$(23\|\bar{3}3)$		Ov.

instead of two; and the same holds for all multiplet terms. The reason for doing so is that it is much easier to get the lacking functions by spin step-up or step-down operators, after getting a spin eigenfunction. Shortly said, we contented ourselves with giving the necessary background to complete the calculation by spin projection operators alone.

We would like to conclude with some remarks about the possibility and expediency of using electronic computers for such kind of computations. The time needed for programming, testing, etc., was somewhat less than two months, while the computer worked out the reported results in a few hours. There is nothing to say about the possibility of carrying out the computation; but what about its expediency? Though it is rather difficult to make precise estimates on this subject, we think that a hand computation would have required a time about equal to that spent by us in total. At this point it must be noted, however, that our experiment was made in rather unfavourable conditions: a bigger machine would have rid us of many troubles, enabling us to save much time; at the same time, a bigger machine would have made a better use of the program, since it would have succeeded in calculating much more interesting cases than our small computer could do.

When all such circumstances are taken into account, the balance is clearly in favour of the electronic computer. Moreover, one should not overtake that hand computing is much more cumbersome and much less interesting a job than programming. The latter has then the further advantage that once made it applies to as many cases as we want, while hand computing must be made every time anew.

Much work is still to be done on this subject; but we hope we have succeeded in giving an example of what an electronic computer can do for a physicist, if he only asks for it.

RIASSUNTO

Si studia l'applicazione di una calcolatrice elettronica numerica al calcolo delle autofunzioni esatte del momento angolare orbitale totale per sistemi di più elettroni. Vengono discussi alcuni aspetti particolari che il problema presenta in confronto alle applicazioni usuali delle calcolatrici elettroniche. I calcoli sono stati condotti col metodo dell'operatore di proiezione; si danno risultati per 3 e 4 elettroni *d* e *f*, e per 5 elettroni *d*. Poichè la calcolatrice usata era relativamente piccola, i risultati non sono completi; la via seguita sembra però promettente in vista di future estensioni del calcolo con una macchina più grande.

IL NUOVO CIMENTO Vol. XIV, N. 1 1° Ottobre 1959

On the Determination of the Mean Life of μ^- Mesons in Ca and Pb.

A. Alberigi Quaranta (*), U. Dore and F. Pieraccini

Istituto di Fisica dell'Università - Roma
Istituto Nazionale di Fisica Nucleare - Sezione di Roma

(ricevuto il 4 Marzo 1959)

Summary. — The results of a series of measurements for the determination of the apparent mean life of μ^--mesons in Ca and Pb, carried out by means of a recently described apparatus are reported. The values obtained are $\tau = (35.7 \pm 3) \cdot 10^{-8}$ s in Ca and $\tau = (7.3 \pm 0.6) \cdot 10^{-8}$ s in Pb. The results are in agreement with those obtained by other investigators and with theoretical estimations.

1. – Introduction.

In a previous paper [1] experimental methods and results connected with the behaviour of μ^- mesons brought to rest in the proximity of atomic nuclei were described in detail and extensively discussed. Moreover, some hints were given about the information which these investigations can provide concerning the nature of the nuclei themselves.

Further interesting experimental results, which appeared [2-4] after the publication of our paper [1], considerably increased our knowledge on the subject. In particular, availability of high intensity meson beams produced by syncro-

(*) Present address: Sezione Acceleratore dell'I.N.F.N., Frascati, Roma.

[1] A. Alberigi Quaranta, D. Broadbent and F. Pieraccini: *Nuovo Cimento*, **6**, 1084 (1957).

[2] J. C. Sens, R. A. Swanson, V. L. Telegdi and D. D. Yovanovitch: *Phys. Rev.*, **107**, 1464 (1957).

[3] A. Astbury, M. A. R. Kemp, N. H. Lipman, H. Muirhead, R. G. P. Voss, C. C. Zuangger and A. Kirk: *Proc. Phys. Soc.*, **72**, 494 (1958).

[4] A. M. Hillas, W. B. Gilboy and R. M. Tennent: *Phil. Mag.*, **3**, 109 (1958).

cyclotrons ([2,3]) made it possible to attain a much greater precision in the determination of the apparent mean lives of μ^- mesons in the presence of nuclei.

Therefore we thought it worth-while to determine the apparent mean life τ of μ^- mesons coming to rest in Pb and Ca, because only in one case the values of τ in these two elements were determined with the same apparatus.

In fact, the value of the ratio between the apparent mean lives as determined by us, is affected by systematic errors (*e.g.* calibration errors) to a much minor degree than the value of this ratio calculated from two separate determinations of these mean lives carried out with different experimental devices. On the other hand, several theoretical papers on the subject ([5-10]) allow calculations of the ratio of the probabilities of μ^- meson absorptions by the nuclei of these two elements to be made. It may be of some interest, therefore, to compare our results with the theoretical estimations put forward in the above papers.

2. – Experimental apparatus.

The experimental apparatus employed in the present investigation has been previously described in detail ([1]).

For the determination of the apparent mean life of μ^- mesons in Ca and Pb, we chose the two different values of the explored interval of meson disappearance times which were most suited ([11]) for the two different values of the apparent mean life in Ca and Pb that we wanted to determine. In the case of Fe, in fact, meson disappearance times were observed in the range from $5 \cdot 10^{-8}$ to $6 \cdot 10^{-7}$ s ([1]), while for the determination of τ in Pb and in Ca we studied disappearance times ranging from $2 \cdot 10^{-8}$ to $26 \cdot 10^{-8}$ s and from $10 \cdot 10^{-8}$ to $106 \cdot 10^{-8}$ s respectively.

In the case of Pb we were able to determine each of the investigated disappearance times with an accuracy of less than $\pm 0.5 \cdot 10^{-8}$ s, while for Ca the accuracy was about $\pm 1 \cdot 10^{-8}$ s.

In each group of measurements, the uncertainty in the time determinations does not affect ([12]) the accuracy of the measurement.

([5]) W. Wheeler: *Rev. Mod. Phys.*, **21**, 133 (1949).
([6]) J. Tiomno and J. A. Wheeler: *Rev. Mod. Phys.*, **21**, 154 (1949).
([7]) J. M. Kennedy: *Phys. Rev.*, **87**, 953 (1952).
([8]) T. Eguchi and M. Ohta: *Nuovo Cimento*, **10**, 1415 (1953).
([9]) H. Primakoff: *Proc. of the Fifth Annual Rochester Conference* (1955).
([10]) H. A. Tolhoek and J. R. Luyten: *Nucl. Phys.*, **3**, 679 (1957).
([11]) R. Peierls: *Proc. Roy. Soc.*, A **149**, 467 (1935).
([12]) N. Nereson and B. Rossi: *Phys. Rev.*, **62**, 417 (1942).

Absorbers of a thickness more or less equivalent to the mean range of decay electrons were used. Mainly because of the different density values of the two elements investigated (density of Ca = 1.6 g/cm^3; density of Pb = 11.3 g/cm^3) the thickness of the absorbers is much greater with Ca than with Pb. Because of this the lower part of the apparatus must have quite a different shape for the two elements. For Pb the device is much more compact than for Ca; consequently we could markedly increase the solid angle for the acceptance of incident mesons and for the detection of the products of μ^- mesons disappearance in the absorbers.

3. – Experimental results.

Measurements for determining the apparent mean life of μ^- mesons in Ca and Pb were carried out by means of the above apparatus. For Ca four pairs of blocks of metallic Ca (*), placed as indicated by A in Fig. 1 of the previous paper (1), were used, so as to obtain four absorbers ($50 \times 18 \times 10$) cm in size.

In order to guarantee the preservation of Ca and to prevent its oxidation, the blocks were kept in thin plexiglass boxes slightly larger and covered with mineral oil.

We used four plates of ($50 \times 20 \times 1{,}5$) cm each, as Pb adsorbers (Pb content 99%).

It should be pointed out that, according to our method (1), we obtained the value of the ratio K (number of events due to capture of the μ^- mesons by the nuclei/number of events due to decay of μ^- mesons in the absorbers).

In Ca the ratio was $K = 1.6$.

In Pb the ratio was $K = 8$.

This shows that the determination of the apparent mean life calculated from the distribution of the disappearance times in Ca is affected, approximately to the same extent, by events related both to the capture and to the disintegration of μ^- mesons.

In the case of Pb most of the measured events are due to capture.

The distribution of the disappearance times due to μ^+ mesons decay in Ca and Pb is in good agreement with the value $\tau = 2.22$ μs for the mean life of μ^+ mesons.

(*) Chemical analysis of a sample of the block employed gave the following results (supplied by Degussa - Wolfgang Hanan, Germany).

Ca	96.2%
Na	2.5%
Cl	1 %
K	0.2%
Other elements	0.1%

The experimental distribution of the disappearance times of μ^- mesons in both elements (Pb and Ca) presents too high a percentage of events at time intervals longer than the apparent mean life evaluated from the experimental distribution obtained at shorter disappearance times.

With an obvious iteration, the number of background events ([1]) was calculated and subtracted from the distribution of the disappearance times determined experimentally. The time distribution of background events was assumed to be the same as the one obtained with μ^+ mesons ($\tau = 2.22$ μs).

The following experimental data for the apparent mean life of μ^- mesons in Ca and Pb were calculated from the time distributions corrected as described above:

$$\text{Ca} \qquad \tau = (35.7 \pm 3.0) \cdot 10^{-8} \text{ s} ,$$

$$\text{Pb} \qquad \tau = (\ 7.3 \pm 0.6) \cdot 10^{-8} \text{ s} .$$

Assuming that the mean decay life of μ^- mesons is 2.22 μs, the following values for the probability of capture by nuclei p_c are obtained from the values of:

$$\text{Ca} \qquad p_c = (\ 23.4 \pm \ 2.2) \cdot 10^5 \text{ s}^{-1} ,$$

$$\text{Pb} \qquad p_c = (132 \quad \pm 11 \ ) \cdot 10^5 \text{ s}^{-1} .$$

The ratio between the two values of the probability capture obtained by the experiments is

$$\frac{p_c \text{ (Ca)}}{p_c \text{ (Pb)}} = 5.7 \pm 0.7 .$$

4. – Conclusions.

Table I gives the values of the apparent mean lives of μ^- mesons (divided by 10^{-8}) and of the capture probabilities p_c (divided by 10^5 s^{-1}), calculated, assuming $\tau = 2.22$ μs, from the values of τ provided by our measurements.

The data obtained by other authors and the theoretical values calculated by PRIMAKOFF are reported, together with our experimental results, in Table I.

As shown in the Table, there is good agreement among the data for τ and p_c found by different authors in each element and with the theoretical values calculated by PRIMAKOFF.

It is worth-while to compare the ratios between the probabilities of capture, determined by us in Pb, Ca and Fe, with some theoretical estimations. Among the data reported in the literature, we shall consider only the pairs of p_c values

TABLE I.

Authors	Elements	Z	τ	p_c
LEDERMAN [13]	Ca	20	—	24.6 ± 4.0
SENS [2]			33.8 ± 1.3	25.1 ± 0.9
Present work			35.7 ± 3.0	23.4 ± 2.2
ASTBURY [3]			—	26.8 ± 0.4
Theoretical value (PRIMAKOFF)			—	27.8
BENADE [14]	Fe	26	21.0 ± 6.0	43 ± 14
KEUFFEL [15]			16.3 ± 2.7	57 ± 10
LEDERMAN [13]			—	44.3 ± 5.0
SENS [2]			20.2 ± 0.7	44.9 ± 1.5
TENNENT [4]			20.4 ± 1.5	44.5 ± 3.0
TENNENT [16]			19.2 ± 1.2	44.3 ± 3.0
ALBERIGI QUARANTA *et al.* [1]			16 ± 1	58 ± 4
Theoretical value (PRIMAKOFF)			—	45
KEUFFEL [15]	Pb	82	7.6 ± 0.4	127 ± 7
MEYER [17]			7.4 ± 0.3	130 ± 6
SENS [2]			7.7 ± 0.4	125 ± 7
Present work			7.3 ± 0.6	132 ± 11
Theoretical value (PRIMAKOFF)			—	146

obtained with the same experimental devices (and consequently affected in a minor degree by systematic errors).

$$\frac{p_c\,(\mathrm{Ca})}{p_c\,(\mathrm{Pb})} = \begin{matrix}\text{SENS [2]} \\ 5 \pm 0.3\end{matrix} \qquad \begin{matrix}\text{Present work} \\ 5.7 \pm 0.7\,.\end{matrix}$$

The value of this ratio (as obtained by us) is in very good agreement with that calculated by KENNEDY [7]:

$$\frac{p_c\,(\mathrm{Ca})}{p_c\,(\mathrm{Pb})} = 5.9\,.$$

Kennedy's estimations were made with no specific assumption as to the type of interaction occurring in the process of meson absorption.

---

[13] L. LEDERMAN and M. WEINRICH: *CERN Symposium* (June 1956).

[14] A. H. BENADE: *Phys. Rev.*, **91**, 971 (1953).

[15] J. W. KEUFFEL, F. B. HARRISON, T. M. K. GODFREY and G. T. REYNOLDS: *Phys. Rev.*, **87**, 942 (1952).

[16] R. M. TENNENT: private communication.

[17] A. J. MEYER: *Thesis* (Princeton University, 1954).

A paper by TOLHOEK and LUYTEN [10] allows a comparison to be made between our experimental results and the ratio between p_c values calculated assuming different types of interactions, in several elements.

The value of the ratio

$$\frac{p_c\ (\mathrm{Fe})}{p_c\ (\mathrm{Ca})} = 2.5 \pm 0.3\,,$$

obtained by us experimentally is in better agreement with the one obtained by Th and Lu [10] assuming a *TA* interaction (1.7) than the one obtained on the assumption of on *SV* interaction (1.08).

Moreover, the value of the coupling constant g was obtained, employing Kennedy's calculations, from the p_c values determined experimentally in Ca and Pb.

The result ($g = (2.9 \pm 0.2) \cdot 10^{-49}$ erg cm^3) agrees, allowance being made for experimental errors, with other values of the coupling constant [18].

* * *

The authors are indebted to Prof. E. AMALDI for constant encouragement.

---

[18] G. N. FOWLER and A. W. WOLFENDALE: *Progress in Elementary Particle and Cosmic Ray Physics* (Amsterdam, 1958), ch. III.

RIASSUNTO

Vengono riportati i risultati di una serie di misure, eseguite con un apparato sperimentale descritto in un precedente lavoro, intese a determinare la vita media apparente τ dei mesoni μ^- in Ca e Pb. I valori ottenuti sono per il calcio $\tau = (35.7 \pm 3.0) \cdot 10^{-8}$ s e per il Pb $\tau = (7.3 \pm 0.6) \cdot 10^{-8}$ s. Si confrontano tali risultati con quelli ottenuti da altri sperimentatori e con talune previsioni teoriche, riscontrando un accordo soddisfacente.

IL NUOVO CIMENTO Vol. XIV, N. 1 1° Ottobre 1959

Photoneutrons from Al.

G. Cortini, C. Milone, T. Papa and R. Rinzivillo

Istituto di Fisica dell'Università - Catania
Centro Siciliano di Fisica Nucleare - Catania

(ricevuto il 9 Marzo 1959)

Summary. — The energy spectra of photoneutrons emitted at 90° from Al under bremsstrahlung of 24 and 30 MeV maximum energy were investigated by means of the recoil protons in photoemulsions. The difference between the two spectra shows that above 24 MeV photon energy the neutrons are emitted mainly by a direct process. This process gives a relevant contribution (> 25%) to the photoneutron yield, at 30 MeV.

1. – Introduction.

The energy spectra of photoneutrons have been investigated for a number of elements by many authors: Cu [1]; Ag [2]; Bi [2]; Cr [3]; Ta [3]; Pb [4]; Au [5]; Ca [6]; Rh [6].

The spectra from heavy elements are in general agreement with the statistical evaporation theory with the exception of a high energy tail which generally accounts for about 10% of the total yield.

This tail is attributed to a « direct » process (Courant [7], Wilkinson [8],

---

[1] P. R. Byerly Jr. and W. S. Stephens: *Phys. Rev.*, **81**, 473 (1951).

[2] G. A. Price: *Phys. Rev.*, **93**, 1279 (1954).

[3] G. Cortini, C. Milone, A. Rubbino and F. Ferrero: *Nuovo Cimento*, **9**, 85 (1957).

[4] M. E. Toms and W. E. Stephens: *Phys. Rev.*, **108**, 77 (1957).

[5] S. Cavallaro, V. Emma, C. Milone and A. Rubbino: *Nuovo Cimento*, **9**, 736 (1957).

[6] A. Agodi, S. Cavallaro, G. Cortini, V. Emma, F. Ferrero, C. Milone, R. Rinzivillo, and A. Rubbino: *Congrès International de Phsique Nucléaire - Paris, Juillet 1958* (Paris, 1959), pag. 625.

[7] E. D. Courant: *Phys. Rev.*, **82**, 703 (1951).

[8] D. H. Wilkinson: *Physica*, **22**, 1039 (1956).

AGODI ([9])) which goes on without involving the intermediate step of a compound nucleus.

The investigation of photoneutrons from light elements is somewhat difficult because of the small (γ, n) cross-sections. However, we found it worth while to examine the behaviour of a selected number of light nuclei in order to extend the range of known photoneutron spectra.

In the present paper the Al spectrum is reported and compared with other known spectra. A short account of the present work was given at the S.I.F. Conference ([10]). Similar results about the Al neutron spectrum from 70 MeV bremsstrahlung were communicated by REVZEN and SARGENT at the Washington Photonuclear Conference ([11]).

2. – Experimental procedure.

The experimental procedure was described in a previous paper ([3]).

A 19 g aluminum target was irradiated with a collimated bremsstrahlung beam from the Brown-Boveri Betatron of Turin. Two exposures were made respectively at 24 and 30 MeV $E_{\gamma\max}$. The photoneutrons emitted at angles of $\theta \sim 90°$ with the photon beam were detected by means of the proton recoil tracks in Ilford 200 μm thick C-2 emulsions. The plates were scanned and screened as in the previous work ([3]). Exposure and scanning data are summarized in Table I.

TABLE I.

$E_{\gamma\max}$ (MeV)	24	30
($\varphi < 15°$)		
Number of tracks $E_n < 5$ MeV	323	570
Number of tracks $E_n \geqslant 5$ MeV	63	136
($15° < \varphi < 30°$)		
Number of tracks $E_n \geqslant 5$ MeV	86	163

([9]) A. AGODI: *Nuovo Cimento*, **8**, 516 (1958).

([10]) G. CORTINI, C. MILONE, T. PAPA and R. RINZIVILLO: *XLIV Congresso della Società Italiana di Fisica - Palermo, Novembre 1958.*

([11]) M. REVZEN and B. W. SARGENT: *Conference on Photonuclear Reactions - Washington, 1958* (private comunication).

3. – Results.

The experimental spectra obtained with the procedure described in [3] are shown in Fig. 1*a* and 1*b*. $F_{E_{\gamma max}}(E_n)$ gives the number of neutrons of energy E_n per unit energy interval, produced by γ-rays of maximum energy $E_{\gamma max}$.

Our apparatus is not suitable for accurate absolute measurements of the yields. Even for relative measurements the efficiency of scanning and other factors can give considerable trouble in the yield evaluations, while as far as the forms of the spectra are concerned the results obtained from different plates and different exposures always are in perfect agreement.

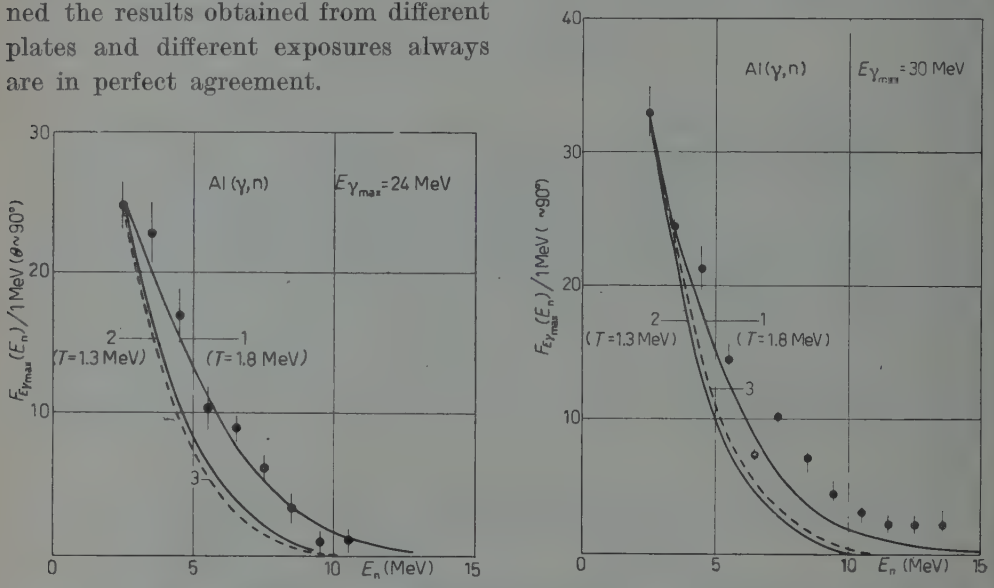

Fig. 1. – Energy spectrum of photoneutrons from Al at $E_{\gamma max}$ 24 MeV (Fig. 1*a*) and $E_{\gamma max} = 30$ MeV (Fig. 1*b*). For the curves see text.

Therefore our curves of Fig. 1, are normalized so as to give the correct relative yields, as obtained by FERRERO *et al.* [12].

The comparison of the two spectra of Fig. 1, shows that the photons in the energy interval (24 ÷ 30) MeV give mainly photoneutrons of rather high energy. In order to stress this point, we have plotted (Fig. 2) against the neutron energy, the values of the ratio $[F_{30}(E_n) - F_{24}(E_n)]/[F_{30}(E_n) + F_{24}(E_n)]$, *i.e.* of the relative increase in the neutron yield, from the 24 MeV to the 30 MeV irradiation. We get a definitely increasing curve.

---

[12] E. FERRERO, R. MALVANO and C. TRIBUNO: *Nuovo Cimento*, **6**, 385 (1957).

The Turin group [13] found that the integrated cross-section in the energy interval between 24 and 30 MeV for production of neutrons with energy > 5 MeV is 23% of the total (γ, n) cross-section integrated up to 24 MeV. From our experimental spectra taking into account the values of the Al(γ, n) threshold (~ 13 MeV) and the behaviour of the bremsstrahlung spectra, we obtain that the integrated cross-section in the energy interval $(24 \div 30)$ MeV, for production of neutrons with energy > 10 MeV amounts at least to about 10% of the total (γ, n) cross-section integrated up to 24 MeV.

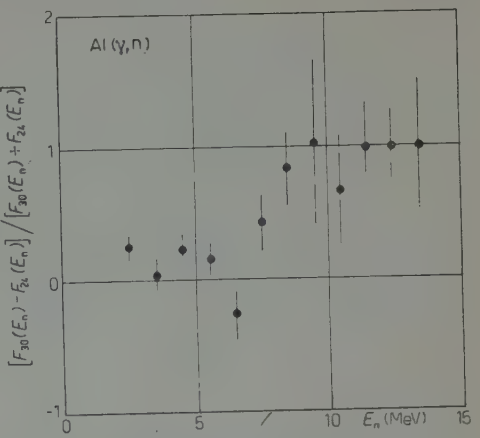

Fig. 2. – The ratio $(F_{30}(E_n) - F_{24}(E_n)) / (F_{30}(E_n) + F_{24}(E_n))$ plotted against E_n.

This result confirms and strengthens those previously quoted [10].

Some type of « direct » process is obviously suggested by these experimental data.

In the 30 MeV spectrum we remark a peak at a neutron energy of ~ 7 MeV. This peak forms a part of a more pronounced peak observed in a similar experiment, under 70 MeV irradiation, by REVZEN and SARGENT [11].

4. – Discussion.

The classical Weisskopf-Ewing [14] evaporation formula, for « monocromatic » incident γ-rays, of energy E_γ is:

$$F(E_n) = \text{const}\, E_n \sigma_c(E_n) \cdot \omega(E_\gamma - B - E_n) \,. \tag{1}$$

Here B is the binding energy of the last neutron. The cross-section for the inverse process $\sigma_c(E_n)$ is supposed to be a slowly varying function of E_n, which can be ignored. For the level density $\omega(E_R)$ of the residual nucleus excited at an energy $E_R = E_\gamma - B - E_n$, the expression:

$$\omega(E_R) = C \exp\left[2\sqrt{\frac{A}{20} E_R}\right] \tag{2}$$

can be derived [14] from the model of a degenerate Fermi-Dirac gas.

---

[13] F. FERRERO, R. MALVANO, S. MENARDI and O. TERRACINI: *Nucl. Phys.*, **9**, 32 (1958).

[14] V. F. WEISSKOPF and D. H. EWING: *Phys. Rev.*, **57**, 472 (1940).

Eq. (1) can be simplified to the commonly used form:

$$F(E_n) = \text{const}\, E_n \exp[-E_n/T] \tag{3}$$

by means of an approximation procedure well known in statistical mechanics (see for inst. MORRISON ([15])). Here T is the « nuclear temperature » in MeV. Eq. (3) can also be deduced exactly from eq. (1) if one substituted eq. (2) with:

$$\omega(E_R) = \text{const} \exp[E_R/T]\,; \tag{4}$$

eq. (4) means ([16]) that the nuclear temperature can be considered constant (independent of E_R).

Of course, eq. (3) can be true only for:

$$E_n < E_\gamma - B \tag{5}$$

and in fact it is expected to be correct only when $E_n \ll E_\gamma - B$.

For irradiation with bremsstrahlung, of spectrum $I(E_\gamma, E_{\gamma\max})$, if $\sigma_{\gamma n}(E_\gamma)$ is the (γ, n) cross-section, we obtain from eq. (1), ignoring σ_c:

$$F(E_n) = \text{const}\, E_n \int_{B+E_n}^{E_{\gamma\max}} \frac{\sigma_{\gamma n}\, I(E_\gamma, E_{\gamma\max})\, \mathrm{d}E_\gamma}{\int_0^{E_\gamma - B} x\omega(E_\gamma - B - x)\,\mathrm{d}x}\,. \tag{6}$$

Under assumption (4), this gives:

$$F(E_n) = \text{const}\, E_n \exp[-E_n/T]\varphi(E_n)\,, \tag{7}$$

with

$$\varphi(E_n) = \int_{B+E_n}^{E_{\gamma\max}} \frac{\sigma_{\gamma n} I(E_\gamma, E_{\gamma\max})\,\mathrm{d}E_\gamma}{\int_0^{E_\gamma - B} x \exp[-x/T]\,\mathrm{d}x}\,. \tag{7'}$$

The integral $\varphi(E_n)$ is a decreasing function of E_n. It assures that the condition (5) be satisfied and that the total numbef of neutrons produced by γ-rays in the $(E_\gamma, \mathrm{d}E_\gamma)$ interval, be equal to $\sigma_{\gamma n} I(E_\gamma, E_{\gamma\max})\,\mathrm{d}E_\gamma$.

If one ignores $\varphi(E_n)$, eq. (7) gives again eq. (3). Certainly this last formula is very convenient, as it is simple, and with adjustement of T it roughly cor-

---

([15]) P. MORRISON, see E. SEGRÈ: *Experimental Nuclear Physics*, vol. **2** (New York, 1953), p. 62.

([16]) D. L. LIVESEY: *Can. Journ. Phys.*, **33**, 391 (1955).

responds to the experimental results. However some caution must be maintained about its physical meaning, every time that (essentially for the limited number of degrees of freedom) condition (5) gives an effective limitation to processes that otherwise would have non-zero probabilities.

For instance, compare curves 1, 2 and 3 in Fig. 1*a* and 1*b*.

Curve 1 and 2 were calculated from the simplified formula (3), with $T=1.8$ MeV and $T=1.3$ MeV, respectively.

Curve 3 was obtained from eq. (6) with the level density (2).

The same curve 3, was also obtained, without appreciable variation, from eq. (7), with $T=1.8$ MeV. This means that by taking account of the integral $\varphi(E_n)$ curve 1 is shifted to curve 3; this shift gives a quite appreciable change in the estimated nuclear temperature.

Note that using another known formula ([17]) for the level density no appreciable change could be found from curve 3.

4·1. *Aluminum results.* – Curve 1 agrees well with the experimental results at 24 MeV (Fig. 1*a*) and also (Fig. 1*b*) at 30 MeV, exception made of the 7 MeV maximum and the subsequent tail. Curve 1 also gives a good fit with the Al photoneutron spectrum obtained by REVZEN and SARGENT ([11]) with 70 MeV bremsstrahlung.

One would be tempted to conclude that a major part of the Al spectra is evaporative in origin (100% at 24 MeV and 85% at 30 MeV).

However, we find this interpretation rather doubtful. Several different ways of calculating the evaporation spectrum from the complete eq. (6) give almost exactly the same curve 3.

Besides, we must consider the following arguments.

Our γ-ray irradiations give a mean excitation energy of the compound nucleus of about (20 ÷ 22) MeV (maximum of giant resonance). This is about the same as in the experiments by GUGELOT ([18]), who bombarded Al (among other elements) with 16 MeV protons. The compound nucleus is different in the two cases, but this difference cannot be relevant for an evaporation process.

Therefore, we must suppose that in our photoneutron spectra the evaporation fraction is not harder than the curve found by Gugelot, which, could itself contain some fraction of direct processes.

Now, GUGELOT approximated his results with eq. (3), taking for Al, $T=1.3$ MeV (curve 2 in Fig. 1) and obtained good agreement with the experimental spectrum between 2 and 6 MeV. For $E_n > 6$ MeV he observed a « tail ».

([17]) S. A. MOSZOKOWSKY: *Handb. d. Phys.*, **39**, 437 (1957).

([18]) P. C. GUGELOT: *Phys. Rev.*, **81**, 51 (1951).

This means that in our photoneutron spectra at 90° a considerable direct emission component is already present at neutron energies as low as $(4 \div 5)$ MeV. If pure evaporation is supposed to give Gugelot's curve 2, the directly emitted neutrons at 90°, for 30 MeV irradiation, are 25% of all neutrons having energy $E_n > 2$ MeV.

4·2. *Other photoneutron spectra.* – A number of neutron spectra measured in this laboratory at $E_{\gamma max} = 30$ MeV are shown in Fig. 3. The spectra are arranged following the reversed mass-number order.

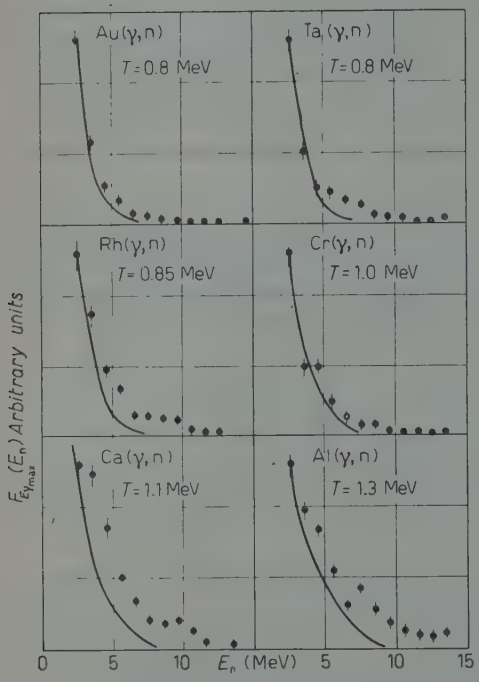

Fig. 3. – Photoneutron spectra at 90° under 30 MeV bremsstrahlung irradiation, obtained through collaboration between Catania and Turin. Bibliography as follows: Au see ([5]); Ta and Cr see ([3]); Rh and Ca see ([6]); Al: present work. The curves are calculated from eq. (3) with the T values shown in inserts (see text).

A general trend is apparent: the high energy tails become more and more important and the spectra harder and harder as the mass-number A decreases. A similar trend is not so clearly apparent in the other known photoneutron spectra (see introduction). These were measured at different values of $E_{\gamma max}$ and with different experimental arrangements; besides the low bremsstrahlung energy used by most of the workers $((20 \div 24)$ MeV) gives a rather high sensitivity to the threshold values of the single nuclides investigated.

The mentioned general trend is expected, as it corresponds to the decreasing level density of the residual nuclei, as A decreases.

Indeed, similar results were found by GUGELOT in the already quoted work. The curves in Fig. 3 are calculated from eq. (3) with the T values found by GUGELOT. We note the remarkable general similarity of the two series of results. For $E_n > (6 \div 8)$ MeV, the experimental points are systematically higher than the curves. This corresponds to the expected contribution of direct processes; similar discrepancies were found by GUGELOT himself.

In the cases of Ca and Rh (apart from Al) a relevant contribution from direct processes at energies of $((3 \div 4)$ MeV) have also been observed ([6]), and

discussed in terms of a modified Wilkinson model ([9]). For the high energy part of the observed photoneutron spectra wich cannot been explained on the basis of the Wilkinson model ([8,9]) a possible explanation can be given in terms of a direct surface process ([19]).

* * *

Our grateful thanks are due to Prof. R. RICAMO and to Prof. G. WATAGHIN who put at our disposal the means for performing the present research. We are indebted to Prof. R. MALVANO, who gave us precious help. Finally, we thank the betatron staff of Turin, for friendly collaboration.

([19]) A. AGODI, E. EBERLE and L. SERTORIO: *XLIV Congresso della Società Italiana di Fisica - Palermo, Novembre 1958.*

RIASSUNTO

Si studia lo spettro dei fotoneutroni emessi dall'alluminio irradiato con raggi X con energia massima di 24 e di 30 MeV. I neutroni sono stati rivelati mediante i protoni di rinculo in emulsioni nucleari. Si trova che i fotoni di energia > 24 MeV danno luogo prevalentemente a processi di emissione diretta. Per $E_{\gamma max} = 30$ MeV l'emissione diretta dà alla resa totale (γ, n) un contributo molto notevole $(> 25\%)$.

Charged Photoparticles from Argon.

V. Emma, C. Milone, R. Rinzivillo and A. Rubbino

Istituto di Fisica dell'Università - Catania
Centro Siciliano di Fisica Nucleare - Catania

(ricevuto il 27 Marzo 1959)

Summary. — The (γ, p) and (γ, α) reactions in argon have been studied by irradiation of an A gas target with the bremsstrahlung beam of the 31 MeV B.B.C. betatron of Turin. Three different maximum bremsstrahlung energies were used: 23, 26 and 30 MeV. The charged photoparticles emitted at an angle around 90° with the γ-ray beam were recorded by nuclear emulsion. Tracks with a total range < 75 μm of emulsion are attributed mainly to $A(\gamma, \alpha)$ process whose $d\sigma/d\Omega$ is given. Thus the apparent anomaly disappears in the spectrum $A(\gamma, p)$ with a high and narrow peak at energy lower than the Coulomb barrier. The (γ, p) yield appears to be lower than that found by Spicer [3] and the Canadian workers [2], while seeming to be in agreement with the recent results [12] on the $A(\gamma, p)$ cross-section. Hence the $A(\gamma, p)$ cross-section does not seem so abnormally high in respect to other nuclei as it has been accepted to this date.

1. – Introduction.

Photoproton spectra arising from the photodisintegration of argon by monochromatic radiation from the $^7Li(p, \gamma)$ reaction have been obtained by D. H. Wilkinson and J. H. Carver [1].

---

[1] D. H. Wilkinson and J. H. Carver: *Phys. Rev.*, **83**, 466 (1951).

The (γ, p) and (γ, n) cross-sections of ^{40}A have been determined by the Canadian group ([2]) by means of the activation method as a function of the photon energy from threshold to 23 MeV.

Results on energy and angular distributions of the protons emitted from ^{40}A irradiated with 22.5 MeV bremsstrahlung have been reported by B. M. SPICER ([3]).

The experimental results show the following anomalies:

a) The energy spectra ([1,2]) show a peak at ~ 2.5 MeV proton energy. This result is surprising because the Coulomb barrier is ~ 5 MeV and the peak is very high and very narrow.

b) The photoproton yield ([2]) is abnormally high.

The peak energies of the (γ, p) and (γ, n) cross-sections are very different: according to the Canadian group ([2]) above 20 MeV the $\sigma(\gamma, n)$ is a decreasing function of E_γ while the $\sigma(\gamma, p)$ is an increasing function of E_γ and its maximum is not yet reached at 24 MeV (maximum energy of their irradiation). At this energy the $\sigma(\gamma, p)/(\sigma(\gamma, n)$ ratio is 5.3.

The experimental integrated $\sigma(\gamma, p)$ cross-section is higher than the integrated cross-section for all processes calculated according to

$$\int \sigma_c(E)\, dE = 0{,}015\, A(1 + 0.8x) \quad ([4]) .$$

For the self-conjugate nuclei—as ^{28}Si, ^{32}S, ^{40}Ca—a predominant proton emission is expected from the calculations of MORINAGA ([5]) and is confirmed by the experimental results of JOHANSSON ([6]). For argon the abnormally high photoproton cross-section is not justified by theoretical predictions.

Because of this surprising behaviour we decided to study the energy spectra and yields of charged photoparticles from argon by irradiation with bremsstrahlung at several maximum energies (*).

([2]) D. MCPHERSON, E. PEDERSON and L. KATZ: *Can. Journ. Phys.*, **32**, 593 (1954).
([3]) B. M. SPICER: *Phys. Rev.*, **100**, 791 (1955).
([4]) J. S. LEVINGER and H. A. BETHE: *Phys. Rev.*, **78**, 115 (1950).
([5]) H. MORINAGA: *Phys. Rev.*, **97**, 1185 (1955).
([6]) S. A. E. JOHANSSON: *Phys. Rev.*, **97**, 1186 (1955).
(*) A short account of the present work was given at the *S.I.F. Conference.* Palermo (November 1958) by V. EMMA, C. MILONE, R. RINZIVILLO and A. RUBBINO: *Recenti risultati sugli spettri dei fotoprotoni.*

2. – Experimental procedure.

The experimental technique used in the present work is described in a previous paper (7). An argon gas target was exposed in a « chamber » at a pressure of 1.2 atmospheres, to the collimated bremsstrahlung beam of the B.B. Betatron of Turin operating successively at 23, 26 and 30 MeV maximum energy.

Photoprotons were detected in 200 μm C_2 Ilford 3in. × 3in. plates with a central hole of 2.5 cm diameter. The plates were perpendicular to the γ-ray beam which had a diameter of 1.4 cm at the center of the plates. In every exposure two C_2 emulsions parallel to each other were placed 0.7 cm apart and at 106 cm from the source of γ-rays.

The dose measured by means of a Victoreen thimble was ~ 5 000 roentgen at the center of the target for every irradiation (see Table I).

TABLE I.

$E_{\gamma\,max}$ (MeV)	23	26	30	30
Pressure of argon (atmospheres)	1.2	1.2	1.2	2.0
Dose (roentgen)	4 850	4 900	4 900	5 300
Slow scanning ($E_p \geqslant 1.6$ MeV)				
Field of view at the microscopes	130 μm	130 μm	80 μm	
Scanned surface (mm²)	209	241	235	
Number of accepted tracks	403	693	753	
Fast scanning ($E_p > 3$ MeV)				
Field of view in the microscopes	320 μm		320 μm	180 μm
Scanned surface (mm²)	362		342	160
Number of accepted tracks	382		797	891

The plates, processed by standard methods, were scanned along circular rings centered on the beam axis. Only protons ejected from the gas target with an angle $70° < \vartheta < 110°$ from the bremsstrahlung beam entered the scanned area of the emulsions.

For any track to be accepted a direction was required compatible with an origin in the irradiated part of the argon target.

A « fast » scanning with 30× immersion oil objectives and 7.8 eyepieces

(7) C. MILONE, S. MILONE-TAMBURINO, R. RINZIVILLO, A. RUBBINO and C. TRIBUNO: *Nuovo Cimento*, **7**, 729 (1958).

(field of view 320 μm) was made in order to rapidly determine the proton spectra from 3 MeV to higher energy.

A « slow » scanning with 100× immersion oil objectives and 8× eyepieces (field of view 130 μm) was made for a better examination of the low energy region. The minimum length of considered tracks was 8 μm.

Results obtained by « slow » and « fast » scanning are in good agreement.

Data on the experimental procedure are summarized in Table I.

The energy loss by the proton in the gas between the target and the emulsion was calculated using the curves of B. H. WILLIS ([8]).

All protons were assumed to start at the center of the gas target.

The uncertainty in locating the beginning of the tracks was $\pm$ 1.25 mg/cm^2 of argon, equivalent to $\sim$ 4 μm of C_2 Ilford emulsion for the irradiation at 1.2 atmospheres (Table I). The total uncertainty in the measurement of proton energy was $\pm$ 0.2 MeV for 2 MeV protons and $\pm$ 0.03 MeV for 12 MeV protons.

The background determined from tracks entering the emulsion but having wrong direction was respectively 15%, 8% and 4% for 2, 3 and 4 MeV protons. In the higher energy region the background was less than 3%.

3. – Results.

The results are summarized in Figs. 1, 2 and 3.

The energy spectrum obtained by SPICER ([3]) at 22.5 MeV irradiation is peaked at $\sim$ 2.5 MeV and shows very few protons above 5 MeV. Our spectrum at 23 MeV irradiation shows above 5 MeV a higher contribution of photoprotons. These two spectra are compared in Fig. 1 after normalizing the results in the (2÷4) MeV region (below 2 MeV the discrimination of the tracks according to the dip angle becomes critical and the background not negligible).

Figs. 2 and 3 show the spectra obtained at 23, 26 and 30 MeV irradiation respectively. The 30 MeV spectrum of Fig. 2(*b*) is obtained in a run differing from the standard condition used in all the other runs as to the pressure and volume of the gas target and for the ϑ interval between γ-rays and protons ($40° < \vartheta < 140°$).

Experimental data were treated taking into account the energy loss of the protons in the gas and the solid angle seen from the target. There is agreement between the two 30 MeV spectra (Fig. 2(*a*) and (*b*)).

In Fig. 3 the values $E_s + (40/39)E_p$ are reported beside the E_p values. Under the assumptions: i) that all accepted tracks are protons; ii) that the residual nucleus is left in its ground state, we have $(40/39)E_p + E_s(\gamma, p) = E_\gamma$,

([8]) Beverly Hill Willis UCRL 2426 (October 1953).

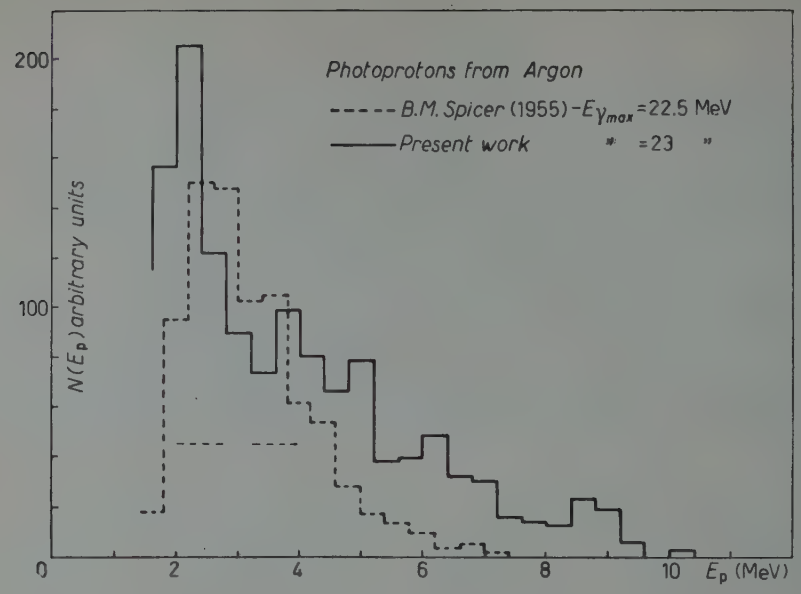

Fig. 1. – Our results and Spicer's on energy distribution of charged photoparticles from argon. Normalization region (2÷4) MeV .

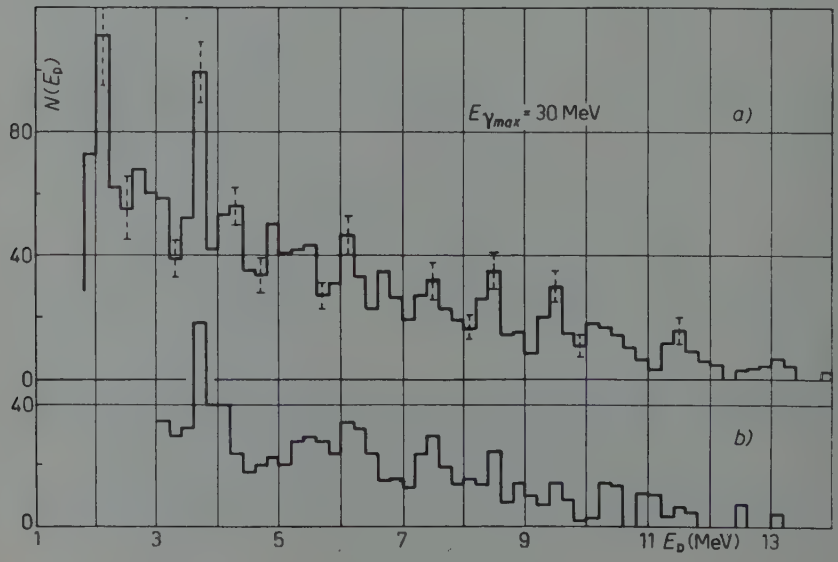

Fig. 2. – Comparison of spectra obtained at 30 MeV peak bremsstrahlung, at different times and in different experimental conditions.

$E_s(\gamma, p) = 12{,}44$ MeV being the threshold energy of the $A(\gamma, p)$ process and E_γ being the energy of γ-rays that generate the protons of energy E_p. The assumptions i) and ii) may be not correct (see following paragraph).

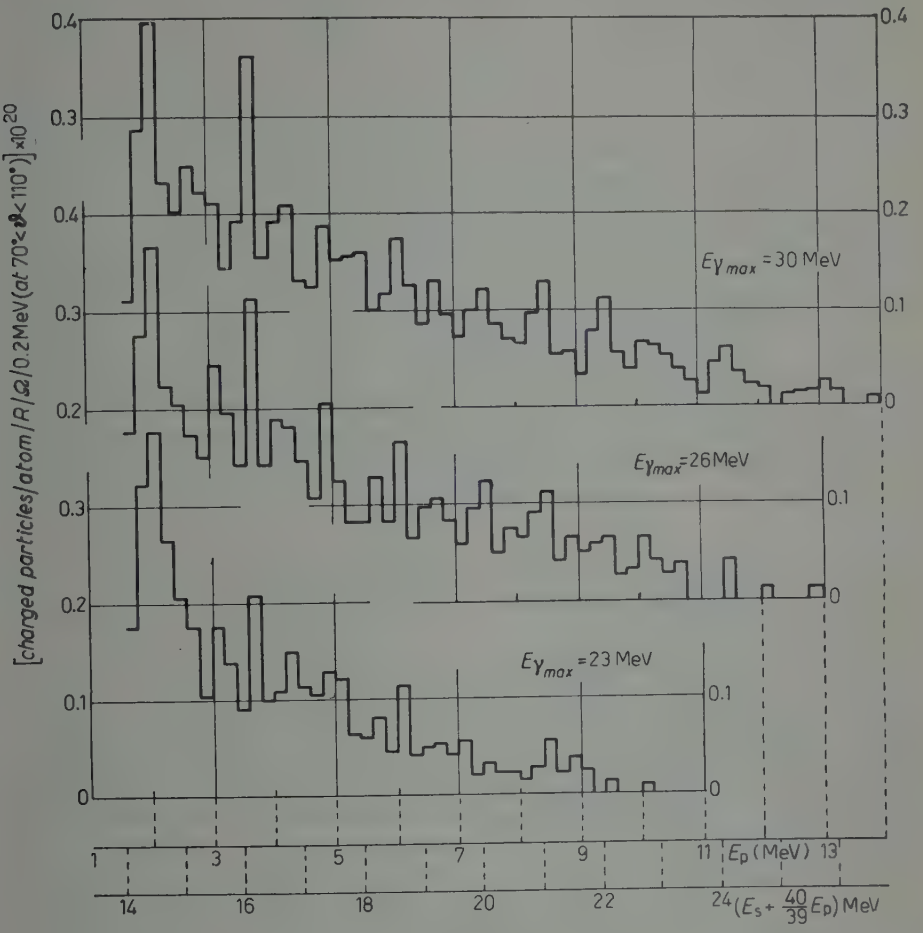

Fig. 3. – Spectra obtained at 23, 26 and 30 meV peak bremsstrahlung in unity of yield in the assumption that all tracks are due to protons (assumption correct for $E_p > 3$ MeV).

4. – Discussion.

Figs. 2 and 3 show for every irradiation a very high and narrow peak for tracks with a total range $l \leqslant 75$ μm of emulsion. Were these tracks due to protons, a peak at 2.2 MeV would be obtained. This result agrees with that

of others workers ([1,3]), but appears very surprising because the Coulomb barrier is ~ 5 MeV.

Assuming that the tracks below 75 μm of emulsion may be due also to other photoparticles, deuterons and tritons are excluded for their high threshold energy (~ 18 MeV).

The A(γ, α) process may give a large contribution to this peak. In fact:

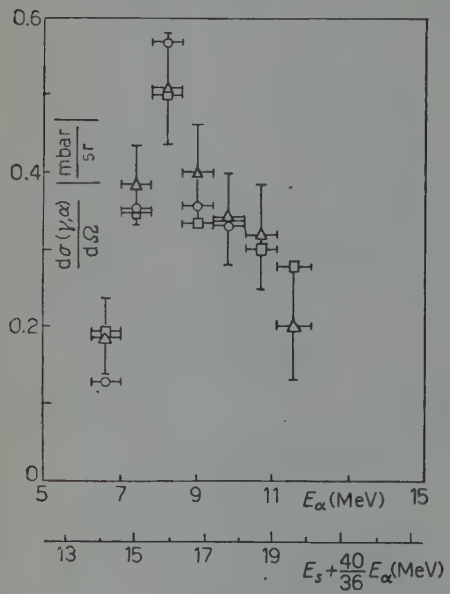

Fig. 4. – Photoalpha cross-section in argon as a function of alpha particle energy. Points $\triangle$, $\square$, $\bigcirc$, refer to $E_{\gamma\,max}=23$, 26, 30 MeV irradiations respectively.

a) For short tracks the α-particles cannot be distinguished ([9]) from the protons in ours plates and in those used by SPICER ([3]).

b) The A(γ, α) threshold is very low (6.8 MeV) ([10]).

c) The (γ, α) cross-section is not negligible in comparison with the (γ, p) cross section. For instance WILKINSON and CARVER ([1]) with irradiation of argon at 17.6 MeV by the ^{7}Li(p, γ) reaction, found charged photoparticles with energy higher than $17.6-E_s(\gamma, p)$. This result may be interpreted with a (γ, α) process contribution.

d) The attribution of the first peak to evaporated protons is to be excluded because this peak is very narrow and its yield is unvaried at various values of $E_{\gamma\,max}$. Besides, SPICER ([3]) in order to interpret the energy spectrum from argon according to the statistical theory needed a drastic modification of the Coulomb barrier so as to attribute the tracks with $l \leqslant 75$ μm to evaporated protons. On the other hand his observed angular distribution ([3]) for $E_p \leqslant 3$ MeV presents a large anisotropy.

Then we consider the first peak (Figs. 2 and 3) as due to the (γ, α) process. The correspondent $d\sigma/d\Omega$ derived from the radiations at 23, 26 and 30 MeV, taking into account the bremsstrahlung function, is shown in Fig. 4 as a function of E_γ.

We think this cross-section is accurate up to $E_\alpha = 10$ MeV.

([9]) M. ADER and M. P. CABANNES: *Journ Phys. Rad.*, **19**, 939 (1958).
([10]) P. M. ENDT and C. M. BRAAMS: *Rev. Mod. Phys.*, **29**, 683 (1957).

5. – Photoproton yield.

Yields of charged photoparticles/atom/R/Ω (taking $70° < \vartheta < 110°$) have been calculated from the formula

$$Y = \frac{N}{S}\frac{1}{\Omega}\frac{1}{RnV}, \tag{1}$$

where N/S is the number of tracks per unit area of the emulsion, Ω is the mean solid angle at the target subtended by the unit area on the emulsion, R is the total dose in roentgen at the center of the gas target, n is the number of atoms per cm³ of the gas, and V is the effective volume of the gas target in cm³.

In Fig. 3 the yields have been reported for charged particles.

The yields for protons refer to $E_p > 3$ MeV.

In order to find other information on the photoproton emission from argon we made the extreme assumption that proton emission will leave the residual nucleus in its ground state. Under these assumptions, taking into account the bremsstrahlung spectra $I(E_\gamma, E_{\gamma\,\max})$ ([7,11]) the functions

$$\left(Y_{26} - Y_{23}\frac{I(E_\gamma, 26)}{I(E_\gamma, 23)}\right) \quad \text{and} \quad \left(Y_{30} - Y_{26}\frac{I(E_\gamma, 30)}{I(E_\gamma, 26)}\right),$$

for $\Delta E_p = 0.6$ MeV become those reported in Fig. 5(*a*) and 5(*b*).

Fig. 5(*c*) shows the ratios $I(E_\gamma, 26)/I(E_\gamma, 23)$ and $I(E_\gamma, 30)/I(E_\gamma, 26)$.

From Figs. 5 (*a*), (*c*) we observe that within the proton energy interval $3 < E_p < 9$ MeV, there is a remarkable contribution of protons emitted owing to absorption of γ-rays having energy $E_\gamma > 21$ MeV (region in which the ratio $I(E_\gamma, 26)/I(E_\gamma, 23)$ rapidly increases above unity). On the contrary, Figs. 5(*b*), (*c*) show that the contribution of protons emitted owing to absorption of γ-rays of energy higher than 26 MeV is negligible.

Photons from 23 to 25 MeV give two groups of protons peaked the one around 3.5 MeV, the other around 7 MeV (Fig. 5(*a*)). These peaks must correspond to transitions to excited states in ^{39}Cl. Besides, the ground state transitions are of rater low intensity. This is true also for the photons from 26 to 30 MeV.

The transitions cannot be identified since the photon energy is known with an uncertainty of about 4 MeV so that the excited states of the nucleus ^{39}Cl are not known.

Yet, we may identify the regions of photon energy which give a larger

---

([11]) L. Katz and A. G. W. Cameron: *Can. Journ. Phys.*, **39**, 437 (1957).

contribution of photoprotons. Thus from Fig. 5 we may derive that the cross section A(γ, p) is very low for $E_\gamma > 25$ MeV, while the Canadian group [2] found a maximum of the A(γ, p) cross-section for $E_\gamma > 25$ MeV.

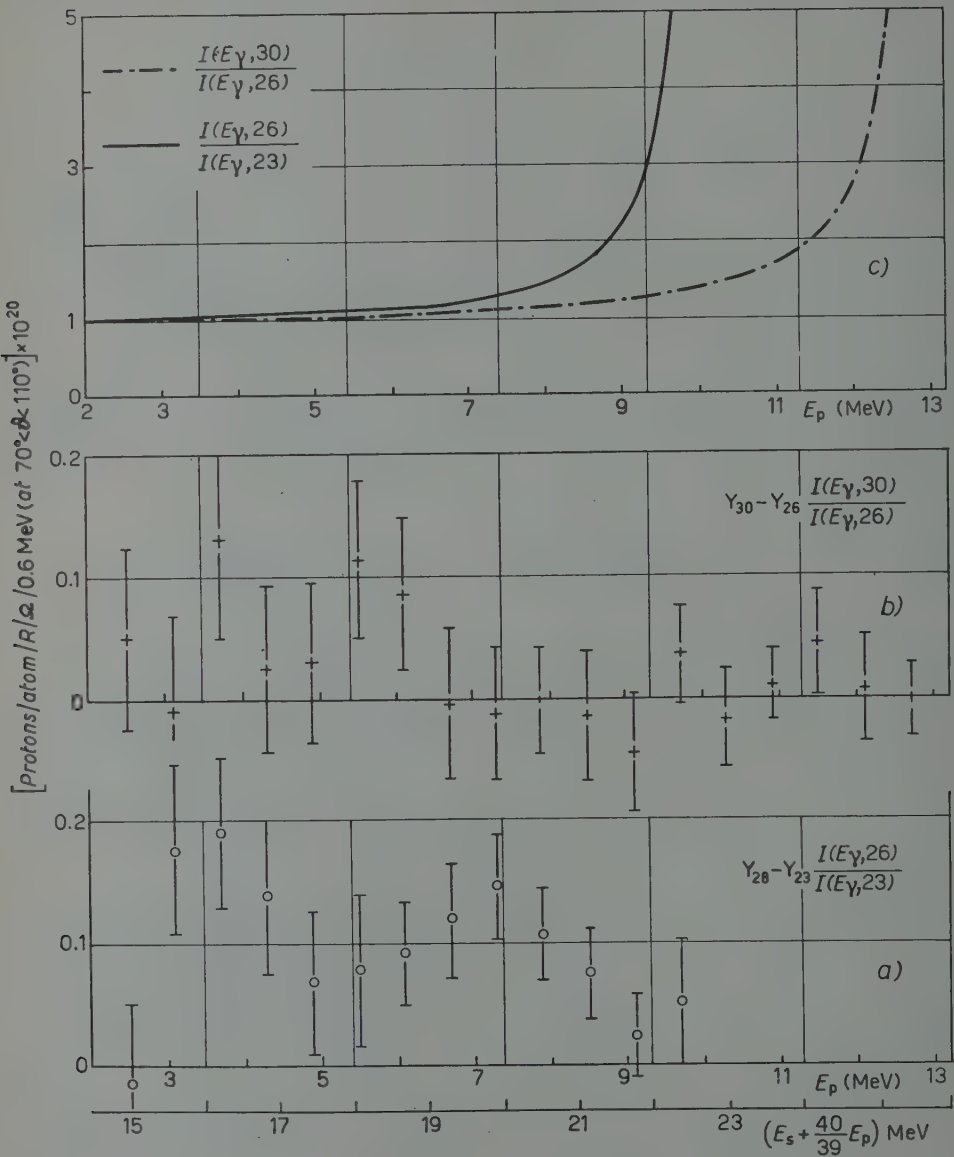

Fig. 5. – *a*) Spectrum of protons produced by photon absorption in the energy interval (21÷26) MeV). *b*) Spectrum of protons produced by photon absorption in the energy internal (24÷30) MeV. *c*) Ratio $I(E_\gamma, 30)/I(E_\gamma, 26)$ [curve ·–·–· and ratio $I(E_\gamma, 26)/I(E_\gamma, 23)$ curve ——.

Recently K. H. LINDENBERGER ([12]) found an A(γ, p) cross-section integrated up to 32 MeV smaller than the A(γ, n) cross-section. This result cannot be reconciled with the results of the Canadian group which found

$$\int_0^{25} \sigma(\gamma, \mathrm{p})\, \mathrm{d}E \Big/ \int_0^{25} \sigma(\gamma, \mathrm{n})\, \mathrm{d}E = 0.54/0.35\,,$$

while at $E_\gamma = 25$ MeV the (γ, n) cross-section is nearly exhausted and the (γ, p) cross-section has not yet reached the maximum value ([2]).

From our result we found at $E_{\gamma\,\max} = 23$ MeV a yield $Y = 4 \cdot 10^{-20}$ charged particles/atom/R/Ω. To this value corresponds a maximum yield of $4 \cdot 10^{-20} \cdot 4\pi N_a = 3 \cdot 10^5$ charged particles/mole/R in the case of isotropic angular distribution. The Canadian group ([2]) and SPICER ([3]) found respectively $7.3 \cdot 10^5$ and $5.5 \cdot 10^5$ protons per mole per roentgen.

In Fig. 6 the A(γ, p) yields are compared with O(γ, p) ([7]) and N(γ, p) ([13]) yields obtained in the same experimental conditions.

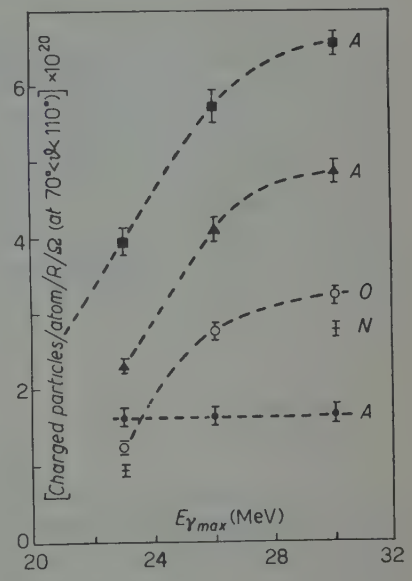

Fig. 6. – Comparison of yields in unities of (charged particles/atom/R/Ω at $90° < \vartheta < 110°$) $\cdot 10^{20}$: argon ⊥ for all accepted tracks; ▲ for tracks with a total range > 75 μm of emulsion; ● for tracks with a total range $\leqslant 75\mu$m of emulsion; oxigen ○ for all accepted tracks. Nitrogen ⊥ for all accepted tracks

6. – Structure of the spectra.

At any irradiation the photoproton spectra exhibit a structure that may be partly due to resonances in the photon absorption and partly to the branching of the proton emission to various excited levels in the residual nucleus ^{39}Cl.

([12]) K. H. LINDERBERGER: *Conference on Photonoclear Reactions* (April 30 and May 1, 1958), Nation. Bureau of Standards, p. 13 (Washington D.C.).

([13]) G. CORTINI, C. MILONE, R. RINZIVILLO and C. TRIBUNO: *Nuovo Cimento*, **9**, 118 (1958).

In order to allow identification of the proton groups it would be necessary to know a high number of spectra obtained making a corresponding high number of irradiations at energies gradually increasing from the threshold to the maximum energy of the Betatron.

We may obtain only qualitative information.

For example, the height of the peak at $E_p = 3.6$ MeV increases more than contiguous proton groups as the maximum bremsstrahlung energy increases. Therefore, this proton group may be due mainly to absorption of γ-rays of energy higher than 20 MeV where $I(E_\gamma, E_{\gamma\,\max})/I(E_\gamma, E'_{\gamma\,\max})$ increases with $E_{\gamma\,\max}$.

High peaks with narrow width in photoproton spectra from elements such as sodium ([14]) and potassium ([15]) have been obtained by ^{7}Li(p, γ) radiation. In these cases the cross-section for the ground state transitions comparative to the cross-section for every transition is lower than 5% for sodium and lower than 8% for potassium.

In the case of the A(γ, p) reaction, the excitation energies of the residual nucleus ^{39}Cl are not known.

Our spectra cannot clearly identify transitions to unknown levels in ^{39}Cl and it is already surprising that the spectra even show a fine structure.

If one wanted to give a significance to the peaks one ought to suppose that only few transitions to excited states of the residual nucleus ^{39}Cl are allowed or that the level density in ^{39}Cl is very low.

7. – Conclusions.

The tracks with a total range < 75 μm of emulsion are attributed to the A(γ, α) process. So the anomaly of a high and narrow peak at ~ 2.5 MeV in the proton energy spectrum ([1,2]) (while the Coulomb barrier is ~ 5 MeV) is eliminated. The cross-section $d\sigma/d\Omega$ for the A(γ, α) process from $E_\gamma = 14$ MeV up to $E_\gamma = 20$ MeV is obtained.

The yield and the cross-section for the A(γ, p) process are not so high as found by SPICER ([3]) and the Canadian workers ([2]), while it seems to be in agreement with Lindenberger's results ([12]).

([14]) T. R. OPHEL and I. F. WIGHT: *Proc. Phys. Soc.*, A **71**, 389 (1958).
([15]) T. R. OPHEL: *Proc. Phys. Soc.*, A **72**, 321 (1958).

* * *

Our thanks are due to Prof. R. RICAMO and Prof. G. WATAGHIN who put at our disposal the means for performing this work.

We thank Prof. G. CORTINI for many illuminating discussions.

We also thank Dr. A. AGODI and Dr. C. TRIBUNO for their friendly help.

RIASSUNTO

Si studiano le reazioni (γ, p) e (γ, α) in argon esponendo targhette gassose di Argon ai raggi γ del betatrone B.B.C. di 31 MeV di Torino. Sono stati eseguiti irraggiamenti alle energie di 23, 26 e 30 MeV. Le tracce con un range totale < 75 μm di emulsione sono attribuite principalmente a processi $A(\gamma, \alpha)$; di questo processo si dà la sezione d'urto $d\sigma/d\Omega$. In questo modo si elimina nello spettro $A(\gamma, p)$ l'apparente anomalia consistente in un alto e stretto picco ad energia inferiore a quella della barriera coulombiana. La resa (γ, p) risulta inferiore a quella determinata da SPICER [3] e dai Canadesi [2], mentre sembra in accordo con i recenti risultati [12] sulla sezione d'urto del processo $A(\gamma, p)$. Si conclude che la sezione d'urto del processo $A(\gamma, p)$ non è così eccezionalmente alta rispetto alla fotodisintegrazione degli altri nuclei come fin ora accettato.

IL NUOVO CIMENTO Vol. XIV, N. 1 1° Ottobre 1959

Meson Production in the Static Charged-Scalar Theory (*) (**).

E. KAZES (***)

University of Chicago - Chicago, Ill.

(ricevuto il 31 Marzo 1959)

Summary. — Meson production amplitudes in the charged-scalar theory are shown to satisfy integral equations which in the one meson approximation reduce to the Riemann-Hilbert boundary problem and the complete solution is given.

1. – Introduction.

In the last few years the static pion-nucleon interaction model of Chew-Low has been used widely in view of its ability to account for the low energy p-phase shifts and of its relative simplicity. This model has also been used in calculating pion production cross-sections in pion-nucleon collisions, with widely different approximations ([1-5]). In (K) using the charge-symmetric pseudoscalar theory a solution to latter problem which partially satisfies the crossing-symmetry but that accounts for unitarity was given. In contrast to the charge-symmetric theory CASTILLEJO, DALITZ and DYSON ([6]) have obtained all the solutions for pion-nucleon scattering in the charged-scalar theory. It will be

(*) Based on a dissertation submitted in partial fulfilment of requirements of the Ph.D. degree at the University of Chicago.

(**) This work was supported in part by a grant from the U.S. Atomic Energy Commission.

(***) Now at Physics Department of the University of Wisconsin.

(1) S. BARSHAY: *Phys. Rev.*, **103**, 1102 (1956).

(2) J. FRANKLIN: *Phys. Rev.*, **105**, 1101 (1957).

(3) L. S. RODBERG: *Phys. Rev.*, **106**, 1091 (1957).

(4) E. KAZES: *Phys. Rev.*, **107**, 1131 (1957), hereafter referred to as (K).

(5) R. OMNÈS: *Nuovo Cimento*, **6**, 780 (1957).

(6) L. CASTILLEJO, R. H. DALITZ and F. J. DYSON: *Phys. Rev.*, **101**, 453 (1956).

shown that the same thing is true for pion production amplitudes in this model, and using the one-meson approximation the complete solution which satisfies unitarity and the crossing-symmetry will be given.

2. – Integral equations.

In the static approximation with a finite source, the Hamiltonian is

$$H = H_0 + H_I ,$$

where

$$H_0 = \sum_{\varkappa} \omega_{\varkappa} a_{\varkappa}^{+} a_{\varkappa} ,$$

$$H_I = \sum_{\varkappa} (V_{\varkappa}^{0} a_{\varkappa} + V_{\varkappa}^{0+} a_{\varkappa}^{+}) .$$

In the charged scalar theory

$$V_{\varkappa}^{(0)} = f_{(r)}^{0} \frac{\tau_{\varkappa} v(\boldsymbol{\varkappa})}{(2\omega_{\varkappa})^{\frac{1}{2}}} ,$$

here $f_{(r)}^{0}$ is the unrenormalized but rationalized coupling constant and $v(\boldsymbol{\varkappa})$ is the Fourier component of the source function. $\varkappa$ is used to indicate momentum and charge variables. And

$$\tau_{\varkappa} = \frac{\tau_x \pm \tau_y}{2} , \qquad \varkappa = \pm 1 .$$

The lowest eigenstate of H will describe the four states of a nucleon at rest and will be denoted by $\Psi_0(m)$. By proper choice of the energy scale

$$H\Psi_0(m) = 0 .$$

Proton-neutron mass difference is ignored.

The state vector that consists of two mesons p_1, p_2 and a nucleon in a state $\Psi_0(m')$ at $t = +\infty$ is

$$\Psi_{p_1 p_2}^{(-)}(t) = \exp[-iHt]\left[a_{p_1}^{+} a_{p_2}^{+} + \frac{1}{\omega_{p_1} + \omega_{p_2} - H - i\varepsilon} (a_{q_1}^{+} V_{p_2}^{(0)} + a_{p_2}^{+} V_{p_1}^{(0)})\right] \Psi_0(m') ,$$

Using the notation that appears in (K) and letting

$$O = a_{p_1} V_{p_2}^{(0)+} + a_{p_2} V_{p_1}^{(0)+} ,$$

the meson production amplitude from an initial nucleon and meson state m, q to a final state characterized with nucleon and meson variables m', p_1, p_2 respectively is $\langle \Psi_0(m') | O | \Psi_q^{(+)}(m) \rangle$. Let

$$t(q, m', m) = \sqrt{\omega_q} \langle \Psi_0(m') | O | \Psi_q^{(+)}(m) \rangle ,$$
$$x(q, m', m) = \sqrt{\omega_q} \langle \Psi_q^{(+)}(m') | O | \Psi_0(m) \rangle ;$$

in terms of these variables the integral equations of the problem, as appears in equations (2.5) and (2.6) of (K) and with possible bound states of the pion-nucleon field, are

$$(1) \quad -t(q, m', m) = \frac{\langle \Psi_0(m') | V^{(0)+}_{p_2} | \Psi_0(m) \rangle t^*(p_1, m) \sqrt{\omega_{p_1}}}{\omega_{p_1} - \omega_q - i\varepsilon} \delta'_{p_1, q} +$$
$$+ \frac{\langle \Psi_0(m') | V^{(0)+}_{p_1} | \Psi_0(m) \rangle t^*(p_2, m) \sqrt{\omega_{p_2}}}{\omega_{p_2} - \omega_q - i\varepsilon} \delta'_{p_2, q} +$$
$$+ \sum_B \left\{ \frac{\langle \Psi_0(m') | O | \Psi_B \rangle \langle \Psi_B | V^{(0)}_q | \Psi_0(m) \rangle}{E_B - \omega_q} + \frac{\langle \Psi_0(m') | V^{(0)}_q | \Psi_B \rangle \langle \Psi_B | O | \Psi_0(m) \rangle}{E_B + \omega_q} \right\} \sqrt{\omega_q} +$$
$$+ \sum_r \frac{(t(r, m', m)\, t^*(r, m)}{\omega_r - \omega_q - i\varepsilon} + \sum_\nu \frac{t(\nu, m')\, x(\nu, m', m)}{\omega_\nu + \omega_q} ,$$

$$(2) \quad -x(\nu, m', m) = \frac{\langle \Psi_0(m') | V^{(0)+}_{p_2} | \Psi_0(m) \rangle t^*(p_1, m) \sqrt{\omega_{p_1}}}{\omega_\nu + \omega_{p_1}} \delta'_{q, p_1} +$$
$$+ \frac{\langle \Psi_0(m') | V^{(0)+}_{p_1} | \Psi_0(m) \rangle t^*(p_2, m) \sqrt{\omega_{p_2}}}{\omega_\nu + \omega_{p_2}} \delta'_{q, p_2} +$$
$$+ \sum_B \left\{ \frac{\langle \Psi_0(m') | V^{(0)+}_\nu | \Psi_B \rangle \langle \Psi_B | O | \Psi_0(m) \rangle}{E_B - \omega_\nu} + \frac{\langle \Psi_0(m') | O | \Psi_B \rangle \langle \Psi_B | V^{(0)+}_\nu | \Psi_0(m) \rangle}{E_B + \omega_\nu} \right\} \sqrt{\omega_\nu} +$$
$$+ \sum_\varrho \frac{t(\varrho, m')\, x(\varrho, m', m)}{\omega_\varrho - \omega_\nu + i\varepsilon} + \sum_s \frac{t(s, m', m) t^*(s, m)}{\omega_\nu + \omega_s} ,$$

where $\sum_B$ is a summation over all bound states of the system including the one nucleons state, *i.e.*, $0 \leqslant E_B < 1$ (7). In equations (1) and (2) the Latin and Greek letters represent mesons of opposite charge and δ' is diagonal in charge variables only, and $t(r, m)$ represents the scattering amplitude of a meson of charge and momentum variable r from a nucleon in state m. The sums r, ν and ϱ, s are on one-pion intermediate states.

---

(7) $\hbar = c = \mu = 1$.

Now defining $T(z, m', m)$ and $X(z, m', m)$ by the following equations

$$(3)\quad -T(z,m',m) \equiv \frac{\langle \Psi_0(m')|V^{(0)+}_{p_2}|\Psi_0(m)\rangle t^*(p_1,m)\sqrt{\omega_{p_1}}}{\omega_{p_1}-z}\,\delta'_{p_1,q} +$$

$$+\frac{\langle \Psi_0(m')|V^{(0)+}_{p_1}|\Psi_0(m)\rangle t^*(p_2,m)\sqrt{\omega_{p_2}}}{\omega_{p_2}-z}\,\delta'_{p_2,q} +$$

$$+\sum_B\left\{\frac{\langle \Psi_0(m')|O|\Psi_B\rangle\langle\Psi_B|V^{(0)}_q|\Psi_0(m)\rangle}{E_B-z}+\frac{\langle\Psi_0(m')|V^{(0)}_q|\Psi_B\rangle\langle\Psi_B|O|\Psi_0(m)\rangle}{E_B+z}\right\}\sqrt{\omega_i}+$$

$$+\frac{1}{2\pi^2}\int_1^\infty\sqrt{\omega^2-1}\,\omega\,\mathrm{d}\omega\left\{\frac{t(r_\omega,m')t^*(r_\omega,m)}{\omega-z}+\frac{t(v_\omega,m)x(v_\omega,m',m)}{\omega+z}\right\}.$$

$$(4)\quad -X(z,m',m) = \frac{\langle \Psi_0(m')|V^{(0)+}_{p_2}|\Psi_0(m)\rangle t^*(p_1,m)\sqrt{\omega_{p_1}}}{\omega_{p_1}+z}\,\delta'_{q,p_1}+$$

$$+\frac{\langle \Psi_0(m')|V^{(0)+}_{p_1}|\Psi_0(m)\rangle t^*(p_2,m)\sqrt{\omega_{p_2}}}{\omega_{p_2}+z}\,\delta'_{q,p_2}+$$

$$+\sum_B\left\{\frac{\langle \Psi_0(m')|V^{(0)+}_\nu|\Psi_B\rangle\langle\Psi_B|O|\Psi_0(m)\rangle}{E_B-z}+\frac{\langle\Psi_0(m')|O|\Psi_B\rangle\langle\Psi_B|V^{(0)+}_\nu|\Psi_0(m)\rangle}{E_B+z}\right\}\sqrt{\omega_\nu}+$$

$$+\frac{1}{2\pi^2}\int_1^\infty\sqrt{\omega^2-1}\,\omega\,\mathrm{d}\omega\left\{\frac{t(\varrho_\omega,)\,m'(\varrho_\omega,m',m)}{\omega-z}+\frac{t(s_\omega,m',m)t^*(s_\omega,m)}{\omega+z}\right\},$$

where the subscripts of the arguments of the scattering and production amplitudes designate meson energies. Note that for $\omega > 1$

$$(5)\quad \lim_{z\to\omega+i\varepsilon} T(z,m',m) = t(q_\omega,m',m)\,,$$

$$(6)\quad \lim_{z\to\omega-i\varepsilon} X(z,m',m) = x(v_\omega,m',m)\,.$$

The crossing theorem now becomes

$$(7)\quad X(z,m',m) = T(-z,m',m)\,.$$

Using equations (3) and (4) and $\omega > 1$

$$(8)\quad \lim_{z\to\omega+i\varepsilon} T(z,m',m) - \lim_{z\to\omega-i\varepsilon} T(z,m',m) =$$

$$= -2\pi i\left\{\langle\Psi_0(m')|V^{(0)+}_{p_2}|\Psi_0(m_0)\rangle t^*(p_1,m)\sqrt{\omega_{p_1}}\,\delta'_{p_1,q}\,\delta(\omega_{p_1}-\omega)+\right.$$

$$+\langle\Psi_0(m')|V^{(0)+}_{p_1}|\Psi_0(m)\rangle t^*(p_2,m)\sqrt{\omega_{p_2}}\,\delta'_{p_2,q}\,\delta(\omega_{p_2}-\omega)-$$

$$\left.-\frac{i}{\pi}\omega\sqrt{\omega^2-1}\,t(r_\omega,m',m)t^*(r_\omega,m)\right\},$$

$$(9)\quad \lim_{z\to-\omega+i\varepsilon} T(z,m',m) - \lim_{z\to-\omega-i\varepsilon} T(z,m',m) = \frac{i}{\pi}\,\omega\sqrt{\omega^2-1}\,t(\nu_\omega,m')\,x(\nu_\omega,m',m).$$

And for $-1\leqslant\omega\leqslant+1$

$$(10)\quad \lim_{z\to\omega+i\varepsilon} T(z,m',m) - \lim_{z\to\omega-i\varepsilon} T(z,m',m) =$$
$$-2\pi i\sum_B \{\langle\Psi_0(m')|O|\Psi_B\rangle\langle\Psi_B|V_q^{(0)}|\Psi_0(m)\rangle\,\delta(E_B-\omega) -$$
$$-\langle\Psi_0(m')|V_q^{(0)}|\Psi_B\rangle\langle\Psi_B|O|\Psi_0(m)\rangle\,\delta(E_B+\omega)\}\sqrt{\omega_q}\,.$$

Using equations (6) and (7)

$$(11)\qquad x(\nu_\omega,m',m) = \lim_{z\to-\omega+i\varepsilon} T(z,m',m)\,.$$

Using equations (5), (11) the original integral equations (3) and (4) are reduced to a standard Riemann-Hilbert boundary problem. In the following the limits to the real axis from above and below be indicated by + and —. Equations (8), (9), (10) for $\omega>1$ become

$$(12)\quad T^+(\omega,m',m) = \frac{1}{1+(i/\pi)\omega\sqrt{\omega^2-1}\,t^*(r_\omega,m)}\,T^-(\omega,m',m) -$$
$$-2\pi i\left\{\frac{\langle\Psi_0(m')|V_{p_2}^{(0)+}|\Psi_0(m)\rangle\,t^*(p_1,m)\sqrt{\omega_{p_1}}}{1+(i/\pi)\omega\sqrt{\omega^2-1}\,t^*(r_\omega,m)}\,\delta'_{q_1,q}\,\delta(\omega_{p_1}-\omega)+\right.$$
$$\left.+\frac{\langle\Psi_0(m')|V_{p_1}^{(0)+}|\Psi_0(m)\rangle\,t^*(p_2,m)\sqrt{\omega_{p_2}}}{1+(i/\pi)\omega\sqrt{\omega^2-1}\,t^*(r_\omega,m)}\,\delta'_{p_2,q}\,\delta(\omega_{p_2}-\omega)\right\},$$

$$(13)\qquad T^+(-\omega,m',m) = \frac{1}{1-(i/\pi)\omega\sqrt{\omega^2-1}\,t(\nu_\omega,m')}\,T^-(-\omega,m',m)\,,$$

and for $-1\leqslant\omega\leqslant+1$

$$(14)\qquad T^+(\omega,m',m) - T^-(\omega,m',m) =$$
$$-2\pi i\sum_B \{\langle\Psi_0(m')|O|\Psi_B\rangle\langle\Psi_B|V_q^{(0)}|\Psi_0(m)\rangle\,\delta(E_B-\omega) -$$
$$-\langle\Psi_0(m')|V_q^{(0)}|\Psi_B\rangle\langle\Psi_B|O|\Psi_0(m)\rangle\,\delta(E_B+\omega)\}\sqrt{\omega_q}\,.$$

Equations (12), (13), (14) form a Riemann-Hilbert boundary problem which with one difference is extensively treated by MUSKHELISHVILI ([8]). As a con

([8]) M. I. MUSKHELISHVILI: *Singular Integral Equations* (Groningen, 1953).

sequence of the δ-functions of energy that appear above the Hölder condition is not satisfied, we shall nevertheless continue to use the methods used by MUSKHEKUSHVILI ([8]) under more restrictive conditions. The problem is to find the sectionally analytic function $T(z)$ having finite degree at infinity, satisfying the boundary condition

$$T^+(t) = G(t)\,T^-(t) + g(t)$$

on the arc L. The solution is ([8])

$$T(z) = \frac{Z(z)}{2\pi i}\int_L \frac{g(t)\,\mathrm{d}t}{Z^+(t)(t-z)} + Z(z)\,P(z)\,, \tag{15}$$

where $Z(z)$ is the solution of the homogeneous boundary problem which for this purpose is

$$Z(z) = \exp\left[\Gamma(z)\right], \tag{16}$$

where

$$\Gamma(z) = \frac{1}{2\pi i}\int_L \frac{\ln G(t)}{t-z}\,\mathrm{d}t\,, \tag{17}$$

and $P(z)$ is an arbitrary polynomial. $T(z)$ is of zero degree at infinity by inspection of equations (3), (4), hence $P(z)$ is zero for our problem. Using equations (12), (13), (14) in (15), (16), (17) the meson production amplitude becomes

$$\begin{aligned} T^+(\omega, m', m) = t(q_\omega, m', m) = \\ = -Z^+(\omega)\Bigg[\int_{-1}^{+1}\mathrm{d}\omega' \sum_B \Bigg\{\frac{\langle\Psi_0(m')|O|\Psi_B\rangle\langle\Psi_B|V_q^{(0)}|\Psi_0(m)\rangle\sqrt{\omega_q}}{Z^+(\omega')(\omega'-\omega)}\,\delta(E_B-\omega') - \\ - \frac{\langle\Psi_0(m')|V_q^{(0)}|\Psi_B\rangle\langle\Psi_B|O|\Psi_0(m)\rangle\sqrt{\omega_q}}{Z^+(\omega')(\omega'+\omega)}\,\delta(E_B+\omega')\Bigg\} + \\ + \frac{\langle\Psi_0(m')|V_{p_2}^{(0)+}|\Psi_0(m)\rangle\, t^*(p_1, m)\sqrt{\omega_{p_1}}\,\delta'_{p_1,q}}{Z^+(\omega_{p_1})(\omega_{p_1}-\omega)\left(1+(i/\pi)\omega_{p_1}\sqrt{\omega_{p_1}^2-1}\,t^*(r_{\omega_{p_1}}, m)\right)} + \\ + \frac{\langle\Psi_0(m')|V_{p_1}^{(0)+}|\Psi_0(m)\rangle t^*(p_2, m)\sqrt{\omega_{p_2}}\,\delta'_{p_2,q}}{Z^+(\omega_{p_2})(\omega_{p_2}-\omega)\left(1+(i/\pi)\,\omega_{p_2}\sqrt{\omega_{p_2}^2-1}\,t^*(r_{\omega_{p_2}}, m)\right)}\Bigg], \end{aligned} \tag{18}$$

where

$$\langle\Psi_B|O|\Psi_0(m)\rangle = -\langle\Psi_B|V_{p_1}^{(0)+}\frac{1}{H+\omega_{p_2}}V_{p_2}^{(0)+} + V_{p_2}^{(0)+}\frac{1}{H+\omega_{p_1}}V_{p_1}^{(0)+}|\Psi_0(m)\rangle\,,$$

$$\begin{aligned}\langle\Psi_0(m')|O|\Psi_B\rangle = \\ = -\langle\Psi_0(m')|V_{p_1}^{(0)+}\frac{1}{H+\omega_{p_2}-E_B}V_{p_2}^{(0)+} + V_{p_2}^{(0)+}\frac{1}{H+\omega_{p_1}-E_B}V_{p_1}^{(0)+}|\Psi_B\rangle\,.\end{aligned}$$

By taking $f_r^2(v(\varkappa)^2/2\pi) < 1$ (9) the bound states disappear (6). Using the Lee-Serber solution (6) for the scattering amplitude with $f_r^2 = 0.2$ and $v(\varkappa) = 1$

TABLE I.

E	$\pi^+ + p \to n + \pi^+ + \pi^+$		$\pi^- + p \to n + \pi^+ + \pi^-$	
	σ in $(\hbar/\mu c)^2 \cdot 10^{-2}$	Born approx.	σ in $(\hbar/\mu c)^2 \cdot 10^{-2}$	Born approx.
2.4	2.0	1.2	0.23	0.62
3.2	5.4	3.7	1.00	1.85
4.0	6.1	4.3	1.25	2.2

in Table I the various meson production cross-sections from protons are shown and compar ed with the Born approximation. E the total C.M. emergy is given in units of the pion rest mass energy.

* * *

The author wants to thank Professor M. L. GOLDBERGER for having suggested this problem and for invaluable help and assistance.

(9) $v(\varkappa)$ is the source function.

RIASSUNTO (*)

Si dimostra che, nella teoria delle particelle scalari cariche, le ampiezze della produzione mesonica soddisfano ad equazioni integrali le quali, nella sola approssimazione mesonica, si riducono al problema al contorno di Riemann-Hilbert. Se ne dà la soluzione completa.

(*) *Traduzione a cura della Redazione.*

IL NUOVO CIMENTO Vol. XIV, N. 1 1° Ottobre 1959

Structures in the Proton Spectra from n, p Reactions.

L. Colli

Istituto di Fisica dell'Università and Laboratori CISE - Milano

F. Cvelbar (*), S. Micheletti and M. Pignanelli

Istituto di Fisica dell'Università and I.N.F.N. - Sezione di Milano

(ricevuto il 2 Aprile 1959)

Summary. — Measurements on proton energy spectra from n, p reactions on Mg, Al, Si and S show the existence of well defined peaks even at excitation energy values where the excitation levels of the residual nucleus are very dense. Comparing our results with some proton spectra from d, p reactions a similarity is found in the position of these peaks on the residual excitation energy scale. By means of this comparison it is possible to establish that the n, p reactions go through a mechanism of the type of surface effect, where the residual nucleus is left preferably in some excited states probably corresponding to single particle excitation.

1. – Introduction.

In the study of the energy distribution of protons emitted in n, p reactions with 14 MeV neutrons, the existence of structure in the shape of large humps, has been shown in some previous works [1-6].

Following this, we have undertaken the systematical study of the proton spectra emitted in n, p reaction with the aim of seeing whether through the

(*) On leave of absence from Jozef Stefan Institute, Ljubljana.

(1) L. Colli and U. Facchini: *Nuovo Cimento*, **4**, 671 (1956).

(2) C. Badoni, L. Colli and U. Facchini: *Nuovo Cimento*, **4**, 1618 (1956).

(3) L. Colli and U. Facchini, *Nuovo Cimento*, **5**, 309 (1957).

(4) D. L. Allan: *Proc. Phys. Soc.*, A **70**, 195 (1957).

(5) P. V. March and W. T. Morton: *Phil. Mag.*, **3**, 1256 (1958).

(6) H. P. Eubank, R. A. Peck jr., and F. L. Hassler: *Nucl. Phys.*, **9**, 273 (1958).

particular characteristics of these humps, once the exact position on the energy scale and their width have been determined, the nature of the process through which the reaction takes place may be illuminated.

From the previous results it was quite evident that the n, p reactions take place at least partly through a mechanism of instantaneous emission type whose true nature is not yet known; by this process a greater probability for the forward emission of the particles is foreseen. Because it seemed probable to us that the peaks of the spectrum could be attributed to this instantaneous effect, we examined the spectrum of forward emitted protons with respect to incident neutrons.

For these measurements a proton detector similar to those used in previous works was set up, but with a much better resolution in energy and in angle than we had obtained so far.

The 14 MeV neutron beam was obtained by means of the reaction D+T, employing the 160 keV deuteron beam from the accelerating apparatus of the INFN, Sezione di Milano.

2. – Experimental results.

The improvement of energy resolution of the scintillator counters was obtained by introducing a light pipe between the crystal and the photomultiplier. This pipe is made up of an aluminium cylinder 5 cm in diameter, and with a length of 8 cm: a layer of MgO powder stuck with collodion diffuses the light inside the cylinder. As has been shown by STOKES *et al.* (7), in this arrangement the light collection is improved because the effect of the dishomogenity of the photocathode is eliminated.

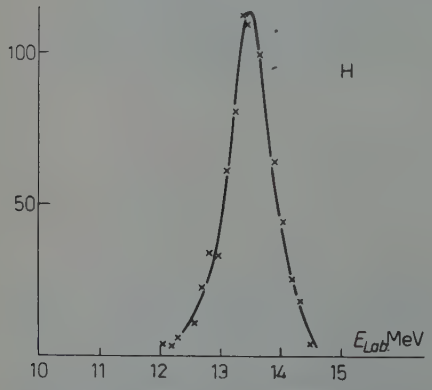

Fig. 1. – Spectrum of recoil protons from a polithene target.

Using a polithene target 1 cm in diameter, the line shown in Fig. 1 is obtained for the spectrum of hydrogen recoil protons; the width of the line turns out to be $\sim 6.5\%$.

A width of 3.5% is to be attributed to the angular opening with which the protons are detected and a further 3% to the widening caused by the self-

(7) R. H. STOKES, J. A. NORTHROP and R. BOYER: *Rev. Scient. Inst.*, **29**, 61 (1958).

absorption in the target. The effective resolution is therefore about 4.5%. All the other characteristics of the detector are the same as those described in a previous work ([8]).

Measurements were taken by placing the target at 14 cm from the neutron source, so that the particles emitted in forward direction of the incident neutrons in an angle of about 30° are detected, the most probable angle being 17°. By this arrangement the energy spectra of particles emitted from Al, Mg, Si and S were obtained. These spectra are shown in Fig. 2, 3, 4 and 5.

Aluminium is a naturally pure isotope. For Mg, Si and S it is possible to attribute the reaction to the lightest isotope, which in these cases is always the most abundant (see also the results of LEVKOWSKI ([9])).

Furthermore, as we have found that the 14 MeV neutrons produce in some elements a notable amount of deuterons from n, d reactions, and as such deuterons are counted by our detector, thus altering the shape of the proton spectra, we have set up an electronic device capable of separating pulses caused by protons from those caused by deuterons in the crystal. This results was obtained using the different pulses given by the two particles in the proportional counter.

In this way we have found a notable amount of deuterons in the S spectrum and a small amount in the Al spectrum. The measurements on deuterons will be published shortly.

The spectra given here are those obtained by substracting the deuteron spectrum from the total one.

3. – Discussion of results.

The spectra given here are rather different from the ones previously published: this is due partly to the improved energy resolution, and partly to the smaller detection angle; with a rather large detection angle, like the one previously used ($\sim 60°$), there is indeed an additional energy smearing due to the different recoil energy of the nucleus in the different possible directions.

The proton spectra presented here put clearly into evidence the existence of well defined peaks in them even at a rather high excitation energy, where the residual nucleus levels are very close to each other compared with the resolution of our apparatus. Because of these conditions, our measurements give an average on the residual level density times the excitation probability of each level. The peaks shown in our results must therefore be interpreted as gross structures.

We can now analize the various spectra studied.

([8]) G. MARCAZZAN, M. PIGNANELLI and A. SONA: *Nuovo Cimento*, **10**, 155 (1958).
([9]) V. N. LEVKOVSKI: *Journ. Exp. Theor. Phys.*, **6**, 1174 (1958).

3·1. *Aluminium.* – In the case of ^{27}Al the spectrum suggests a peak at 3.7 MeV on the proton scale and one at 5 MeV; the two peaks at 7.5 and at 9.3 MeV are very well shown, and a peak at 11.3 MeV, corresponding to the ground level of the residual nucleus ^{27}Mg, is hardly visible.

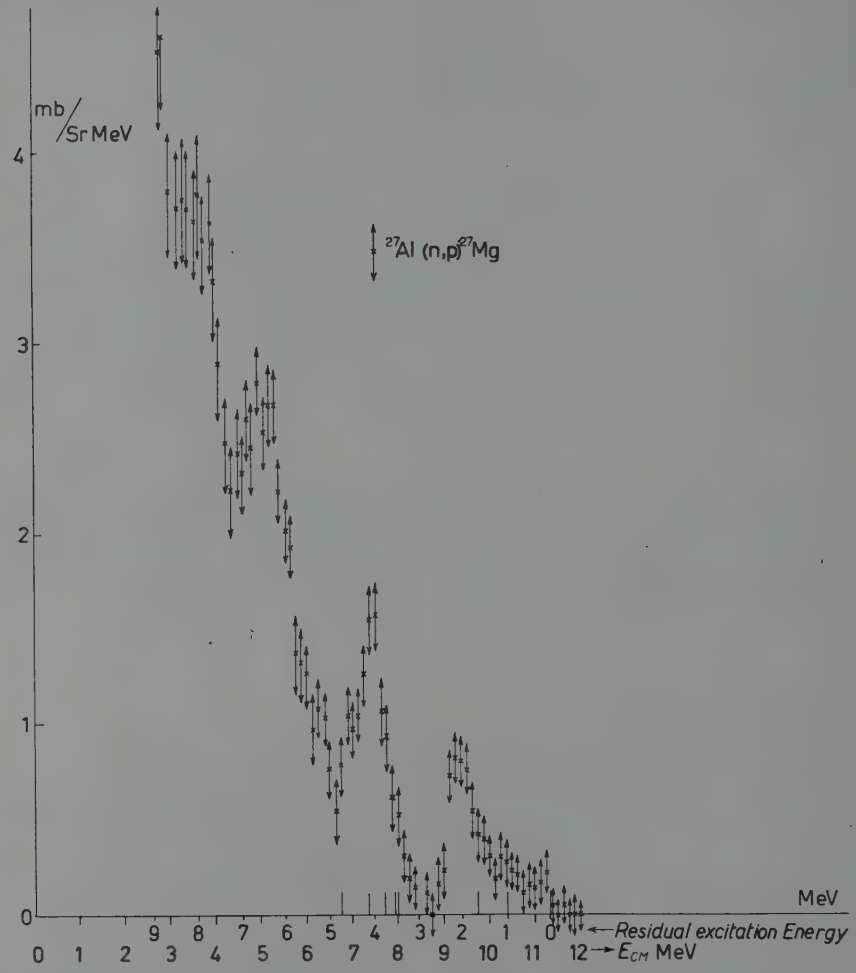

Fig. 2. – Spectrum of protons from ^{27}Al (n, p) ^{27}Mg. Known excitation levels of ^{27}Mg are shown on the residual excitation energy scale.

It is interesting to compare this spectrum with the already known levels of the residual nucleus ^{27}Mg recently studied by means of the d, p reaction by HINDS *et al.* ([10]). These levels are above the ground level at 1 – 1.66 – 3.5 – 3.56 – 3.75

([10]) S. HIND, R. MIDDELTON and G. PARRY: *Proc. Phys. Soc.*, **71**, 49 (1958).

4.13 – 4.75 MeV. The level structure of the ^{27}Mg excited levels above this energy is not known. The first two levels are not resolved in our spectrum, whilst the first resolved peak corresponds to an excitation energy of the residual nucleus of 2.2 MeV. A level in this position had not yet been found.

The peak at 7.5 MeV, corresponding to an excitation energy of 4 MeV, may contain the levels included between 3.50 and 4.75 MeV.

It is probable that at higher excitation energy the levels become more dense. The proton peaks at 3.7 and 5 MeV, corresponding to an excitation energy of 7.9 and 6.6 MeV, are found in a zone where the levels should be already so dense that they can be interpreted as explained above: an average on the density level and on their excitation probability.

3·2. *Magnesium.* – In the ^{24}Mg(n, p)^{24}Na spectrum shown in Fig. 3 a peak is found at 4.25 MeV on the proton scale, another one at 6.8 MeV, is very clearly resolved, and a small peak can be seen at 8.3 MeV, corresponding to the ^{24}Na ground state.

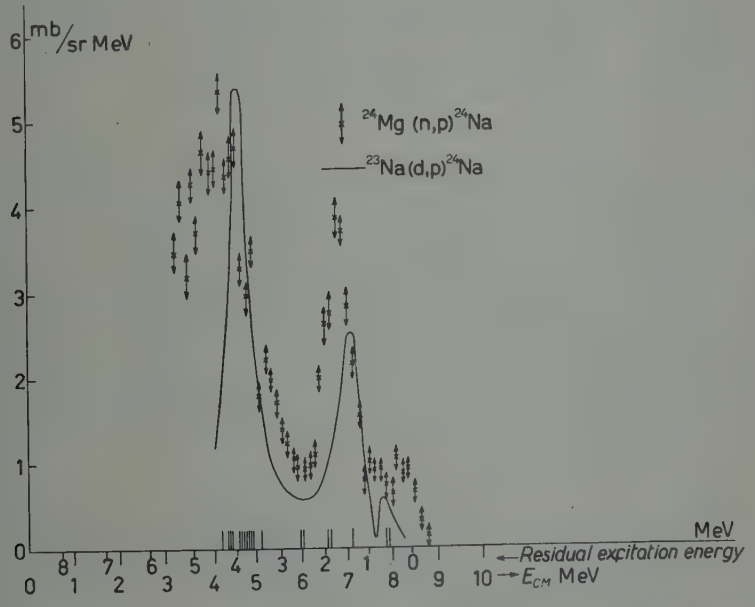

Fig. 3. – Spectrum of protons from ^{24}Mg(n, p)^{24}Na compared with ^{23}Na(d, p)^{24}Na. Residual excitation levels are also shown.

The ^{24}Na excited levels have been studied by the ^{23}Na(d, p)^{24}Na reaction by SPERDUTO and BUECKNER ([11]).

([11]) A. SPERDUTO and W. W. BUECKNER: *Phys. Rev.*, **88**, 574 (1952).

It was first pointed out by BLOK and JONKER ([12]) that a similarity exists between the peaks in the n, p proton spectrum and the structures shown by the spectra of protons from some d, p reactions. The existence of such structures in d, p proton spectra is now a well established fact ([13,14]); moreover we have now for n, p protons pectra much better resolved peaks than were given by the previous results; as a consequence, we can now discuss these peaks much more easily.

Applying to the proton spectrum from the ^{23}Na(d, p)^{24}Na an energy smearing as given by a 4.5% energy resolution, (the effective resolution of our detector) a spectrum is obtained very similar to ours, with two peaks at 1.5 and 3.9 MeV on the ^{24}Na excitation energy scale; this spectrum is shown in Fig. 3; the positions of the peaks are close enough to the ones which we obtain, namely 1.7 and 4.3; the differences between these values can be due to errors of energy scale. It is also interesting to note that both peaks have an intensity roughly similar in both spectra. These facts show that in the two reactions compared here the residual nucleus ^{24}Na is left in some levels or groups of levels with greater probability than in others, and that these more favourable levels are the same for both reactions.

Comparing our spectrum with these levels, it can be seen that the first peak includes three levels, whilst the second includes about ten.

3·3. *Silicon.* – The Silicon spectrum (Fig. 4) shows five peaks: at 3 – 5.5 – 7 –8.1 and 9.3 MeV, the last corresponding to the ground level. Positions on the residual ^{28}Al excitation scale are: 6.7 – 4 – 2.4 and 1.3 MeV.

We can compare this spectrum with the one obtained by ENGE *et al.* ([15]) for the ^{27}Al(d, p)^{28}Al, to the latter of which an energy smearing having been applied as mentioned above.

The first peak at 1,3 MeV is not shown in the d, p spectrum, but the second (at 2.5 MeV) and the third (here at 3.7 MeV) are. The peak at 4.75 MeV in the d, p curve is not shown in ours.

3·4. *Sulphur.* – The ^{32}S n, p spectrum is shown in Fig. 5. Peaks are found at 6.2 (uncertain) and at 8.1 – 9.5 MeV. Another small uncertain peak is found at 11.2 MeV. The ground level is not shown.

([12]) J. BLOK and C. C. JONKER: *Nuovo Cimento*, **6**, 378 (1957).

([13]) L. COLLI and S. MICHELETTI: *Nuovo Cimento*, **6**, 1001 (1957).

([14]) J. P. SCHIFFER and L. L. LEE jr.: *Phys. Rev.*, **109**, 2098 (1958) and J. P. SCHIFFER, L. L. LEE jr., J. L. YNTEMA and B. ZEIDMAN: *Comptes Rendus du Congrès Int. de Phys. Nucl. de Paris*, Juillet 1958, p. 536 (Paris, 1959).

([15]) H. A. ENGE, W. W. BUECKNER and A. SPERDUTO: *Phys. Rev.*, **88**, 936 (1952).

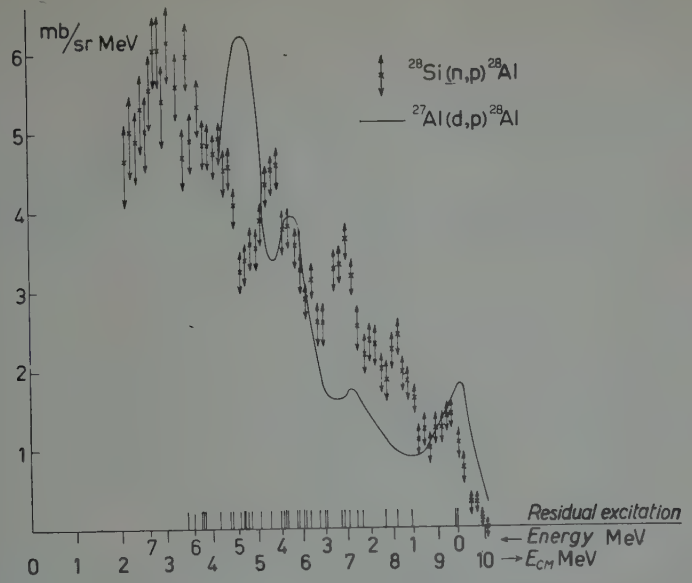

Fig. 4. – Spectrum of protons from ^{28}Si(n, p)^{28}Al compared with ^{27}Al(d, p)^{28}Al.

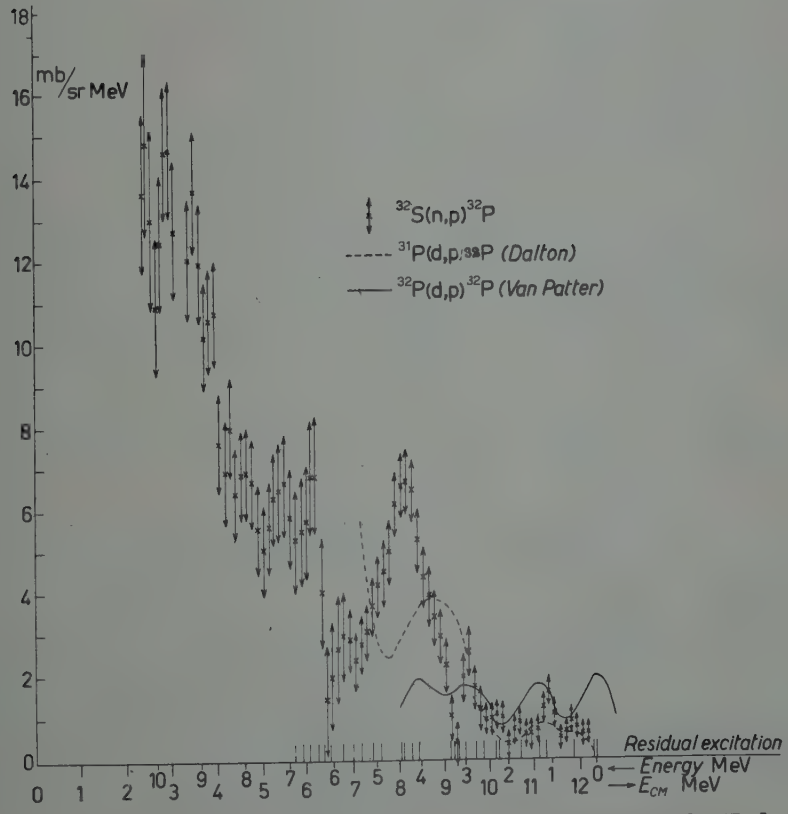

Fig. 5. – Spectrum of protons from ^{32}S(n, p)^{32}P compared with ^{31}P(d, p)^{32}P

On the residual excitation energy scale the peaks are at 6.4 – 4.3 – 2.8 and 1.1 MeV.

The d, p curves, obtained by smearing the result of VAN PATTER *et al.* ([16]) and of DALTON *et al.* ([16]), are shown on the same Fig. 5.

All the three curves show the last peak at 1.2. The peaks at 2.8 and at 4.3 MeV on the n, p are found at about the same energy on one of the d, p curves, while the other d, p curve shows a large hump, at 3.8 MeV.

4. – Conclusion.

The comparison between the n, p and d, p reactions permits us to reach the conclusion that the mechanism which gives rise to the n, p reaction in the studied nuclei presents certain similarities to the mechanisms by which the d, p reactions take place.

The d, p reactions are explained on the basis of the « stripping process » where the neutron is stripped from the deuteron, and captured by the target nucleus; this is essentially a surface process, in which the nucleus core is left undisturbed.

It has been suggested by some authors that the structures present in the spectra of protons emitted in the d, p reactions ([17]) must be interpreted as single particle levels in which the residual nucleus is preferably left, and this follows the arguments of LANE, THOMAS and WIGNER ([18]).

In the case of the d, p reactions the structure would correspond to single particle levels of the neutron which falls in the nucleus target.

The fact that the n, p reactions studied here show in a number of cases peaks in the proton spectra at the same residual nucleus excitation energy which are found for the d, p reactions, should mean that in the n, p reactions too, the residual nucleus remains with greater probability in the excitation levels corresponding to a neutron captured in a single particle level.

In the reactions n, p and d, p the proton emitted under this hypothesis absorbs the energy difference between the incident energy and the single particle levels of the neutron in the nucleus.

As in the n, p reaction, the proton emission may be believed to proceed through an instantaneous process (it can be deduced by the peaked forward

---

([16]) D. M. VAN PATTER, P. M. ENDT, A. SPERDUTO and W. W. BUECKNER: *Phys. Rev.*, **86**, 502 (1952); A. W. DALTON, S. HINDS and G. PARRY: *Proc. Phys., Soc.*, A **70**, 586 (1957).

([17]) A. M. LANE: private communication (1957), and *Comptes Rendus du Congrès Int. de Phys. Nucl.* (Paris, 1959), pag. 113.

([18]) A. M. LANE, R. G. THOMAS and E. P. WIGNER: *Phys. Rev.*, **98**, 693 (1955).

angular distribution ([19])) and as the conditions of the residual nucleus are the same as in the d, p reactions, we can deduce that the n, p reaction also goes through a surface interaction, where the less bound proton is emitted and the neutron is captured in the single particle state. In these conditions the nucleus core is left undisturbed. Following this deduction, the protons at the surface would be the ones determinating the reaction.

GROSHEV *et al.* ([20]), while studying the spectrum of the γ emitted in n, γ reactions by thermal neutrons, showed in some instances a result similar to the one discussed here. Even in those γ spectra it is found that some lines or groups of lines are particularly intense, corresponding to the residual nucleus energies where peaks in the d, p spectra are found. This effect is found in some light nuclei, where the compound nucleus resonance levels are absent.

Even in this case the authors suggest that each group of lines correspond to one single particle state of the captured neutron. LANE ([21]) assumes that these effects are due to direct capture processes.

The results on (d, p), (n, p), and (n, γ) reactions would therefore show that the residual nucleus remains preferably excited in a state in which one single neutron has all the excitation energy.

It should be noted that in all these three types of reactions the captured particle is a neutron.

* * *

We gladly thank Prof. P. CALDIROLA, U. FACCHINI and C. SALVETTI for stimulating discussions and Dr. R. CHAMINADE for interesting discussions on the detection technique.

([19]) Preliminary results by L. COLLI, M. G. MARCAZZAN and A. M. SONA.

([20]) L. V. GROŠEV, A. V. DEMIDOV, V. N. LUTSENKO and V. I. PELEHOV: *II United Nations Int. Conf. on the Paceful Uses of Atomic Energy*, A/conf/15/P/2029 (1958)

([21]) A. M. LANE: private communication.

RIASSUNTO

Le misure di spettri di energia di protoni dalla reazione n, p su Mg, Al, Si e S qui presentate mostrano l'esistenza di picchi ben definiti in questi spettri, anche in corrispondenza a valori dell'energia di eccitazione del nucleo residuo dove i livelli eccitati di questo nucleo sono molto fitti. Confrontando i nostri risultati con alcuni spettri di protoni emessi da reazioni d, p, si trova che i picchi esistenti in ambedue queste reazioni si trovano agli stessi valori dell'energia di eccitazione. Questo confronto permette di concludere che le reazioni n, p qui studiate procedono attraverso un meccanismo del tipo ad interazione di superficie, dove il nucleo residuo rimane preferibilmente in stati eccitati che corrispondono a livelli di eccitazione di particella singola.

IL NUOVO CIMENTO Vol. XIV, N. 1 1° Ottobre 1959

Primary Heavy Cosmic Rays Near the Geomagnetic Equator.

O. B. Young and F. W. Zurheide

Southern Illinois University - Carbondale, Ill.

(ricevuto il 22 Aprile 1959)

Summary. — G-5 emulsions were exposed in February, 1957 during the Operation EQUEX on two flights of about 100000 foot altitudes for about $7\frac{1}{2}$ h each. Tracks of nuclei of $Z \geqslant 10$ were studied. The δ-ray method of counting was used. Results are given for the angular distribution, charge spectrum, flux at the top of the atmosphere, and attenuation mean free path.

1. – Introduction.

In recent years a great deal of direct investigation has been done on the high energy primary cosmic rays which enter our atmosphere from the outer space. This investigation was restricted to the heavy nuclei with charges equal to or greater than ten. The electron sensitive photographic emulsions used in this investigation were of the Ilford G-5 type manufactured by Ilford Ltd. of London. All emulsions had a thickness, before development, of 600 μm. Three stacks of emulsions were exposed on two different balloon flights from Guam, Marianas Island, 4° N G.M. latitude during February, 1957, as part of the United States Office of Naval Research 1957 Equatorial Expedition. The flight paths, time of day, and weather conditions were practically identical for these two flights organized jointly by the Winzen Research, Inc. and the United State Navy. Complete flight data are given in Table I.

The δ-ray method of counting was used to determine the relative characteristics of the tracks. The fixing of $Z = 10$ was made by taking scattering measurements on lighter tracks.

2. – Experimental procedure.

After processing in our laboratory, each emulsion was scanned for tracks of heavy nuclei, and the length and azimuthal angle of each track were measured. The total area scanned for each plate is given in Table I. The δ-rays of each track were counted by a procedure which is in accordance with the counting criteria developed and adopted by this laboratory (1).

TABLE I. – *Flight data.*

Flight number	Plate number	Date of flight	Altitude (g/cm²)	Eff. time of flight (h)	Area scanned (cm²)
6	GC-3	Feb. 10, 1957	8.2	7.58	193.0
7	GA-2	Feb. 12, 1957	9.0	7.58	132.8
7	GB-1	Feb. 12, 1957	9.0	7.58	66.4

From the data obtained by the above measurements, the zenith angle and the number of δ-rays per 100 μm before shrinkage were calculated for each track by methods similar to those used in a previous article by YOUNG and HARVEY (2). These were used in drawing the angular distribution and charge spectrum for each plate and for flux and mean free path determinations.

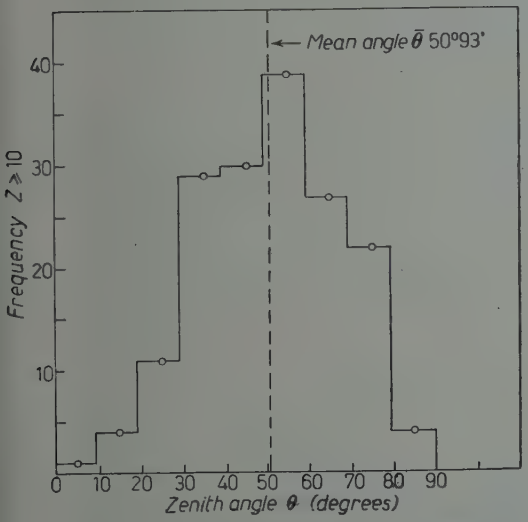

Fig. 1. – Angular distribution for flight 6.

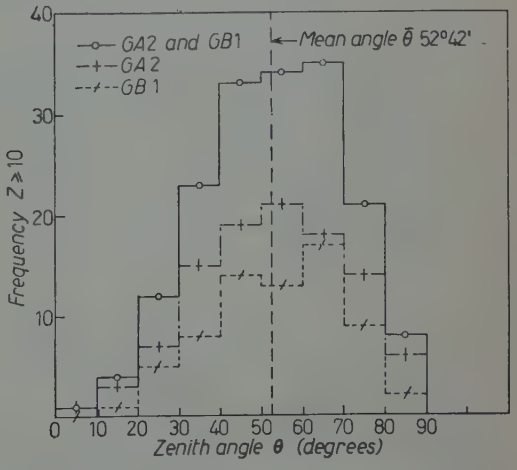

Fig. 2. – Angular distribution for flight 7.

(1) O. B. YOUNG and W. C. BALLOWE: *Am. Journ. Phys.*, **24**, 157 (1956).
(2) O. B. YOUNG and F. E. HARVEY: *Phys. Rev.*, **109**, 529 (1958).

The scanning and all other measurements were made using five Bausch and Lomb microscopes. One of the microscopes was equipped with a special scattering substage and a filar micrometer eyepiece which made possible measurements to the accuracy of $\pm .1\,\mu$m.

The angular distribution for the nuclei with $Z \geqslant 10$ for each flight and their combination are shown in Figs. 1, 2 and 3. The mean zenith angle for the combination was found to be $\bar{\theta} = 51.7°$.

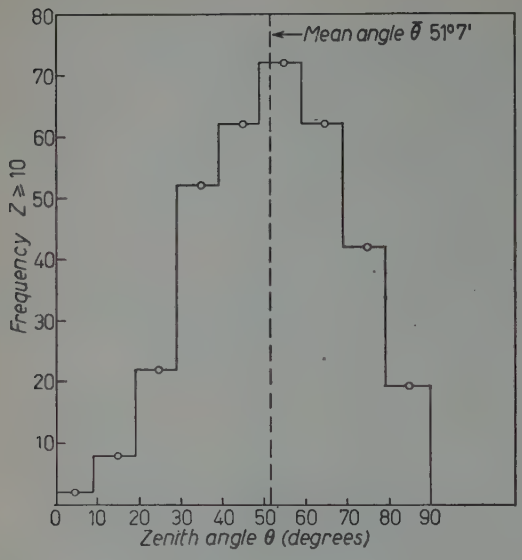

Fig. 3. – Angular distribution for flights 6 and 7.

3. – Charge spectrum.

The cut-off energy at 4° N G.M. latitude is about 8 GeV per nucleon; consequently, the velocity of the primary nuclei can be assumed to be relativistic. Therefore the charge Z of each nucleus can be determined from the

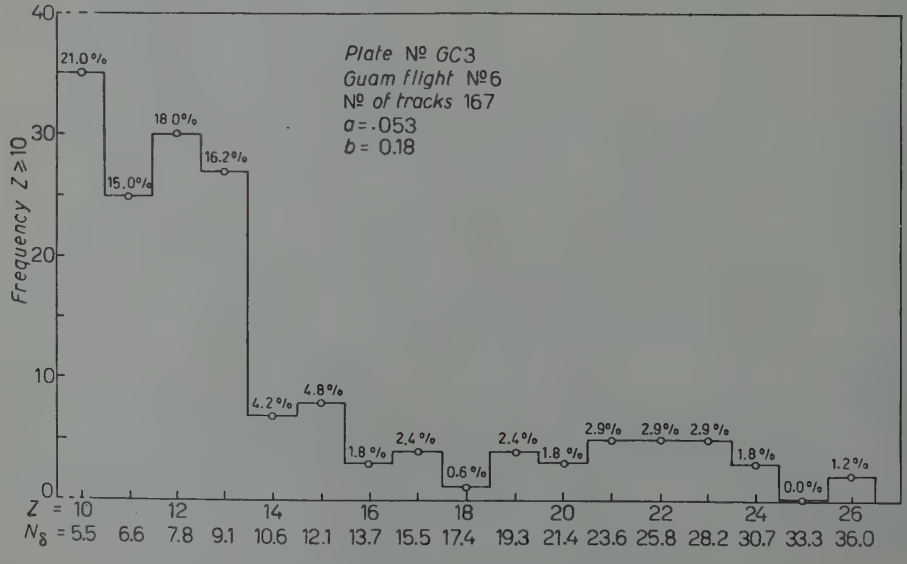

Fig. 4. – Charge spectrum for flight 6.

number of δ-rays per 100 μm by (3)

$$N_\delta = aZ^2 + b \,,$$

where a and b are constants for each plate.

To evaluate the constants a and b, long light tracks were counted for δ-rays and their mean scattering angles $\bar{a}$ measured (2). In addition to these, long tracks from the CNOF (carbon, nitrogen, oxygen, fluorine) group were

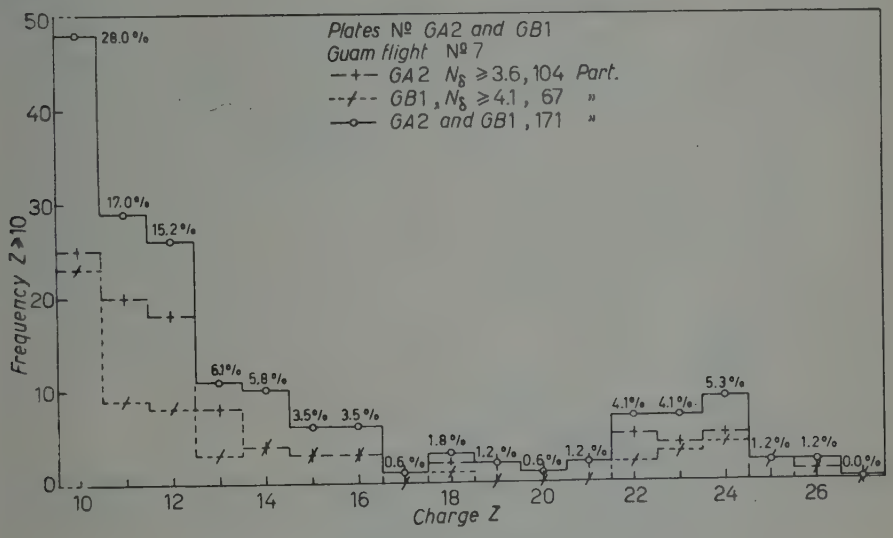

Fig. 5. – Charge spectrum for flight 7.

also used. The δ-ray density for each charge was obtained by plotting the number of δ-rays per hundred microns against the mean scattering angle per hundred microns (4). From each graph the calibration constants a and b were obtained by the least square method, and the results are given in Table II.

From the results in Table II, the value for the charge of each particle was determined, and the results are shown in the charge spectra for each flight in Figs. 4 and 5. A summary charge spectrum is shown in Fig. 6.

TABLE II. – *Calibration constants.*

Plate number	a	b
GA-2	0.038	0.20
GB-1	0.044	0.20
GC-3	0.053	0.18

(3) A. D. DAINTON and D. W. KENT: *Phil. Mag.*, **41**, 963 (1950).
(4) A. D. DAINTON, P. H. FOWLER and D. W. KENT: *Phil. Mag.*, **42**, 327 (1951).

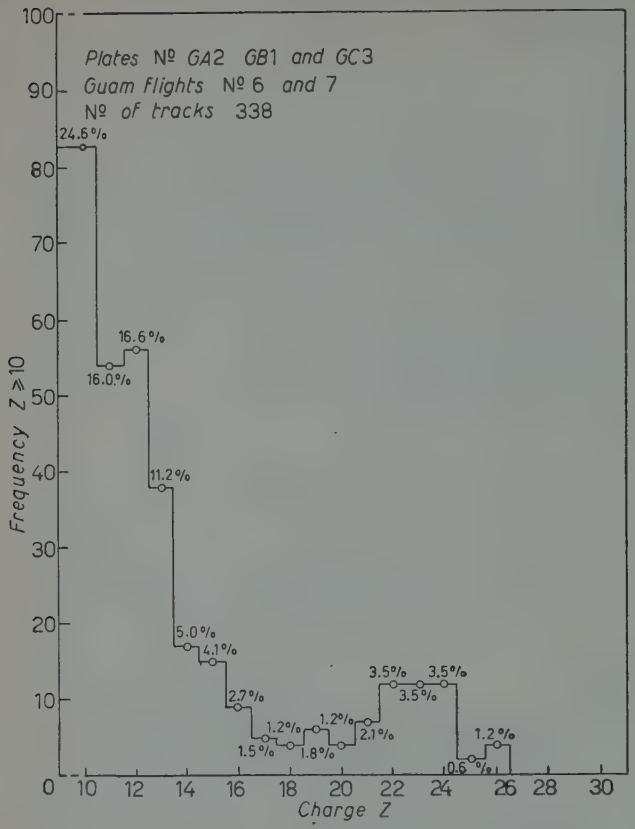

Fig. 6. – Summary charge spectrum for flight 6 and 7.

The relative abundances for the charges are compared with the corresponding charges from a like spectrum of 2 021 particles obtained by this laboratory from flights at altitudes varying from 7.7 to 17.5 g/cm² at 41° N geomagnetic latitude (Texas) and are shown in Table III. This indicates a correct matching in the charges for both spectra. It is to be observed that no particles with charges $Z > 26$ appear in either set of results.

TABLE III. – *Abundance of elements at Texas and Guam.*

Element	Z	Abundance (%) of 2 021 tracks from Texas	Abundance (%) of 338 tracks from Guam
Ne	10	21.70	24.6
Na	11	13.65	16.0
Mg	12	15.96	16.6
Al	13	11.17	11.2
Si	14	8.66	5.0
P	15	5.79	4.1
S	16	2.37	2.7
Cl	17	3.41	1.5
A	18	2.41	1.2
K	19	2.57	1.8
Ca	20	2.27	1.2
Sc	21	2.27	2.1
Ti	22	1.93	3.5
V	23	1.53	3.5
Cr	24	1.88	3.5
Mn	25	0.79	0.6
Fe	26	1.43	1.2

4. – Flux and mean free path.

Assuming the flux of the heavy primary cosmic rays to be isotropic with respect to the zenith angle, the flux at the zenith angle θ can be expressed in terms of the average atmospheric depth h and the flux at the top of the atmosphere I_0 by

$$I(\theta) = I_0 \exp\left[-h/\lambda \cos\theta\right],$$

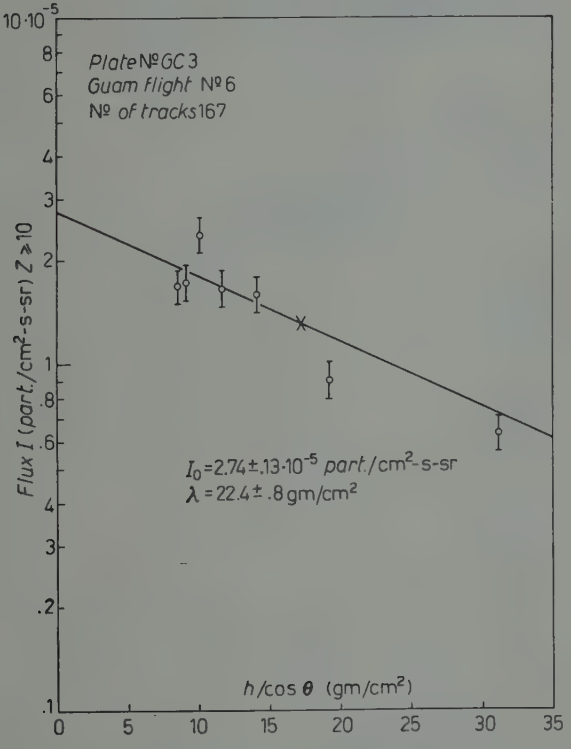

Fig. 7. – Flux for flight 6.

where λ is the attenuation mean free path. The number of particles in a unit angle interval at the zenith angle θ is given for a plate flown in vertical position by

$$N(\theta) = 4AT \cdot I(\theta) \cdot \sin^2\theta\,,$$

where A is the scanned area in cm², T is the effective flight time in seconds, and $I(\theta)$ is in particles per cm² s sr. If the two equations are combined and

the common logarithm is taken, we have (3)

$$\log\left(\frac{N(\theta)}{\sin^2\theta}\right) = \log\left(4ATI_0\right) - \left(\frac{\log e}{\lambda}\right)\frac{h}{\cos\theta}.$$

A plot of this equation, as in Figs. 7, 8 and 9, gives the slope as $-(\log e)/\lambda$ and the flux intercept as $\log(4ATI_0)$. The best fit straight line was found by

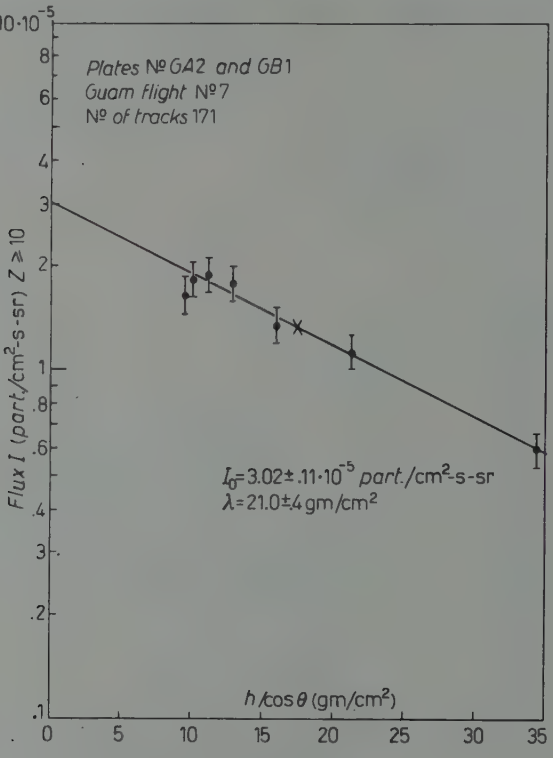

Fig. 8. – Flux for flight 7.

the least squ are method. This line determined the slope and the flux intercept. I_0 and λ were then computed directly and are given in Table IV.

TABLE IV. – *Flux and attenuation mean free path.*

Flight number	Number of nuclei with $Z \geqslant 10$	I_0 (part./m^2 s sr)	λ (g/c m^2)
6	167	0.274 ± .013	22.4 ± .8
7	171	0.302 ± .011	21.0 ± .4
6 and 7	338	0.281 ± .010	22.9 ± .3

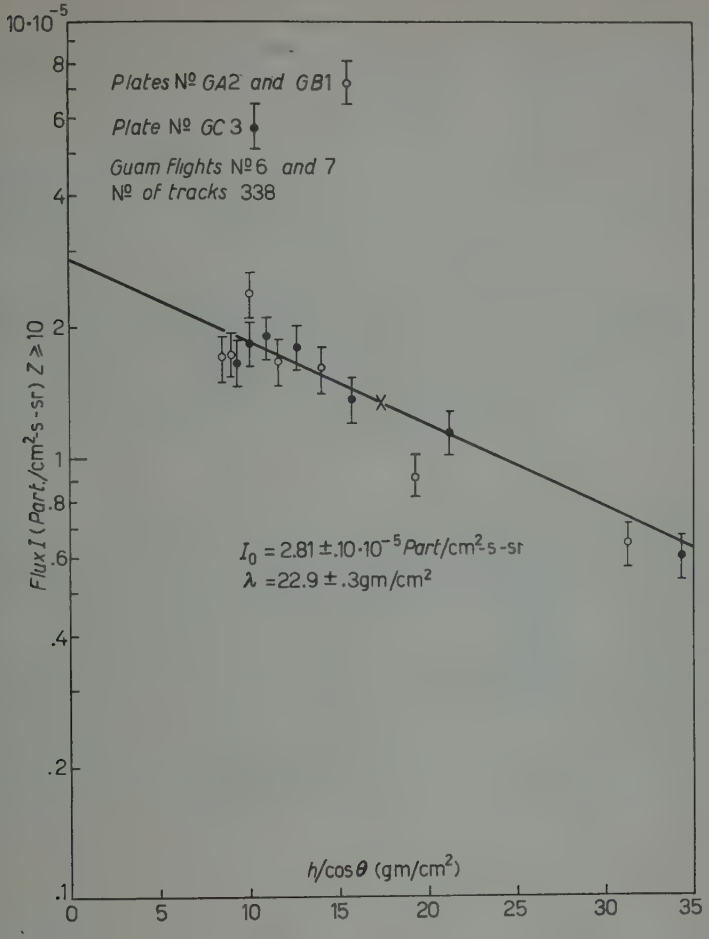

Fig. 9. – Flux for flights 6 and 7.

5. – Summary and conclusions.

In this experiment, two flights were made near the geomagnetic equator where all of the primary cosmic rays have relativistic velocities. A summary charge spectrum was given for a total of 338 nuclei with $Z \geqslant 10$. The abundance ratios compared closely with those obtained at 41° N G.M. latitude.

The total angular distribution for $Z \geqslant 10$ indicated a mean zenith angle of 51.7 degrees.

The total flux value for $Z \geqslant 10$ at the top of the atmosphere obtained from both fligths was found to be

$$I_0 = 0.281 \pm .010 \text{ particles/m}^2 \text{ s sr}.$$

This value is approximately one-ninth of the value for the flux obtained by this laboratory for 41° N G.M. latitude. Since the cut-off energy at 41° N is 1.5 GeV per nucleon (2), more particles are admitted than are at Guam where the cut-off energy is 8 GeV per nucleon.

The attenuation mean free path of heavy nuclei with $Z \geqslant 10$ was found to be

$$\lambda = 22.9 \pm .3 \text{ g/cm}^2 .$$

This result agrees with the mean free path value of 23 g/cm² obtained from the Texas flights, but gives no indication that the mean free path is energy dependent above the 6 GeV per nucleon range (5). More flights are needed at this latitude to increase the data so that the charge spectrum might be more definite.

* * *

The authors are grateful for the financial support given this research by the Office of Ordnance Research of the U.S. Army and by the International Geophysical Year Program. Also appreciated is the assistance given by Prof. MARCEL SCHEIN and his Cosmic Ray Group at the University of Chicago.

(5) Y. H. NOON and M. F. KAPLON: *Phys. Rev.*, **97**, 769 (1955).

RIASSUNTO (*)

Nel Febbraio 1957, durante l'operazione EQUEX, furono esposte in due lanci, all'altezza di 100 000 piedi circa e per la durata approssimativa di 7½ h ciascuno, delle emulsioni G-5. Furono esaminate le tracce dei nuclei di $Z \geqslant 10$. Fu adottato il metodo del conteggio dei raggi δ. Si riportano i risultati relativi alla distribuzione angolare, allo spettro della carica, al flusso sulla sommità dell'atmosfera ed al cammino libero medio di attenuazione.

(*) *Traduzione a cura della Redazione.*

IL NUOVO CIMENTO Vol. XIV, N. 1 1° Ottobre 1959

Coincidence Studies of the Radiations from the Decay of ^{182}Ta.

B. P. Singh, H. S. Hans and P. S. Gill

Department of Physics, Muslim University - Aligarh

(ricevuto l'11 Maggio 1959)

Summary. — γ-rays at 68 keV, 100 keV, 152 keV, 1.122 MeV, 1.189 MeV, and 1.222 MeV have been found in the decay of ^{182}Ta using a scintillation spectrometer. The γ-ray of 68 keV is found to be in coincidence with 57 keV, 100 keV, 264 keV, 1.122 MeV and 1.222 MeV energy γ-rays. The γ-ray of 152 keV is found to be in coincidence with 57 keV, 100 keV, 1.122 MeV and 1.222 MeV energy γ-rays and also the 222 keV γ-ray is found to be in coincidence with 57 keV, 100 keV and 1.231 MeV energy γ-rays. Two β-ray groups of maximum energy of (560 ± 50) keV and (460 ± 40) keV have been found by coincidence studies. These coincidence studies have established the levels at 100 keV, 1.222 MeV, 1.290 MeV, 1.331 MeV, 1.374 MeV and 1.554 MeV in ^{182}W.

1. – Introduction.

Radiations from the decay of ^{182}Ta have been investigated by several workers making use of different techniques. The conversion electron spectrum and β-ray spectrum have been measured by Beach *et al.* [1], O'Meara [2], Cork *et al.* [3], and Murray *et al.* [4]. The energies of γ-rays were measured by means of photoelectrons from a radiator in β-ray spectrometer by Rall and Wilkinson [5], Goddard and Cook [6], and Beach *et al.* [1]. But later on,

---

[1] L. A. Beach, C. L. Peacock and R. G. Wilkinson: *Phys. Rev.*, **76**, 1585 (1949).

[2] F. E. O'Meara *Phys. Rev.* **79**, 1032 (1950).

[3] J. M. Cork, H. B. Keller, W. G. Rutledge and A. E. Stoddard: *Phys. Rev.*, **78**, 95 (1950).

[4] J. J. Murray, F. Bohem, P. Marmier and J. W. M. DuMond: *Phys. Rev.*, **97**, 1007 (1955).

[5] W. Rall and R. G. Wilkinson: *Phys. Rev.*, **71**, 321 (1947).

[6] C. H. Goddard and C. S. Cook: *Phys. Rev.*, **76**, 1419 (1949).

due to large number of γ-rays, curved crystal spectrometers were used by MULLER *et al.* ([7]), FOWLER *et al.* ([8]), and MURRAY *et al.* ([4]). MULLER *et al.* ([7]) proposed four possible decay schemes for the low energy γ-ray spectrum by «topological maps» considering the energies of γ-rays. MURRAY *et al.*, on the other hand, reported 27 γ-transitions. Also internal conversion coefficient and multipolarities were deduced for most of these transitions. By energy considerations, they proposed a decay scheme with 11 levels in ^{182}W. The β-ray group of maximum energy of 0.530 MeV has been reported by BEACH *et al.* ([1]) and others. But recently DEMUYNCK *et al.* ([9]) have reported two more β-ray groups of maximum energy of 440 keV and 360 keV.

The coincidence studies by MANDEVILLE and SCHERB ([10]) resulted in the identification of one β-ray group of maximum energy of 510 keV. They further reported that high energy γ-ray transitions are not in cascade. Further coincidence studies have been made using scintillation spectrometers by WILLIAMS and ROULSTON ([11]), and also by MIHELICH ([12]). WILLIAM and ROULSTON ([11]) reported that the 67.74 keV γ-ray is in coincidence with the 1.122 and 1.222 MeV γ-rays. They also reported that the 152 keV γ-ray is in coincidence with the 1.222 MeV γ-ray. They further measured angular correlations of these cascades. MIHELICH ([12]) reported that the 100 keV γ-ray is in coincidence with the 1.189 MeV and 1.122 MeV γ-rays but not with the 1.222 MeV γ-ray.

The present study has been taken up in order to build a decay scheme on the basis of γ-γ and β-γ coincidences which have not been established before; *e.g.* all coincidences of low energy γ-rays with γ-rays of high energies have not yet been established. Similarly, coincidences of low energy γ-rays with low energy γ-rays and β-γ coincidences require investigation.

2. – Experimental.

The source was obtained from the Oak Ridge National Laboratory in the form of $K_8Ta_4O_{19}$ in KOH solution with specific activity of 617 mc/g. The strength of the source used is about 0.10 mc.

2·1. *γ-ray spectrum.* – The single channel scintillation spectrometer using a NaI(Tl) crystal of $1\frac{1}{2}$ inches diameter and 1 inch length was used for the

([7]) D. E. MULLER: *Phys. Rev.*, **88**, 775 (1952).

([8]) C. M. FOWLER, H. W. KRUSE, V. KESHISHIAN, R. J. KLOTZ and G. P. MELLOR: *Phys. Rev.*, **94**, 1082 (1954).

([9]) J. DEMUYNCK, J. VERHAEGHE and B. VAN DER VELDE: *Compt. Rend.*, **244**, 3050 (1957).

([10]) C. E. MANDEVILLE and M. V. SCHERB: *Phys. Rev.*, **73**, 340 (1948).

([11]) R. C. WILLIAM and K. I. ROULSTON: *Can. Journ. Phys.*, **34**, 1087 (1956).

([12]) J. W. MIHELICH: *Phys. Rev.*, **95**, 626 (1954).

study of the γ-rays. The spectrometer was calibrated for various γ-ray energies. The differential pulse height spectrum of γ-rays is given in Fig. 1 (*A*, *B*). Fig. 1 (*A*) represents the spectrum keeping one volt channel width. The photo-peaks due to 68 keV, 100 keV, 152 keV and 222 keV γ-ray transitions

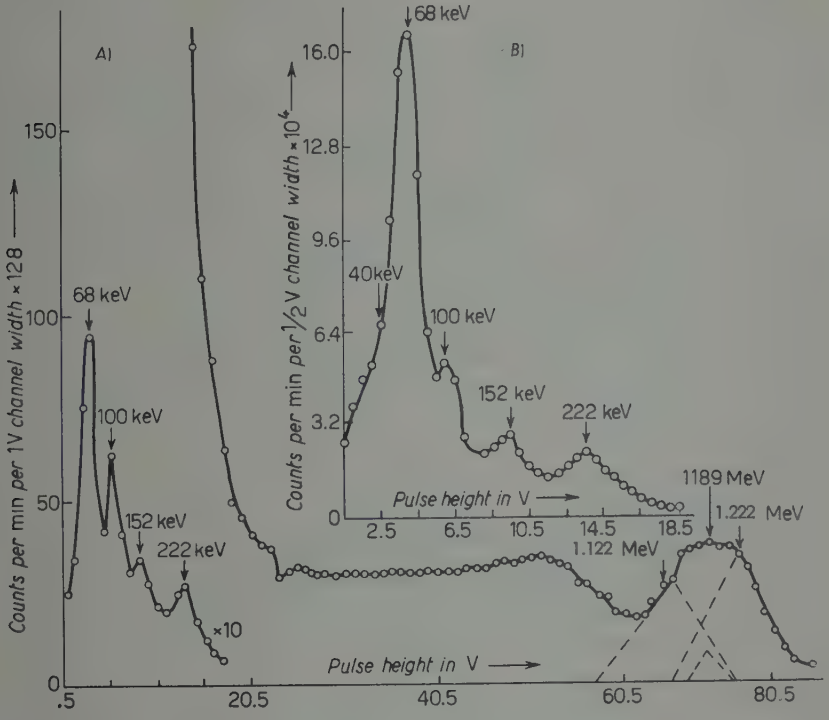

Fig. 1.

are clearly indicated in the low energy spectrum. The high energy γ-ray spectrum has been analysed into three γ-rays of 1.122 MeV, 1.189 MeV and 1.222 MeV γ-transitions. The analysis is shown by dotted lines in the spectrum. The dotted line for 1.122 MeV has been drawn by considering the resolution of γ-rays from the decay of ^{65}Zn (1.112 MeV). And by similar considerations, the analysis for 1.222 MeV γ-ray has been made. The remaining counts correspond to a photo-peak of 1.189 MeV γ-ray. These energies of γ-rays were earlier reported using a crystal spectrometer ([4,7,8 etc]).

The low energy spectrum has been again taken, keeping the half volt channel width which further clearly indicates the photo-peaks due to γ-rays as mentioned above. At 40 keV, there is an indication of an escape peak (shown in Fig. 1 (*B*)).

2·2. *β-ray spectrum.* – The energy spectrum of β-rays and conversion electrons has been studied using a plastic scintillator. The peak in the spectrum may be due to conversion electrons and the spectrum extends up to 550 keV as shown in Fig. 2 (*I*).

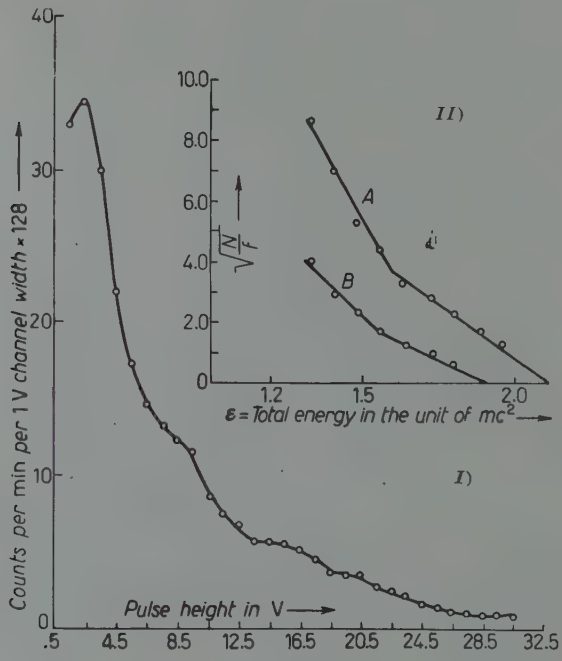

Fig. 2.

2·3. *γ-γ coincidence studies.* – The coincidence studies on the γ-ray spectrum have been done in the following three parts using two single channel scintillation spectrometers in coincidence. The resolution of the coincidence circuit is $2 \cdot 10^{-7}$ s.

PART I. The coincidence studies of low energy spectrum with low energy spectrum.

a) One channel accepts only γ-rays due to the photo-peak of 68 keV in one volt channel width. The other channel scans the low energy spectrum keeping one volt channel. The observed coincidence peaks as shown in Fig. 3 (*A*), correspond to 57 keV, 100 keV, and 264 keV γ-ray energies.

b) In the second set of coincidence experiments, one channel accepts the photo-peak due to the 152 keV γ-ray in one volt channel width and

the other channel scans the low energy spectrum. The coincidence peaks correspond to 57 keV and 100 keV γ-rays as shown in Fig. 3 (*C*).

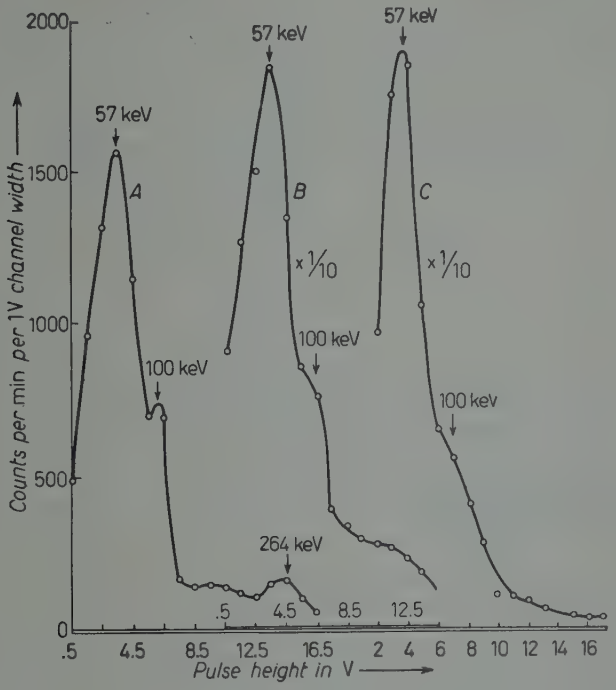

Fig. 3.

c) In the third set of coincidence experiments, one channel accepts the photo-peak due to the 222 keV γ-ray in one volt channel width and the other channel scans the low energy spectrum. The coincidence peaks correspond to 57 keV and 100 keV γ-rays. (as shown in Fig. 3 (*B*)).

It was confirmed that the peak indicated at 57 keV is not due to 68 keV. This was done by comparing it with 57 keV X-rays from ^{181}W.

PART II. The coincidence studies of high energy spectrum with low energy spectrum.

a) One channel accepts all the γ-rays above 500 keV (using a discriminator) and the other channel scans the spectrum in the low energy region. The coincidence spectrum is shown in Fig. 4 (*I*). The photopeaks in the coincidence spectrum due to 68 keV, 100 keV, 152 keV and 222 keV are indicated. The coincidence peak at 222 keV is a broad maximum indicating that other γ-rays of about 222 keV are also in coincidence with high energy γ-rays.

b) In the second set of observations, one channel accepts the peaks due to the 68 keV γ-ray in one volt channel width and the other channel scans the high energy γ-ray spectrum keeping two volts channel width. The coincidence peaks due to 1.122 MeV and 1.222 MeV are clearly indicated (Fig. 4 (II *A*)).

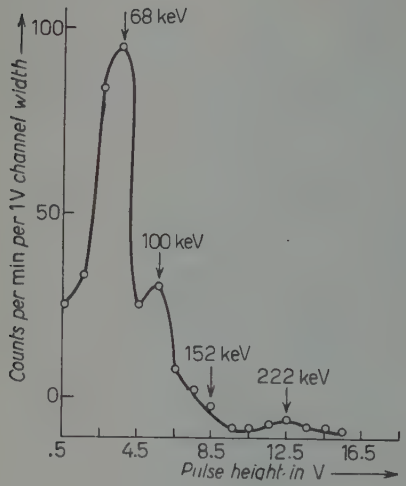

Fig. 4 I.

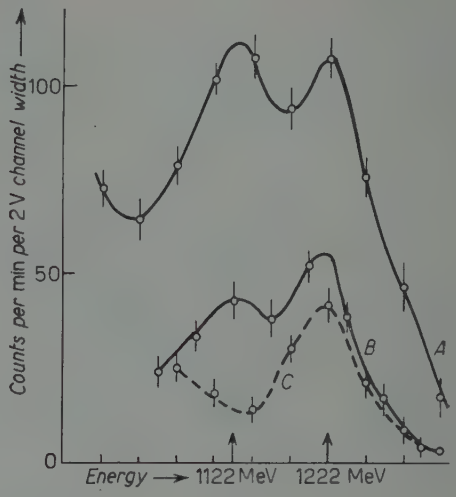

Fig. 4 II.

c) In the third set of observations, one channel accepts the photo-peak due to the 152 keV γ-ray in one volt channel width and the other channel scans the high energy γ-ray spectrum, keeping two volt channel width. The coincidence peaks due to 1.122 MeV and 1.222 MeV are clearly indicated (Fig 4 (II *B*)).

d) In the fourth set of observations, one channel accepts the 222 keV γ-ray in one volt channel width and the other channel scans the high energy spectrum keeping two volt channel width. The coincidence peak due to the 1.222 MeV γ-ray is clearly indicated (Fig. 4 (II *C*)).

PART III. Attempts were made to find the coincidences of the high energy γ-ray spectrum with γ-rays of high energy. No genuine coincidences were found.

2·4. β-γ *coincidence studies.* – The following two experiments were performed:

a) In one set of observations, one channel (using NaI(Tl) crystal) accepts γ-ray spectrum at 57 keV in two volt channel width and the other channel (using a plastic scintillator) scans the β-ray spectrum. A Fermi-Kurie plot for the coincidence spectrum for allowed transition is given in Fig. 2 II (*A*),

(after applying resolution correction to the spectrum). The maximum energy of the β-ray group thus obtained is (560 ± 50) keV.

b) In the second set of observations, one channel (NaI(Tl) crystal) accepts the γ-ray spectrum at 222 keV in two volts channel width and the other channel (plastic scintillator) scans the β-ray spectrum. A Fermi-Kurie plot for this spectrum for allowed transition is shown in Fig. 2 II (*B*) (after applying resolution correction to the spectrum). The maximum energy of the β-ray group, thus obtained is (460 ± 40) keV.

3. – Discussion.

The γ-ray spectrum from the decay of ^{182}Ta is supposed to give a large number of γ-rays, some of which are quite weak. All the γ-rays in the present spectrum may not be resolved. The coincidences may, however, give definite indication of the sequential relationship of some of the γ-rays.

The level at 100 keV has been established by Coulomb excitation studies (McGrown and Stelson ([13]) and others).

Muller *et al.* ([7]) have proposed the four possible decay schemes for the low energy spectrum by « topological maps » considering the energies of the γ-rays. Out of the four proposed decay schemes, the present coincidence measurements result in favour of the first one. The coincidence studies show that the 68 keV γ-ray is in coincidence with the 264 keV γ-ray and is not in coincidence with the 222 keV γ-ray and also the coincidences of the 68 keV γ-ray do not show any peak at 152 keV. This is in accordance with the first scheme and contradicts the other schemes.

Murray *et al.* ([4]) have proposed a decay scheme with 11 levels in ^{182}W by energy considerations. Their decay scheme of low energy γ-rays is like the 1-st one of Muller *et al.* ([7]), which is supported by the present coincidence studies. Further the 68 keV γ-ray is in coincidence with the 1.122 and 1.222 MeV γ-rays and the 152 keV γ-ray is in coincidence with the 1.122 MeV and 1.222 MeV γ-rays. Also the 68 keV and 152 keV γ-rays are in coincidence with the 100 keV γ-ray and the 57 keV X-ray, which should be the case according to the proposed decay scheme by Murray *et al.* ([4]). In the present coincidence measurements, 1.222 MeV and 1.231 MeV γ-rays can not be distinguished as the channel width is kept two volts which corresponds to about 35 keV. If the 222 keV γ-ray is in coincidence with the 1.222 MeV γ-ray, then, in the scheme by Murray *et al.* ([4]), it should also be in coincidence with the

---

([13]) F. K. McGrown and P. H. Stelson: *Phys. Rev.*, **109**, 901 (1958).

1.122 MeV γ-ray which is not the case. So it is argued that the 222 keV γ-ray is in coincidence with the 1.231 MeV γ-ray which is the case in the proposed decay scheme. Further, the study of the coincidences of all the high energy γ-rays with the low energy spectrum reveals that around 222 keV, the spectrum is broad as if the other γ-rays in this region were also in coincidence with high energy γ-rays. This is in favour of the proposed decay scheme.

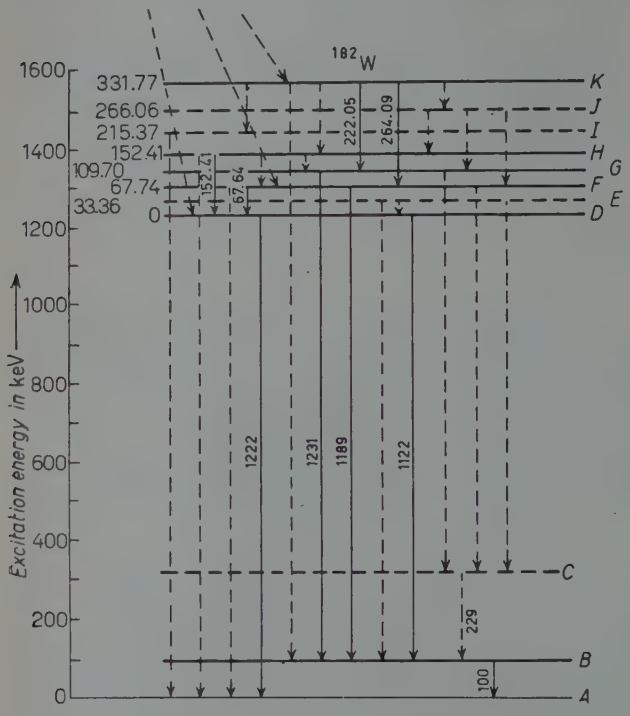

Fig. 5.

The present coincidence studies have firmly established the levels *A*, *B*, *D*, *F*, *G*, *H*, *K* as shown in Fig. 5. It is not possible to establish other levels, *i.e.* *C*, *E*, *J*, and *I*, by the coincidence method, because of the weak transitions from these levels.

The Fermi-Kurie plot of the coincidence spectrum of β-rays (after applying resolution correction to the β-ray spectrum) with X-rays of 57 keV to which there is a certain contribution due to the 68 keV γ-ray, is shown in Fig. 2 II *A*. This spectrum has an end point energy of (560 ± 50) keV which is the same as the maximum energy of the β-ray spectrum shown in Fig. 2 I. The low energy portion of the spectrum deviates from the Fermi-Kurie plot, because of the contribution of conversion electrons in this region or of other groups of low energy β-rays.

A Fermi-Kurie plot of the coincidence spectrum of β-rays (after resolution correction to the spectrum) with γ-rays around 222 keV is shown in Fig. 2 II *B*. This spectrum has an end point energy of (460 ± 40) keV. Again the low energy portion of the spectrum deviates from the straigth line because of the contribution of conversion electrons and other β-ray groups of low energy. Though the estimates of the end points of these Fermi-Kurie plots are quite approximate due to the limitations of the scintillation technique (bad resolution and channel width which corresponds to 38 keV). One thing is apparent

from these Fermi-Kurie plots that γ-rays around 222 keV are not in coincidence with β-ray group of maximum energy of (560 $\pm$ 50) keV. From the decay scheme proposed by MURRAY *et al.* [4] and β-ray groups reported by DEMUYNCK *et al.* [9], the 222 keV γ-ray should be in coincidence with the β-ray group of 184 keV and the 229 keV γ-ray may be in coincidence with the β-ray group of 440 keV through the level *F* whose intensity should however be quite small. The Fermi-Kurie plot of the coincidence spectrum shown in Fig. 2 II *B*, may, therefore be attributed to the coincidence between the 229 keV γ-ray and the 440 keV β-ray group.

RIASSUNTO (*)

Facendo uso di uno spettrometro a scintillazione si sono trovati nel decadimento del ^{182}Ta raggi γ di energie di 68 keV, 100 keV, 152 keV, 1 122 MeV, 1 189 MeV e 1 222 MeV. Si riscontra che il raggio γ di 68 keV è in coincidenza con i raggi γ aventi energia di 57 keV, 100 keV, 264 keV, 1 122 MeV e 1 222 MeV. Si trova che i raggi γ di 152 keV sono in coincidenza con i raggi γ aventi energia di 57 keV, 100 keV, 1 122 MeV e 1 222 MeV, e che il raggio γ di 222 keV sono in coincidenza con i raggi γ aventi energia di 57 keV, 100 keV e 1 231 MeV. Da studi di coincidenza sono stati trovati due gruppi di raggi β aventi energia massima rispettivamente di (560$\pm$50) keV e (460$\pm$40) keV. Questi studi di coincidenza hanno stabilito i livelli nel ^{182}W, a 100 keV, 1 222 MeV, 1 290 MeV, 1 331 MeV, 1 374 MeV e 1 554 MeV.

(*) *Traduzione a cura della Redazione.*

IL NUOVO CIMENTO Vol. XIV, N. 1 1° Ottobre 1959

Investigations of the Decay of ^{185}W.

B. P. Singh and H. S. Hans

Department of Physics, Muslim University - Aligarh

(ricevuto l'11 Maggio 1959)

Summary. — The half life of 57 keV electromagnetic radiation as obtained in the γ-ray spectrum of the decay of ^{185}W has been measured to be (140±5) days. The 57 keV radiation has, therefore, been assigned to ^{181}W. Two more γ-rays of low intensity have been observed at 136 keV and 152 keV. By energy and intensity considerations, these γ-rays are also considered to be due to ^{181}W. The maximum energy of the β-ray group has been measured to be (420±20) keV. No genuine coincidences were found between any part of β-ray spectrum and γ-rays and also no γ-γ coincidences were found. Neither the γ-ray of 125 keV (0.005%), nor any inner β-ray group can be assigned to the spectrum of ^{185}W.

1. – Introduction.

The decay of ^{185}W has been the subject of much controversy. Early workers (Saxon [1], Shull [2], etc.) established that the radiation from ^{185}W consists of only one β-ray group of maximum energy 430 keV. Cork *et al.* [3] reported a γ-ray of 133.7 keV. On the other hand Lazer *et al.* [4] reported

---

(1) D. Saxon: *Phys. Rev.*, **74**, A 1264 (1948).
(2) F. B. Shull: *Phys. Rev.*, **74**, 917 (1948).
(3) J. M. Cork, H. B. Keller and A. E. Stoddard: *Phys. Rev.*, **76**, 575 (1949).
(4) N. Lazar, R. J. D. Moffat and L. M. Langer: *Phys. Rev.*, **91**, A 498 (1953).
(5) A. Bisi, S. Terrani and L. Zappa: *Nuovo Cimento*, **1**, 291 (1955).
(6) S. K. Bhattacherjee and S. Raman: *Nuovo Cimento*, **3**, 1131 (1956).
(7) W. E. Dreger, L. D. McIsaac, J. L. Mackin and J. R. Lai: *Phys. Rev.*, **100**, 953 (1955).
(8) T. C. Sebastian and A. H. Weber: *Bull. Am. Phys. Soc.*, **1**, 134 (1956).
(9) V. S. Dubey, C. E. Mandeville, A. Mukerji and V. R. Potnis: *Phys. Rev.*, **106**, 785 (1957).
(10) B. H. Armitage and W. G. W. Rosser: *Proc. Phys. Soc.*, **71**, 335 (1958).

no such γ-ray. BISI *et al.* [5] reported an electromagnetic radiation of 57 keV which they attributed to the excited state of ^{185}Re by measuring its half life. They further predicted an inner β-ray group which should be in coincidence with the 57 keV γ-ray. BHATTACHARJEE and SHREE RAMAN [6] found the inner β-ray group by observing the coincidences with the 57 keV radiation which were 15% of the total number of β-rays. They further showed the total conversion coefficient to be 3.3. KREGER *et al.* [7] observed two more γ-rays of 570 keV and 770 keV from the decay of ^{185}W. SEBASTIAN and WEBER [8] again reported one more γ-ray of 132 keV. DUBEY *et al.* [9] found no γ-ray in enriched ^{185}W. ARMITAGE and ROSSER [10] observed a peak at 125 keV probably arising from an inner β group of 0.005%.

The study has been taken up in order to find the decay products of ^{185}W and to ascertain the nature of these radiations.

2. – Experimental.

The source of ^{185}W was obtained from the Oak Ridge National Laboratory U.S.A. It was produced by the reaction $^{184}W(n, \gamma)$. The final source was in the chemical form of K_2WO_4 in KOH solution. The purity of tungsten radiation in the source was greater than 98%. Specific activity at the time of measurement was 0.46 mc/mg.

2·1. *β-ray spectrum.* – β-ray spectrum was measured using a plastic scintillator (resolution for the internal conversion line of ^{137}Cs of 630 keV was 21.5%). A Fermi-Kurie plot of the β group of (420 $\pm$ 20) keV end energy was obtained.

2·2. *γ-ray spectrum.* – A γ-ray spectrum of the source was obtained with a scintillation spectrometer using an NaI(Tl) crystal of $1\frac{1}{2}$ in. diameter and $\frac{1}{2}$ in. thickness. The source with high activity used for the spectrum was made on a cellulose tape.

The spectrum revealed two γ-ray peaks, one at 28 keV and other at 57 keV (*). It was noted that the spectrum extends further but no distinguishable peak was observed. It was considered desirable that the spectrum above 57 keV should be studied very carefully. For this various spectra were taken by introducing different thicknesses of copper strips between the source and the detector. This was done in order to reduce the relative intensity of the 57 keV rays with respect to the higher energy spectrum, so that this latter spectrum should not be masked by the tail of the 57 keV peak. The spectrum obtained

(*) The peak at 28 keV is apparently due to the escape of *K*-X-rays of Iodine in the process of photoelectric absorption of 57 keV radiation in the NaI(Tl) crystal.

in this way is shown in Fig. 1-*a* and *b*. The full spectrum in Fig. 1-*a*, was taken after using 500 mg/cm² of copper strips, as absorber. Apart from the sharp peaks of 28 keV and 57 keV, a broad maximum is also clearly observable

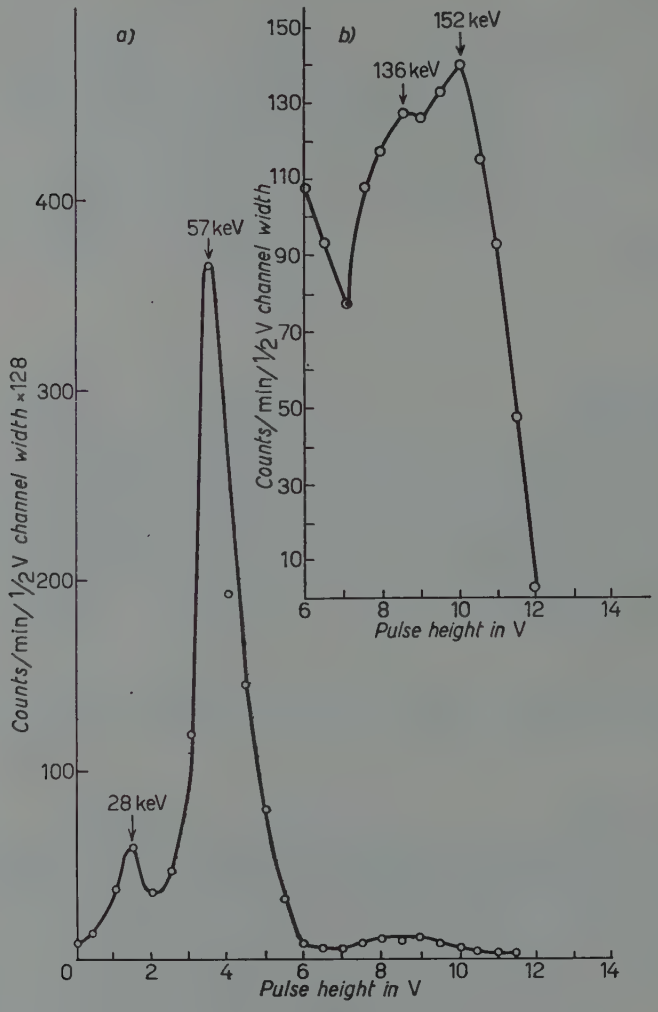

Fig. 1.

at about 140 keV. The high energy spectrum in Fig. 1-*b* was taken using 1000 mg/cm² copper strips as absorber and using a channel width of 6 keV. The spectrum in Fig. 1-*b* reveals two peaks one at 136 keV and the other at 152 keV. This portion of the spectrum was taken many times under various conditions of the spectrometer and these peaks were always clearly observable.

The intensity of various parts of the spectrum was measured with respect to the intensity of the 57 keV peak as given below.

Energy interval of γ-rays	Intensity ratio
(110÷175) keV	$5 \cdot 10^{-3}$
(175÷360) keV	$7 \cdot 10^{-4}$
> 360 keV	$4 \cdot 10^{-3}$

2·3. *Half life measurement.* – To ascertain the origin of the 57 keV radiation its half life measurement was undertaken by using the scintillation spectrometer. As very long half lives are involved only three points at different times could be taken. The decay curve is shown in Fig. 2-*a, b* giving a half life of (140 ± 5) days. While measuring the intensity of the 57 keV radiation at different times extra care was taken to keep the geometry and the conditions of the spectrometer unaltered.

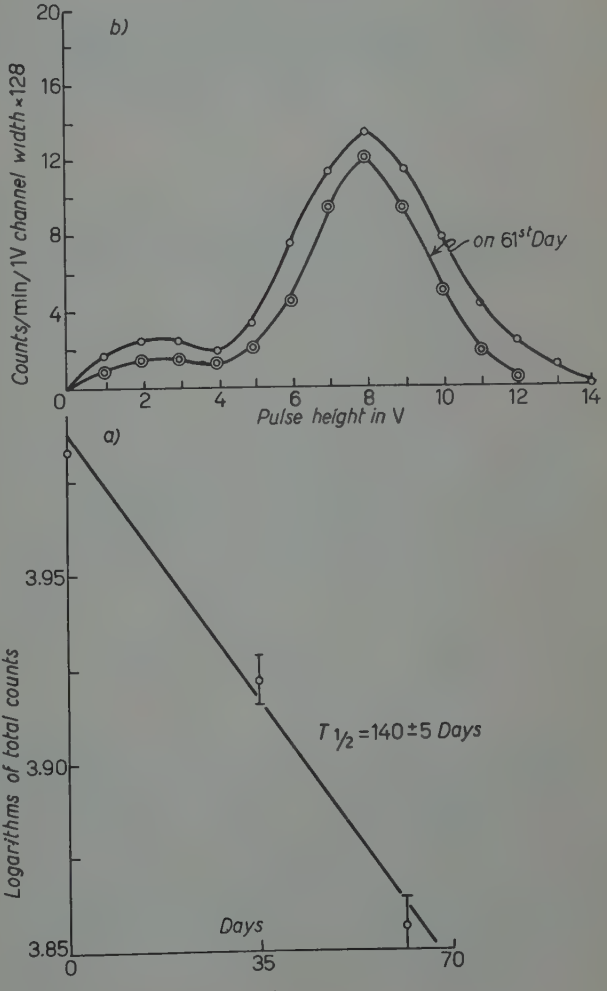

Fig. 2.

2·4. *Coincidence measurements.* – Coincidence measurements were made between β-ray and γ-ray spectrum. For this purpose, two scintillation spectrometers were used in coincidence with a resolving time of the order of $2 \cdot 10^{-7}$ s. β-rays were detected by a plastic scintillator and NaI(Tl) crystals were used for γ-rays. A high intensity source was used in these measu-

rements as was done in the measurement of the γ-rays. The following two experiments were performed.

a) For β-γ coincidences, one channel accepts pulses of all energies due to γ-rays (using it as discriminator) and the other channel accepts the β-ray spectrum in channel width of one volt (one volt = 20 keV). No coincidences were found.

b) For γ-γ coincidences, one γ-channel accepts pulses of all energies and the other γ channel accepts the spectrum in channel width of one volt. No coincidences were found.

Thus no genuine coincidences were found between β-rays and any part of the γ-ray spectrum, or between any two parts of the γ-ray spectrum, so that the 57 keV radiation was not found to be in coincidence with the 152 keV and 136 keV radiations and also the 136 keV and 152 keV radiations were not in coincidence with each other.

3. – Discussion.

The maximum energy of the β-ray spectrum is the same as reported in the literature for ^{185}W. The half life measurement of the 57 keV radiation shows quite conclusively that it is an X-ray arising from the electron capture of ^{181}W. This also supports the conclusion of DUBEY *et al.* ([9]) that the 57 keV radiation does not belong to ^{185}W. The γ-rays of 136 keV and 152 keV also seem to be due to the decay of ^{181}W to ^{181}Ta. These γ-rays have also been observed by DEBRUNNER *et al.* ([11]) and CORK *et al.* ([12]). The energies and relative intensities of these two γ-rays with respect to each other and with the X-rays as measured by us are the same as those of the above authors. This supports our conclusion. It seems that the γ-ray of about 133 keV reported by various authors may be the same γ-rays as observed by us but not resolved enough to give two peaks. The absence of any coincidence between β-rays and the 57 keV radiation is in contradiction to the observations of BHATTACHARJEE and RAMAN ([6]). But this confirms the opinion that the 57 keV radiation belongs to ^{181}W.

Our measurements also do not show the coincidences between the γ-ray spectrum near 125 keV and β-rays as observed by ARMITAGE and ROSSER ([10]). As the source used by us was prepared from natural tungsten, activity due to both ^{185}W and ^{181}W should be present in the ratio determined by the

---

([11]) P. DEBRUNNER, E. HEER, W. KÜNDIG and R. RÜESCHI: *Helv. Phys. Acta*, **29**, 235, 463 (1956).

([12]) J. M. CORK, W. H. NESTER, J. M. LEBLANC and M. K. BRICE: *Phys. Rev.*, **92**, 119 (1953).

relative abundances and capture cross-sections for the production of these activities. Taking 0.005 % as the ratio of intensity of the 125 keV radiation of β-rays as measured by ARMITAGE and ROSSER ([10]) and using the ratio of natural isotopes of ^{181}W and ^{185}W as mentioned above, the expected intensity for the 125 keV rays was calculated. This turned out to be nearly the same as the measured intensity of the 152 keV γ-ray. No peak of 125 keV of this intensity can be accounted for in our spectrum. ARMITAGE and ROSSER used a comparatively thicker and more intense source *e.g.* 2 mg/cm² while our source was 0.25 mg/cm². They were, therefore, expected to have much more external bremsstrahlung over and above the internal bremsstrahlung due to β-rays. Most of their coincidences with β-rays were accounted for by this bremsstrahlung.

Our results of coincidence measurements and intensity considerations do not support the evidence of the existence of a γ-ray of 125 keV. ARMITAGE and ROSSER who reported the coincidences of 125 keV γ-rays and β-rays, themselves are uncertain about the γ-rays of 125 keV, there being bremsstrahlung of that energy.

* * *

The authors wish to express their sincere thanks to Prof. P. S. GILL for his kind interest and continuous encouragement in this work. One of the authors (B.P.S.) is thankful to the Union Education Ministry for the grant of a Senior Research Scholarship.

Note added in proof.

The paper « On the decay of ^{185}W » by BISI and ZAPPA (*Nuovo Cimento*, **10**, 90 (1958)) came to the notice of the authors after this paper was submitted for publication. Our results are in contradiction to those of Bisi and Zappa as regards the half life of 57 keV. Our β-γ coincidence measurements do not support their view that 57 keV radiation is due to the conversion of 125 keV radiation from the decay of ^{185}W.

RIASSUNTO (*)

La vita media della radiazione elettromagnetica di 57 keV presente nello spettro di decadimento γ del ^{185}W è stata determinata in (140 ± 5) giorni. La radiazione di 57 keV è stata pertanto assegnata al ^{181}W. Si sono osservati altri due raggi γ di debole intensità a 136 keV e 152 keV. In base a considerazioni energetiche e di intensità anche questi raggi si attribuiscono al ^{181}W. L'energia massima del gruppo di radiazione β è risultata di (420 ± 20) keV. Non si sono trovate coincidenze genuine tra le singole parti dello spettro β e i raggi γ nè coincidenze γ-γ. Al ^{185}W non si possono attribuire nè il raggio γ di 125 keV (0.005%) nè un gruppo di radiazione β interna.

(*) *Traduzione a cura della Redazione.*

IL NUOVO CIMENTO Vol. XIV, N. 1 1° Ottobre 1959

Universality in the Non-Leptonic Decay Interaction of Hyperons.

O. Hara

Department of Physics, College of Science and Engineering
Nihon University - Tokyo

(ricevuto il 23 Maggio 1959)

Summary. — If we assume the $\Delta I = \frac{1}{2}$ rule and make some other plausible assumptions, decay interactions for Λ and Σ can be determined except for the coupling constants g_Λ and g_Σ. g_Λ and g_Σ were determined from the life times of Λ and Σ, and it was found that they agree within the experimental error

---

Recently, Feynman and Gell-Mann (1) showed that there exists a remarkable universality in the coupling constants of various lepton processes. In this note we shall show that a similar universality seems to exist in the non-leptonic decay interactions of hyperons.

If we assume that

a) the spin of the hyperon is $\frac{1}{2}$,

b) the $\Delta I = \frac{1}{2}$ rule holds,

c) T-invariance is satisfied,

d) the coupling is of derivative type,

---

(1) R. P. Feynman and M. Gell-Mann: *Phys. Rev.*, **109**, 193 (1958).

the decay hamiltonians for Λ and Σ are given as follows:

i) for the Λ-decay:

$$(1)\quad H_\Lambda = \sqrt{\tfrac{1}{3}}\, g_\Lambda \varkappa \{\sqrt{2}\,\bar{\psi}_P \gamma_\mu (1+\varepsilon\gamma_5)\psi_\Lambda \cdot \partial_\mu \varphi - \bar{\psi}_N \gamma_\mu (1+\varepsilon\gamma_5)\psi_\Lambda \cdot \partial_\mu \varphi^0\} + \text{h. c.},$$

where g_Λ and ε are real, and $\varkappa$ is the Compton wave length of the pion. ε is restricted to be ± 1 since the asymmetry factor in $\Lambda \to p + \pi^-$ is nearly unity. $\sqrt{\frac{1}{3}}$ comes from the Clebsch-Gordon coefficient. We shall write it explicitly for later purposes.

ii) for the Σ-decay:

$$(2)\quad H_\Sigma = -\sqrt{\frac{1}{6}}\, g_\Sigma \varkappa \left\{ \bar{\psi}_p \gamma_\mu (1+\varepsilon\gamma_5)(\partial_\mu \varphi^+, \partial_\mu \varphi^0, \partial_\mu \varphi^-)^* (I_1 - iI_2) \begin{pmatrix} \psi_{\Sigma^+} \\ \psi_{\Sigma^0} \\ \psi_{\Sigma^-} \end{pmatrix} - \right.$$

$$\left. - \bar{\psi}_N \gamma_\mu (1+\varepsilon\gamma_5)(\partial_\mu \varphi^+, \partial_\mu \varphi^0, \partial_\mu \varphi^-)^* \, I_3 \begin{pmatrix} \psi_{\Sigma^+} \\ \psi_{\Sigma^0} \\ \psi_{\Sigma^-} \end{pmatrix} \right\} +$$

$$+ \sqrt{\frac{1}{3}}\, g'_\Sigma \varkappa \left\{ \bar{\psi}_N \gamma_\mu (1+\varepsilon'\gamma_5)(\partial_\mu \varphi^+, \partial_\mu \varphi^0, \partial_\mu \varphi^-)^* \begin{pmatrix} \psi_{\Sigma^+} \\ \psi_{\Sigma_0} \\ \psi_{\Sigma^-} \end{pmatrix} \right\} + \text{h. c.},$$

where g_Σ, g'_Σ, ε and ε' are real as before, and I_1, I_2 and I_3 are given by

$$I_1 = \frac{1}{\sqrt{2}} \begin{pmatrix} 0 & -1 & 0 \\ -1 & 0 & 1 \\ 0 & 1 & 0 \end{pmatrix}, \quad I_2 = \frac{1}{\sqrt{2}} \begin{pmatrix} 0 & i & 0 \\ -i & 0 & -i \\ 0 & i & 0 \end{pmatrix}$$

$$\text{and} \quad I_3 = \begin{pmatrix} 1 & 0 & 0 \\ 0 & 0 & 0 \\ 0 & 0 & -1 \end{pmatrix}.$$

$\sqrt{\frac{1}{6}}$ and $\sqrt{\frac{1}{3}}$ come from the Clebsch-Gordon coefficient as before. Experimental data on the asymmetry factor [2] ($\alpha_+ \simeq \alpha_- \simeq 0$, $\alpha_0 \simeq \pm 1$) impose the restric-

---

[2] Private communication from M. MIYAZAWA.

tions $\varepsilon' = -\varepsilon$, $\varepsilon = \pm 1$ and $g'_\Sigma = \pm g_\Sigma/\sqrt{2}$: It can be shown that under the assumptions *a*)–*d*), this is the only one that is consistent with experimental data concerning the asymmetry factor, so long as we assume that the effect of the pion cloud is not so large (*).

It is satisfying that (2) gives

$$\frac{\Sigma^+ \to \mathrm{p} + \pi^0}{\Sigma^+ \to \mathrm{n} + \pi^+} \simeq 1 \qquad \text{and} \qquad \frac{\tau_{\Sigma^+}}{\tau_{\Sigma^-}} \simeq \frac{1}{2}.$$

Therefore, (2) is consistent with all data concerning the Σ-decay (**).

Decomposing (2), we get as the decay hamiltonian for $\Sigma^\pm$:

$$(3)\quad \begin{cases} H_\Sigma = \sqrt{\frac{1}{3}}\, g_\Sigma \varkappa \{\bar{\psi}_\mathrm{p}\gamma_\mu(1+\varepsilon\gamma_5)\psi_{\Sigma^+}\cdot\partial_\mu\varphi^0 + \sqrt{2}\,\bar{\psi}_\mathrm{N}\gamma_\mu\psi_{\Sigma^+}\cdot\partial_\mu\varphi^* + \\ \qquad + \sqrt{2}\,\varepsilon\bar{\psi}_\mathrm{N}\gamma_\mu\gamma_5\psi_{\Sigma^-}\cdot\partial_\mu\varphi\} + \mathrm{h.\,c.} \qquad \text{for } g'_\Sigma = g_\Sigma/\sqrt{2}\,, \\ H_\Sigma = \sqrt{\frac{1}{3}}\, g_\Sigma \varkappa \{\bar{\psi}_\mathrm{p}\gamma_\mu(1+\varepsilon\gamma_5)\psi_{\Sigma^+}\cdot\partial_\mu\varphi^0 + \sqrt{2}\,\varepsilon\bar{\psi}_\mathrm{N}\gamma_\mu\gamma_5\psi_{\Sigma^+}\cdot\partial_\mu\varphi^* + \\ \qquad + \sqrt{2}\,\bar{\psi}_\mathrm{N}\gamma_\mu\psi_{\Sigma^-}\cdot\partial_\mu\varphi\} + \mathrm{h.\,c.} \qquad \text{for } g'_\Sigma = -g_\Sigma/\sqrt{2}\,. \end{cases}$$

Using (1) and (3), we get easily

$$(4)\quad \frac{1}{\tau_\Lambda} = \frac{2}{3}\cdot\left(\frac{g_\Lambda^2}{\hbar c}\right)\cdot\frac{M_\mathrm{n}}{M_\Lambda}\cdot\left[\frac{P_\Lambda^0 c}{\hbar}\left\{1+2\,\frac{(P_\Lambda^0 c)^2}{\mu_0^2}\left(1+\frac{E_\Lambda^0}{M_\mathrm{n}c^2}\right)\right\} + 2\,\frac{P_\Lambda^- c}{\hbar}\left\{1+2\,\frac{(P_\Lambda^- c)^2}{\mu_-^2}\left(1+\frac{E_\Lambda^-}{M_\mathrm{n}c^2}\right)\right\}\right],$$

and

$$(5)\quad \frac{1}{\tau_{\Sigma^-}} = \frac{4}{3}\cdot\left(\frac{g_\Sigma^2}{\hbar c}\right)\cdot\frac{M_\mathrm{n}}{M_{\Sigma^-}}\cdot\frac{P_{\Sigma^-}c}{\hbar}\cdot\begin{cases} \dfrac{(P_{\Sigma^-}c)^2}{\mu_-^2}\left(1+\dfrac{E_{\Sigma^-}}{M_\mathrm{n}c^2}\right) & \text{for } g'_\Sigma = g_\Sigma/\sqrt{2}, \\ \dfrac{E_{\Sigma^-}^2}{\mu_-^2}\left\{1+\dfrac{(P_{\Sigma^-}c)^2}{M_\mathrm{n}c^2\cdot E_{\Sigma^-}}\right\} & \text{for } g'_\Sigma = -g_\Sigma/2\,, \end{cases}$$

where E_Λ, E_{Σ^-}, P_Λ and P_{Σ^-} are energy and momentum of the emitted pion (E_Λ^0 corresponds to $\Lambda \to \mathrm{n} + \pi^0$ and so on), and $\mu_{0,-}$ are their rest energy.

(*) Contrary to this, TAKEDA and KATO [3] tried to explain this asymmetry factor, starting from $A - V$ (or $A + V$) interaction, by assuming that the effect of the pion cloud is large.

[3] G. TAKEDA and M. KATO: *Prog. Theor. Phys.*, **21**, 441 (1959).

(**) (2) was given by NAKAGAWA and UMEZAWA [4].

[4] K. NAKAGAWA and K. UMEZAWA: *Nuovo Cimento*, **10**, 911 (1958); K. NAKAGAWA: *Nuclear Physics*, **10**, 20 (1959).

M_n, M_Λ and M_{Σ^-} are the rest mass of the nucleon, Λ and Σ^-, and terms of order $(\mu/M_n c^2)^3$ or smaller were neglected against unity.

From (4) and (5) we get, using $\tau_\Lambda = (2.60^{\pm 0.16}_{-0.14})\cdot 10^{-10}$ s and $\tau_{\Sigma^-} = (1.72^{+0.17}_{-0.10})\cdot \cdot 10^{-10}$ s, [5]

$$g_\Lambda^2/\hbar c = (6.5 \pm 0.7)\cdot 10^{-15}\,, \tag{6}$$

and

$$|g_\Lambda/g_\Sigma| = \begin{cases} 0.91 \pm 0.07 & \text{for } g'_\Sigma = g_\Sigma/\sqrt{2}\ (*), \\ 1.08 \pm 0.08 & \text{for } g'_\Sigma = -g_\Sigma/\sqrt{2}\,. \end{cases} \tag{7}$$

Thus, we see that g_Λ and g_Σ agree within the experimental error, and there seems to exist a remarkable universality.

The decay hamiltonian for Ξ is given as follows (**)

$$H_\Xi = \sqrt{\frac{1}{3}}\, g_\Xi \varkappa \{\sqrt{2}\,\bar\psi_\Lambda \gamma_\mu (1+\varepsilon\gamma_5)\psi_{\Xi^-}\cdot\partial_\mu\varphi - \bar\psi_\Lambda\gamma_\mu(1+\varepsilon\gamma_5)\psi_{\Xi^0}\cdot\partial_\mu\varphi^0\} + \text{h. c.} \tag{8}$$

by exactly the same way as before. From this we get, in the same approximation as before,

$$\frac{1}{\tau_\Xi} = \frac{4}{3}\cdot\left(\frac{g_\Xi^2}{\hbar c}\right)\cdot\frac{M_n}{M_\Xi}\cdot\frac{P_{\Xi^-}c}{\hbar}\cdot\left\{1 + 2\,\frac{(P_{\Xi^-}c)^2}{\mu_-^2}\left(1+\frac{E_{\Xi^-}}{M_\Lambda c^2}\right)\right\}. \tag{9}$$

From (8) we get, if we assume that the same universality can be extended to the decay of Ξ and take $g_\Xi = g_\Lambda$,

$$\tau_{\Xi^-} \simeq 2.2\cdot 10^{-10}\ \text{s}\,. \tag{10}$$

The universality suggested here, which asserts that the coupling constants of the weak interactions between pion and baryon are all the same, may be

---

[5] D. A. GLASER: *Report of 1958 Annual International Conference on High Energy Physics at CERN.*

(*) These two cases can be discriminated from the angular distribution of the emitted pion. In the first case, π^+ in $\Sigma^+ \to n + \pi^+$ is emitted in the S-state and π^- in $\Sigma^- \to n + \pi^-$ in the P-state. In the latter case, this is reversed.

(**) From (8) we get at once

$$\tau_{\Xi^0}/\tau_{\Xi^-} = 2\,.$$

This may be used as another test for the $\Delta I = \frac{1}{2}$ rule.

regarded as an analogue of the global symmetry of GELL-MANN (6), which asserts that the coupling constants of the strong interactions between pion and baryon are all the same (*).

---

(6) M. GELL-MANN: *Phys. Rev.*, **106**, 1296 (1957).

(*) This universality has been supposed by several authors (7). The emphasis of this note is that it is made more clear by taking into account the Clebsch-Gordon coefficient explicitly.

(7) For example, H. UMEZAWA: *Prog. Theor. Phys., Suppl.* no. 7, 67 (1959).

RIASSUNTO (*)

Se si assume la regola $\Delta I = \frac{1}{2}$ e si fanno ulteriori plausibili ipotesi, si possono determinare le interazioni di decadimento per le Λ e le Σ, fatta esclusione per le costanti di accoppiamento g_Λ e g_Σ. Le g_Λ e le g_Σ sono state determinate dalle vite delle Λ e delle Σ, e si è trovato che esse concordano entro i limiti degli errori sperimentali.

(*) *Traduzione a cura della Redazione.*

IL NUOVO CIMENTO Vol. XIV, N. 1 1° Ottobre 1959

A Method for the Measurement of the Nuclear Transversal Relaxation Time.

G. Bonera, L. Chiodi, L. Giulotto and G. Lanzi

Istituto di Fisica dell'Università - Pavia

(ricevuto il 29 Maggio 1959)

Summary. — A method for measuring transverse relaxation times in liquids is described. The method is based on the observation of the decay of the nuclear magnetization when it precesses in a plane perpendicular to the constant magnetic field. This condition is realized by stopping the variation of the constant magnetic field during a fast adiabatic passage at a proper time. The constant magnetic field is modulated with a saw-tooth current from a relaxation oscillator and an amplifier. When the voltage induced by the nuclear precession reaches a fixed value the relaxation oscillator is stopped with a delay such that the constant field stops its variation at the value for which the signal has the largest amplitude. Measurements have been made on some pure liquids and the preliminary results indicate that the values of T_2 are very close to those of T_1.

1. – Introduction.

Various methods have been used previously in nuclear magnetic resonance to measure the nuclear transverse relaxation time T_2.

If the constant magnetic field $\boldsymbol{H}_0$ is sufficiently homogeneous and T_2 is sufficiently small, it is possible to deduce the value of T_2 from the line-width of the signal. The value of T_2 is in general too large in the case of liquids for this method to be applicable.

A well known method is that of « spin echoes » due to Hahn [1]. It consists in applying to the sample two brief and intense r.f. pulses so that the first pulse

[1] E. L. Hahn: *Phys. Rev.*, **80**, 580 (1950).

brings the nuclear magnetization into the xy plane, normal to the direction of the constant magnetic field, and the second pulse causes the nuclear magnetization to turn of 180°. If τ is the time interval between the two pulses, after a time τ from the second pulse one observes an « echo » signal due to the fact that the nuclear magnetizations of the various parts of the sample have become in-phase again. Increasing the time τ between the pulses one obtains a sequence of echo signals whose amplitude decreases exponentially with time constant T_2. In the case of liquids where T_2 is quite large, measurements of T_2 with Hahn's method can be affected by self-diffusion phenomena.

Some considerable improvements to the spin echo method have been introduced by CARR and PURCELL ([2]). They take into account self-diffusion phenomena and are able to measure indirectly the diffusion constants of some liquids.

A further improvement was made by MEIBOOM and GILL ([3]). The pulse sequence is identical to the one proposed by CARR and PURCELL, but the r.f. of the successive pulses is coherent and on the first pulse a phase shift of 90° is introduced. With this method quite large values of T_2 can be measured.

Measurements of T_2 by the spin echo phenomena have been also carried out by SOLOMON ([4]) and by POWLES and CUTLER ([5]).

Two other methods to be recalled are due to TORREY ([6]) and GABILLARD ([7]). Torrey's method consists in submitting the sample to a sharp-fronted pulse, which remains constant during the time of the observation of the signal. The signal looks then like a damped oscillation, due to slow changes of the nuclear magnetization about the effective field $\boldsymbol{H}_{\text{eff}}$ (RABI, RAMSEY and SCHWINGER ([8])). At the resonance condition the time constant of the decay of the signal is given by $2[1/T_1 + 1/T_2]^{-1}$ and when T_1 is known, T_2 can be determined. Torrey's method is limited by the inhomogeneity of $\boldsymbol{H}_0$ and of $\boldsymbol{H}_1$ (rotating field) and is applicable in practice only when $T_2 \leqslant 10^{-2}$ s.

Gabillard's method is based on the observation of transient phenomena. When one passes through resonance in a time short compared to T_1 and T_2 and with small oscillating fields, one observes damped oscillations of increasing frequency called « wiggles », studied by JACOBSOHN and WANGSNESS ([9]). If the constant field $\boldsymbol{H}_0$ is very homogeneous the « wiggles » decay exponentially with

---

([2]) H. Y. CARR and E. M. PURCELL: *Phys. Rev.*, **94**, 630 (1954).
([3]) S. MEIBOOM and D. GILL: *Rev. Sci. Instr.*, **29**, 688 (1958).
([4]) I. SOLOMON: *Phys. Rev.*, **99**, 559 (1955).
([5]) J. G. POWLES and D. CUTLER: *Arch. des Sci.*, **11**, 209 (1958).
([6]) M. C. TORREY: *Phys. Rev.*, **76**, 1059 (1949).
([7]) R. GABILLARD: *Compt. Rend.*, **233**, 39 (1951).
([8]) I. I. RABI, N. F. RAMSEY and J. SCHWINGER: *Rev. Mod. Phys.*, **26**, 167 (1954).
([9]) B. A. JACOBSOHN and R. K. WANGSNESS: *Phys. Rev.*, **73**, 942 (1948).

time constant T_2. When one passes again through the resonance condition before the signal has decayed completely, the amplitude of the signal will increase to decay again with time. GABILLARD has shown that the ratio of the amplitudes before and after resonance is given by $\exp[t_m/2T_2]$, with $t_m =$ period of the sweep modulating the constant field. From this T_2 can be easily obtained. Because of the self diffusion of molecules in liquids Gabillard's method is limited to values of T_2 less than 0.1 s.

Another method similar to Gabillard's method has been developed independently by BRADFORD, CLAY, STRICK and CRAFT [10]. Methods based on transient phenomena to measure T_2 have been also used by GOODEN [11] and SALPETER [12].

In the present paper we describe a method for measuring T_2 which consists of stopping a rapid adiabatic passage while the nuclear magnetization is precessing in a plane perpendicular to the constant magnetic field $\boldsymbol{H}_0$. We observe then a signal which decays exponentially with time constant T_2, under certain conditions rather easy to realize in practice. The main advantage of this method is that, if $\boldsymbol{H}_1$ is large enough, a small inhomogeneity of $\boldsymbol{H}_0$ does not greatly affect the measurement of T_2. Furthermore the measurements of T_2 in this case are not affected by self-diffusion phenomena.

Another way of bringing the nuclear magnetization into the xy-plane in order to measure T_2 consists in applying to the sample a pulse of 90 degrees with a phase shift of $\pi/2$ with respect to the radiofrequency, which produces the field $\boldsymbol{H}_1$. This method has been recently used by SOLOMON [13].

Before we describe in detail the method we propose for a measurement of T_2, we recall the conditions under which a rapid adiabatic passage takes place:

$$\text{(1)} \qquad \left|\frac{\mathrm{d}H_0}{\mathrm{d}t}\right| \ll \gamma H_1^2 ,$$

$$\text{(2)} \qquad \frac{H_1}{T_1} \ll \left|\frac{\mathrm{d}H_0}{\mathrm{d}t}\right| , \qquad \frac{H_1}{T_2} \ll \left|\frac{\mathrm{d}H_0}{\mathrm{d}t}\right| ,$$

from which follows

$$\text{(3)} \qquad \frac{1}{T_1} \ll \gamma H_1 , \qquad \frac{1}{T_2} \ll \gamma H_1 .$$

Let us consider a system of cartesian axes x', y', z', ($z' = z$), rotating with

---

[10] E. STRICK, R. BRADFORD, C. CLAY and A. CRAFT: *Phys. Rev.*, **84** 363 (1951).
[11] J. S. GOODEN: *Nature*, **165**, 1014 (1950).
[12] E. E. SALPETER: *Proc. Phys. Soc.* (*London*), A **63**, 337 (1950).
[13] I. SOLOMON: *Compt. Rend.*, **248**, 92 (1959).

the same frequency ω as the field $\boldsymbol{H}_1$ ([8]). With respect to such a reference the effective magnetic field $\boldsymbol{H}_{\text{eff}}$, whose components are H_1, 0, $H_0 - \omega/\gamma$, reverses during the passage through resonance. Since in the adiabatic rapid passage the magnetization is always oriented parallel to $\boldsymbol{H}_{\text{eff}}$, also it is reversed and its modulus is unchanged.

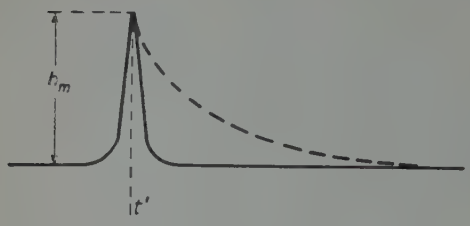

Fig. 1. – Full line: signal due to a rapid adiabatic passage. Broken line: decay signal when the passage is stopped at resonance.

The signal observed is proportional to the component of the magnetization along x'; so one finds directly the equation given by BLOCH ([14]) for such a passage:

$$M_{x'}(t) = M \frac{1}{(1+\delta^2)^{\frac{1}{2}}} \qquad \text{where} \qquad \delta = \frac{\gamma H_0 - \omega}{\gamma H_1} .$$

The signal reaches its highest value at resonance ($\delta = 0$) and has the shape indicated with a full-line in Fig. 1.

2. – The stopping of a rapid adiabatic passage.

Let us see what happens when one stops a rapid adiabatic passage, stopping the variation of the magnetic field H_0 when it reaches the value $H_0(t') = H'$. Let us suppose in general $H' \neq H^*$, where $H^* = \omega/\gamma$ is the resonance value.

The effective field and consequently the magnetization $\boldsymbol{M}$ will stop in a direction forming with the z' axis an angle

$$\theta' = \text{arc tg} \frac{\gamma H_1}{\gamma H' - \omega} . \tag{4}$$

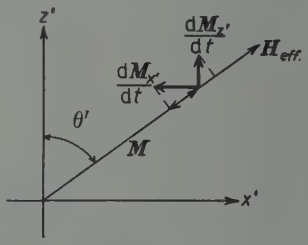

Fig. 2. – If $\boldsymbol{M}$ is pointed in the direction of $\boldsymbol{H}_{\text{eff}}$, relaxation effects cause only changes of its modulus.

It can be easily seen that after the stopping of the passage the effect of the relaxation will be to change the modulus of the magnetization and not the direction.

For this reason the rate of change of M is (see Fig. 2)

$$\frac{dM}{dt} = \left(\frac{dM_{z'}}{dt}\right) \cos\theta' + \left(\frac{dM_{x'}}{dt}\right) \sin\theta' ,$$

([14]) F. BLOCH: *Phys. Rev.*, **70**, 460 (1946).

where

$$\frac{dM_{z'}}{dt} = \frac{1}{T_1}(M_0 - M_{z'}), \qquad \frac{dM_{x'}}{dt} = -\frac{1}{T_2} M_{x'},$$

are the components of the rate of change of M far from resonance. Noticing that $M_{x'} = M \sin\theta'$ and $M_{z'} = M \cos\theta'$, the above expression can be written:

$$\frac{dM}{dt} = -M\left(\frac{\sin^2\theta'}{T_2} + \frac{\cos^2\theta'}{T_1}\right) + \frac{1}{T_1} M_0 \cos\theta'.$$

The general solution of the above differential equation is:

$$M(t) = A \exp\left[-\left(\frac{1}{T_2}\sin^2\theta' + \frac{1}{T_1}\cos^2\theta'\right)(t-t')\right] + \frac{(1/T_1)M_0\cos\theta'}{(1/T_2)\sin^2\theta' + (1/T_1)\cos^2\theta'}. \tag{5}$$

In particular, if the magnetic field is stopped at the resonance for which $\theta' = 90°$, the component of M along x' is

$$M_{x'}(t) = M(t) = M(t') \exp[-(t-t')/T_2]$$

and the signal approaches the value 0 with time constant T_2.

This result could have been easily predicted from the fact that the magnetization at the resonance lies in the plane xy and will be affected by the transversal relaxation only since it must stay on that plane.

The nuclear signal one obtains in this case after the adiabatic rapid passage has been stopped is represented by the broken line of Fig. 1. This portion of the signal (decay signal) makes it possible to obtain directly the value of the transversal relaxation time T_2.

Equation (5) indicates that generally, when the magnetic field H_0 has been stopped at the value H', the modulus of the magnetization approaches the limiting value

$$M_r = \frac{(1/T_1)M_0\cos\theta'}{(1/T_2)\sin^2\theta' + (1/T_1)\cos^2\theta'}, \tag{6}$$

with time constant T given by

$$\frac{1}{T} = \frac{1}{T_2}\sin^2\theta' + \frac{1}{T_1}\cos^2\theta'. \tag{7}$$

The limiting value M_r will be called « residual magnetization ». It can be easily seen that the vector $\boldsymbol{M}_r$, as the angle θ' varies, describes an ellipse passing through the origin, whose major semiaxis, oriented along the z' axis, has the value $M_0/2$ and whose minor semiaxis has the value $(M_0/2)(T_2/T_1)^{\frac{1}{2}}$ (see Fig. 3).

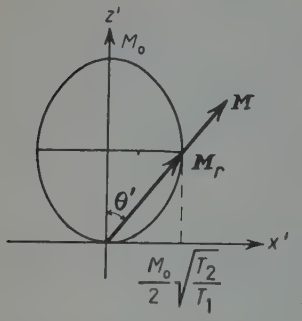

Fig. 3. – Residual magnetization as a function of θ'.

If we project $M(t)$ given by equation (5) on the x' axis we obtain in the general case, the shape of the nuclear signal after the field has been stopped:

$$(8) \qquad M_{x'}(t) = M(t)\sin\theta' = \\ = A\sin\theta'\exp\left[-(t-t')/T\right] + M_r\sin\theta' ,$$

where $A = M(t') - M_r$.

The signal will approach a limiting value h_r, which we will call the « residual signal », with time constant T given by equation (7). The residual signal h_r is proportional to

$$(9) \qquad M_{rx'} = \frac{(1/T_1)M_0\cos\theta'\sin\theta'}{(1/T_2)\sin^2\theta' + (1/T_1)\cos^2\theta'} .$$

If we put $\operatorname{cotg}\theta' = \delta$ into equation (9), we obtain:

$$(10) \qquad M_{rx'} = M_0\frac{\delta}{\delta^2 + T_1/T_2} .$$

$M_{rx'}$ varies with δ as indicated in Fig. 4 and assumes the extreme values $\pm(M_0/2)(T_2/T_1)^{\frac{1}{2}}$ for $\delta = \pm(T_1/T_2)^{\frac{1}{2}}$ (*). We have drawn by a broken line in Fig. 5 and in Fig. 6 the decays of the signal in the cases when the field is stopped before resonance ($\delta > 0$) and after resonance ($\delta < 0$) respectively.

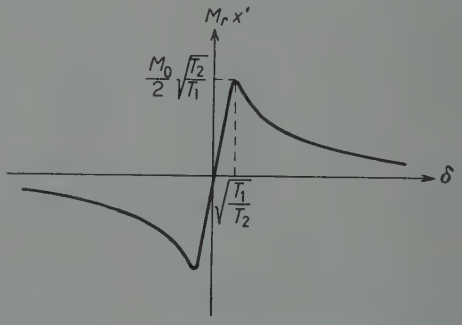

Fig. 4. – Residual signal as a function of δ.

(*) It can be noticed that equation (10) coincides with the expression for the component of the magnetization in the xy plane, given by BLOCH [14] for the case of a slow adiabatic passage under conditions (3).

This coincidence is not surprising because, when the oscillating field is strong enough, a slow passage can be regarded as obtained by a succession of small rapid variations of the magnetic field H_0 in which the magnetization reaches its equilibrium value after every small variation of the field.

In principle it is possible to measure separately T_1 and T_2 stopping the rapid passage out of resonance. In fact the shape of the decay signal gives the value T of equation (7). Furthermore if we compare the value h_r of the re-

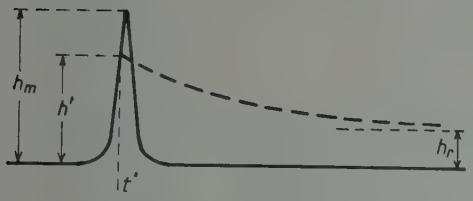

Fig. 5. – Full line: signal due to a rapid adiabatic passage. Broken line: decay signal when the passage is stopped before resonance.

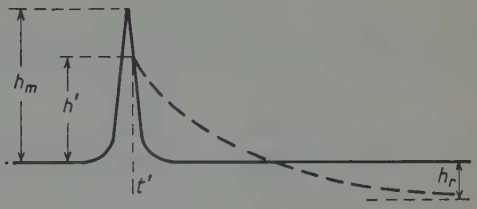

Fig. 6. – Full line: signal due to a rapid adiabatic passage. Broken line: decay signal when the passage is stopped after resonance.

sidual signal with the value h_0 the signal reaches in a normal rapid adiabatic passage when M has reached its equilibrium value M_0, we obtain from equation (9)

$$\frac{h_r}{h_0} = \frac{M_{rx'}}{M_0} = \frac{(1/T_1)\cos\theta'\sin\theta'}{(1/T_2)\sin^2\theta' + (1/T_1)\cos^2\theta'}. \tag{11}$$

When one passes periodically through resonance with periods not very great with respect to T_1, one can still calculate h_0 from the value of the signal h_m, smaller than h_0 ([15]). Finally, noticing that the value h' of the signal at the time the field is stopped is proportional to

$$M_{x'}(t') = M(t')\sin\theta',$$

we can obtain

$$\sin\theta' = \frac{M_{x'}(t')}{M(t')} = \frac{h'}{h_m}. \tag{12}$$

From equations (7), (11) and (12) it is then possible to obtain θ' and both relaxation times T_1 and T_2.

It must be pointed out, however, that the procedure described above does not allow great precision and requires a knowledge of h_0. It seems better to make use of two records, one in which the passage is stopped at resonance, the other with the passage stopped out of resonance. From the two decay

([15]) G. Chiarotti, G. Cristiani, L. Giulotto and G. Lanzi: *Nuovo Cimento*, **12**, 519 (1954).

signals one can obtain T_1 and T_2 without knowing h_0 and h_r. However it is still preferable to obtain T_1 separately with a different method described elsewhere ([15]).

3. – Limitations to the use of the method.

To apply successfully the method described it is required that $\boldsymbol{H}_{\text{eff}}$ be homogeneous in the sample. This is the case when the oscillating field is uniform in the region of the sample and when the condition

$$H_1 \gg \Delta H_0 \tag{13}$$

is satisfied, where ΔH_0 is the inhomogeneity of the constant magnetic field in the region of the sample.

To measure T_2 in pure liquids the method described seems preferable to the method of spin-echoes, since it is not limited by self-diffusion phenomena.

Condition (13) may not be difficult to satisfy. It is always easy to check if condition (13) is satisfied. In fact let us suppose that condition (13) is not satisfied and let us imagine separating the sample into three equal parts, each of which is subjected to a uniform magnetic field $H_0 - \Delta H_0$, H_0, $H_0 + \Delta H_0$ respectively. Let us suppose we stop the passage when the signal has reached its highest value. At that time the positions of the three magnetization vectors $\boldsymbol{M}_1$, $\boldsymbol{M}_2$, $\boldsymbol{M}_3$, corresponding to the three parts of the sample are those represented in Fig. 7. After a time long with respect to T_1 and T_2, $\boldsymbol{M}_2$ will become 0 while $\boldsymbol{M}_1$ and $\boldsymbol{M}_3$ will have become $\boldsymbol{M}_{r1}$ and $\boldsymbol{M}_{r3}$ respectively. The residual signal will be equal to 0 also in this case as when $\Delta H_0 \ll H_1$.

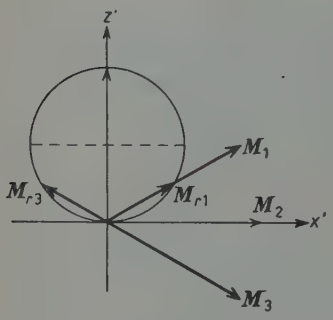

Fig. 7. – Simplified model of the behavior of the nuclear magnetization of the different parts of the sample after the stopping of passage.

However the presence of appreciable inhomogeneity can be detected by starting again the passage through resonance.

No signal takes place if the inhomogeneity of H_0 is negligible; an « exit signal » takes place when this is not the case. The exit signal is due to the fact that $\boldsymbol{M}_{r3}$ tends to orient itself in the positive direction of the z' axis and $\boldsymbol{M}_{r1}$ tends to orient itself in the negative direction of the z' axis when one goes out of resonance.

In practice one can consider that condition (13) is obeyed when, stopping the passage at resonance, and starting it again after a time long compared with T_1, no exit signal is observed or the height of the exit signal is less than 1/20 of h_0.

However it is not convenient to use very strong oscillating fields, since the value of T_2 can be dependent on H_1, when this is of the order of the local field ([16,17]).

4. – Experimental apparatus.

The principle on which the present device is based is that of using the nuclear signal due to a rapid adiabatic passage to stop the passage when the nuclear magnetization precesses in the xy plane, perpendicular to the direction z of the constant magnetic field. Precisely, let us consider a nuclear signal due to a rapid adiabatic passage as indicated in Fig. 8 (full line). When the height of the signal has reached a certain value h^* a special discriminator connected to the vertical deflection plates of the oscillograph gives a pulse. The pulse is delayed by a time Δt by a delay circuit and sets a special device to stop the variation of the current in the modulating coils. The delay time Δt is determined in such a way that the modulation current is stopped at resonance or eventually before or after reaching the resonance. The block diagram to illustrate the experimental apparatus is given in Fig. 9.

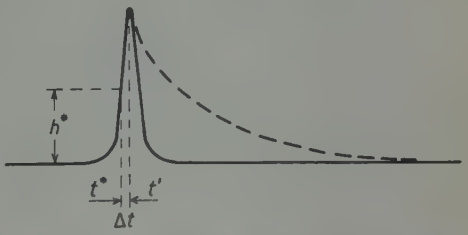

Fig. 8. – Full line: signal due to a rapid adiabatic passage. Broken line: decay signal.

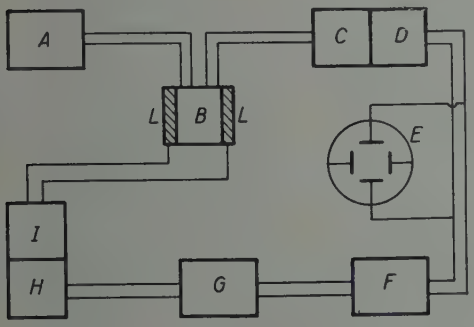

Fig. 9. – Block diagram of the experimental apparatus: *A*) high frequency generator; *B*) r.f. head; *C*) r.f. amplifier and detector; *D*) d.c. amplifier (including the d.c. amplifier of the oscilloscope); *E*) oscilloscope; *F*) discriminator; *G*) delay circuit; *I*) generator of the modulating current with stopping device *H*); *L*) modulating coils.

([16]) A. G. Redfield: *Phys. Rev.*, **98**, 1787 (1955).
([17]) N. Bloembergen and P. Sorokin: *Phys. Rev.*, **110**, 865 (1958).

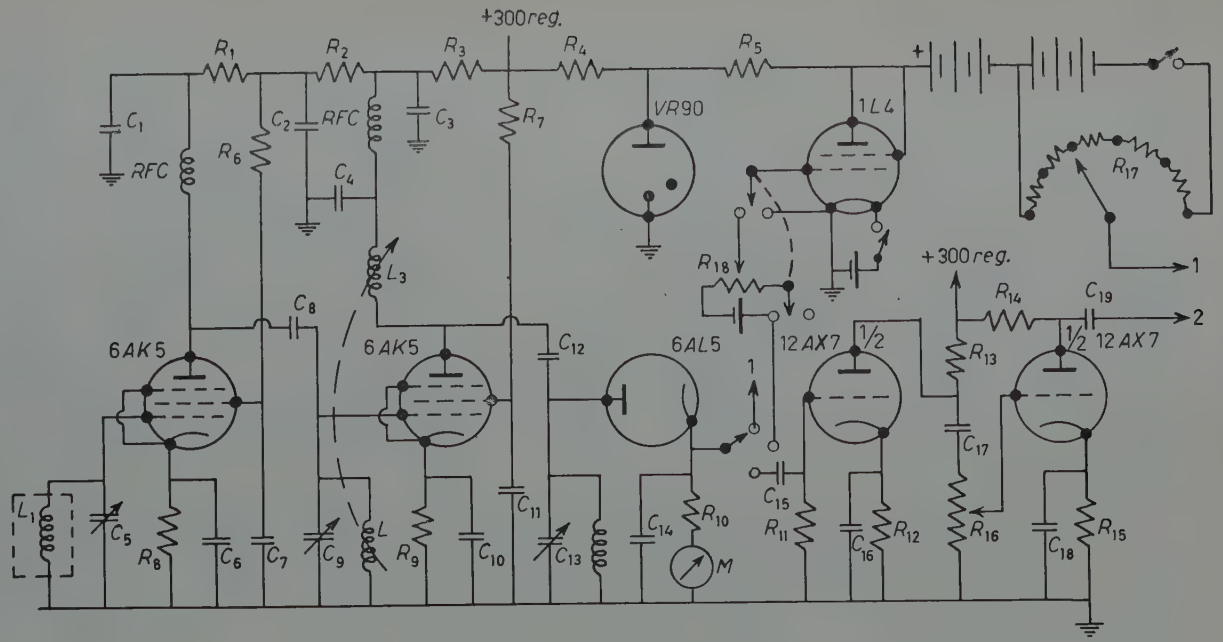

Fig. 10. – Circuit diagram of the receiver.

R_1 – 2.2 kΩ	R_7 – 68 kΩ	R_{13} – 47 kΩ	C_1 – 20 μF	C_7 – 10000 pF	C_{13} – 50 pF
R_2 – 22 kΩ	R_8 – 220 Ω	R_{14} – 68 kΩ	C_2 – 20 μF	C_8 – 10000 pF	C_{14} – 150 pF
R_3 – 22 kΩ	R_9 – 150 Ω	R_{15} – 1500 Ω	C_3 – 20 μF	C_9 – 50 pF	C_{15} – 0.2 μF
R_4 – 25 kΩ	R_{10} – 500 kΩ	R_{16} – 1 MΩ	C_4 – 680 pF	C_{10} – 1200 pF	C_{16} – 25 μF
R_5 – 45 kΩ	R_{11} – 470 kΩ	R_{17} – 100 kΩ	C_5 – 50 pF	C_{11} – 10000 pF	C_{17} – 0.2 μF
R_6 – 47 kΩ	R_{12} – 1400 Ω	R_{18} – 50 kΩ Helipot	C_6 – 1200 pF	C_{12} – 3.3 pF	C_{18} – 25 μF
					C_{19} – 0.2 μF

L_1 – receiving coil (in the r.f. head); 1 – to d.c. amplifier of the c.r.o; 2 – to a.c. amplifier of the c.r.o. Heating supplied by 6 V storage battery.

The transmitter with the phase shifter, the radiofrequency head and the magnet are similar to those described in another paper ([15]). The only significant difference concerns the modulating coils which are now placed on the walls of the radiofrequency head in order to obtain a modulating field in phase with the modulating voltage. We describe here in some detail the other parts of the experimental apparatus.

4·1. *Receiver.* – The receiver consists of two r.f. tuned amplifying stages, a diode detector and a d.c. amplifier (Fig. 10).

The coil L_3, variably coupled to the coil L_2, allows a positive or negative feedback to the second 6AK5 tube. A microammeter measuring the diode current is used to tune the amplifying stages. When it is aligned the microammeter is used to regulate the level of the leakage in the receiving coil in order to avoid saturation in the first r.f. stage. The output of the detector is directly connected either to a d.c. amplifier or also directly to the d.c. amplifier of the c.r.o., when the signals are quite strong.

We may also connect the detector output to a two stage a.c. amplifier. The latter is preferred, out of practical convenience, in checking operations, principally in order to facilitate the regulation of the phase of the leakage in the receiving coil.

4·2. *Nuclear signal recording.* – The horizontal sweep of the c.r.o. can be driven by a voltage delivered by the modulating current generator itself. In this manner the observation of the rapid adiabatic signals becomes quite easy and the discriminator and the delay and stopping device of the modulating current can be easily adjusted as desired. The nuclear signals can be recorded with a photographic apparatus or with a high speed pen recorder.

4·3. *Modulating and stopping devices.* – A first attempt to stop the passage at resonance has been made modulating the constant magnetic field with an electrolytic bridge analogous to the one described and used in the measurement of T_1 ([15]).

Actually we adopt a modulating device, in which a relaxation oscillator is used. The saw-tooth generator indicated in Fig. 11, allows to obtain sweep periods between 0.2 and 80 seconds. To stop the variation of the modulating magnetic field the charging of the condenser C_1 of the relaxation oscillator can be stopped at the proper time by a relay S.

An electromagnetic relay can be used if the relaxation times to be measured are sufficiently long. To measure small values of T_2 the electromagnetic relay should be replaced by a special electronic relay.

The modulation coils are connected between the cathodes of the power stage and a potentiometric circuit. In this way we can adjust the potentio-

meter so that the modulating current at resonance is very small in order to avoid inhomogeneities of the constant magnetic field due to the modulating current.

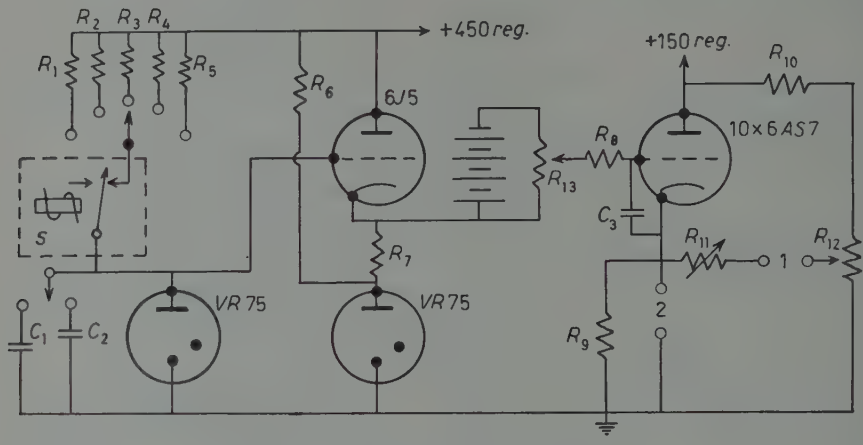

Fig. 11. – Circuit diagram of the modulating current generator.

R_1 – 2.7 MΩ	R_6 – 33 kΩ	R_{11} – 200 Ω
R_2 – 3.9 MΩ	R_7 – 47 kΩ	R_{12} – 10 Ω
R_3 – 8.2 MΩ	R_8 – 10 kΩ	R_{13} – 100 kΩ
R_4 – 17 MΩ	R_9 – 15 Ω	C_1 – 32 μF
R_5 – 35 MΩ	R_{10} – 40 Ω	C_2 – 1 μF
		C_3 – 10000 pF

S relay (see Fig. 12); 1 to modulating coils; 2 to horizontal deflection amplifier of the c.r.o. Heating supplied by a 6 V storage battery.

4'4. *Discriminator and delay circuit.* – Let us describe now the discriminator and the delay circuits (Fig. 12). The grid of a thyratron V_2 is connected to the vertical plates of the c.r.o. through a buffer stage V_1. The resistor R_1 increases the input impedance so that signals on the c.r.o. are not distorted by the discriminator. The potentiometer R_7 regulates the firing potential of the thyratron V_2. The thyratron V_3 is connected in series with the electromagnetic relay S which stops the relaxation oscillator. V_3 is triggered after a delay with respect to V_2, which depends on the values of R_5 and R_6 and of C_1 or C_2 or C_3 and also depends on the voltage from the battery B_3.

With the values of B_3, R_5, R_6, C_1, C_2, C_3 indicated in Fig. 12 it is possible to control the delay time in the range between 3 and 10^{-3} s.

To avoid disturbance of the signals on the c.r.o. it was found convenient

to supply this device with separate batteries. It is also convenient to stabilize the voltage of these batteries in order to obtain delays independent of the conditions of the batteries.

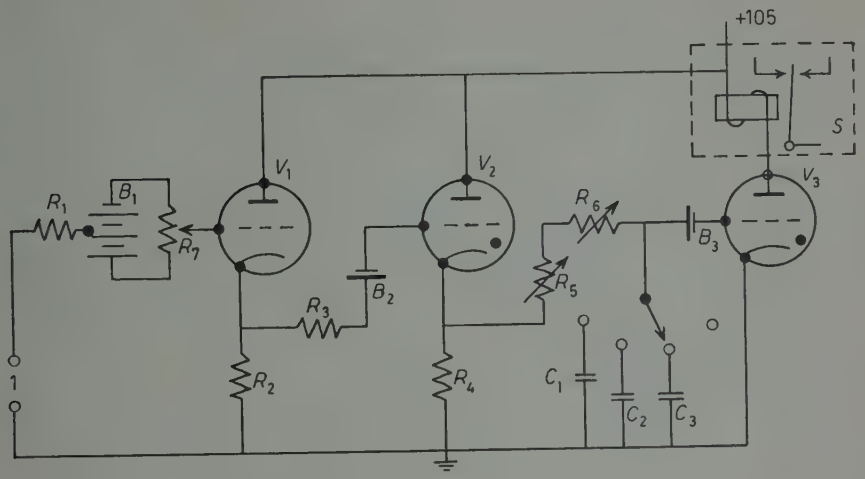

Fig. 12. – Diagram of the discriminator and delay circuit.

R_1 – 1.5 MΩ	R_6 – 50 KΩ	B_1 – 12 V
R_2 – 39 KΩ	R_7 – 50 KΩ	B_2 – 6 V
R_3 – 18 KΩ	C_1 – 0.1 μF	B_3 – 67.5 V
R_4 – 12 KΩ	C_2 – 0.3 μF	V_1 – 6C4
R_5 – 1 MΩ	C_3 – 1 μF	V_2 – PL2D21
		V_3 – PL2D21

S relay (see Fig. 11); 1 to vertical deflection plates of the c.r.o. Heating supplied by a 6 V storage battery.

4·5. *Some improvements introduced in the device for the measurement of* T_2. – For a correct interpretation of the record the strong magnetic field should remain rigorously constant after the stopping of the passage. In practice the constant magnetic field can change slightly after the stopping because of the following two effects.

A first cause of instability of the constant field after stopping can be a small spontaneous discharge of the condensers used in the relaxation oscillator. The spontaneous discharge can be easily observed and controlled on the oscillograph and can be compensated delivering to the condensers a very small current: this can be done with a very high variable resistor in parallel with the relay contacts. We have used a resistor variable between $7 \cdot 10^8$ and 10^{13} Ω. This resistor consists of a disc of nylon sponge between two metallic electrodes one of which is convex. The variation of the resistance is obtained by means of a screw which varies the distance between the electrodes.

There is another cause of instability of the magnetic field after stopping, which may be more important. It is due to the fact that not all the lines of force coming out of the system of the two modulating coils close themselves in the air gap but a part of them cross the iron of the electromagnet. This part of the flux follows the modulating current with a certain delay so that, when the modulating current is stopped, the magnetic field still varies in the same direction. The effect on H_0 can be appreciable even a few seconds after the variation of the modulating current has been stopped and may cause remarkable deformations on the decay signal. The delay by which that part of the flux through the magnet follows the modulating current is due mainly to the current induced in the energizing coils of the magnet.

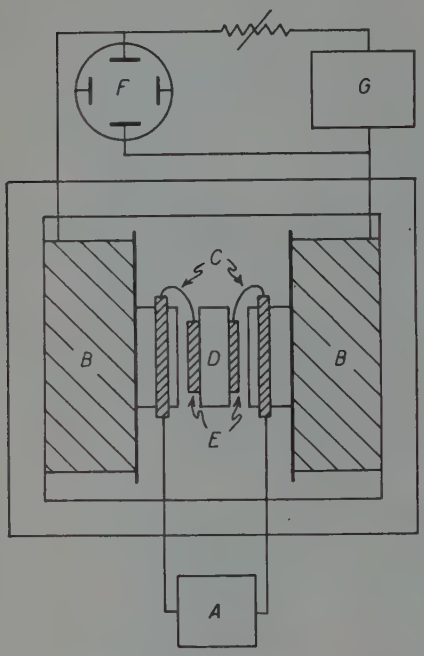

Fig. 13. – Experimental arrangement for checking the decoupling coils. A) modulation current generator; *B*) field coils; *C*) decoupling coils; *D*) r.f. head with modulation coils *E*; *F*) c.r.o.; *G*) field coils power supply.

This inconvenience can be reduced by increasing the distance between the modulating coils and the pole faces. This can be done but there are practical limitations. An artifice which has been found very effective consists of preventing the modulating flux from passing through the magnet, with the use of special decoupling coils *C* placed on the poles (Fig. 13). The decoupling coils are connected in series with the modulating coils in the r.f. head so that the modulation current flows through them in the direction opposite to that of the modulating current. The number of turns of the decoupling coils is found by trial so that if an a.c. flows through the system formed by the modulating coils, an oscilloscope connected across the terminals of the energizing coils of the magnet detects a negligible induced voltage.

5. – Some experimental results.

We have recorded a large number of nuclear signals after stopping a rapid adiabatic passage near the resonance. The main purpose of these records was to test the experimental apparatus and to confirm the prediction made in the second part of the present paper.

In a previous paper ([15]) we described the various aspects of the signal obtained in a rapid adiabatic passage. In particular with a sinusoidal symmetric modulation of the constant field with respect to the resonating field, one obtains a succession of signals of the same amplitude and alternatively up and down.

However, if the modulating current generator consists of a relaxation oscillator followed by an amplifier and the recorder runs with the proper speed the return signals are so fast that they cannot be detected. For this reason with a saw-tooth modulation of H_0 we obtain a succession of signals of the same amplitude and all at the same side.

In Fig. 14 we reproduce three typical records obtained with the saw-tooth generator, with the device to stop the passage used with three different delays. Each one of the three records 1, 2 and 3, contains the signal of a regular adiabatic rapid passage.

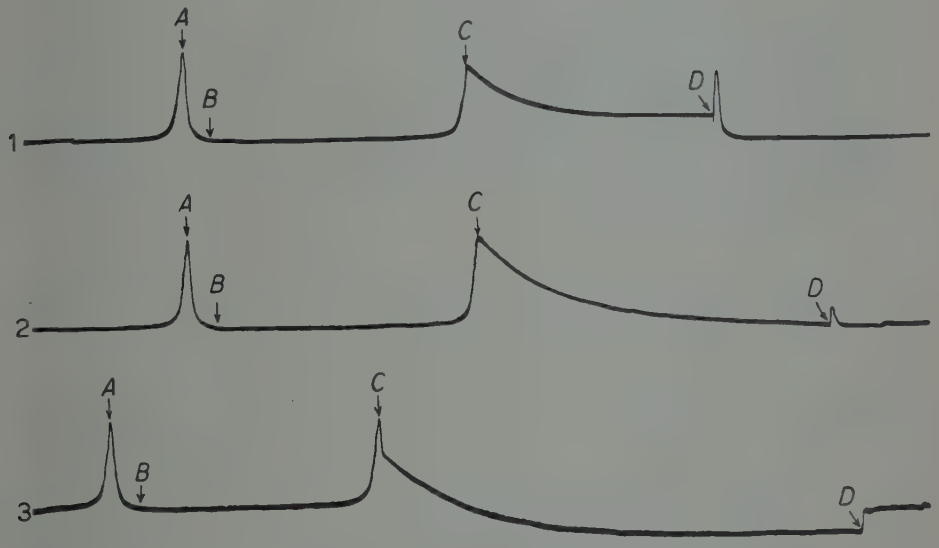

Fig. 14. – Decay signals in three typical cases.

This signal reaches its maximum in A). After this signal we can observe in the three records the signal of an adiabatic rapid passage stopped in C). Between the two signals there should exist in B) a return signal which is not visible however. In record 1 the stopping of the passage at C) is made before reaching the resonance; in record 2 the stopping takes place at resonance; in record 3, some time after the resonance has been reached.

As predicted in Section 2 of this paper, in 1 the decay signal tends towards a positive residual signal; in 2 the signal tends to zero; in 3, to a negative re-

sidual signal. At *D*) the passage starts again. We can then notice a rapid disappearance of the residual signal. In 1 the disappearance of the residual signal is preceded by a quite large signal due to the fact that the passage had been stopped before reaching the resonance.

Even in 2 there is a small exit signal due to the inhomogeneities of the field, as discussed in Section **3**.

Some preliminary results have been obtained for the longitudinal and transverse relaxation times of some liquids. In particular we have obtained for water $T_2 = 3.1$ s at a temperature of about 20°. This value of T_2 coincides within the experimental error with the value which we found for T_1 at the same temperature ([18]). We also find values of T_2 coinciding with values of T_1, within the experimental error of other pure liquids, in agreement with the more recent developments of the theory of relaxation in liquids ([19-21,4,22,23]) and with some recent experimental results obtained by SOLOMON ([13]).

* * *

The authors are grateful to Professor A. ABRAGAM and to Professor I. SOLOMON for helpful discussions and to Doctor L. TOSCA for his collaboration.

The authors also wish to express their gratefulness to the Consiglio Nazionale delle Ricerche for its grant, and to the Office, Chief of Research and Development, U.S. Department of Army, who has sponsored in part this work through its European Office.

([18]) L. GIULOTTO, G. LANZI and L. TOSCA: *Arch. des Sci.*, **10**, 250 (1957).
([19]) N. BLOEMBERGEN, E. M. PURCELL and R. V. POUND: *Phys. Rev.*, **73**, 679 (1948).
([20]) N. BLOEMBERREN: *Nuclear Magnetic Relaxation* (The Hague, 1948).
([21]) A. ABRAGAM and R. V. POUND: *Phys. Rev.*, **92**, 953 (1953).
([22]) F. BLOCH: *Phys. Rev.*, **102**, 104 (1956).
([23]) E. M. PURCELL: *Suppl. Nuovo Cimento*, **3**, 961 (1957).

RIASSUNTO

Si descrive un metodo per la misura del tempo di rilassamento trasversale. Il metodo è basato sulla osservazione del decadimento della magnetizzazione nucleare quando essa precede in un piano perpendicolare al campo magnetico costante. Questa condizione è realizzata bloccando, al momento opportuno, la variazione del campo magnetico costante, durante un passaggio veloce adiabatico. Il campo magnetico costante è modulato con una corrente a dente di sega, generata da un oscillatore a rilassamento seguito da un amplificatore. Quando la f.e.m. indotta dalla precessione nucleare raggiunge un valore prefissato, l'oscillatore a rilassamento viene bloccato con un ritardo tale che la variazione del campo magnetico costante sia arrestata al valore per il quale il segnale ha la massima altezza. Sono state eseguite varie misure su alcuni liquidi puri ed i risultati preliminari indicano che i valori di T_2 sono molto prossimi ai valori di T_1.

IL NUOVO CIMENTO Vol. XIV, N. 1 1° Ottobre 1959

Gravitation and Electromagnetism.

A. H. Klotz

Rutherford College of Technology - Newcastle upon Tyne

(ricevuto il 1° Giugno 1959)

Summary. — A unified field theory is developed from a generalized metric involving skew symmetric tensor elements. The field gravitational equations of an empty world together with the set of Maxwell's equations independent of electromagnetic vector potentials are derived from modified affine relations based on the geodesic equations. The invariants suggested by the above are used in an action integral variation similar in form to Infeld's and Plebanski's [1] to obtain the most general relations consistent with their work on electrodynamics without vector potentials. Invariant equations resulting from a contraction of these offer a possible empirical test of the action invariants used in unified field theories.

1. – Introduction.

Einstein's Unified Field Theory [2] was shown by M. Ikeda [3] to yield equations of motion of a test particle which were independent of the electromagnetic tensor $g_{\mu\nu}$ to the first order of small quantities. To remedy this defect, G. Stephenson and C. W. Kilmister [4], proposed adoption of the metric

$$\mathrm{d}s = -A_\mu \mathrm{d}x^\mu \pm \sqrt{g_{\mu\nu}\mathrm{d}x^\mu \mathrm{d}x^\nu}\,,$$

with symmetric metric tensor $g_{\mu\nu}$ as the starting point of a new Unified Field Theory. $(m_0c^2/e)A_\mu$ is to be identified with the electromagnetic four vector

(1) L. Infeld and J. Plebanski: *Proc. Roy. Soc.*, **224**, 222 (1954).
(2) A. Einstein: *Meaning of Relativity* (1954), App. II.
(3) M. Ikeda: *Progr. Theor. Phys.*, **7**, 127 (1952).
(4) G. Stephenson and C. W. Kilmister: *Nuovo Cimento*, **10**, 230 (1953).

potential so that the theory depends on its use *a priori*. Thus it appears to exclude the work of INFELD and PLEBANSKI [1], on electromagnetism without potentials. In the present work I shall endeavour to construct an analogous, affine theory which avoids this difficulty.

Our point of departure is in the assumption that the fundamental metric relation should depend explicitly on the skew symmetric part of the metric tensor. The latter takes then, necessarily, the form

$$(1) \qquad ds^2 = a_{\mu\nu}\,dx^\mu dx^\nu + \varphi_{\mu\nu}\,d_2 s^{\mu\nu}, \qquad (\mu, \nu = 1, 2, 3, 4),$$

where $a_{\mu\nu} = +a_{\nu\mu}, \varphi_{\mu\nu} = -\varphi_{\nu\mu}\, d_2 s^{\mu\nu}$ is a skew symmetric, infinitesimal tensor whose character as a second order quantity is indicated by the suffix « 2 ». This element may be regarded as a two dimensional area associated uniquely with any two given world points. A physical interpretation of it appears possible in three dimensional space with separate (not to say absolute) time scale. Since geodesics are to represent paths of material particles the usual Principle of Uncertainty will apply. Instead of a sharply defined path of a test particle between two points of the world A_1, A_2, we should obtain a bundle of possible tracks surrounding A_1 and A_2 as a tube. Any cross-section of this tube will serve our purpose. « $d_2 s^{\mu\nu}$ » thus appears as a four dimensional generalization of this concept.

2. – Geodesics of the world.

The geodesics joining any two points A_1 and A_2 of the world are obtained, in the usual way, from the variation

$$\delta \int ds = 0,$$

the integral being taken from A_1 to A_2 along the curve, and the metric (1) is used. In integration by parts, the integrated terms will be assumed to vanish at the boundaries.

The variation gives

$$0 = \int \delta x^\lambda\, ds \left\{ \left(-[\mu\nu, \lambda]\, \dot{x}^\mu \dot{x}^\nu + a_{\alpha\lambda} \ddot{x}^\alpha \right) + \frac{1}{2} \left(\varphi_{\mu\nu,\lambda} \frac{d_1 \dot{s}^{\mu\nu}}{ds} - \frac{d\varphi_{\mu\nu}}{ds} \frac{\partial_1 \dot{s}^{\mu\nu}}{\partial x^\lambda} \right) \right\},$$

where $d_1 \dot{s}^{\mu\nu}$ is written for $d_2 s^{\mu\nu}/ds$ and $[\mu\nu, \lambda]$ are Christoffel brackets of the first kind formed from $a_{\mu\nu}$. Since δx^λ is arbitrary, the differential equations

of the geodesics become

$$\ddot{x}^\gamma + \left\{ {\gamma \atop \mu\nu} \right\} \dot{x}^\mu \dot{x}^\nu + a^{\gamma\lambda} F_{\beta\lambda} \dot{x}^\beta = 0 \,, \tag{2}$$

where $\dot{s}^{\mu\nu}_{,\lambda} \equiv \partial_1 \dot{s}^{\mu\nu} / \partial x^\lambda$ in

$$F_{\beta\lambda} \equiv \tfrac{1}{2} (\varphi_{\mu\nu,\beta} \dot{s}^{\mu\nu}_{,\lambda} - \varphi_{\mu\nu,\lambda} \dot{s}^{\mu\nu}_{,\beta}) \,.$$

If $F_{\beta\lambda}$ is identified with the electromagnetic tensor, the equations (2) yield, in the absence of gravitation characterized by the potentials $a_{\mu\nu}$, the Lorentz equations of motion of a charged particle.

3. – Field equations.

We obtain the field equations in the way similar to that in which Einstein formulated both the theory of general relativity and his unified field theory. Accordingly we adopt as field equations, at least of an empty world, the vanishing of contracted, generalized « curvature » tensors. Geodesic equations (2) suggest the following form for the relationship analogous to the affine equation:

$$\delta A^\alpha = - \Gamma^\alpha_{\mu\nu} A^\mu \delta x^\nu - F^\alpha_\mu A^\mu \delta s \,, \tag{3}$$

where $F^\alpha_\beta = a^{\alpha\lambda} F_{\beta\lambda}$ and A_μ is any vector. Indeed, if Γ_s are assumed to be symmetric it is possible to identify

$$\Gamma^\beta_{\mu\nu} = \left\{ {\beta \atop \mu\nu} \right\} .$$

Consider next the difference

$$\Delta = \mathrm{d}\,\delta A^\alpha - \delta\,\mathrm{d} A^\alpha ,$$

where « d » and « δ » are two distinct operators of parallel transfer (*e.g.* [5]). If we let « d » refer to differentiation with respect to $x^\varkappa$ and « δ » to differentiation with respect to x^ν we obtain

$$\Delta = \{ - \Gamma^\alpha_{\mu\nu,\varkappa} + \Gamma^\alpha_{\mu\varkappa,\nu} + \Gamma^\alpha_{\beta\nu} \Gamma^\beta_{\mu\varkappa} - \Gamma^\alpha_{\beta\varkappa} \Gamma^\beta_{\mu\nu} \} A^\mu \,\mathrm{d}x^\varkappa \delta x^\nu +$$
$$+ \{ - F^\alpha_{\mu,\varkappa} + \Gamma^\beta_{\mu\varkappa} F^\alpha_\beta - \Gamma^\alpha_{\beta\varkappa} F^\beta_\mu \} A^\mu \,\mathrm{d}x^\varkappa \delta s + \{ F^\alpha_{\mu,\nu} - \Gamma^\beta_{\mu\nu} F^\alpha_\beta + \Gamma^\alpha_{\beta\nu} F^\beta_\mu \} A^\mu \delta x^\nu \,\mathrm{d}s \,,$$

having assumed that $\mathrm{d}\,\delta x^\mu = \delta\,\mathrm{d}x^\mu$, $\mathrm{d}\,\delta s = \delta\,\mathrm{d}s$. Thus sufficient conditions of

---

[5] T. Levi Civita: *Absolute Differential Calculus* (London), (for general reference).

integrability in our world are given by two tensor equations:

$$B^{\alpha}_{\mu\nu\varkappa} = -\Gamma^{\alpha}_{\mu\nu,\varkappa} + \Gamma^{\alpha}_{\mu\varkappa,\nu} + \Gamma^{\alpha}_{\beta\nu}\Gamma^{\beta}_{\mu\varkappa} - \Gamma^{\alpha}_{\beta\varkappa}\Gamma^{\beta}_{\mu\nu} = 0\,, \tag{4a}$$

$$F'^{\alpha}_{\mu;\varkappa} = F'^{\alpha}_{\mu,\varkappa} - \Gamma^{\beta}_{\mu\varkappa}F'^{\alpha}_{\beta} + \Gamma^{\alpha}_{\beta\varkappa}F'^{\beta}_{\mu} = 0\,. \tag{4b}$$

The conditions are also necessary providing δs does not vanish with δx^{ν}. This is contingent on the particular interpretation of the area element $\mathrm{d}_2 s^{\mu\nu}$. The field equations become

$$R_{\mu\nu} = B^{\alpha}_{\mu\nu\alpha} = 0\,, \tag{5a}$$

$$F'^{\alpha}_{\mu;\alpha} = \operatorname{div} F'_{\mu} = 0\,. \tag{5b}$$

Since the covariant derivative of $a_{\mu\nu}$ with respect to Christoffel brackets of the second kind vanishes identically, equations (5*b*) may be written in the form

$$F'^{\mu\alpha}{}_{;\alpha} = 0\,. \tag{6}$$

They are, thus, identical with the second set of Maxwell's equations in the absence of current, while equations (5*a*) are, of course, the well known gravitational equations of an empty world of Einstein.

4. – Hamiltonian theory.

The foregoing interpretation of the generalized world geometry suggests that the two fundamental invariants to be used in the Lagrangian are

$$R = a^{\mu\nu}R_{\mu\nu} \qquad \text{and} \qquad F' = -\tfrac{1}{4}F'_{\mu\nu}F'^{\mu\nu}\,,$$

of Weyl-Eddington theory. Infeld and Plebanski introduce electrically charged matter by defining the four current vector as

$$j^{\mu} = \varrho_e \dot{x}^{\mu} = F'^{\mu\alpha}{}_{;\alpha}\,.$$

In the world with metric given by (1)

$$1 = a_{\mu\nu}\dot{x}^{\mu}\dot{x}^{\nu} + \varphi_{\mu\nu}\frac{\mathrm{d}_2 s^{\mu\nu}}{\mathrm{d}s^2} = \frac{1}{\varrho_m^2}j_{\lambda}j^{\lambda} + p\,, \quad \text{say}\,.$$

Hence the charge density, ϱ_e, is given by

$$\varrho_e^2 = \frac{j_{\lambda}j^{\lambda}}{1-p} = \frac{a_{\lambda\beta}F'^{\beta\gamma}{}_{;\gamma}F'^{\lambda\alpha}{}_{;\alpha}}{1-p}\,.$$

If we assume, with them, that the magnitude of ϱ_e is proportional to the material density

$$\varrho = \frac{k}{\sqrt{1-p}} \{a_{\lambda\beta} F^{\beta\gamma}{}_{;\gamma} F^{\lambda\alpha}{}_{;\alpha}\}^{\frac{1}{2}} .$$

We assume now that the Lagrangian invariant Ω is a function of R, F and ϱ, so that the action principle becomes

$$\delta \int \mathscr{L} \, d\tau = \delta \int \sqrt{-a}\, \Omega(R, F, \varrho)\, d\tau = 0 , \tag{7}$$

where $d\tau$ is the four dimensional volume element and $a = \det \{a_{\mu\nu}\}$.

In carrying out the variation we shall neglect δp which refers to the change of electromagnetic terms in the metric equation. This is equivalent to postulating high neutrality of macroscopic matter (*e.g.* [6]).

We have

$$\delta \mathscr{L} = \Omega\, \delta\sqrt{-a} + \sqrt{-a} \left\{ \frac{\partial \Omega}{\partial R} \delta R + \frac{\partial \Omega}{\partial F} \delta F + \frac{\partial \Omega}{\partial \varrho} \delta \varrho \right\} ,$$

whence, neglecting integrals over three dimensional domains,

$$\int \delta \mathscr{L} \, d\tau = \int d\tau \sqrt{-a}\, P_{\alpha\beta}\, \delta a^{\alpha\beta} - \int d\tau \sqrt{-a}\, Q_{\alpha\beta}\, \delta F^{\alpha\beta} = 0 .$$

where

$$P_{\alpha\beta} = \frac{\partial \Omega}{\partial R} R_{\alpha\beta} - \frac{1}{2} a_{\alpha\beta} \Omega + \frac{1}{2} \frac{\partial \Omega}{\partial F} a_{\alpha\gamma} F_{\beta\varepsilon} F^{\gamma\varepsilon} + \\ + \frac{\partial \Omega}{\partial \varrho} (-j_\alpha j_\beta + a_{\alpha\beta} j_\gamma j^\gamma) \frac{k_0^2}{2\varrho} + \frac{1}{2} a_{\alpha\beta} \left\{ \frac{\partial \Omega}{\partial \varrho} \frac{k_0^2}{\varrho} j_\gamma \right\}_{,\varepsilon} F^{\gamma\varepsilon} , \quad k_0 = \frac{k}{\sqrt{1-p}} ,$$

and

$$Q_{\alpha\beta} = \frac{1}{2} \frac{\partial \Omega}{\partial F} F_{\alpha\beta} + \left\{ \frac{\partial \Omega}{\partial \varrho} \frac{k_0^2}{\varrho} j_\alpha \right\}_{,\beta} .$$

Equating to zero the coefficients of $\delta a^{\alpha\beta}$ and $\delta F^{\alpha\beta}$ we obtain two sets of equations:

$$\frac{\partial \Omega}{\partial F} R_{\alpha\beta} - \frac{1}{2} a_{\alpha\beta} \Omega + \frac{1}{4} \frac{\partial \Omega}{\partial F} \{a_{\alpha\gamma} F_{\beta\varepsilon} F^{\gamma\varepsilon} + a_{\beta\gamma} F_{\alpha\varepsilon} F^{\gamma\varepsilon}\} + \\ + \frac{\partial \Omega}{\partial \varrho} (-j_\alpha j_\beta + a_{\alpha\beta} j_\gamma j^\gamma) \frac{k_0^2}{2\varrho} + \frac{1}{2} a_{\alpha\beta} F^{\gamma\varepsilon} \left[\left\{ \frac{\partial \Omega}{\partial \varrho} \frac{k_0^2}{\varrho} j_\gamma \right\}_{,\gamma} - \left\{ \frac{\partial \Omega}{\partial \varrho} \frac{k_0^2}{\varrho} j_\varepsilon \right\}_{,\gamma} \right] = 0 , \tag{8}$$

[6] A. S. EDDINGTON: *Relativity Theory of Protons and Electrons*, (Cambridge, 1936).

and

$$\frac{\partial \Omega}{\partial F} F_{\alpha\beta} = \left\{ \frac{\partial \Omega}{\partial \varrho} \frac{k_0^2}{\varrho} j_\beta \right\}_{,\alpha} - \left\{ \frac{\partial \Omega}{\partial \varrho} \frac{k_0^2}{\varrho} j_\alpha \right\}_{,\beta} . \tag{9}$$

Equations (9) have been obtained by INFELD and PLEBANSKI [1]. Equations (8), on the other hand, are the most general field equations of a unified field containing charged matter. Contracting those equations we obtain

$$R \frac{\partial \Omega}{\partial R} - 2\Omega - 2F \frac{\partial \Omega}{\partial F} + \frac{3}{2} \varrho \frac{\partial \Omega}{\partial \varrho} + 2F^{\gamma\varepsilon}(A_{\gamma,\varepsilon} - A_{\varepsilon,\gamma}) = 0 , \tag{10}$$

where

$$A_\gamma = \frac{\partial \Omega}{\partial \varrho} \frac{k_0^2}{\varrho} j_\gamma .$$

For different functional forms of Ω, the equation (10) provides the general relation between the curvature invariant R, the electromagnetic invariant F and the density of charged matter ϱ.

5. – Conclusions.

The essential features of the theory presented above are as follows. I have introduced an area element to make the metric depend explicitly on a skew symmetric tensor essential in the description of the electromagnetic field. An attempt was made to interpret this as a link with quantum mechanical uncertainty by analogy with the case of absolute time. The field equations for a world void of matter are derived from a generalization of the affine relationship. This makes it possible to develop a simple form of unified theory without an *a priori* use of electromagnetic vector potentials. In ref. [1] a further link is established between such a theory and nuclear fields. Thirdly, the Lagrangian function of ref. [1] is generalized to include curvature invariant of general relativity. This leads to the most general set of equations of a unified field, involving classical equations only. Indeed, matter is introduced in this way. Since ϱ, F and R are all of dimension of density providing velocity of light, c is taken as numerical unity, Ω must be a homogeneous function of these variables. For example, if (ref. [1]),

$$\Omega = \varrho + F + R$$

then

$$F_{\alpha\beta} = A_{\beta,\alpha} - A_{\alpha,\beta}$$

and equation (10) becomes

$$\varrho = 2(4F - R) .$$

A relation such as this should be amenable to verification on cosmic scale, providing suitable units are used, as a suggestion we may take Eddington's « natural units » with $c = 1$ and $\gamma h^2 = \pi/2$, where γ is the gravitational constant and h Planck's constant, with reference to density as scale variable.

* * *

I should like to express my gratitude to Dr. C. GILBERT of King's College, Newcastle upon Tyne, for helpful discussions.

RIASSUNTO (*)

Si sviluppa una teoria unificata del campo partendo da una metrica generalizzata concernente elementi di tensori antisimmetrici. Da relazioni affini modificate basate sulle equazioni delle geodetiche, si deducono le equazioni gravitazionali del campo per un universo vuoto, e l'insieme delle equazioni di Maxwell indipendenti dai potenziali vettori elettromagnetici. Gli invarianti proposti sopra sono usati, in una variazione dell'azione simile formalmente alle variazioni di Infeld e di Plebanski [3], allo scopo di ottenere, senza ricorrere a potenziali vettori, relazioni più generali in armonia con i lavori di detti autori sull'elettrodinamica. Le equazioni invarianti, risultanti da una contrazione di tali relazioni generali, offrono la possibilità di una riprova empirica degli invarianti di azione usati nelle teorie unificate del campo.

(*) *Traduzione a cura della Redazione.*

IL NUOVO CIMENTO Vol. XIV, N. 1 1° Ottobre 1959

On the Transformation Properties of Strong Interactions.

N. Dallaporta and T. Toyoda (*)

Istituto di Fisica dell'Università - Padova
Istituto Nazionale di Fisica Nucleare - Sezione di Padova

(ricevuto il 18 Giugno 1959)

Summary. — By extending the procedure outlined in previous papers of grouping several baryon states to form many-component spinors obeying symmetry properties which are not apparent for the separate states, a general Dirac equation satisfied by a 32-component spinor including all the known baryon states is proposed and its properties are discussed. The baryon states, apart from the normal space time co-ordinates, are described by two kinds of independent internal parameters: the isospin variables and the hypercharge variables. The K interactions are expressed by two independent terms with two different interaction constants F and F', each of which is invariant for rotations in a 4 dimensional hypercharge space, and the pion interactions by the usual expression invariant for rotations in a 3 dimensional isospin space, quite independent from the hypercharge space; and finally electromagnetic interactions are formulated by the combination of two terms which allow to obtain the experimentally known charge labellings of the different baryon states when a two step separation process is applied to the equation, which leads for the K transitions to selection rules expressing naturally the conservation of hypercharge or strangeness as it is formulated in the doublet approximation. The combination of the two K interaction terms allows further to obtain two kinds of coupling constants $F+F'$ and $F-F'$ for the different interaction terms, disposed in such a way as to explain the observed different self masses of the baryons. It is further shown that the 32-component equation is invariant under boson, spinor and charge conjugation operations separately, which are rigorously valid even when the different baryon masses are included. Finally some aspects of the γ_5 transformation properties of the equation are discussed. The present approach seems therefore adequate to unify under few common points-of-view the treatment of the baryon states and to put into evidence some general invariance properties which otherwise should not be revealed.

(*) Now at Rikkyo University, Tokyo.

It is generally believed that the most characteristic features of the interactions to which the different particle states are subject are their invariance properties; and after the great advance accomplished recently in their understanding for weak interactions, the same problem related to strong interactions has now become one of the main points on which physical interest is concentrated. It appears, however, that the usual way of representing baryons is not always the most suitable to put into light these invariance properties and therefore the problem of referring to the spinors adequate to this aim has already been considered in some aspects. Thus, SCHREMP (1) and on the same line, GÜRSEY (2), have shown that, by representing nucleons with 8-component spinors which are mixtures of the definite charge states, *i.e.* proton and neutron, one may write for them a wave equation, invariant under an extended γ_5 transformation (3) and under the TOYODA (4) and PAULI (5) transformations, into which isotopic spin formalism and charge independence are naturally included. On a somewhat different line, the present authors (6) have shown that by taking instead an 8-component mixture of baryonic states with opposite electric charge or/and opposite hypercharge, such as $p\,\Xi^-$, or $n\,\Xi^0$ or $\Sigma^+\Sigma^-$, one satisfies with them a modified wave equation which, when mass differences between baryons are neglected, offers the right behaviour for the operations defined and termed as boson conjugation and spinor conujgation by BUDINI, DALLAPORTA and FONDA (7) and for their product which is normal charge conjugation. These two examples seem therefore to show that, by combining together different baryons or, which is equivalent, by increasing the order of the spinors describing them, one may be able to put into evidence properties which are not apparent when the charge states are considered separately.

Thus, one could hope that, by pursuing this process up to the limit in which all different states should be unified into a single physical entity, the baryon, it would be possible to attribute to the equations obeyed by this unique entity all the properties observed to be singly verified in the different partial attempts.

Up to now, only two 4-component spinors were unified into a single 8-component system; while according to our present knowledge of the baryon charge and hypercharge states, four of such 8-component systems should exist, wichever way of grouping the separate particles has been chosen. Therefore,

---

(1) E. J. SCHREMP: *Phys. Rev.*, **99**, 1603 (1955).
(2) F. GÜRSEY: *Nuovo Cimento*, **7**, 411 (1958).
(3) B. TOUSCHEK: *Nuovo Cimento*, **5**, 1281 (1957).
(4) T. TOYODA: *Nucl. Phys.*, **8**, 661 (1958).
(5) W. PAULI: *Nuovo Cimento*, **6**, 204 (1957).
(6) N. DALLAPORTA and T. TOYODA: *Nuovo Cimento*, **12**, 593, (1959).
(7) P. BUDINI, N. DALLAPORTA and L. FONDA: *Nuovo Cimento*, **9**, 316 (1958).

the last step we have just considered should imply to gather these four 8-component states into a single 32-component one, including all the charge, hypercharge and spin states of the baryon, which should combine the properties which were present in the partial groupings of the Schremp-Gürsey (SG) type or of the present authors (DT) type.

Such an attempt will be discussed in the present paper: first a free particle equation for a 32-component baryon will be considered which shall be constructed by gathering two separate 16-component groups, and some of its properties will be investigated. The main purpose of the paper, however, is to study the way to insert in this formalism the different types of strong interactions and to determine the invariance properties to which they obey. From the known elementary properties of the three main groups of electromagnetic, pion and K phenomena, it will be easily recognized that only the K interactions are such as to require a 32-component representation as they are the only ones to cause transitions between the two 16-component groups; and this in some sense gives to the K interactions a kind of priority in order to understand the general structure of the baryon. The insertion of electromagnetic interactions will allow, at the same time, to partly differentiate the charge states. The first separation of states from the original mixed one, due essentially to K interactions, will be obtained with a (DT) type of transformation and this will lead to a twofold degenerate 16-component system.

The further separation of these double states is then obtained by introducing the pion interactions and by completing the electromagnetic differentiation of the states; and this is given by a second transformation of the (SG) type. One thus arrives to the well-known interaction equations for the different charge states according to the so-called doublet approximation scheme proposed indipendently by TIOMNO ([8]), one of the authors ([9]) and PAIS ([10]) and the equivalence of this system with the initial one will prove that all the properties valid for the original system are also valid for the doublet approximation.

A result of particular interest of the present approach will be that the mass differences between baryons may be interpreted not as due to a secondary perturbation but to the fundamental form itself of the K interactions and most of the transformational properties of the system will be shown to hold rigorously even when these mass differences are considered, according to a general idea outlined by one of the present authors ([11]).

([8]) J. TIOMNO: *Nuovo Cimento*, **6**, 69 (1957).

([9]) N. DALLAPORTA: *Proc. Intern. Conf. on Mesons and recently discovered Particles* (Padua-Venice, Sept. 1957), V, 3; *Nuovo Cimento*, **7**, 200 (1958).

([10]) A. PAIS: *Phys. Rev.*, **110**, 574 (1958).

([11]) N. DALLAPORTA: *Nuovo Cimento*, **13**, 159, (1959).

2. – In both the previously quoted attempts ([2,6]) the 8-component free particle equation was written as

$$\left(\Gamma^\mu \frac{\partial}{\partial x_\mu} + \Gamma_5 m\right) X^{(8)} = 0\,, \tag{1}$$

where m is the bare mass of the baryon and the Γ's are reducible 8-component Dirac matrices given as (*)

$$\Gamma^\mu = \begin{pmatrix} 0 & \gamma^\mu \\ \gamma^\mu & 0 \end{pmatrix}, \qquad \Gamma_5 = \begin{pmatrix} -\gamma_5 & 0 \\ 0 & \gamma_5 \end{pmatrix}. \tag{2}$$

Now, the two different interpretations given in the two papers ([2]) and ([6]) for the 8-component spinor may be unified, if we extend our framework to the following 16-component Dirac equation:

$$\left(\mathbf{\Gamma}^\mu \frac{\partial}{\partial x_\mu} + \mathbf{\Gamma}'_5 m\right) X^{(16)} = 0\,, \tag{3}$$

where

$$\mathbf{\Gamma}^\mu = \begin{pmatrix} 0 & \Gamma^\mu \\ \Gamma^\mu & 0 \end{pmatrix}, \qquad \mathbf{\Gamma}'_5 = \begin{pmatrix} -\Gamma^5 & 0 \\ 0 & \Gamma^5 \end{pmatrix} \Gamma_5\,, \qquad \Gamma^5 = \begin{pmatrix} \gamma_5 & 0 \\ 0 & \gamma_5 \end{pmatrix}. \tag{4}$$

The 16-component $X^{(16)}$ spinor represents now a mixing of either the two nucleon and the two Ξ states, or of the four Y hyperon states.

Let us apply a separation transformation defined analogously to the 8-component case by

$$\boldsymbol{S} = \boldsymbol{S}^{-1} = \begin{vmatrix} B & A \\ A & -B \end{vmatrix}, \tag{5}$$

where

$$A = \tfrac{1}{2}(1 + \Gamma^5)\,, \qquad B = \tfrac{1}{2}(1 - \Gamma^5)\,, \tag{6}$$

to eq. (3) and denote a first partially separated 16-component spinor by $\Psi^{(16)}$.

$$X^{(16)} = \begin{vmatrix} X_a^{(8)} \\ X_b^{(8)} \end{vmatrix} = \boldsymbol{S}\,\Psi^{(16)} = \boldsymbol{S} \begin{pmatrix} \Psi_a^{(8)} \\ \Psi_b^{(8)} \end{pmatrix}. \tag{7}$$

(*) In the present paper we shall adopt the conventional Hermitian representation for all γ_μ; then the i in front of the mass term in our previous paper ([6]) is dropped.

The first separation corresponds to the (DT) operation (8) in [6] so that Ψ_a is a mixture of the two nucleon states only and Ψ_b a mixture of the two Ξ states (correspondingly for the hyperon states a second 16-component pair may be separated in a Ψ_c state mixture of Σ^+ Y and a Ψ_d mixture of $Z^0\,\Sigma^-$).

The further separation of (GS) type (see GÜRSEY [2] eq. (15)) may now be obtained for each of the Ψ_n, $(n = a, b, c, d)$, by applying to them the transformation $s = \begin{vmatrix} \beta & \alpha \\ \alpha & -\beta \end{vmatrix}$ (with $\alpha = \frac{1}{2}(1+\gamma_5)$, $\beta = \frac{1}{2}(1-\gamma_5)$),

$$\Psi_n^{(8)} = s\psi_n^{(8)} = s \begin{vmatrix} \psi_n^{(4)} \\ \tilde{\psi}_n^{(4)} \end{vmatrix}; \tag{8}$$

which operates the complete separation of all the double mixtures (proton and neutron, Ξ^0 and $\bar{\Xi}^-$ and so on).

So, starting from a 16-component representation would be sufficient if we should only wish to achieve these separations. However, K interactions are causing transitions between the two 16-component groups just now defined, so, in order to introduce them, we shall need to extend the Dirac equation to a 32-component representation. The simplest way of doing this is then obviously to write:

$$\left[G^\mu \frac{\partial}{\partial x_\mu} + G^5\right] X^{(32)} = 0\,, \tag{9}$$

where

$$G^\mu = \begin{pmatrix} \boldsymbol{\Gamma}^\mu & 0 \\ 0 & \boldsymbol{\Gamma}^\mu \end{pmatrix}, \qquad G_5 = \begin{pmatrix} \boldsymbol{\Gamma}'_5 & 0 \\ 0 & \boldsymbol{\Gamma}'_5 \end{pmatrix}. \tag{10}$$

Two other possible types of vector matrices which will be used later on are:

$$\begin{cases} G''^\mu = \begin{vmatrix} \boldsymbol{\Gamma}^\mu\boldsymbol{\Gamma}_5 & 0 \\ 0 & \boldsymbol{\Gamma}^\mu\boldsymbol{\Gamma}_5 \end{vmatrix} \\ G'^\mu = \begin{vmatrix} \boldsymbol{\Gamma}^\mu\boldsymbol{\Gamma}^5 & 0 \\ 0 & \boldsymbol{\Gamma}^\mu\boldsymbol{\Gamma}^5 \end{vmatrix} \end{cases} \quad \text{with} \quad \boldsymbol{\Gamma}_5 = \begin{vmatrix} \Gamma_5 & 0 \\ 0 & \Gamma_5 \end{vmatrix} \quad \boldsymbol{\Gamma}^5 = \begin{vmatrix} -\Gamma^5 & 0 \\ 0 & \Gamma^5 \end{vmatrix}. \tag{10a}$$

Although such an extension looks like a trivial unification of the two independent 16-component equations just by putting them in parallel in the case of no K interactions, it already involves some transformation properties which will be later considered. Writing explicitly a solution of eq. (9) by using the 8-component spinor notations $X_n^{(8)}$ as

$$X^{(32)} = \begin{vmatrix} X_a^{(8)} \\ X_b^{(8)} \\ X_c^{(8)} \\ X_d^{(8)} \end{vmatrix}, \tag{11}$$

γ_5 invariance may be obtained with the following two independent transformations

$$(12) \qquad X_1^{(32)} \to \begin{vmatrix} BX_a^{(8)} \\ AX_b^{(8)} \\ p_1 BX_c^{(8)} \\ p_1 AX_d^{(8)} \end{vmatrix} \quad \text{or} \quad X_2^{(32)} \to \begin{vmatrix} BX_a^{(8)} \\ AX_b^{(8)} \\ p_2 AX_c^{(8)} \\ p_2 BX_d^{(8)} \end{vmatrix},$$

where p_1 and p_2 are arbitrary numerical factors.

Two other possible transformations obtained from these by just interchanging the A and B factors are discarded, according to the discussion in a preceding paper by one of us ([11]). Therefore, it is in general possible to construct a 2-parameter transformation or projection by combining the two relations (12), under which eq. (9) is invariant, that is:

$$(13) \qquad X^{(32)} \to rX_1^{(32)} + sX_2^{(32)} = \begin{pmatrix} (r+s)B & & & \\ & (r+s)A & & \\ & & rp_1 B + sp_2 A & \\ & & & rp_1 A + sp_2 B \end{pmatrix} X^{(32)},$$

(r and s arbitrary parameters).

We shall now considerer the geometrical structure of the 32-component spinor space and we shall assume that it consists in a direct product of three physical spaces

$$\begin{pmatrix} \text{hypercharge spin space} \\ \text{4 dimensions} \end{pmatrix} \times \begin{pmatrix} \text{isospin space} \\ \text{2 dimensions} \end{pmatrix} \times \begin{pmatrix} \text{ordinary spin space} \\ \text{4 dimensions} \end{pmatrix}.$$

A similar interpretation has already been suggested and developed by TIOMNO ([8]). In order to avoid confusion, we shall always use Greek indices to label 4 dimensional space time coordinates, small Latin letters for the 3 dimensional isospin space and capital Latin letters for the 4 dimensional hypercharge space.

Of course, the geometrical properties of these spaces can be understood only through their invariances. Usually, one derives some quantum numbers from the non-interacting system which in invariant with respect to some groups in these spaces. However, in our opinion, if the interactions are very strong, we may start from the invariant interactions. Then, it may happen to find the free-system to be non-invariant as will be shown later. This fact may be interpreted as some kind of violation of the symmetrical interaction form.

We shall now introduce for 32×32 Dirac matrices which will rule the transitions in the hypercharge 4 dimensional space, as direct products of 8×8 unit matrix elements, each of which is disposed in the familiar way of the 4×4 Dirac γ matrices:

$$\mathbf{\Omega}_K = \Omega_K \times I^{(8)}, \tag{18}$$

where

$$\left\{\begin{array}{l} \Omega_1 = \begin{vmatrix} 0 & i\omega_1 \\ -i\omega_1 & 0 \end{vmatrix}, \quad \Omega_2 = \begin{vmatrix} 0 & i\omega_2 \\ -i\omega_2 & 0 \end{vmatrix}, \quad \Omega_3 = \begin{vmatrix} 0 & i\omega_3 \\ -i\omega_3 & 0 \end{vmatrix}, \quad \Omega_4 = \begin{vmatrix} 0 & I \\ I & 0 \end{vmatrix}, \\ \omega_1 = \begin{pmatrix} 0 & 1 \\ 1 & 0 \end{pmatrix}, \quad \omega_2 = \begin{pmatrix} 0 & -i \\ i & 0 \end{pmatrix}, \quad \omega_3 = \begin{pmatrix} 1 & 0 \\ 0 & -1 \end{pmatrix}, \quad I = \begin{pmatrix} 1 & 0 \\ 0 & 1 \end{pmatrix}, \\ \mathbf{\Omega}_K G^\mu = \pm\, G^\mu \mathbf{\Omega}_K \begin{array}{l} +\text{ for } \{K = 1, 4 \\ -\text{ for } \{K = 2, 3 \end{array}, \\ \mathbf{\Omega}_L \mathbf{\Omega}_K + \mathbf{\Omega}_K \mathbf{\Omega}_L = 2\delta_{KL}, \quad \mathbf{\Omega}_K G_5 = \pm\, G_5 \mathbf{\Omega}_K \begin{array}{l} +\text{ for } \{K = 2, 3 \\ -\text{ for } \{K = 1, 4 \end{array}. \end{array}\right. \tag{19}$$

If one writes G^μ and G_5 as

$$G^\mu = \begin{pmatrix} \omega_1 & 0 \\ 0 & \omega_1 \end{pmatrix} \times \Gamma^\mu = -i\Omega_2\Omega_3 \times \Gamma^\mu, \qquad G^5 = i\Omega_1\Omega_2 \times \Gamma^5, \tag{20}$$

Eq. (9) may be rewritten in such a way as to manifest in a familiar way its transformation property in the hypercharge space:

$$\left(-i\Omega_2\Omega_3 \times \Gamma^\mu \frac{\partial}{\partial x^\mu} + i\Omega_1\Omega_2 \times \Gamma^5 m\right) X^{(32)} = 0\,. \tag{21}$$

Although eq. (21) is not invariant with respect to the rotation group in the hypercharge space, it is invariant under the transformation:

$$X^{(32)} \to \mathbf{\Omega}_5 X^{(32)}, \tag{22}$$

with

$$\mathbf{\Omega}_5 = \Omega_5 \times I^{(8)} = \Omega_1\Omega_2\Omega_3\Omega_4 \times I^{(8)} = \begin{pmatrix} -I^{16} & 0 \\ 0 & +I^{16} \end{pmatrix},$$

as well as under the Lorentz transformation in space time.

From the $\mathbf{\Omega}$ matrices we may now build a pseudo-hypercharge spin vector

$\mathbf{\Omega}'_K$ which has the same commutation relations with G^μ and G_5 as $\mathbf{\Omega}_K$.

$$
(23)\qquad \begin{cases} \mathbf{\Omega}'_1 = -i\mathbf{\Omega}_2\mathbf{\Omega}_5 \equiv \Omega'_1 \times I^8 = \begin{pmatrix} 0 & \omega_2 \\ \omega_2 & 0 \end{pmatrix} \times I^8 , \\ \mathbf{\Omega}'_2 = +i\mathbf{\Omega}_1\mathbf{\Omega}_5 \equiv \Omega'_2 \times I^8 = \begin{pmatrix} 0 & -\omega_1 \\ -\omega_1 & 0 \end{pmatrix} \times I^8 , \\ \mathbf{\Omega}'_3 = -i\mathbf{\Omega}_4\mathbf{\Omega}_5 \equiv \Omega'_3 \times I^8 = \begin{pmatrix} 0 & -iI \\ iI & 0 \end{pmatrix} \times I^8 , \\ \mathbf{\Omega}'_4 = +i\mathbf{\Omega}_3\mathbf{\Omega}_5 \equiv \Omega'_4 \times I^8 = \begin{pmatrix} 0 & -\omega_3 \\ -\omega_3 & 0 \end{pmatrix} \times I^8 . \end{cases}
$$

All the $\mathbf{\Omega}'_K$ anticommute with each other as do the $\mathbf{\Omega}_K$:

$$\mathbf{\Omega}'_K\mathbf{\Omega}'_L + \mathbf{\Omega}'_L\mathbf{\Omega}'_K = 2\,\delta_{KL} .$$

We have further

$$
(24)\qquad \begin{cases} (\mathbf{\Omega}_K \text{ or } \mathbf{\Omega}'_K)\mathbf{\Omega}_5 = -\mathbf{\Omega}_5(\mathbf{\Omega}_K \text{ or } \mathbf{\Omega}'_K) , \\ \mathbf{\Omega}'_1\mathbf{\Omega}'_2\mathbf{\Omega}'_3\mathbf{\Omega}'_4 = \mathbf{\Omega}_5 . \end{cases}
$$

3. – The framework now developed (with a few other additions of already well known elements of the isotopic spin formalism) will be now used to introduce and describe the three main types of strong interactions into eq. (9). We assume as fundamental complete equation:

$$
(25)\qquad \left\{ G^\mu \frac{\partial}{\partial x_\mu} + G_5 m - i\sum_K [F\mathbf{\Omega}_K + F'\Gamma^5\mathbf{\Omega}'_K](\Gamma^5)^{K+1}\varphi_K - \right.
$$
$$
\left. - \frac{i\,e}{2}[G'^\mu + G''^\mu]A_\mu - g\sum_j T_j(\Gamma^5)^{j+1}\pi_j \right\} X^{(32)} = 0 .
$$

In this formula, the φ_K are four real scalar functions in the space-time space and form a four vector in the hypercharge space which will be used to describe the K field, according to a later definition: the $\mathbf{\Omega}_K$ and $\mathbf{\Omega}'_K$ are the two sets of four vector matrices in the hypercharge space as discussed in the previous paragraph, and F and F' are two different interaction constants; further the A^μ are the four vector components of the electromagnetic potential, G'^μ and G''^μ the two 32×32 matrices defined by (10a) and e the electric charge; finally π_j is the isospin vector pseudo scalar pion field and T_j the well-known isospin matrices defined by

$$
(26)\qquad T_j = I^{(4)} \times \tau_j \times I^{(4)} ,
$$

where

$$\tau_1 = \begin{vmatrix} & 1 \\ 1 & \end{vmatrix}, \qquad \tau_2 = \begin{vmatrix} & i \\ -i & \end{vmatrix}, \qquad \tau_3 = \begin{vmatrix} -1 & \\ & +1 \end{vmatrix},$$

and g the interaction constant for the pion interactions.

In the K and pion interactions, the supplementary $(\Gamma^5)^{K+1}$ and $(\Gamma^5)^{j+1}$ factors weighing differently the field components are introduced in order to obtain definite charge state for the mesons in the final results.

We shall now discuss the physical properties implied by these interaction expressions and we shall first show by separation of the definite charge states that equation (25) is equivalent to the doublet approximation scheme.

If we apply successively the two transformations (7) and (8) extended to 32-components with

$$S = \left|\begin{array}{cc:cc} B & A & & \\ A & -B & & \\ \hdashline & & B & A \\ & & A & -B \end{array}\right|, \tag{27}$$

$$s = I^{(4)} \times \begin{vmatrix} \beta & \alpha \\ \alpha & -\beta \end{vmatrix}, \tag{28}$$

and define the K field by:

$$\varphi_1 + i\varphi_2 = K_c, \quad \varphi_1 - i\varphi_2 = K_c^*, \quad \varphi_3 + i\varphi_4 = K_n, \quad \varphi_3 - i\varphi_4 = K_n^* \tag{29}$$

K_c destroys K^+ and creates $\overline{K}^-$, K_n destroys K^0 and creates $\overline{K}^0$,
K_c^* destroys $\overline{K}^-$ and creates K^+ K_n^* destroys $\overline{K}^0$ and creates K^0

Then the first separation (7) gives us:

$$\left\{\begin{aligned}
&\left\{\Gamma_\mu\left[\frac{\partial}{\partial x_\mu} - \frac{ie}{2}(1+\Gamma_5)A_\mu\right] + m\Gamma_5 - g\tau_j \times I^{(4)}(\Gamma^5)^{j+1}\pi_j\right\}\Psi_A + \\
&\qquad + (F+F')\Gamma^5 K_c \Psi_D - (F+F')\Gamma^5 K_n \Psi_C = 0\,, \\
&\left\{\Gamma_\mu\left[\frac{\partial}{\partial x_\mu} + \frac{ie}{2}(1-\Gamma_5)A_\mu\right] + m\Gamma_5 + g\tau_j \times I^{(4)}(\Gamma^5)^{j+1}\pi_j\right\}\Psi_B - \\
&\qquad - (F-F')\Gamma^5 K_C^* \Psi_c - (F-F')\Gamma^5 K_n^* \Psi_D = 0\,, \\
&\left\{\Gamma_\mu\left[\frac{\partial}{\partial x_\mu} - \frac{ie}{2}(1+\Gamma_5)A_\mu\right] + m\Gamma_5 - g\tau_j \times I^{(4)}(\Gamma^5)^{j+1}\pi_j\right\}\Psi_C - \\
&\qquad - (F-F')\Gamma^5 K_c \Psi_B + (F+F')\Gamma^5 K_n^* \Psi_A = 0\,, \\
&\left\{\Gamma_\mu\left[\frac{\partial}{\partial x_\mu} + \frac{ie}{2}(1-\Gamma_5)A_\mu\right] + m\Gamma_5 + g\tau_j \times I^{(4)}(\Gamma^5)^{j+1}\pi_j\right\}\Psi_D + \\
&\qquad + (F+F')\Gamma^5 K_c^* \Psi_A + (F-F')\Gamma^5 K_n \Psi_B = 0\,.
\end{aligned}\right. \tag{30}$$

By applying now the second separation and further defining the pion field as

$$\pi_1 - i\pi_2 = \pi\,, \qquad \pi_1 + i\pi_2 = \pi^*\,, \tag{31}$$

$$\begin{cases} \pi \text{ destroys } \pi^+ \text{ and creates } \pi^- \\ \pi^* \text{ destroys } \pi^- \text{ and creates } \pi^+\,, \\ \pi_3 \text{ destroys and creates } \pi_0 \end{cases}$$

we obtain for the complete separate set of baryon equations:

$$\begin{cases} \left\{\gamma^\mu\left(\frac{\partial}{\partial x_\mu} - ieA_\mu\right) + m\right\}\psi_A - g\gamma_5\,(\pi\tilde{\psi}_A + \pi_3\psi_A) + \\ \qquad + (F + F')\gamma_5(K_c\psi_D - K_n\psi_C) = 0\,, \\ \left\{\gamma^\mu\frac{\partial}{\partial x^\mu} + m\right\}\tilde{\psi}_A + g\gamma_5\,(\pi^*\psi_A - \pi_3\tilde{\psi}_A) - \\ \qquad - (F + F')\gamma_5(K_c\tilde{\psi}_D - K_n\tilde{\psi}_C) = 0\,, \\ \left\{\gamma^\mu\frac{\partial}{\partial x_\mu} + m\right\}\psi_B + g\gamma_5\,(\pi\tilde{\psi}_B + \pi_3\psi_B) - \\ \qquad - (F' - F')\gamma_5(K_c^*\psi_C + K_n^*\psi_D) = 0\,, \\ \left\{\gamma_\mu\left(\frac{\partial}{\partial x_\mu} + ieA_\mu\right) + m\right\}\tilde{\psi}_B - g\gamma_5(\pi^*\psi_B - \pi_3\tilde{\psi}_B) + \\ \qquad + (F - F')\gamma_5(K_c^*\tilde{\psi}_C + K_n^*\tilde{\psi}_D) = 0\,, \\ \left\{\gamma^\mu\left(\frac{\partial}{\partial x_\mu} - ieA_\mu\right) + m\right\}\psi_C - g\gamma_5(\pi\tilde{\psi}_C + \pi_3\psi_C) - \\ \qquad - \gamma_5\{(F - F')K_c\psi_B - (F + F')K_n^*\psi_A\} = 0\,, \\ \left\{\gamma^\mu\frac{\partial}{\partial x_\mu} + m\right\}\tilde{\psi}_C + g\gamma_5(\pi^*\psi_C - \pi_3\tilde{\psi}_C) + \\ \qquad + \gamma_5\{(F - F')K_c\tilde{\psi}_B - (F + F')K_n^*\tilde{\psi}_A\} = 0\,, \\ \left\{\gamma_\mu\frac{\partial}{\partial x_\mu} + m\right\}\psi_D + g\gamma_5(\pi\tilde{\psi}_D + \pi_3\psi_D) + \\ \qquad + \gamma_5\{(F + F')K_c^*\psi_A + (F - F')K_n\psi_B\} = 0\,, \\ \left\{\gamma_\mu\left(\frac{\partial}{\partial x_\mu} + ieA_\mu\right) + m\right\}\tilde{\psi}_D - g\gamma_5(\pi^*\psi_D - \pi_3\tilde{\psi}_D) - \\ \qquad - \gamma_5\{(F + F')K_c^*\tilde{\psi}_A + (F - F')K_n\tilde{\psi}_B\} = 0\,, \end{cases} \tag{32}$$

These are the equations satisfying the doublet approximation if we make the following identifications:

$$\begin{cases} \psi_A = p & \psi_B = \Xi^0 & \psi_C = \Sigma^+ & \psi_D = Z^0\,, \\ \tilde{\psi}_B = n & \tilde{\psi}_B = \Xi^- & \tilde{\psi}_C = Y^0 & \tilde{\psi}_D = \Sigma^-\,, \end{cases} \tag{33}$$

which result first from the sign or the absence of the electromagnetic interaction terms ([12]), while the display of the K interaction transitions shown in Fig. 1 reproduces the well-known selection rules which are generally expressed with the concept of strangeness conservation.

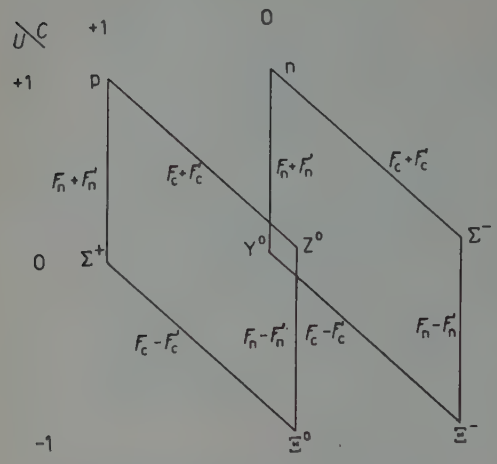

Fig. 1.

A very similar description of the K interactions in a four dimensional space has already been proposed by TIOMNO ([8]) who has used for the interaction term matrices analogous to the $\boldsymbol{\Omega}_K$ set. Further, these $\boldsymbol{\Omega}_K$ matrices are also strictly connected with the ζ_K and ω_K ($K = 1, 2$) isospin matrices, which were used in a formalism developed by one of us ([9]) for the description of the charged and respectively neutral K's interactions considered as independent transitions.

Moreover, the third components of these two partial isospins ζ_3 and ω_3 are the same as the quantum numbers S_1 and S_2 introduced by PAIS ([10]). Thus it seems that these two partially independent groups of transitions are now unified by the aid of the concept of 4-dimensional hypercharge space.

However, the most important new feature of the K interactions depends on the fact of having expressed them in eq. (25) as a combination of two terms with coupling constants F and F', the second of which, owing to the factors Γ^5 and Ω_5 it contains, may be considered as pseudoscalar in respect to the first, both in normal and hypercharge spaces.

This amounts to assuming that K interactions are obtained as a combination of different individually parity non-conserving expressions and this, as was already shown in a previous paper ([11]), leads to different coupling constants $F+F'$ or $F-F'$ (and therefore different self-masses) for the different baryon states. It may be easily recognized that the actual form of the interaction succeeds in attributing the right separation for the masses, as in fact both nucleon states are coupled only through $F+F'$, both Ξ states only through $F-F'$, and the four hyperon states through a mixture of both $F+F'$ and

---

([12]) We have been privately informed by Dr. H. P. DÜRR that a very similar treatment of the electromagnetic interaction is given in a preprint *Zur Theorie der Elementarteilchen* by DÜRR, HEISENBERG, MITTER, SCHLIEDER and YAMAZAKI.

$F - F'$, which makes rather plausible for them an intermediate mass value in respect to nucleons and Ξ's.

Thus if the previous assumption for the K interactions is true, the different mass values for the baryons acquire a fundamental meaning instead of being, as was thought before, only a simple secondary disturbance in an otherwise symmetrical scheme.

The choice we have made leads us to pseudoscalar K interactions in the final form (32) for the equations. Should we have written in eq. (25) the interaction term as

$$(F\Omega_K + F'\Gamma\Omega'_K)(\Gamma^5)^K\varphi^K , \tag{35}$$

we should have obviously obtained scalar K interactions; and other mixed possibilities might also be easily taken into account. This arbitrariness leaves us free to adapt the present interaction form to the future experimental results concerning the relative parity of K-mesons and hyperons.

For what concerns electromagnetic interactions, it may be remarked that the different charge labellings are obtained by the interference effects of two different kinds of vector couplings represented by the matrices G'^μ and G''^μ. From the point-of-view of the individual states of the whole set, this interference may be considered as a kind of mixing of different apparently parity non-conserving terms, as is most obvious in the intermediate representation stage given in eq. (30) where all electromagnetic interactions appear as containing the factors $1 \pm \Gamma_5$. There is therefore a great similarity of formulation between K and electromagnetic interactions, still increased if one considers that the cancellation of electromagnetic interaction in some states as the neutron, the Ξ^0 and so on is only due to the fact that the coupling constant e is assumed to be exactly the same for the two couplings G'^μ and G''^μ. Should we have assumed also $F = F'$ for K interactions, we should have obtained the disappearance of the interaction for the Ξ states in exactly the same way. Under this aspect the only difference between K and electromagnetic interactions depends on the fact that, while for the former we must have $F \neq F'$, there is only a single value for the electromagnetic constant.

Turning now to the pions, in order to obtain a uniform self mass contribution due to them as seems up to now required by experimental evidence, a single conventional pion interaction term has been introduced into (25). One could not exclude, however, some very small mass splittings (let us say between Σ^+ Y and Z Σ^-) which could be introduced by the addition of a second type interaction with a very small constant g' analogous to the second term in the K and electromagnetic cases. Here also it may be remarked that the choice made for the γ_5 factors of the different pion components is such as to obtain pseudoscalar coupling in the final form (32) as desired.

4. – We shall now examine some of the transformation properties of eq. (25).

a) Let us first begin with those concerning rotations in the isospaces which result from the form itself of the interaction terms. Thus, it may be easily shown that the two K interaction terms are invariant under the proper rotation group in the hypercharge space (*). Moreover, if φ_K is such that

$$\mathbf{\Omega}_5 \varphi_K = -\varphi_K \Omega_5 \tag{36}$$

then the K interaction terms turn out to be invariant also with respect to an $\mathbf{\Omega}_5$ transformation, as was eq. (9). However, it should be noted that in the absence of the interaction term, the system is not invariant with respect to the rotation group in the hypercharge space. This means that one gets the most conspicuous features of the K-interactions which depend on the combination of the two coupling constants F and F' by violation of the symmetry of the total system in the hypercharge space.

For what concerns pions, the interaction term is invariant for three dimensional rotations in the isotopic spin space (as already shown in (2)) that is pion interactions are charge independent.

b) As a second point, we shall examine as was done in our first paper (6) the behaviour of eq. (25) under the operations of charge conjugation and of boson and spinor conjugations (7).

To this aim, let us first define the adjoint of X by

$$\overline{X}^{(32)} = X^{+(32)} G^4 . \tag{38}$$

With our choice of representation for the γ^μ matrices, this gives us for the adjoint equation:

$$\overline{X}^{(32)} \left\{ G^\mu \frac{\partial}{\partial x^\mu} - G_5 m + i \sum_K (F \mathbf{\Omega}_K + F' \Gamma^{\mathrm{r}} \mathbf{\Omega}'_K)(\Gamma^5)^{K+1} \varphi_K + \right. \tag{39}$$

$$\left. + \frac{ie}{2} \left((G'^\mu + G''^\mu) A_\mu + g \sum_j T_j (\Gamma^5)^{j+1} \pi_j \right\} = 0 .$$

We now define the boson, the spinor and the charge conjugate states as:

$$X^{B(32)} = \mathscr{B} X^{(32)}, \qquad X^{S(32)} = \mathscr{S} \overline{X}^{T(32)}, \qquad X^{C(32)} = \mathscr{C} \overline{X}^{T(32)} \tag{40}$$

(*) This point will be investigated more closely in a forthcoming note by DALLAPORTA and DE SANTIS to be published in *Nuovo Cimento*.

in which the matrices $\mathscr{B}$, $\mathscr{S}$, $\mathscr{C}$ are given by:

$$
\left\{
\begin{array}{lll}
\mathscr{B}^{(32)} = \begin{vmatrix} v^{(8)} & & & \\ & v^{(8)} & & \\ & & v^{(8)} & \\ & & & v^{(8)} \end{vmatrix} & & v^{(8)} = \begin{vmatrix} 0 & I^{(4)} \\ I^{(4)} & 0 \end{vmatrix} \\
\mathscr{S}^{(32)} = \begin{vmatrix} s^{(8)} & & & \\ & s^{(8)} & & \\ & & s^{(8)} & \\ & & & s^{(8)} \end{vmatrix} & & s^{(8)} = \begin{vmatrix} 0 & c \\ c & 0 \end{vmatrix} \\
\mathscr{C}^{(32)} = \begin{vmatrix} c^{(8)} & & & \\ & c^{(8)} & & \\ & & c^{(8)} & \\ & & & c^{(8)} \end{vmatrix} & & c^{(8)} = \begin{vmatrix} c & 0 \\ 0 & c \end{vmatrix}
\end{array}
\right. \tag{41}
$$

and c is the normal 4×4 charge-conjugation matrix.

Of course, the relation

$$\mathscr{B}\mathscr{S} = \mathscr{C} \tag{42}$$

holds. If, as usual, we assume:

$$c\gamma_\mu^T = -\gamma_\mu c\,, \qquad c\gamma_5^T = \gamma_5 c\,, \tag{43}$$

the main commutation properties are found to be the following: $\{[\ ]_-$ means commutation; $[\ ]_+$ anticommutation; $[\ ]_-^T$, $[\ ]_+^T$ commutation respectively anticommutation with transposition: *i.e.* $[\mathscr{S}G_\mu]_+^T = \mathscr{S}G_\mu^T + G_\mu\mathscr{S}\}$.

$$
\left\{
\begin{array}{llllllll}
[\mathscr{B}G^\mu\ ]_- = 0 & [\mathscr{B}\mathbf{\Omega}_1]_- = 0 & [\mathscr{S}G^\mu\ ]_+^T = 0 & [\mathscr{S}\mathbf{\Omega}_1]_+^T = 0 & [\mathscr{C}G^\mu\ ]_+^T = 0 & [\mathscr{C}\mathbf{\Omega}_1]_+^T = 0 \\
[\mathscr{B}G_5\ ]_- = 0 & [\mathscr{B}\mathbf{\Omega}_2]_+ = 0 & [\mathscr{S}G_5\ ]_-^T = 0 & [\mathscr{S}\mathbf{\Omega}_2]_+^T = 0 & [\mathscr{C}G_5\ ]_-^T = 0 & [\mathscr{C}\mathbf{\Omega}_2]_-^T = 0 \\
[\mathscr{B}G'^\mu]_+ = 0 & [\mathscr{B}\mathbf{\Omega}_3]_+ = 0 & [\mathscr{S}G'^\mu]_-^T = 0 & [\mathscr{S}\mathbf{\Omega}_3]_-^T = 0 & [\mathscr{C}G'^\mu]_+^T = 0 & [\mathscr{C}\mathbf{\Omega}_3]_+^T = 0 \\
[\mathscr{B}G''^\mu]_+ = 0 & [\mathscr{B}\mathbf{\Omega}_4]_- = 0 & [\mathscr{S}G''^\mu]_-^T = 0 & [\mathscr{S}\mathbf{\Omega}_4]_-^T = 0 & [\mathscr{C}G''^\mu]_+^T = 0 & [\mathscr{C}\mathbf{\Omega}_4]_-^T = 0 \\
[\mathscr{B}T_1\ ]_- = 0 & [\mathscr{B}\mathbf{\Omega}'_1]_+ = 0 & [\mathscr{S}T_1\ ]_-^T = 0 & [\mathscr{S}\mathbf{\Omega}'_1]_-^T = 0 & [\mathscr{C}T_1\ ]_-^T = 0 & [\mathscr{C}\mathbf{\Omega}'^T_1]_+ = 0 \\
[\mathscr{B}T_2\ ]_+ = 0 & [\mathscr{B}\mathbf{\Omega}'_2]_- = 0 & [\mathscr{S}T_2\ ]_-^T = 0 & [\mathscr{S}\mathbf{\Omega}'_2]_-^T = 0 & [\mathscr{C}T_2\ ]_+^T = 0 & [\mathscr{C}\mathbf{\Omega}'^T_2]_- = 0 \\
[\mathscr{B}T_3\ ]_+ = 0 & [\mathscr{B}\mathbf{\Omega}'_3]_- = 0 & [\mathscr{S}T_3\ ]_+^T = 0 & [\mathscr{S}\mathbf{\Omega}'_3]_+^T = 0 & [\mathscr{C}T_3\ ]_-^T = 0 & [\mathscr{C}\mathbf{\Omega}'^T_3]_+ = 0 \\
 & [\mathscr{B}\mathbf{\Omega}'_4]_+ = 0 & & [\mathscr{S}\mathbf{\Omega}'_4]_+^T = 0 & & [\mathscr{C}\mathbf{\Omega}'^T_4]_- = 0
\end{array}
\right. \tag{44}
$$

Now, by applying the three operations $\mathscr{B}$, $\mathscr{S}$, $\mathscr{C}$ to eq. (25) and to the transpose of eq. (39) we get the three transformed equations:

$$
(45)\quad \begin{cases}
\Big[G^\mu \dfrac{\partial}{\partial x^\mu} + mG_5 - i\{[F\boldsymbol{\Omega}_1 - F'\Gamma^5\boldsymbol{\Omega}'_1]\varphi_1 - [F\boldsymbol{\Omega}_2 - F'\Gamma^5\boldsymbol{\Omega}'_2]\Gamma^5\varphi_2 - \\
\qquad - [F\boldsymbol{\Omega}_3 - F'\Gamma^5\boldsymbol{\Omega}'_3]\varphi_3 + [F\boldsymbol{\Omega}_4 - F'\Gamma^5\boldsymbol{\Omega}'_4]\Gamma^5\varphi_4\} + \\
\qquad + \dfrac{ie}{2}(G'^\mu + G''^\mu)A_\mu - g(T_1\pi_1 - T_2\Gamma^5\pi_2 - T_3\pi_3)\Big] X^{\mathscr{B}} = 0\,, \\
\Big[G^\mu \dfrac{\partial}{\partial x_\mu} + mG_5 + i\{[F\boldsymbol{\Omega}_1 - F'\Gamma^5\boldsymbol{\Omega}'_1]\varphi_1 + [F\boldsymbol{\Omega}_2 - F'\Gamma^5\boldsymbol{\Omega}'_2]\Gamma^5\varphi_2 - \\
\qquad - [F\boldsymbol{\Omega}_3 - F'\Gamma^5\boldsymbol{\Omega}'_3]\varphi_3 - [F\boldsymbol{\Omega}_4 - F'\Gamma^5\boldsymbol{\Omega}'_4]\Gamma^5\varphi_4\} - \\
\qquad - \dfrac{ie}{2}(G'^\mu + G''^\mu)A_\mu - g(T_1\pi_1 + T_2\Gamma^5\pi_2 - T_3\pi_3)\Big] X^{\mathscr{S}} = 0\,, \\
\Big[G^\mu \dfrac{\partial}{\partial x^\mu} + mG_5 + i\{[F\boldsymbol{\Omega}_1 + F'\Gamma^5\boldsymbol{\Omega}'_1]\varphi_1 - [F\boldsymbol{\Omega}_2 + F'\Gamma^5\boldsymbol{\Omega}'_2]\Gamma^5\varphi_2 + \\
\qquad + [F\boldsymbol{\Omega}_3 + F'\Gamma^5\boldsymbol{\Omega}'_3]\varphi_3 - [F\boldsymbol{\Omega}_4 + F'\Gamma^5\boldsymbol{\Omega}'_4]\Gamma^5\varphi_4\} + \\
\qquad + \dfrac{ie}{2}(G'^\mu + G''^\mu)A_\mu - g(T_1\pi_1 - T_2\Gamma^5\pi_2 + T_3\pi_3)\Big] X^{\mathscr{C}} = 0\,.
\end{cases}
$$

From these we conclude that in the three operations the following transformations occur:

$$
(46)\quad \begin{cases}
\text{Boson conj.} & \begin{array}{l} e \to -e \quad F \to F \quad F' \to -F' \quad \varphi_1 + i\varphi_2 \to \varphi_1 - i\varphi_2 \quad \varphi_3 + i\varphi_4 \to -(\varphi_3 - i\varphi_4) \\ g \to g \quad \pi_1 + i\pi_2 \to \pi_1 - i\pi_2 \quad \pi_3 \to -\pi_3 \end{array} \\
\text{Spinor conj.} & \begin{array}{l} e \to e \quad F \to -F \quad F' \to F' \quad \varphi_1 + i\varphi_2 \to \varphi_1 + i\varphi_2 \quad \varphi_3 + i\varphi_4 \to -(\varphi_3 + i\varphi_4) \\ g \to g \quad (\pi_1 + i\pi_2) \to (\pi_1 + i\pi_2) \quad \pi_3 \to -\pi_3 \end{array} \\
\text{Charge conj.} & \begin{array}{l} e \to -e \quad F \to -F \quad F' \to -F' \quad \varphi_1 + i\varphi_2 \to \varphi_1 - i\varphi_2 \quad \varphi_3 + i\varphi_4 \to (\varphi_3 - i\varphi_4) \\ g \to g \quad (\pi_1 + i\pi_2) \to (\pi_1 - i\pi_2) \quad \pi_3 \to \pi_3\,. \end{array}
\end{cases}
$$

In order to discuss the physical meaning of these relations, let us first remind that, according to the definitions given in our earlier papers ([6,7]) boson conjugation is expected to reverse the signs of the electric charge and hypercharge both of baryons and of mesons without touching the spinor structure of the baryon (*i.e.* it changes proton into Ξ^-), while spinor conjugation reverses the sign of nuclear charge (that is makes the transition from particle to antiparticle) without changing the electric charge and hypercharge (*i.e.* it changes proton into $\overline{\Xi^-} = (\overline{\Xi})^+$), while the charge conjugation reverses the signs of all quantities (*i.e.* it changes proton into antiproton). Now, this behaviour is quite apparent here in all meson fields, whose sign is reversed (for both

electric charge and hypercharge) by boson and charge conjugation but not by spinor conjugation, and for the electromagnetic term which was already discussed in (6). The most interesting feature is given, however, by the K interactions; here we see that the transformation properties of the two constants F and F' are different, F transforms as a nuclear charge and F' as a hyper or electric charge. This ensures that, while $F+F'$ remains invariant for charge conjugation (so that proton and antiproton have the same mass), it goes into $F-F'$ for both boson and spinor conjugations; these two operations are able therefore to transform the mass values of the baryons and are rigorously valid for eq. (25) even when we take into account the different baryon masses: the nucleon mass is transformed into the Ξ mass by both boson and spinor conjugations, while it does not change for charge conjugation.

This main result obtained with the present Hamiltonian (25) differs from the preceding ones given in (6) and (7), where boson and spinor conjugations were studied in the assumption of equal masses for all the baryons.

For what concerns pion interactions, it is seen that the g constant does not transform under any of the three operations discussed. One may remark, however, that should we have adopted a pseudovector form of type either

$$f \sum_j T_j G^\mu \frac{\partial \pi_{j\mu}}{\partial x_\mu} \tag{47a}$$

or

$$f' \sum_j T_j G'^\mu \frac{\partial \pi_{j\mu}}{\partial x_\mu} \tag{47b}$$

the situation should have been rather different. In effect, if we insert these two terms in eq. (25) and proceed to study their conjugation behaviour for all the cases we have now examined, in the same way as was done for the other terms, we find for them the following properties

$$\left\{\begin{array}{llllll} \text{for boson conj.} & f \to f & f' \to -f' & \pi_1 + i\pi_2 \to \pi_1 - i\pi_2 & \pi_3 \to -\pi_3\,, \\ \text{for spinor conj.} & f \to -f & f' \to f' & \pi_1 + i\pi_2 \to \pi_1 + i\pi_2 & \pi_3 \to -\pi_3\,, \\ \text{for charge conj.} & f \to -f & f' \to -f' & \pi_1 + i\pi_2 \to \pi_1 - i\pi_2 & \pi_3 \to \pi_3\,. \end{array}\right. \tag{48}$$

Thus the interaction constant for the first choice (47a) of pseudovector coupling behaves under the different conjugations as a nuclear charge, while in case of the second choice (47b) it behaves as an hyper or electric charge. As up to now the question concerning the real form (pseudoscalar or pseudovector) for pion interactions cannot be considered as settled, these different transformation properties of the two cases may be of interest in order to

understand the real physical meaning of the interaction constants and the true interrelation between the different meson fields.

In this connection, it may be generally observed that the present scheme does not require the introduction of an hypercharge as a real physical quantity (as a source of a field in the sense of SCHWINGER [13]) in order to justify the empirical fact of strangeness conservation, because strangeness is automatically conserved by the natural display of the properties of the matrices, which allow only some definite transitions between baryon states to take place. This, by the way, could explain why strangeness should play no role in any kind of interactions not ruled by matrices of the kind of the Ω's as may well be the case for weak interactions. However, the fact that F' and perhaps f' have the transformation properties required for a hypercharge may induce to consider these constants as possible sources of parts of the K and pion fields and thus provide some physical insight to the concept of hypercharge.

c) As a third case, let us finally consider briefly the γ_5 transformation properties.

While the free particle eq. (9) has been shown to be invariant under appropriate γ_5 transformations such as (12) or (13), it may be easily seen that this invariance does not hold any more when complicated K interactions as given in eq. (25) are introduced. However, an approximate γ_5 invariance may be obtained for a particular case which, owing to the rather peculiar physical situation it leads to, may perhaps be worth while to be pointed out.

According to the spirit of a previous paper [11], form (13) was proposed as the most general solution of eq. (9), expressing γ_5 invariance properties. Now let us specialise this general solution by taking

$$r = s\,, \qquad p_1 = p_2 = 2$$

thus obtaining $X^{(32)} \to RX^{(32)}$

$$\text{with } R = \begin{pmatrix} \dfrac{I^{(16)} - \omega_3 \times \Gamma^5}{2} & 0 \\ 0 & I^{(16)} \end{pmatrix} \tag{49}$$

where $I^{(16)}$ is a 16×16 unit matrix and ω_3 is defined by (19). Now it may be easily shown that (*), provided $F = F'$, the transformation (49) leaves invariant the K interaction term of eq. (25).

---

[13] J. SCHWINGER: *Phys. Rev.*, **104**, 1164 (1956).

(*) For example, let us commute with R the first component of the K interaction term. By using the well-known formulae

$$\omega_1\omega_3 = -i\omega_2\,, \qquad \omega_2\omega_3 = i\omega_1\,,$$

Thus, if $F = F'$ were the case, we could correlate γ_5 invariance with the assumption of taking two different interaction terms ruled by two different matrices Ω_K and Ω'_K for the K interactions. However, $F = F'$ would mean that the Ξ states not only do not interact through K interactions but if solution (49) is adopted, do not exist at all, so that $F = F'$ is an essential condition. Thus, one could conclude that rigorous γ_5 invariance for the K interactions could be achieved only in the case of so extreme $N - \Xi$ mass difference that the Ξ states become inexistent. This point is probably related with the difficulties concerning the true meaning of the interaction constants and cannot be discussed in a phenomenological approach.

We would like to sum the results obtained in the present paper by saying that the gathering of all baryon states into the description of a single 32-component spinor leads us to express the strong interactions in such a way as to allow to put into evidence many important transformation properties, and that these properties are compatible with the different values of the baryon masses, which result as a natural consequence of the fundamental form adopted for K interactions.

---

we get

$$(50) \qquad [(F\Omega_1 \times I^{(8)} + F'\Omega'_1 \times \Gamma^5), R] =$$

$$= \begin{pmatrix} 0 & iF\omega_1 \times I^{(4)} + F'\omega_2 \times \Gamma^5 \\ -i\left(\frac{F+F'}{2}\right)\omega_1 \times I^{(4)} + \left(\frac{F+F'}{2}\right)\omega_2 \times \Gamma^5 & 0 \end{pmatrix} -$$

$$- \begin{pmatrix} 0 & i\left(\frac{F+F'}{2}\right)\omega_1 \times I^{(4)} + \left(\frac{F+F'}{2}\right)\omega_2 \times \Gamma^5 \\ -iF\omega_1 \times I^{(4)} + F'\omega_2 \times \Gamma^5 & 0 \end{pmatrix}.$$

which is 0 provided $F = F'$.

A similar derivation may be given for the other components.

RIASSUNTO

Estendendo un procedimento, già descritto in altri lavori, consistente nel raggruppare diversi stati barionici per formare spinori a più componenti che obbediscono a proprietà di simmetria non apparenti per gli stati separati, viene proposta e discussa una equazione di Dirac soddisfatta da uno spinore a 32 componenti che comprende

tutti gli stati barionici finora noti. Gli stati barionici, a parte la normale dipendenza dalle coordinate spazio-temporali, sono descritti da due specie di parametri interni, le variabili di spin isotopico e di ipercarica. Le interazioni K sono espresse mediante due termini indipendenti con due costanti di interazione F ed F', ognuno dei quali risulta invariante per rotazioni in uno spazio di ipercarica tetradimensionale, e le interazioni pioniche dalla espressione usuale invariante per rotazioni nello spazio isotopico tridimensionale, che è del tutto indipendente dallo spazio di ipercarica; infine le interazioni elettromagnetiche sono formate tramite la combinazione di due termini che permettono di ottenere i valori sperimentali della carica elettrica per i diversi stati barionici quando viene applicato all'equazione originaria un processo di separazione a due tappe, processo che porta per le transizioni K a regole di selezione che esprimono naturalmente la conservazione dell'ipercarica o stranezza come risulta formulata nella « approssimazione di doppietto ». La combinazione dei due tipi di interazione K permette finalmente di ottenere due tipi di costanti di accoppiamento $F+F'$ e $F-F'$ per i diversi termini di interazione disposti in modo tale da spiegare le note differenze di massa dei barioni. Si fa inoltre vedere che la equazione a 32 componenti è separatamente invariante per le operazioni di coniugazione bosonica, coniugazione spinoriale e coniugazione di carica e che queste sono rigorosamente valide anche quando si tenga conto delle diverse masse dei barioni. Per finire, si discutono alcuni aspetti della invarianza per le trasformazioni in γ_5 delle equazioni. La presente formulazione sembra quindi adatta ad unificare notevolmente il trattamento degli stati barionici sotto un numero ristretto di punti di vista ed a porre in evidenza alcune proprietà di invarianza che altrimenti non apparirebbero.

On the Dielectric Constant of some Aqueous Solutions.

A. Carrelli and L. Della Caggia

Istituto di Fisica Sperimentale dell'Università - Napoli

(ricevuto il 20 Giugno 1959)

Summary. — Measurements of the dielectric constant of some aqueous solutions have been made, at a frequency of 8 MHz. After a description of the method and of the device used in the measurements, it is shown how it is possible to calculate the number of water dipoles blocked by each ion in solution, taking into account the variation of the dielectric constant.

This note is a report of the measurements carried out to determine the dielectric constant of aqueous solutions of salts. High frequencies were used, that is, currents having frequencies of $\nu = 8$ MHz. The device used is the one described in a previous note [1]. It is based on the phenomenon of the resonance in an oscillating circuit (Fig. 1). L is a coil allowing an inductive link with an oscillator that is not represented. The cell containing the solution, of which we want to determine the dielectric constant, is represented by the capacity C_1; R is a resistance connected in parallel. By causing C to vary, a maximum of current is obtained, in resonance conditions, in the circuit. Each solution placed in the cell represents a particular value of the capacity C_1 and of the resistance R and therefore, particular values are obtained for the capacity C and for the maximum of the current.

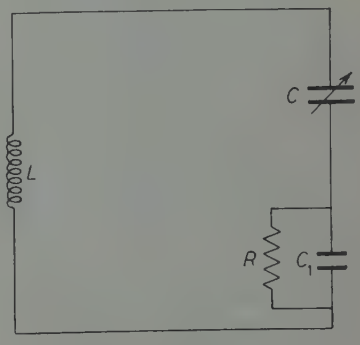

Fig. 1.

---

[1] A. Carrelli and M. Rescigno: *Nuovo Cimento*, **9**, 1 (1952).

In order to carry out the measurement, a series of solutions of acetone in water, having a known dielectric constant K, is placed in the cell C_1 and, for each solution, a series of resistances R are shunted at the electrodes so as to know for each single value of the capacity C_1 and of the resistance R the position D_c of the condenser C at the maximum of current D_g (read on a galvanometer set in series with R) in resonance conditions.

By plotting the values of D_c and of D_g on a diagram, two groups of curves are obtained; the first are those concerning a constant R and a variable C_1; the second are those concerning a constant C_1 and a variable R. The curves thus obtained may be termed *iso-ohmic* and *iso-faradic*.

Having plotted this network of curves (calibration network), a salt solution of known concentration may be placed in the cell. The figurative point of this substance (ordinate D_c, abscissa D_g) shall appear on one of the iso-faradic curves directly plotted during the calibration, or on one of the curves that may be obtained by interpolation of the given ones.

The value of K belonging to this curve gives the dielectric constant of the solution.

1. – Description of the apparatus.

The apparatus we made use of for our measurements consists mainly of a high frequency generator, a resonating circuit in which the cell containing the liquid is inserted, a device which makes the measurement of the resonance current in the testing circuit.

The whole is enclosed in a single block containing also the feeder for the high frequency generator.

The circuit of this oscillator has a high stability of frequency and this is necessary in order to avoid errors due to variations in the generated frequency.

In order to obtain such a result it has been considered advisable to follow up the oscillating stage with a duplicator-separator stage. This stage is obtained by employing the anodic circuit of the same 5763 tube of the high frequency generator by inserting a resonating circuit tuned to a frequency double of the one generated by the oscillator.

The coupling between the two stages is, thus, purely electronic and has excellent stability.

In this way the variations of the load effected on the testing circuit do not influence the circuit of the oscillator and do not displace the pre-established frequency.

The frequency that can be produced by the oscillator may vary from 3.5 to 6 MHz and consequently, in view of the presence of a duplicator stage, the circuit may be tuned at frequencies from 7 MHz to 12 MHz. The frequency

of the oscillator and the tuning of the anodic circuit are controlled by means of two variable condensers.

The coupling of the testing circuit to the radio frequency generator takes place through a variable inductive coupler.

It gives the possibility of transferring to the testing circuit a quantity of energy that can vary according to the requirements.

The testing circuit is formed by an inductance of about 3 henry and by the capacity of the cell set in series with a variable condenser. The instrument for the measurement of the resonance current in the testing circuit is constituted by a high frequency transformer having a toroidal iron nucleus that transforms the resonance current of the circuit into voltage that, having been rectified by a germanium diode of the OA-70 type, is conveyed to a milliammeter.

The preliminary operation consists in the construction of the calibration network formed by the two groups of curves: the iso-ohmic and the iso-faradic.

We therefore made use of substances having a known dielectric constant, specifically solutions of acetone in water. Thus was obtained the network of Fig. 2 in which the full lines indicate the iso-faradic curves that correspond to the values of the dielectric constants: 81.0; 73.9; 67.7.

The dotted lines represent the iso-ohmic curves concerning the values (in ohms) of the resistance: 50, 75, 100, 200, 250, 300, 500.

The reliability of the results depends, before all, on the stability of the calibration network.

By stability we mean the possibility to reproduce, at a lat-

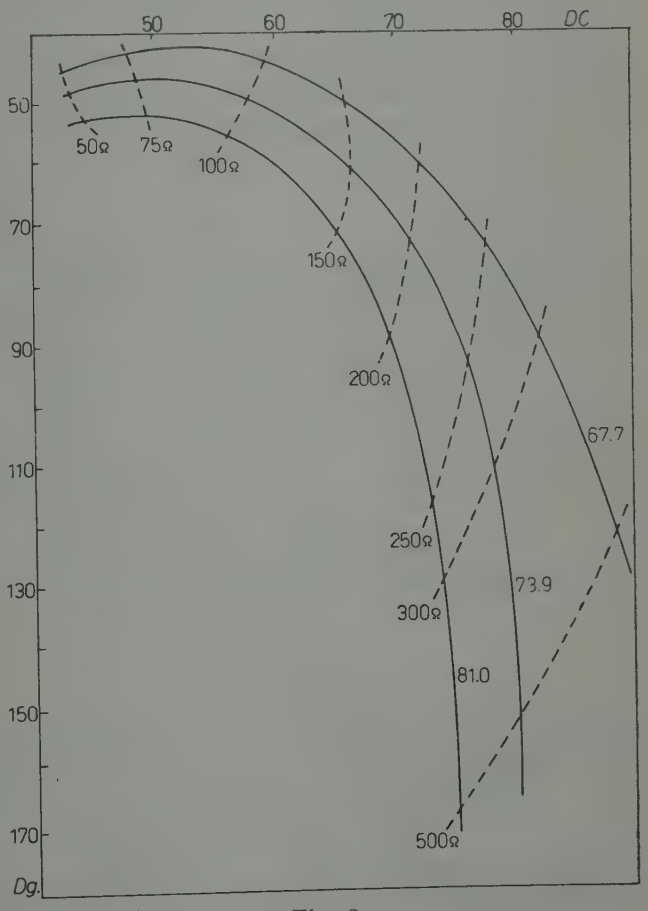

Fig. 2.

er date and under different circumstances, the same calibration network.

To obtain this, we acted as follows: having plotted a certain number of networks, we remarked that only in appearance they were different because, indeed, it was only question of a rigid (that is, without any deformation) displacement of the same network. This observation gives the possibility of simplifying in a remarkable way the research by making the calibration once only, and by returning always to the first network with few operations. Specifically, having placed in the cell any one of the solutions used during the calibration and having set the variable condenser in the position corresponding to the figurative point of the initial diagram, the eventual difference in the current is compensated by varying the position of the inductive coupling. Thus, were determined the values of the dielectric constant for the aqueous solutions of the following salts

mono-monovalent	KF – KCl – KBr – KI .
bi-valent	$CuSo_4$ – $MnSO_4$ – $MgSO_4$.
mono-bivalent	K_2CO_3 – K_2SO_4 .
mono-trivalent	K_3PO_4 .
mono-tetravalent	$K_4Fe(CN)_6$.

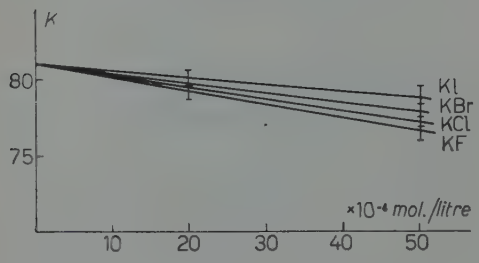

Fig. 3.

The values of the dielectric constant K thus obtained are plotted as function of the molecular concentration c and, as may be seen in Fig. 3, 4 and 5 for our range of concentration, for all salts there is a diminution of K, as C increases.

It is obvious to think that the diminution of the dielectric constant of water produced by a ion is due to the presence of its electric field attracting a certain number of dipoles.

Let us now consider the behaviour of KF: the ions K^+ and F^- having an

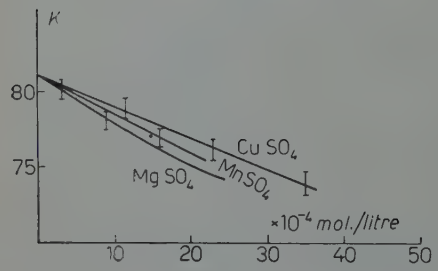

Fig. 4.

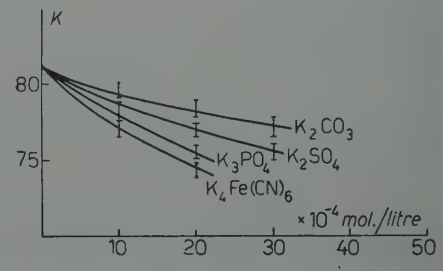

Fig. 5.

equal radius (1.33 Å), shall surround themselves with an electric field that may be considered as being equal, thus they block the same number of dipoles. It may therefore be believed that the diminution of K is due for one half to the ion K^+ and for the other half to the ion F^-, and therefore, if dK/dC stands for the diminution of K relative to a unitary variation of the concentration, we have

$$(1) \qquad \left(\frac{dK}{dC}\right)_{KF} = \left(\frac{dK}{dC}\right)_{K^+} + \left(\frac{dK}{dC}\right)_{F^-} = 2\left(\frac{dK}{dC}\right)_{K^+} = 2\left(\frac{dK}{dC}\right)_{F^-}$$

For KCl we similarly have:

$$(2) \qquad \left(\frac{dK}{dC}\right)_{KCl} = \left(\frac{dK}{dC}\right)_{K^+} + \left(\frac{dK}{dC}\right)_{Cl^-},$$

from which, having obtained from (1) the value for $(dK/dC)_{K^+}$ and having substituted it in (2), the value of $(dK/dC)_{Cl^-}$ is obtained and, in the same way, the dK/dC connected to the various ions may be obtained.

The experimental values thus obtained are reproduced in the Table I.

TABLE I.

Ions	dK/dC	Radii (Å) [1]	Ions	dK/dC	Radii (Å) [1]
F^-	0.42	1.33	Mg^{++}	1.54	0.78
Cl^-	0.28	1.81	Sr^{++}	0.73	1.27
Br^-	0.13	1.96	Ba^{++}	0.59	1.43
J^-	0.01	2.20			
			Zn^{++}	0.59	0.83
Li^+	1.00	0.78	Cd^{++}	0.19	1.03
Na^+	0.74	0.98			
K^+	0.42	1.33			

[1] *Phys. Chem. Tabellen*, vol. IV.

It is to be remarked that for ions having equal charge a greater drop in the dielectric constant is found, as the radius decreases.

This is to be expected because a diminution of the radius calls for an increase of the electric field around the ion. Indeed, if the charge were uniformly distributed on a sphere having its radius equal to the radius of the ion an inverse proportion should be expected between the dK/dC and the

square of the radius, the electric field being given by e/r^2, $2e/r^2$ for ions that are monovalent, bivalent, etc.

Let us plot on a diagram (Fig. 6) the results obtained; a remarkable influence of the electrical structure of the ion on the diminution of the dielectric constant is to be noted.

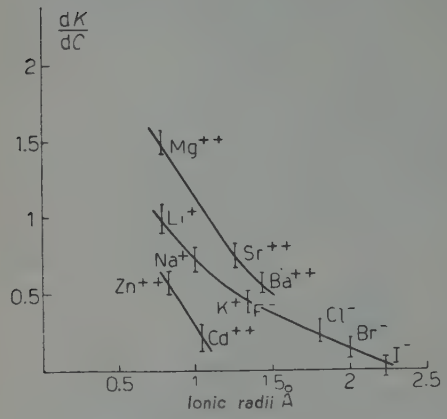

Fig. 6.

In fact, in Fig. 6, it appears that the curve (the shape of which is nearly rectilinear) joining the points concerning halogens presents a deviation when from halogens we pass over to alkali metals.

As to bivalent ions it is to be noticed that the diminution of K due to Zn^{++} is less than that produced by Mg^{++}. This behaviour may be justified as follows: they both have equal charge and their radius is nearly the same (respectively 0.83 and 0.78 Å), they should therefore cause the same diminution of K, however Zn^{++} has 18 electrons more distributed over the M shell, similarly Cd^{++} has 10 electrons more than Sr^{++} distributed over the N shell.

For these ions, therefore, the presence of a greater number of electrons over an external shell appears to reduce the action of the central charge. The experiments we described above may also be used to determine approximately the number of dipoles blocked by each ion.

With reference to the Debye equation:

$$\frac{K-1}{K+2}\frac{M}{d} = \frac{4\pi}{3} N \left(\alpha + \frac{\mu^2}{3KT}\right), \tag{3}$$

it may be believed that when ions are dissolved in water the number of dipoles of water that orient themselves under the action of the external field is $N' < N$ because $N - N'$ dipoles are held back around the dissolved ion; (3) therefore becomes:

$$\frac{K'-1}{K'+2}\frac{M}{d} = \frac{4\pi}{3} N \left(\alpha + \frac{N'}{N}\frac{\mu^2}{3KT}\right), \tag{4}$$

in which K' is the value of the dielectric constant of the solution. From the equations (3) and (4) we can obtain the ratio N'/N and by means of this ratio we can calculate the number of dipoles blocked by the ions. These numbers are reported in Table II.

Other authors (2) have obtained (by means of various methods such as the study of compressibility, mobility, diffusion) values that are not in very good agreement with each other.

TABLE II.

Ions	Blocked dipoles	Ions	Blocked dipoles
F^-	13	K^+	13
Cl^-	5	Mg^{++}	40
Br^-	1	Sr^{++}	20
I^-	1	Ba^{++}	13
Li^+	30	Zn^{++}	15
Na^+	20	Cd^{++}	2

Generally, it may be said that the number of dipoles blocked by the ions, calculated by our method, is greater than the others.

(2) BARNATT: *Quart. Rev. Chem. Soc. London*, **7**, 84 (1953); H. REMY: *Zeits. Phys. Chem.*, **89**, 469 (1915); R. A. ROBINSON and E. H. STOKES: *Electrolyte Solution* (London, 1955).

RIASSUNTO

Sono state fatte misure di costante dielettrica di soluzioni acquose di vari sali, a frequenza di 8 MHz. Dopo una descrizione del metodo e dell'apparecchio usati, è mostrato come dalla variazione della costante dielettrica si possa risalire al numero di dipoli dell'acqua bloccati da ciascun ione in soluzione.

IL NUOVO CIMENTO Vol. XIV, N. 1 1° Ottobre 1959

On the Problem of Causality (*).

G. WANDERS

Max-Planck-Institut für Physik und Astrophysik - München

(ricevuti il 20 Giugno 1959)

Summary. — The possibility of formulating the causality principle in terms of observable transition probabilities is discussed. It is found that only a very weak asymptotic condition can be plausibly deduced from the causality requirement. This condition implies regularity of the forward scattering amplitude $S(p)$ in an infinitesimal strip of the first quadrant along the real p-axis. Singularities of $S(p)$ located at a finite distance of the real axis have also observable effects, but they cannot be interpreted as obvious acausalities.

1. – Introduction.

The condition of local commutativity, according to which two field operators $\Phi_1(x_1)$ and $\Phi_2(x_2)$ have to commute (or anticommute) for space-like separations $(x_1 - x_2)$:

$$[\Phi_1(x_1), \Phi_2(x_2)]_{\pm} = 0 \,, \qquad (x_1 - x_2) \text{ space-like} \tag{1}$$

is one of the basic axioms of quantum field theory implying analytic properties of transition amplitudes. These properties are, in some cases, equivalent to dispersion relations. Local commutativity is usually interpreted as a causality condition, and it certainly leads to a causal theory, as is appearent from the fact that it allows any transition amplitude to be expressed in terms of vacuum expectation values of invariant retarded products of field operators (1). However, condition (1) itself has no clear physical meaning, in spite of its mathe-

(*) Work performed under a grant from the Swiss National Fond for Scientific Research.

(**) Present address: Institut für Theoretische Physik der Universität Hamburg, Hamburg.

(1) H. LEHMANN, K. SYMANZIK and W. ZIMMERMANN: *Nuovo Cimento*, **6**, 319 (1957).

matical simplicity. This arises mainly from the fact that the fields $\Phi_1(x)$ and $\Phi_2(x)$ are, in general, not observable. Thus, strictly speaking, (1) cannot be interpreted directly as a causality condition (2). On the other hand, the remaining axioms (Lorentz invariance, asymptotic condition, positive energy spectrum) have all an immediate physical significance. Thus local commutativity is a weak point in the system of axioms of field theory, in the sense that it is a postulate on the mathematical structure of the field operators, rather than a physical hypothesis.

Therefore an alternative formulation of the causality principle in terms of observables would be desirable. If we adopt the point of view of the pure S-matrix formalism, in which only transition probabilities are observable, we have to look for the direct consequences of causality on transition probabilities. We call macrocausality that type of causality, which can be expressed as a property of transition probabilities. Our main point is to illustrate that this concept of macrocausality is not a sharp one, and that there is little hope to deduce from it consequences as strong as dispersion relations.

In order to point out the difficulties, let us consider qualitatively the scattering of two particles, that is, a transition $(\varphi, \chi) \to (\varphi', \chi')$; $\varphi(x)$ and $\chi(x)$ are the wave packets of the incoming particles, $\varphi'(x)$ and $\chi'(x)$ those of the outgoing ones. We assume that these packets are all confined, for finite times, into narrow space-time regions; φ and χ overlap in a domain D, φ' and χ' in D'. Clearly, the process is causal if its transition probability $P[\varphi', \chi'/\varphi, \chi]$ is great only when D' lies in the forward light-cone of D (Fig. 1). (We assume, of course, a short-range interaction.) However it is impossible to put this condition in the strong and simple form: $P[\varphi', \chi'/\varphi, \chi] = 0$ unless D' is in the forward cone of D. This is

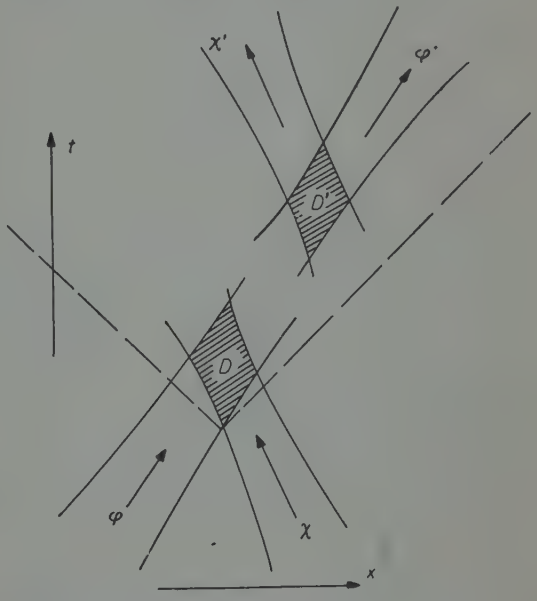

Fig. 1. – Example of a causal transition.

(2) If, according to R. HAAG (Varenna Lectures, 1958), one assumes that $\Phi[g] = \int (dx)^4 g(x) \Phi(x)$ defines a « quasi-localizable » state $\Phi[g]|0\rangle$, $g(x)$ being a smooth test-function, causality implies only: $\langle 0| [\Phi_1(x_1), \Phi_2(x_2)]|0\rangle = 0$ for $(x_1 - x_2)^2 \to -\infty$.

so because of two reasons: *a*) there exists no wave packet with sharp fronts, *i.e.* vanishing exactly outside some space-time region, *b*) the interaction of the particles does not, in general, vanish outside its range. *a*) results from the fact that every admissible wave packet has a spectrum containing only positive frequencies ($m \leqslant \omega < \infty$). Therefore the lines limiting the wave packets in Fig. 1 indicate their half-widths rather than their fronts, and the domains D and D' are not well-defined. Causality requires only that the transition probability has to be small if D' is outside the forward cone of D and no general principle prescribes how small it should be.

Thus the situation is quite different from classical dispersion theory, where signals with sharp fronts can be constructed and where the causality condition is a strong requirement of the type « No output for $x > t$ if no input for $x > t$ ». In quantum theory, the concept of macrocausality is intrinsically unsharp and has only relatively weak consequences. There is no way of introducing unallowed frequencies, of filling up the « unphysical region » $-\infty < \omega < m$ in order to obtain wave packets with sharp fronts, which does not alter the physical content of the theory.

In order to avoid unessential mathematical complications, we shall consider only scattering processes in a two-dimensional world (one space co-ordinate, x, and one time, t). Section **2** introduces the quantities which are convenient for a quantitative formulation of the previous, qualitative, discussion. In Section **3** we propose an asymptotic causality condition and examine its implications on the analytic properties of the forward scattering amplitude $S(p)$. This investigation is incomplete and suggests that asymptotic causality implies regularity of $S(p)$ in an infinitesimal strip of the upper half p-plane, along the positive real axis. Therefore, singularities in the first quadrant of the p-plane are not excluded, as is the case when microcausality is required. However, this does not mean that such singularities have no observable effects on the transition probabilities. This is shown in Section **4** for the special case where $S(p)$ has only a single pole in the first quadrant.

2. – The method of displaced wave packets.

For the sake of clarity, we consider first the elastic scattering of a scalar particle of mass m by a fixed scatterer. The in- and outgoing states are then completely defined by the wave packets $\varphi(x, t)$ and $\varphi'(x, t)$ of the in- and outgoing particle:

$$(2.1) \qquad \begin{cases} \varphi(x, t) = \dfrac{1}{\sqrt{2\pi}} \displaystyle\int_{-\infty}^{+\infty} \mathrm{d}p \, \frac{1}{\sqrt{2\omega_p}} \, \tilde{\varphi}(p) \exp\left[ipx - i\omega_p t\right] ; \quad \omega_p = \sqrt{p^2 + m^2} \\ \varphi'(x,t) = \dots . \end{cases}$$

In the one dimensional space, energy conservation allows only forward and backward scattering ($p \to p$ and $p \to -p$) characterized by the scattering amplitudes $S(p)$ and $R(p)$. As we wish to obtain restrictions from macrocausality on the forward scattering amplitude $S(p)$ alone, we have to choose φ and φ' in such a way that forward scattering alone contributes to the transition $\varphi \to \varphi'$. This is the case if both φ and φ' contain only positive momenta ($\tilde{\varphi}(p) = \tilde{\varphi}'(p) = 0$ for $p < 0$). The transition amplitude $A[\varphi'\varphi]$ is then given by:

$$A[\varphi'/\varphi] = \int_0^\infty \mathrm{d}p\, \tilde{\varphi}'^*(p)\, S(p) \tilde{\varphi}(p)\,. \tag{2.2}$$

It has been assumed that the scatterer is such that the asymptotic condition holds and therefore (2.2) is valid. It is useful to introduce, as a comparison element, the amplitude $A_0[\varphi'/\varphi]$ which one would observe in the absence of the scatterer ($S(p) \to 1$):

$$A_0[\varphi'/\varphi] = \int_0^\infty \mathrm{d}p\, \tilde{\varphi}'^*(p)\, \tilde{\varphi}(p)\,. \tag{2.3}$$

At this point we have to decide which quantities we consider as observables. We assume the idealized situation where the in- and outgoing states are pure states, *i.e.* both the apparatus preparing the ingoing particle and the detector analyzing the scattered particle correspond to well-defined and known wave packets φ and φ'. Therefore $A_0[\varphi'/\varphi]$ can be calculated for each experiment, and is known. On the other hand all the experimental information on the scattering $\varphi \to \varphi'$ is contained in the measurable transition probability $P[\varphi'/\varphi] = |A[\varphi'/\varphi]|^2$. Therefore $P[\varphi'/\varphi]$ and $A_0[\varphi'/\varphi]$ are our observables, and macrocausality has to be formulated as a property of these functionals.

We take advantage of the particular structure of the functionals $A[\varphi'/\varphi]$ and $A_0[\varphi'/\varphi]$ by introducing a monoparametric family of wave packets φ'_ξ, obtained from φ' by spatial translation:

$$\varphi'_\xi(x, t) = \varphi'(x - \xi, t)\,. \tag{2.4}$$

The substitution $\varphi' \to \varphi'_\xi$ transforms $A_0[\varphi'/\varphi]$ in a function of ξ:

$$A_0(\xi) = A_0[\varphi'_\xi/\varphi] = \int_0^\infty \mathrm{d}p\, \tilde{A}_0(p) \exp[ip\xi]\,; \qquad \tilde{A}_0(p) = \tilde{\varphi}'^*(p)\, \tilde{\varphi}(p)\,, \tag{2.5}$$

and $A[\varphi'/\varphi]$ becomes a ξ-dependent functional of $A_0(\xi)$

$$A[A_0, \xi] = A[\varphi'_\xi/\varphi] = \int_0^\infty \mathrm{d}p\, \tilde{A}_0(p)\, S(p) \exp[ip\xi]\,. \tag{2.6}$$

As we loose no information about the scattering amplitude $S(p)$ in going from the correspondence $A_0[\varphi'/\varphi] \to A[\varphi'/\varphi]$ to $A_0(\xi) \to A[A_0, \xi]$ we may confine our further investigations to the latter one (3).

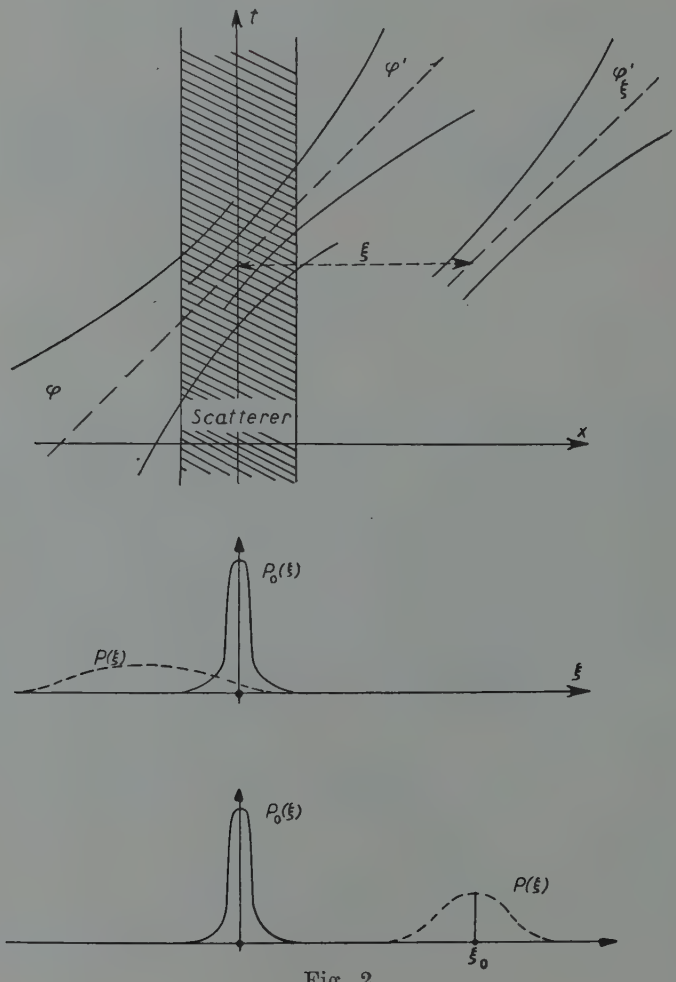

Fig. 2.

(3) It may be shown that the knowledge of the correspondence $A_0(\xi) \to A[A_0, \xi]$ uniquely defines $S(p)$.

We get a qualitative understanding of the restrictions on the relative behaviour of $A_0(\xi)$ and $P(\xi) = |A(\xi)|^2$ (4) resulting from causality by considering an $A_0(\xi)$ having a sharp maximum at $\xi = 0$. This means that φ and φ'_ξ overlap strongly for $\xi \simeq 0$ only (Fig. 2). If the corresponding $P(\xi)$ has a maximum for a positive and very large value ξ_0 of ξ (large compared to the width of $A_0(\xi)$ and the range of the scatterer), the scattered particle leaves the scatterer much earlier, in the mean, than the incoming particle reaches it, and this is presumably an acausality. Thus we see that causality may impose restrictions on the relative behaviour of $A_0(\xi)$ and $P(\xi)$ for very large and positive values of ξ. The following sections are devoted to an investigation of the possible nature of these restrictions.

The method of displaced wave packets works also in the case of the scattering of two particles: $\varphi, \chi \to \varphi', \chi'$. Let M be the mass of the χ-particle ($M \neq m$) and:

$$\text{(2.7)} \qquad \begin{cases} \chi(x,t) = \dfrac{1}{\sqrt{2\pi}} \displaystyle\int_{-\infty}^{+\infty} \mathrm{d}q \, \frac{1}{\sqrt{2\Omega_q}} \tilde{\chi}(q) \exp[iqx - i\Omega_q t]; \qquad \Omega_q = \sqrt{q^2 + M^2}\,, \\ \chi'(x,t) = \dots\,. \end{cases}$$

It is easy to see that, if $\tilde{\varphi}(p) = \tilde{\varphi}'(p) = 0$ for $p < 0$ and $\chi(q) = \chi'(q) = 0$ for $q > 0$, the scattering occurs through forward scattering only. From relativistic invariance, the forward scattering amplitude is a function of $(p, q) = \omega_p \Omega_q - pq$, and the transition amplitude is given by:

$$\text{(2.8)} \qquad A[\varphi', \chi'/\varphi, \chi] = \int_0^\infty \mathrm{d}p \int_{-\infty}^0 \mathrm{d}q \, \tilde{\varphi}'^*(p) \tilde{\chi}'^*(q) \, S(\omega_p \Omega_q - pq) \tilde{\varphi}(p) \tilde{\chi}(q)\,.$$

$A_0[\varphi', \chi'/\varphi, \chi]$ is obtained from (2.8) by putting $S = 1$. Introducing as above the translated wave packet φ'_ξ, keeping χ and χ' fixed, one gets:

$$\text{(2.9)} \qquad \begin{cases} A_0(\xi) = A_0[\varphi'_\xi, \chi'/\varphi, \chi] = \displaystyle\int_0^\infty \mathrm{d}p \, \tilde{A}_0(p) \exp[ip\xi]\,, \\ A[A_0, \xi] = A[\varphi'_\xi, \chi'/\varphi, \chi] = \displaystyle\int_0^\infty \mathrm{d}p \tilde{A}_0(p) \bar{S}(p) \exp[ip\xi]\,, \end{cases}$$

(4) For shortness, we write $A(\xi)$ instead of $A[A_0, \xi]$.

where:

$$(2.10)\qquad \begin{cases} \tilde{A}_0(p) = \tilde{\varphi}'^*(p)\,\tilde{\varphi}(p)\int_{-\infty}^{0} \mathrm{d}q\,\tilde{\chi}'^*(q)\,\tilde{\chi}(q)\,, \\ \bar{S}(p) = \Big[\int_{-\infty}^{0} \mathrm{d}q\,\tilde{\chi}'^*(q)\,S(\omega_p\Omega_q - pq)\,\tilde{\chi}(q)\Big]\Big[\int_{-\infty}^{0} \mathrm{d}q\,\tilde{\chi}'^*(q)\,\tilde{\chi}(q)\Big]^{-1}. \end{cases}$$

The interpretation of the relative behaviour of $A[A_0, \xi]$ and $A_0(\xi)$ is similar to the preceding one. In particular, if $\chi = \chi'$, one gets the situation of Fig. 2, the fixed scatterer being replaced by χ.

3. – Asymptotic causality.

For definiteness we consider again the case of the scattering of a particle by a fixed scatterer. We first remark that, according to (2.5) and (2.6), the spectrum of $A_0(x)$ and $A(x)$ contains only positive p's. Therefore these functions never have sharp fronts, and the causality condition cannot be: $A(x) = 0$ for $x > x_0$ if $A_0(x) = 0$ for $x > x_0$. Moreover, $A(x)$ may well be advanced against $A_0(x)$ without violation of causality because the interaction with the scatterer can be attractive (5). Then the particle is accelerated inside the scatterer and leaves it earlier as if there were no interaction, or only a repulsive interaction. The detailed structure of this possible advancement depends on the particular nature of the scatterer, and one has no feeling how to characterize it in general. However, it is evident that a scatterer of finite range and finite strength, as we assume it, will produce an advancement whose effects are limited to finite values of x. More precisely, we are certainly allowed to require that *asymptotically, for* $x \to +\infty$, $A(x)$ *has to be retarded against* $A_0(x)$. Remembering footnote (5), we propose to formulate this condition in the following way:

$$(3.1)\qquad \limsup_{x_0 \to +\infty} \left[\frac{\int_{x_0}^{\infty} \mathrm{d}x\,P(x)}{\int_{x_0}^{\infty} \mathrm{d}x\,P_0(x)}\right] \leqslant 1\,,$$

(5) Retardation of $A(x)$ against $A_0(x)$ can be characterized, in spite of the impossibility of sharp fronts, by the condition: $\int_{x_0}^{\infty} \mathrm{d}x\,|A(x)|^2 \leqslant \int_{x_0}^{\infty} \mathrm{d}x\,|A_0(x)|^2$ for every x_0. Arguments similar to those of Van Kampen (*Phys. Rev.*, **91**, 1267 (1953)) show that this condition implies analiticity of $S(p)$ in the upper half-plane. Therefore strict retardation excludes the occurence of poles on the positive imaginary axis, due to bound states.

where $P_0(x) = |A_0(x)|^2$. We call this requirement the *condition of asymptotic causality*. This is of course a very weak condition, but, in our opinion, it is the sole condition which is immediately accepted and recognized as a direct consequence of macrocausality. Any stronger condition would fail to have this high degree of plausibility which basic assumptions should have.

Now the question arises if our condition of asymptotic causality implies some analytic properties for $S(p)$. As it will be made clear in the following section, singularities of $S(p)$ in the upper half p-plane never affect in a significant way the asymptotic behaviour of $A(x)$. Therefore asymptotic causality is correlated with the analytic structure of $S(p)$ only in an infinitesimal neighbourhood of the real axis, and we suggest that *the condition of asymptotic causality* (3.1) *holds if, and only if, $S(p)$ has an analytic continuation into an infinitesimal strip $\mathcal{S}$ of the upper half plane, along the positive real axis* ($0 \leqslant \operatorname{Im} p < \varepsilon$, $\operatorname{Re} p \geqslant 0$, ε arbitrarily small).

We have no complete proof of our last statement, but we will demonstrate in the following two theorems which exhibit its plausibility.

$S(p)$ is separable into two terms, $S_-(p)$ and $S_-(p)$ which are boundary values of functions which are analytic and regular respectively in the upper and the lower half plane:

$$S(p) = S_+(p) + S_-(p)\,,$$

$$S_\pm(p) = \mp\, i\frac{\pi}{2} \lim_{\varepsilon \to 0+} (p+q) \int_0^\infty \mathrm{d}p' \, \frac{S(p')}{(p-p' \pm i\varepsilon)(p'+q)}\,, \tag{3.2}$$

where q is real and positive (the integral converges, because $|S(p)| \leqslant 1$ from unitarity) [6].

Thus we claim that $S_-(p)$ has an analytical continuation into the infinitesimal strip $\mathcal{S}$. Now our first theorem reads: *Suppose $S_-(p)$ to be continuous and infinitely often continuously differentiable in the interval (p_1, p_2), except at the point p_0 $(p_1 < p_0 < p_2)$ where some derivatives are discontinuous or unbounded, then the condition* (3.1) *of asymptotic causality is violated for some $A_0(x)$'s.* For the proof of this theorem, we choose an $A_0(x)$ whose Fourier transform $\tilde{A}_0(p)$ has the compact support (p_1, p_2) ($\tilde{A}_0(p) \neq 0$ for $p_1 < p < p_2$ only), and is indefinitely often differentiable with bounded derivatives ($|(\mathrm{d}^n/\mathrm{d}p^n)\tilde{A}_0(p)| \leqslant C_n < \infty$ for every p and every n). Then $A_0(x)$ decreases faster than any power of $1/x$ at infinity. The decomposition (3.2) of $S(p)$ induces a decomposition of $A(x)$:

$$A(x) = A_+(x) + A_-(x) \qquad \tilde{A}_\pm(p) = S_\pm(p)\,\tilde{A}_0(p)\,. \tag{3.3}$$

---

[6] $S_\pm(p)$ are uniquely defined up to a constant, *i.e.*, the substitution $q \to q'$ leads to $S_\pm(p) \to S_\pm(x) \pm \text{const.}$

We can also write:

$$A_{\pm}(x) = \int_{-\infty}^{+\infty} \mathrm{d}x' \, \Sigma_{\pm}(x - x') \, A_0(x') \,, \tag{3.4}$$

where

$$\Sigma_{\pm}(x) = \frac{1}{2\pi} \int_{-\infty}^{+\infty} \mathrm{d}p \, S_{\pm}(p) \exp[ipx] \,. \tag{3.5}$$

As a consequence of the analytic properties of $S_{\pm}(p)$, $\Sigma_{\pm}(x) = 0$ for $x \gtrless 0$.

In order to get information on the asymptotic behaviour of $A_+(x)$ it is convenient to introduce the functions:

$$\begin{cases} \bar{\Sigma}_+(x) = \dfrac{1}{2\pi} \displaystyle\int_{-\infty}^{+\infty} \mathrm{d}p \, \frac{1}{p + i\mu} \, S_+(p) \exp[ipx] \,; & \mu \text{ real}, > 0, \\ \bar{A}_0(x) = i\left(\mu - \dfrac{\mathrm{d}}{\mathrm{d}x}\right) A_0(x) \,. \end{cases} \tag{3.6}$$

Then

$$A_+(x) = \int_{-\infty}^{+\infty} \mathrm{d}x' \, \bar{\Sigma}_+(x - x') \bar{A}_0(x') \,, \tag{3.7}$$

$\bar{\Sigma}_+(x)$ is square integrable (which has not to be the case for $\Sigma_+(x)$) and $\bar{A}_0(x)$ still decreases faster than any power of $1/x$. Schwarz's inequality gives:

$$|A_+(x)|^2 \leqslant \int_{-\infty}^{0} \mathrm{d}x' \, |\bar{\Sigma}_+(x')|^2 \int_{x}^{\infty} \mathrm{d}x' \, |\bar{A}_0(x')|^2 \leqslant \frac{\pi}{\mu} \int_{x}^{\infty} \mathrm{d}x' \, |\bar{A}_0(x')|^2 \,. \tag{3.8}$$

As the remaining integral decreases faster than any power of $1/x$ for $x \to +\infty$, the same is true for $A_+(x)$.

From the assumed properties of $S_-(p)$ follows that the derivatives of $\tilde{A}_-(p)$ are not all bounded at $p = p_0$. Therefore, the integral

$$I_n = \int_{-\infty}^{+\infty} \mathrm{d}x \, |A_-(x)|^2 x^{2n} = \int_{p_1}^{p_2} \mathrm{d}p \left| \frac{\mathrm{d}^n}{\mathrm{d}p^n} \tilde{A}_-(p) \right|^2$$

diverges for some value N of n and converges for $n < N$. This means that

$|A_-(x)|$ behaves as some finite power of $1/x$ at infinity:

$$A_-(x) \sim C \frac{1}{x^\alpha}; \qquad N - \frac{1}{2} < \alpha < N + \frac{1}{2}.$$

On the other hand an argument similar to that on $A_+(x)$ shows that $A_-(x)$ decreases faster than any power of $1/x$ for $x \to -\infty$, so that for $x \to +\infty$

$$|A(x)| \sim |A_-(x)| > C \frac{1}{x^\alpha}, \qquad 0 < \alpha < \infty, \tag{3.9}$$

and (3.1) is violated.

The relevance of this theorem is that, if we make the physically reasonable assumption that $S(p)$, and therefore also $S_-(p)$, is piecewise continuous and infinitely often differentiable, it implies that $S_-(p)$ has to be continuous and infinitely often differentiable on the whole positive real axis. This is of course an essential condition for the possibility of a continuation of $S_-(p)$ into some domain of the first quadrant. Our second theorem asserts that the existence of an analytic continuation of $S(p)$ into the infinitesimal strip $\mathscr{S}$ of the upper half-plane, along the positive real axis is *sufficient* for the validity of (3.1) for a *special class* of $A_0(x)$'s defined by

$$\begin{cases} A_0(x) = \displaystyle\int_{p_1}^{p_2} \mathrm{d}p\, f(p) \exp\left[-g(p) + ipx\right], \\ g(p) = \dfrac{\beta_1}{(p - p_1)^{\alpha_1}} + \dfrac{\beta_2}{(p_2 - p)^{\alpha_2}}. \end{cases} \tag{3.10}$$

α_1 and α_2 are real and positive, β_1 and β_2 may be complex, with $\mathrm{Re}\,\beta_1$, $\mathrm{Re}\,\beta_2 > 0$, $f(p)$ is analytic and regular in some domain $\mathscr{D}$ containing the interval (p_1, p_2) (Fig. 3).

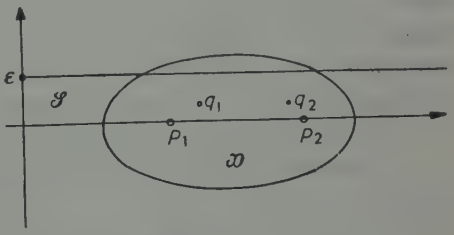

Fig. 3.

The particular form of $A_0(x)$ permits (with the aid of the saddle-point method) an evaluation of the asymptotic form appearing in (3.1). The term $\exp\left[-g(p) + ipx\right]$ has two saddle-points,

$$\begin{cases} q_1 = p_1 + \left(\dfrac{i\alpha_1\beta_1}{x}\right)^{1/(1+\alpha_1)} \\ q_2 = p_2 - \left(\dfrac{\alpha_2\beta_2}{ix}\right)^{1/(1+\alpha_2)}. \end{cases} \tag{3.11}$$

They lie in the upper half plane if $x > 0$, and are inside $\mathscr{D}$ for x sufficiently large. Therefore the path of integration can be replaced by a path passing through the saddle points, and if $\alpha_1 < \alpha_2$ the asymptotic form of $A_0(x)$ results from the contribution of q_1:

$$A_0(x) \sim cf(p_1) \frac{1}{x^{1-a/2}} \exp\left[-bx^a + ip_1 x\right] \qquad \text{for} \quad x \to +\infty, \tag{3.12}$$

where a, b and c are some constants (a real, $\operatorname{Re} b > 0$).

As for sufficiently large values of x the saddle points q_1 and q_2 are also inside the strip into which $S(p)$ is supposed to have a continuation, the asymptotic behaviour of $A(x)$ can also be calculated by the saddle-point method, and one gets

$$A(x) \sim S(p_1) A_0(x) \qquad \text{for } x \to +\infty \tag{3.13}$$

As $|S(p_1)| \leqslant 1$, the condition of asymptotic causality (3.1) is verified.

If we consider the mutual scattering of two particles, instead of the scattering of a particle by a fixed scatterer, it is still justified to require the condition (3.1) of asymptotic causality to be fulfilled. The resulting analyticity in the strip $\mathscr{S}$ holds now for $\overline{S}(p)$, defined in (2.10). It will be shown in Appendix A that analyticity of $\overline{S}(p)$ in $\mathscr{S}$ implies analyticity of $S(p)$ itself in the same domain.

It is known that in potential scattering, $S(p)$ has an analytic and regular continuation into the first quadrant of the p-plane ($\operatorname{Re} p > 0$, $\operatorname{Im} p \geqslant 0$) if the potential decreases as some finite power of $1/x$ at infinity. The first quadrant contains of course our infinitesimal strip $\mathscr{S}$. A potential with slower decrease leads in general to an $S(p)$ having no regular continuation into the first quadrant. However, such a potential corresponds to a very extended scatterer for which it is not legitimate to require (3.1) to hold.

In the field theoretical case $S(p)$ has been shown to be analytic and regular in the first quadrant whenever one has succeeded to prove a dispersion relation for $S(p)$.

Therefore we may conclude that the regularity of $S(p)$ in the strip $\mathscr{S}$ seems to be equivalent to the condition of asymptotic causality (3.1) and that it is not in contradiction with known consequences of the usual condition of microcausality. Of course, regularity in $\mathscr{S}$ is a very weak restriction on $S(p)$, which is far from leading to a dispersion relation; it mainly predicts the relative behaviour of its real and imaginary parts in the neighbourhood of eventual points of discontinuity, corresponding to thresholds.

4. – Observable effects of a pole of $S(p)$ in the first quadrant.

In the preceding section, we discussed a general and quite plausible asymptotic causality condition, which seems to imply only very weak consequences for $S(p)$. It is an open question if there exist stronger conditions, which still can be recognized as causality conditions and which lead to further restrictions on the possible singularities of $S(p)$ in the first quadrant of the p-plane. As one has no direct feeling how to formulate such conditions, the most instructive thing to do is to consider an $S(p)$ with given singularities in the first quadrant and to investigate the specific consequences of these singularities on the behaviour of $P(x)$. We restrict ourselves to the simplest case, where a pole is the unique singularity of $S(p)$ in the first quadrant:

$$S(p) = \frac{1}{2i\pi}\frac{\alpha}{p-\varkappa} + R(p)\,, \tag{4.1}$$

where $\varkappa = \mu + iv$ $(\mu, v > 0)$ and $R(p)$ is regular and bounded in the first quadrant. We write:

$$\begin{cases} A(x) = A_1(x) + A_2(x)\,, \\ A_1(x) = \dfrac{\alpha}{2i\pi}\displaystyle\int_0^\infty \mathrm{d}p\,\frac{1}{p-\varkappa}\,\tilde{A}_0(p)\exp[ipx] = \alpha\int_{-\infty}^{x}\mathrm{d}x'\exp[i\varkappa(x-x')]\,A_0(x')\,, \\ A_2(x) = \displaystyle\int_0^\infty \mathrm{d}p\,R(p)\tilde{A}_0(p)\,\exp[ipx]\,. \end{cases} \tag{4.2}$$

From the fact that the spectrum of $A_0(x)$ contains only positive p's, results that (7):

$$\int_{-\infty}^{+\infty}\mathrm{d}x\,\frac{|\log A_0(x)|}{1+x^2} < \infty\,.$$

Therefore $A_0(x)$ decreases at infinity more slowly than exponentially, and $A_1(x)$ never behaves asymptotically like $\exp[i\varkappa x]$. Therefore it is impossible to infer the existence of the pole $p = \varkappa$ of $S(p)$, and more generally of any singularity in the upper half-plane from the asymptotic behaviour of $A(x)$

(7) Cf. Theorem XII, p. 16 in PALEY and WIENER: *Fourier Transforms in the Complex Domain* (American Mathematical Society, 1934).

for $x \to +\infty$. This fact leads us in Section 3 to suggest that asymptotic causality implies regularity of $S(p)$ in an infinitesimal strip only.

Nevertheless it may be that $|A(x)|$ behaves fairly well like $|\exp[i\varkappa x]| = \exp[-\nu x]$ in some finite, but large interval (x_1, x_2). In order to see this, we introduce a function $\delta(x, y)$ which measures the deviation of $|A(x)|$ from the exponential in the interval $(x, x+y)$

$$\delta(x, y) = \left| \left| \frac{A(x+y)}{A(x)} \exp[-i\varkappa y] \right| - 1 \right| . \tag{4.3}$$

For practical convenience, we take:

$$A_0(x) = \frac{1}{[x + ia]^{2n}} , \tag{4.4}$$

with a real and positive. After some lengthy calculation, whose principal steps are indicated in Appendix B, one gets an upper bound for $\delta(x, y)$:

$$\delta(x, y) < K \sqrt{\frac{2}{2\pi(n-1)}}\ \mathrm{tg}\,\theta\,(\sin\theta)^{2n-1} \exp[a\mu] \left[1 + \bar{R} \left| \frac{\varkappa}{\alpha} \right| \cos\theta \right] , \tag{4.5}$$

if

$$x > \frac{2n}{\nu} K^{-(1/2n)} \quad \text{and} \quad (x+y) < \frac{2n}{\nu} + \frac{1}{\nu} \log K .$$

$\theta = \arg \varkappa = \mathrm{tg}^{-1} \nu/\mu$ and $\bar{R}$ is an upper bound of $2\pi|R(p)|$ in the first quadrant. (n has been assumed large and some factorials have been approximated according to Stirling's formula.) Putting $x = 2n/\nu$ and $K = \exp[2c\sqrt{\pi n}]$ $(c > 1)$ (4.5) gives:

$$\delta\left(\frac{2n}{\nu}, y\right) < \sqrt{\frac{2}{2\pi(n-1)}} \exp[(2n-1)\log(\sin\theta) + C\sqrt{\pi n}] \cdot \\ \cdot \mathrm{tg}\,\theta \exp[a\mu] \left[1 + \bar{R} \left| \frac{\varkappa}{\alpha} \right| \cos\theta \right] , \tag{4.6}$$

for $y < 2c(\sqrt{\pi n}/\nu)$. This shows that, by choosing n large enough $\delta((2n/\nu), y)$ can be made arbitrarily small, for $y < 2c(\sqrt{\pi n}/\nu)$ and as long as $\theta \neq \pi/2$. On the other hand, one finds that if the pole $\varkappa$ is on the imaginary axis $(\varkappa = i\nu)$, $\delta(2n/\nu, 2c\sqrt{\pi n}/\nu)$ has a finite lower limit:

$$\delta\left(\frac{2n}{\nu}, 2c\frac{\sqrt{\pi n}}{\nu}\right) > 2(c-1) + 0\left(\frac{1}{\sqrt{n}}\right) . \tag{4.7}$$

Therefore, we have found an experimental test distinguishing a pole in the first quadrant from a pole on the imaginary axis. (Of course, the experiment in question is an ideal one). Choosing $A_0(x)$ according to (4.4), with n sufficiently large, $|A(x)|$ fits the exponential $\exp[-xv]$ arbitrarily well in the arbitrarily large interval $((2n/v), (2n/v) + 2c\sqrt{\pi n}/v)$ if $\varkappa$ is in the first quadrant. If $\varkappa$ is on the imaginary axis, such a good fit will never be obtained in that interval. However, as one has no convincing physical argument against a quasi-exponential behaviour of $|A(x)|$ in some interval, it is doubtful if there exists a plausible condition of macrocausality excluding a pole of $S(p)$ in the first quadrant, as microcausality does. Therefore, one gets the impression that macrocausality is intrinsically a much weaker concept than microcausality.

* * *

I would like to thank Professor W. Heisenberg for the kind hospitality of the Max-Planck-Institut für Physik. I am especially indebted to Dr. K. Symanzik for many helpful discussions.

Appendix A

Remark first that:

$$\omega_p \frac{\partial}{\partial p} S(\omega_p \Omega_q - pq) = \Omega_q \frac{\partial}{\partial q} S(\omega_p \Omega_q - pq) \,. \tag{A.1}$$

Therefore, according to (2.10):

$$\omega_p \frac{\mathrm{d}\bar{S}(p)}{\mathrm{d}p} = C \int_{-\infty}^{0} \mathrm{d}q \, \Omega_q \, \tilde{\chi}'^*(q) \, \tilde{\chi}(q) \frac{\partial}{\partial q} S(\omega_p \Omega_q - pq) = \tag{A.2}$$

$$= MC\tilde{\chi}'^*(0)\chi(0) \, S(M\omega_p) - C \int_{-\infty}^{\blacksquare} \mathrm{d}q \frac{\mathrm{d}}{\mathrm{d}q} (\tilde{\chi}'^*(q) \, \chi(q) \, \Omega_q) \, S(\omega_p \Omega_q - pq) \,,$$

if

$$\tilde{\chi}'^*(-\infty) \, \tilde{\chi}(-\infty) = 0 \quad \text{and} \quad C^{-1} = \int_{-\infty}^{0} \mathrm{d}q \tilde{\chi}'^*(q) \, \tilde{\chi}(q) \,.$$

Choose now χ_1' and χ_1 in such a way that $\tilde{\chi}_1^*(q)\tilde{\chi}_1(q) = (\mathrm{d}/\mathrm{d}q) \, (\tilde{\chi}'^*(q)\chi(q)\Omega_q)$. These wave packets define a new function $S_1(p)$ and a new constant C_1, and (A.2)

gives:

$$MC\tilde{\chi}'^{*}(0)\tilde{\chi}(0)\,S(M\omega_p) = \omega_p \frac{\mathrm{d}\bar{S}(p)}{\mathrm{d}p} + \frac{C}{C_1}\,\bar{S}_1(p)\,. \tag{A.3}$$

As $\bar{S}(p)$ and $\bar{S}_1(p)$ are assumed to be regular in the strip $\mathcal{S}$, (A.3) shows that the same is true for $S(M\omega_p)$.

Appendix B

$\varkappa$ in the first quadrant.

According to (4.2) and (4.4):

$$A_1(x) = \alpha \int_0^\infty \mathrm{d}x' \frac{\exp\,[i\varkappa x']}{[x - x' + ia]^{2n}}\,. \tag{B.1}$$

The path of integration can be shifted on the positive imaginary axis, if one takes into account the residue at $x' = x + ia$. This gives:

$$A_1(x) = B(x) + B'(x)\,, \tag{B.2}$$

with:

$$B(x) = 2i\pi\alpha \frac{(i\varkappa)^{2n-1}}{(2n-1)!} \exp\,[-a\varkappa] \exp\,[i\varkappa x]\,,$$

$$B'(x) = i^{-(2n-1)}\alpha \int_0^\infty \mathrm{d}u \frac{\exp\,[-\varkappa u]}{[u - a + ix]^{2n}}\,.$$

One has:

$$|B'(x)| < |\alpha| \int_0^\infty \mathrm{d}u \frac{\exp[-u\mu]}{[(u-a)^2 + x^2]} < \frac{|\alpha|}{\mu x^{2n}}\,. \tag{B.3}$$

$A_2(x)$ is given by:

$$A_2(x) = \frac{2\pi}{(2n-1)!}\, i^{-2n} \int_0^\infty \mathrm{d}p\, R(p)\, p^{2n-1} \exp\,[-ap + ipx]\,. \tag{B.4}$$

After shifting the path of integration on the positive imaginary axis, one gets an upper limit for $|A_2(x)|$:

$$|A_2(x)| < \bar{R}\frac{1}{x^{2n}}\,. \tag{B.5}$$

One has now:

$$A(x) \overset{\text{as}}{=} B(x) + B_1(x)\,, \tag{B.6}$$

with $B_1(x) = B'(x) + A_2(x)$. According to (B.3) and (B.5):

$$|B_1(x)| < \frac{|\alpha|}{\mu}\left(1 + \bar{R}\,\frac{\mu}{|\alpha|}\right)\frac{1}{x^{2n}}\,. \tag{B.7}$$

From (B.2) and (B.7) one can deduce that:

$$\frac{|B(x)|}{|B_1(x)|} > \frac{1}{K}\sqrt{2\pi(2n-1)}\,\operatorname{ctg}\theta\,\frac{1}{(\sin\theta)^{2n-1}}\exp[-a\mu]\,\frac{1}{1+\bar{R}(\mu/|\alpha|)}\,. \tag{B.8}$$

if $(2n/\nu)K^{-1/2n} < x < (2n/\nu) + (1/\nu)\log K$. The upper limit (4.5) follows directly from (B.8).

x on the imaginary axis.

We write:

$$\delta(x, y) = |\,|1 + \eta(x, y)| - 1|\,, \tag{B.9}$$

with

$$\eta(x, y) = \frac{A(x+y)\exp[\nu y] - A(x)}{A(x)}\,. \tag{B.10}$$

One has

$$\eta(x, y) = \frac{\int_0^y \mathrm{d}x' \exp[\nu x']/[x + x' + ia]^{2n} + (1/\alpha)\,(\exp[\nu y]\,A_2(x+y) - A_2(x))}{\int_0^\infty \mathrm{d}x' \exp[-\nu x']/[x - x' + ia]^{2n} + (1/\alpha)\,A_2(x)}\,. \tag{B.11}$$

Using the same method as above, one gets an upper limit for the denominator of (B.11):

$$|\mathrm{Den}| < \frac{1}{x^{n-1}}\left(\frac{\sqrt{\pi}}{2}\,\frac{1}{\sqrt{n-1}} + \frac{\bar{R}}{|\alpha|}\,\frac{1}{x}\right). \tag{B.12}$$

If x is large enough, the integral in the numerator of (B.11) can be evaluated in the following way:

$$\left|\int_0^y \mathrm{d}x'\,\frac{\exp[\nu x']}{[x + x' + ia]^n}\right| \sim$$

$$\sim \int_0^y \mathrm{d}x'\,\frac{\exp[\nu x']}{[x + x']^{2n}} > \frac{1}{x^n}\int_0^y \mathrm{d}x'\,\exp\left[\left(\nu - \frac{2n}{x}\right)x'\right] \geqslant \frac{y}{x^{2n}}\,, \tag{B.13}$$

the last inequality holding if $x > 2n/v$. On the other hand:

$$\text{(B.14)} \quad \left|\frac{1}{\alpha}(\exp[vy]A_2(x+y) - A_2(x)\right| < \frac{\bar{R}}{|\alpha|}\frac{1}{x^{2n}}\left[\frac{\exp[vy]}{(1+(y/x))^{2n}} + 1\right] <$$

$$< \frac{\bar{R}}{|\alpha|}\frac{1}{x^{2n}}\left[\exp\left[\left(v - \frac{2n}{x}\right)y + \frac{n}{x^2}y^2\right] + 1\right] < \frac{\bar{R}}{|\alpha|}\frac{1}{x^{2n}}(\exp[\pi c^2] + 1),$$

the last inequality holding if $x > 2n/v$ and $y < 2c(\sqrt{\pi n}/v)$.

From (B.13) and (B.14) one gets:

$$\text{(B.15)} \quad |\text{Num}| > \frac{1}{x^{2n}}\left(y - \frac{\bar{R}}{|\alpha|}(1 + \exp[\pi c^2])\right),$$

as long as $y > (\bar{R}/|\alpha|)(1 + \exp[\pi c^2])$. (4.7) follows from (B.10) and (B.15).

RIASSUNTO (*)

Si discute la possibilità di formulare il principio di causalità in funzione delle probabilità di transizioni osservabili. Si constata che dall'esigenza di causalità si può dedurre, plausibilmente, solo una condizione asintotica molto debole. Questa condizione implica regolarità dell'ampiezza $S(p)$ dello scattering in avanti in una striscia infinitesima del primo quadrante lungo l'asse reale p. Le singolarità di $S(p)$ situate ad una distanza finita dall'asse reale, hanno anche effetti osservabili, ma non possono essere interpretate come ovvie acausalità.

(*) *Traduzione a cura della Redazione.*

IL NUOVO CIMENTO Vol. XIV, N. 1 1° Ottobre 1959

Regularization and Renormalization.

II - Necessary and Sufficient Conditions (*).

E. R. Caianiello (**)

Istituto di Fisica Teorica dell'Università - Napoli
Scuola di Perfezionamento in Fisica Teorica e Nucleare del C.N.R.N. - Napoli

(ricevuto il 3 Luglio 1959)

Summary. — The analysis begun in Part I of the conditions under which the regularization, performed by the adoption of the modified integrals introduced there, acts as a renormalization is completed. The « conditions of the second type » announced in I are formulated and discussed; a quantitative analysis may give results different from the standard requirements for renormalizability: as an example, it is shown that the neutral scalar meson theory is not renormalizable, contrary to current belief. The Lie equations of the renormalization group can be derived without difficulty, and their integrability conditions investigated. Finally, it is shown that using our modified integrals amounts to solving the differential branching equations for kernels under the condition that the solutions belong to a certain well-defined mathematical class $\mathscr{K}$. In this way, ultraviolet infinities never appear, and the search for the renormalizability conditions becomes a search for the self-consistency of a theory, which need be made once for all and cannot cause inconvenience in computations. The result is a rigorous mathematical formulation of the renormalized theory, which avoids all mentions of « bare particles », is completely rid of ambiguities and is suited both for practical computations and for the study of fundamental questions. The unphysical splitting of processes into Feynman graphs is avoided; the troubles due to overlaps are shown to have a trivial origin and are altogether eliminated; all vertex-part contributions vanish with this method, at least in electrodynamics, since the cancellation of them against electron self-energy contributions occurs prior to actual computation. These criteria will be applied in a forthcoming work to an exhaustive study of electrodynamics; they are expected to play a relevant rôle in a search for consistent theories of elementary particles.

(*) The research reported in this document has been sponsored in part by the Office, Chief of Research and Development, U.S. Department of Army.

(**) Part of this research was performed at the Institut des Hautes Etudes Scientifiques, Paris. The author takes pleasure in thanking its Director, M. L. Motchane, for the kind hospitality extended to him.

1. – Introduction.

1·1. – The present work continues and concludes some considerations recently published (1), the purpose of which was to understand the mathematical origin of the so-called ultraviolet divergencies of field theory and to attain a rigorous mathematical formulation of the problems presented by their renormalization. We have stated in I that a regularization procedure acts as renormalization provided it satisfies conditions of two sorts: a first set (conditions *a*, *b*, *c*, *d* of I) of a very general character, which are clearly necessary in order that the theory be mathematically meaningful, and guaranty also that all combinatorial problems are dealt with correctly (this is the hardest, and the most important aspect of the question); a second set, which depend specifically on the theory which is being studied.

All requirements of the first type have been studied in detail in I, where they are shown to be equivalent to a single, very simple mathematical condition given by formula (I-46). As matter of fact, (I-46) (which is required to be true only for *symmetric* integrands) imposes very severe restrictions on the prescription; although it may be satisfied by an infinite number of prescriptions (to within, that is, a finite renormalization), we do not expect that these, different as they may be as regards formal appearance or ease of computation, have substantially different contents. We shall have, time and again, the occasion of using (I-46) to deduce results very relevant for our purposes.

In the present work we study the second set of conditions, which will guaranty, without the need of further checks, that all the divergent parts suppressed by a regularization procedure which satisfies them (and (I-46)) are formally identical with those that the customary counter-terms would have produced; this suffices to prove that the procedure is actually a renormalization, in the standard sense.

We obtain, actually, much more than this. First of all, this treatment is entirely rigorous from a mathematical point of view (*e.g.* it contains, as a by-product, a strict proof of the often stated fact that renormalization of a perturbative expansion in a renormalizable theory can be carried through consistently to all orders) and totally rid of ambiguities (individual Feynman graphs, which are the main sources of them, are never used; overlaps are automatically taken care of; all divergencies due to vertex parts disappear in electrodynamics, because they cancel against the corresponding electron self-energy

(1) E. R. CAIANIELLO: *Nuovo Cimento*, **13**, 637 (1959), referred to hereafter as I; see also all references quoted there.

parts *prior* to computation; etc.). Furthermore, it leads, quite naturally, to the formulation of the differential Lie equations of the renormalization group (*i.e.*, for any fixed prescription, to the differential equations of the transformation that carries unrenormalized into renormalized parameters). The integrability conditions of these are easily written; it turns out that they are satisfied in the case of electrodynamics and of pseudoscalar meson theory, but not of neutral scalar meson theory: the latter is, therefore, *not* renormalizable, contrary to current belief. (Dyson's conditions, which are known to be not necessary for renormalization, are thus seen to be also not sufficient; they give very useful indications, but are not the substitute for a rigorous analysis).

We do not give here a full treatment of any specific theory, because each case presents its own peculiarities and is better treated apart; we give, rather, a complete account of our method in the case of electrodynamics (with a finite photon mass), where, however, on the one hand we accept without criticism, for the sake of brevity, the usual arguments to discard contributions which are not gauge-invariant, and on the other hand we assume that the divergent parts (which turn out, from actual computation, to have in this case a remarkably simple structure) are of unknown complexity. This will permit, in future works dedicated to specific theories (including, possibly, theories deemed thus far to be not renormalizable) to proceed with a minimum effort, all relevant points being already contained in the present discussion. A complete study of electrodynamics is not made the subject of this paper because it would raise other, minor but lengthy, questions (*e.g.*, renormalization changes also the gauge), and also because the simplifications that occur in that case might hide important aspects of the problems; we differ this discussion to the near future, and ask the reader's forgiveness if he is begged, at one or two points, to accept the result of calculations not reported here in detail.

1˙**2.** – After all proofs are given and identification with the current formulation and terminology is completed, one finds an extremely simple conclusion: that a rigorous, consistent and entirely unambiguous renormalization is obtained *ipso facto* if one changes, throughout in the perturbative equations and in the branching equations, the customary ordinary (Riemann or Lebesgue) integrals into somewhat different operations, denoted by us with the symbol $\int$, which generalize (and include) principal-value integrals, Hadamard's finite parts, Riesz's α-parametrized integrals, etc.; different definitions of such operations give results which differ by a finite renormalization. All one has to do, to find whether a regularization prescription is acceptable as a renormalization, is to check whether it fulfils condition (I-46) and to perform the few calculations which are necessary to test whether the conditions given in the present work are verified.

If one takes this point of view, the formulation given by us is only a restatement of the problem of renormalization with a different technique. This identification is indeed very important, because we would have, otherwise, no justification for dropping the infinite quantities that our re-defined integrals suppress. Once this is proved, though, one is tempted to go some steps farther.

First, no mention need ever be made, from our point of view, of infinite quantities (of ultraviolet origin): in a theory which fulfils our requirements and is written throughout in terms of $\int$ integrals, they have been already renormalized away in a consistent manner. A finite renormalization will still be necessary (cf. I); but this means simply that the parameters of the theory, which are indeterminate to begin with, can only, and must, be determined from experiment. We can eliminate all mention of infinities from our discussion, by requesting, instead of the usual conditions, that a theory be self-consistent, *i.e.* that, by expressing its parameters (finite in number) in terms of experimental data (as calculated from the theory) one obtains always consistent results, regardless *a*) of the number of the experimental data which are compared (this presupposes of course that the theory be physically correct to begin with!), *b*) of the particular prescription which has been adopted for the calculation of the integrals. This requirement is clearly equivalent to that of renormalizability: in either case, we have to ask that the numerical determination of any element of the S (or U) matrix be left invariant by the prescription adopted. The analysis that follows can be interpreted in this fashion without any change, since passage from a prescription $\int$ to another $\int'$ has the same properties as the passage from $\int$ to $\int$ integrals, except that the subtracted parts are now finite. Clearly, a theory which is not self-consistent is, at best, only a fragment of a self-consistent theory.

Finally, the question poses naturally itself, whether our integration prescriptions are just a mathematical disguise for hiding in a new way infinities which have an essential physical meaning (cf. I), or whether they can be simply understood in terms of the mathematical nature of the problem. We shall see that the latter alternative is the correct one: redefined $\int$ integrals must necessarily be used if the systems of coupled hyperbolic equations of field theory are to be handled correctly and unambiguously. Infinite ultraviolet quantities are automatically suppressed by a rigorous mathematical treatment: they arose only as correctives to inadequate mathematics.

The search for renormalizable theories becomes thus a search for self-consistent theories. This yields a classification which, at a crude estimate, coincides with the customary division into renormalizable and non-renormalizable theories, but may well give different, non-conventional results after a rigorous study, which appears now possible.

2. – Analysis of divergencies; a crude estimate.

2·1. – For the sake of concreteness, we shall refer throughout to the particular prescription for the calculation of $\int$ integrals which is specified at the end of I-4·2, based on Laurent (or allied) expansions of the integrands around points of confluence (this is always possible: obviously for perturbative expansions, by recourse to the branching equations in more general cases). We impose also that $\int$ integrals coincide, by virtue of their definition, with ordinary integrals whenever the latter are convergent; this criterion, which is desirable mathematically (principle of permanence), is clearly satisfied by our present choice; it may be relaxed if it is so desired (the discussion in I is independent of its validity), but we need not concern ourselves with this possibility here, our present aim being only a consistent elimination of infinite quantities. It is important to remark, though, that different questions may be advantageously studied with different, suitably chosen prescriptions. In order to show the full equivalence of our analysis with the classical treatments of renormalization, it is convenient to begin with a study of perturbative expansions; the formal identification of the divergent terms suppressed by the use of $\int$ integrals with the contributions that standard counter-terms would produce is made thereby perspicuous. After this is done, it will be a simple matter to recognize that the procedure is actually independent of perturbative techniques and of special methods of approximation.

2·2. – We have to find, as was indicated in I, under which conditions formula (I-47):

$$(1)\qquad \frac{\partial}{\partial\lambda} K\begin{pmatrix} x_1\, x_2 \dots x_{N_0} \\ y_1\, y_2 \dots y_{N_0} \end{vmatrix} t_1\, t_2 \dots t_{P_0}\Big) = \\ = \sum_{h=0}^{\infty} \frac{\lambda^h}{h!} \int \mathrm{d}\xi \sum \gamma^{\xi}\gamma^1 \dots \gamma^h \; D_{\xi}^1 \dots D_{\xi}^h K^{(\xi)}\begin{pmatrix} x_1 \dots x_{N_0} & \xi\,\xi_1 \dots \xi_h \\ y_1 \dots y_{N_0} & \xi\,\xi_1 \dots \xi_h \end{vmatrix} \xi\,\xi_1 \dots \xi_h\, t_1 \dots t_{P_0}\Big),$$

reduces to formula (I-49):

$$(2)\qquad \frac{\partial}{\partial\bar{\lambda}} \bar{K}\begin{pmatrix} x_1 \dots x_{N_0} \\ y_1 \dots y_{N_0} \end{vmatrix} t_1 \dots t_{P_0}\Big) = \int\!\!\!\!\!\!- \mathrm{d}\xi \sum \gamma^{\xi} \bar{K}\begin{pmatrix} x_1 \dots x_{N_0}\xi \\ y_1 \dots y_{N_0}\xi \end{vmatrix} \xi\, t_1 \dots t_{P_0}\Big).$$

This is necessary in order that replacement of $\int$ with $\int$ may yield a correctly renormalized theory (cf. I). Passage from (1) to (2) will be the starting point of our discussion and will set the pattern for other such calculations.

The equivalence of (1) and (2), when it holds, can be proved by using for-

mula (I-19) at r.h.s. of (1), and then the combinatorial lemmas proved in I-2·5 (formulae (I-26) to (I-31)). (I-19) serves to bring the divergencies which arise from ξ-confluences of any order *out* of the kernels $K^{(\xi)}$ which appear at r.h.s. of (1); the discussion would be clearly impossible otherwise. One finds:

$$(3)\qquad \frac{\partial}{\partial\lambda}K\begin{pmatrix} x_1 \dots x_{N_0} \\ y_1 \dots y_{N_0}\end{pmatrix} t_1 \dots t_{P_0}\Big) = \sum_{h=0}^{\infty}\frac{\lambda^h}{h!}\int \mathrm{d}\xi \sum \gamma^{\xi}\gamma^1 \dots \gamma^h D^1_{\xi}\dots D^h_{\xi}\cdot$$

$$\cdot \sum_{r=0}^{h+1}\sum_{p=0}^{[(h+1)/2]}\sum_{\sigma_r^R}\sum_{\sigma_r^{\sigma}}\sum_{\sigma_{\varrho}} (-1)^{I(h,k)}\begin{pmatrix}\xi_{h'_1}\dots\xi_{h'_r}\\ \xi_{k'_1}\dots\xi_{k'_r}\end{pmatrix}[\xi_{l'_1}\dots\xi_{l'_{2\varrho}}]\cdot$$

$$\cdot K^{(\xi)}\begin{pmatrix}\overset{\circ}{\xi}_{h''_1}\dots\overset{\circ}{\xi}_{h''_s} & x_1\dots x_{N_0}\\ \overset{\circ}{\xi}_{k''_1}\dots\overset{\circ}{\xi}_{k''_s} & y_1\dots y_{N_0}\end{pmatrix}\overset{\circ}{\xi}_{l''_1}\dots\overset{\circ}{\xi}_{l''_s}\ t_1\dots t_{P_0}\Big),$$

where: $\xi_{h'_1}\dots\xi_{h'_r}$, $\xi_{h''_1}\dots\xi_{h''_s}$ is a combination of $\xi\xi_1\dots\xi_h$ with $h'_1<\dots<h'_r$; $h''_1<\dots<h''_s$; likewise for indices k and l; $r+s=2\varrho+\sigma=h+1$; $p(h,k)$ is the parity of the permutation $h'_1\dots h'_r\,h''_1\dots h''_s$ with respect to $k'_1\dots k'_r\,k''_1\dots k''_s$. We use henceforth $\sum_{\sigma_r}$ for $\sum_{\sigma_r}\sum_{\sigma_r}$, thus including in $\sum_{\sigma_r}$ summations over combinations of both row and column indices.

Formula (3) has two remarkable features: the first is that it factors, as was wanted, all ξ-divergencies out of each term; the second is that the kernels

$$(4)\qquad K^{(\xi)}_{\overset{\circ}{s}+N_0,\overset{\circ}{\sigma}+P_0} = K^{(\xi)}\begin{pmatrix}\overset{\circ}{\xi}_{h''_1}\dots\overset{\circ}{\xi}_{h''_s} & x_1\dots x_{N_0}\\ \overset{\circ}{\xi}_{k''_1}\dots\overset{\circ}{\xi}_{k''_s} & y_1\dots y_{N_0}\end{pmatrix}\overset{\circ}{\xi}_{l''_1}\dots\overset{\circ}{\xi}_{l''_\sigma}\ t_1\dots t_{P_0}\Big),$$

are infinitesimal of order $s-4$ for $s\geqslant 5$ (with four-component spinors) when $\xi_1\xi_2\dots\xi_h$ *coincide* with ξ. The latter property, which is clearly due to the exclusion principle, is not used in the present work; it is recorded because of its importance in a study of the behavior of non-renormalizable spinor theories.

2·3. – To obtain the wanted formal identification of the divergent parts D (to be dropped by adoption of $\int$ instead of $\int$) with the standard divergent terms, we must rearrange the terms at r.h.s. of (3) as follows. First, we set apart the first term of $\sum_h$ ($h=0$); it gives no contribution to $\sum_r$ because we *define* $(\xi\xi)=0$ (Heisenberg's prescription; see also later). Then, we consider separately all the contributions coming to $\partial K_{N_0P_0}/\partial\lambda$ from different values of s, σ (and all $h\geqslant 1$); these we denote with $(\partial K_{N_0P_0}/\partial\lambda)^{(\xi)}_{s,\sigma}$, with reference to (4). Thus:

$$(5)\qquad \frac{\partial K_{N_0P_0}}{\partial\lambda} = \int \mathrm{d}\xi \sum \gamma^{\xi}K^{(\xi)}\begin{pmatrix} x_1\dots x_{N_0}\xi\\ y_1\dots y_{N_0}\xi\end{pmatrix}\xi\, t_1\dots t_{P_0}\Big) + \sum_{s,\sigma\geqslant 0}\left(\frac{\partial K_{N_0P_0}}{\partial\lambda}\right)^{(\xi)}_{s,\sigma}.$$

In the rigorous study of a given theory, all terms $(\partial K/\partial\lambda_{\mathcal{N}_0 P_0})^{(\xi)}_{s,\sigma}$ have to be calculated, or at least estimated; this is a painstaking, but less forbidding task than it may appear. In the case of electrodynamics, to which the present work is restricted (see Introduction), a preliminary crude estimate of the order of the infinities contributed by them to (5) suffices to show, luckily, that only a small number of such terms is actually non-vanishing. We show, accordingly, firstly how this reduction obtains, then proceed with the consideration of the surviving terms; the latter will serve as a pattern for similar analyses, which may be required by more complicated theories.

The (ultraviolet!) divergencies are at their worst when all variables ξ_h *coincide* with ξ, and all possible cancellations among different terms (*e.g.* Furry's theorem) are ignored. Since they arise from four-fold integrations, a confluence of order h in (3) cannot cause infinities of order greater than that of

$$(6)\qquad \int \mathrm{d}\xi \int_{\omega(\xi)} \mathrm{d}\xi_1 \dots \int_{\omega(\xi)} \mathrm{d}\xi_h \gamma^{\xi}\gamma^{1} \dots \gamma^{h} \begin{pmatrix} \xi_{h'_1} \dots \xi_{h'_r} \\ \xi_{k'_1} \dots \xi_{k'_r} \end{pmatrix} [\xi_{l'_1} \dots \xi_{l'_{2\varrho}}] ,$$

where $\omega(\xi)$ is some suitable infinitesimal region of volume $0(\varepsilon^4)$ around the light-cone of ξ.

With

$$(7)\qquad \begin{cases} (\xi'\xi'') \sim 0(\varepsilon^{\,f}) , \\ [\xi'\xi'] \sim 0(\varepsilon^{-b}) , \end{cases} \qquad \text{for } \xi'' \to \xi' ,$$

it follows that divergencies *may* arise from (6) for h-fold confluences only if

$$(8)\qquad \lim_{\varepsilon \to 0} \varepsilon^{4h - fr - b\varrho} \neq 0 ;$$

(a finite value might indicate a logarithmic divergence; the integration over ξ, when it gives a divergent result, does so for reasons which have nothing to do with ultraviolet infinities - cf. I).

Since: $r = h+1-s$, $2\varrho = h+1-\sigma$, we conclude that divergent terms can (but need not) occur in (3) only if

$$fs + \frac{b}{2}\sigma \leqslant h\left(f + \frac{b}{2} - 4\right) + f + \frac{b}{2} ,$$

which is the familiar result. The reader will notice by himself the conceptual difference between this derivation of (9) and the standard treatments. Clearly, (9) is sufficient, but not at all necessary to obtain estimates of the maximum permissible order of infinity; it does not suffice in any case to prove the existence of a transformation which brings unrenormalized into renormalized parameters (cf. Section 4).

2·4. – In electrodynamics ($f = 3$, $b = 2$):

$$3s + \sigma \leqslant 4 . \tag{10}$$

By virtue of this estimate it suffices to consider explicitly, in (5), only the terms which satisfy (10): all others are identically vanishing.

The terms with $s = 0$, $\sigma = 1, 3$ are zero because of Furry's theorem: this can also be proved directly with simple algebraic considerations [2].

The term $s = 0$, $\sigma = 4$ is always neglected on the grounds of gauge invariance; we accept this result here for the sake of brevity and differ a thorough study of this and related questions to a future occasion. We are left with only four cases for which a detailed analysis is necessary:

$$a) \qquad s = 0 , \quad \sigma = 0 ,$$

$$b) \qquad s = 0 , \quad \sigma = 2 ,$$

$$c) \qquad s = 1 , \quad \sigma = 0 ,$$

$$d) \qquad s = 1 , \quad \sigma = 1 .$$

The divergencies are (at worst), respectively, of order 4, 2, 1 and logarithmic. They are analyzed in the next Section.

3. – Analysis of divergencies; conditions of the second type.

3·1. – In view of the character and of the results of the present analysis, the traditional nomenclature (« self-energy » and « vertex » parts) is inappropriate. It is convenient, for our purposes, to define instead the quantities:

$$L^{(\lambda)}\left(\begin{matrix}\hat{u}_1 \dots \mathring{u}_n \xi \\ \mathring{v}_1 \dots \mathring{v}_n \xi\end{matrix}\middle| \xi\, \hat{w}_1 \dots \mathring{w}_P\right) = \tag{11}$$

$$= \sum_{M(p+1)} \frac{\lambda^M}{M!} D_\xi^1 \dots D_\xi^M \gamma^1 \dots \gamma^M \begin{pmatrix} \mathring{u}_1 \dots \mathring{u}_n & \xi\xi_1 \dots \xi_M \\ \mathring{v}_1 \dots \mathring{v}_n & \xi\xi_1 \dots \xi_M \end{pmatrix} \cdot [\xi\xi_1 \dots \xi_M \mathring{w}_1 \dots \mathring{w}_P] ,$$

which have the same formal expansions and properties as the kernels, except that $\int$ is replaced with D_ξ; then, to define the corresponding « divergent cores »

---

[2] E. R. Caianiello: *Nuovo Cimento*, **11**, 492 (1954), Appendix III.

of rank n, p:

$$(12) \qquad C^{(\lambda)}_{n,p} = C\left(\begin{matrix}\mathring{u}_1 \dots \mathring{u}_n \\ \mathring{v}_1 \dots \mathring{v}_n\end{matrix}\middle|\, \mathring{w}_1 \dots \mathring{w}_P\right) = \int \mathrm{d}\xi \sum \gamma^\xi L\left(\begin{matrix}\mathring{u}_1 \dots \mathring{u}_n \xi \\ \mathring{v}_1 \dots \mathring{v}_n \xi\end{matrix}\middle|\, \xi\, \mathring{w}_1 \dots \mathring{w}_P\right).$$

(we shall drop henceforth the superscript λ).

(12) contains, summed to all orders, all and only the divergent terms arising in L from confluences in a single point ξ, when n ingoing, n outgoing fermion lines and p boson lines concur all in ξ because of the confluences, and the resulting expression is integrated over all space-time.

Actual computation of (11) and (12), when infinities are somehow regularized, is a far simpler task than the evaluation of the kernels $K_{N_0P_0}$. A complete analysis of renormalization requires also the consideration of other similar quantities

$$L^{(m_f)}\left(\begin{matrix}\mathring{u}_1 \dots \mathring{u}_n \xi \\ \mathring{v}_1 \dots \mathring{v}_n \xi\end{matrix}\middle|\, \mathring{w}_1 \dots \mathring{w}_P\right), \quad \text{etc.},$$

and of the corresponding « divergent cores ». We forego the obvious extension of (11) and (12) to such cases and refer for comments on this point to Sections **4** and **5**.

We consider next cases *a*), *b*), *c*), *d*) of Part I-3.

3·2. – *Case a*): $s = 0$, $\sigma = 0$.

We obtain here immediately:

$$(13) \qquad \left(\frac{\partial K_{N_0P_0}}{\partial \lambda}\right)^{(\xi)}_{0,0} = \sum_{M(1)} \frac{\lambda^M}{M!} \int \mathrm{d}\xi \sum \gamma^\xi \gamma^1 \dots \gamma^M \; D^1_\xi \dots D^M_\xi \begin{pmatrix} \xi\, \xi_1 \dots \xi_M \\ \xi\, \xi_1 \dots \xi_M \end{pmatrix} [\xi\, \xi_1 \dots \xi_M] =$$

$$= C_{0,0} \cdot K_{N_0P_0},$$

with $C_{0,0}$ given by (12), and $K^{(\xi)}_{N_0P_0} = K_{N_0P_0}$, $\int\limits_\xi \mathrm{d}\xi_h \equiv \int \mathrm{d}\xi_h$, because ξ is not contained in $K_{N_0P_0}$.

3·3. – *Case b*): $s = 0$, $\sigma = 2$.

We find:

$$(14) \qquad \left(\frac{\partial K_{N_0P_0}}{\partial \lambda}\right)^{(\xi)}_{0,2} = \sum_{M(1)} \frac{\lambda^M}{M!} \int \mathrm{d}\xi \sum \gamma^\xi \gamma^1 \dots \gamma^M \; D^1_\xi \dots D^M_\xi \cdot$$

$$\cdot \begin{pmatrix} \xi\, \xi_1 \dots \xi_M \\ \xi\, \xi_1 \dots \xi_M \end{pmatrix} \sum_{c_Q} [\xi_{i'_1} \dots \xi_{i'_{2Q}}] K^{(\xi)}\left(\begin{matrix} x_1 \dots x_{N_0} \\ y_1 \dots y_{N_0} \end{matrix}\middle|\, \mathring{\xi}_{i''_1} \mathring{\xi}_{i''_2}\, t_1 \dots t_{P_0}\right).$$

$K^{(\xi)}$ at r.h.s. of (14) (and similarly for the other cases) can be analyzed by means of the perturbative expansions or of the branching equations, with identical results. The former method is simpler. Denote, to avoid confusion, with primes all integration and summation variables which appear when $K^{(\xi)}$ is expanded in power series:

$$(15)\qquad K^{(\xi)}\begin{pmatrix} x_1 \dots x_{N_0} \\ y_1 \dots y_{N_0} \end{pmatrix} \overset{\circ}{\xi}_{l_1''} \overset{\circ}{\xi}_{l_2''}\ t_1 \dots t_{P_0}\Big) = \sum_{N(P_0)} \frac{\lambda^N}{N!} \int_{\xi} \mathrm{d}\xi_1' \dots \int_{\xi} \mathrm{d}\xi_N' \cdot$$

$$\cdot \sum \gamma^{1'} \dots \gamma^{N'} \cdot \begin{pmatrix} x_1 \dots x_{N_0}\ \xi_1' \dots \xi_N' \\ y_1 \dots \xi_{N_0}\ \xi_1' \dots \xi_N' \end{pmatrix} [\overset{\circ}{\xi}_{l_1''} \overset{\circ}{\xi}_{l_2''}\ t_1 \dots t_{P_0}\ \xi_1' \dots \xi_N'] .$$

Substitution of (15) into (14) and use of Lemma (I-26) and of (11) yield:

$$(16)\qquad \left(\frac{\partial K_{N_0P_0}}{\partial \lambda}\right)_{0,2}^{(\xi)} = \sum_{N(P_0)} \frac{\lambda^N}{N!} \int \mathrm{d}\xi \sum \gamma^{\xi} \int_{\xi} \mathrm{d}\xi_1' \dots \int_{\xi} \mathrm{d}\xi_N'\, \gamma^{1'} \dots \gamma^{N'} \cdot$$

$$\cdot \sum_{\sigma_\tau} L \begin{pmatrix} \xi \\ \xi \end{pmatrix} \xi\ \mathring{u}_{m_1''} \mathring{u}_{m_2''} \Big) \begin{pmatrix} x_1 \dots x_{N_0}\ \xi_1' \dots \xi_N' \\ y_1 \dots y_{N_0}\ \xi_1' \dots \xi_N' \end{pmatrix} [u_{m_1'} \dots u_{m_{2\tau}'}] ,$$

where $2\tau + 2 = P_0 + N$; u_m'', u_m' are $t_1 \dots t_{P_0}\, \xi_1' \dots \xi_N'$, with the definitions and the conditions which go with (I-26). After (I-28) and (12), (16) becomes:

$$(17)\qquad \left(\frac{\partial K_{N_0P_0}}{\partial \lambda}\right)_{0,2}^{(\xi)} = \sum_{N(P_0)} \frac{\lambda^N}{N!} \int \mathrm{d}\xi_1' \dots \int \mathrm{d}\xi_N'\ \gamma^{1'} \dots \gamma^{N'} \cdot$$

$$\cdot \sum_{\sigma_\tau} C\,(\mathring{u}_{m_1''} \mathring{u}_{m_2''}) \begin{pmatrix} x_1 \dots x_{N_0}\ \ \xi_1' \dots \xi_N' \\ y_1 \dots y_{N_0}\ \ \xi_1' \dots \xi_N' \end{pmatrix} [u_{m_1'} \dots u_{m_{2\tau}'}] .$$

(17) yields the first of the conditions of the second type which are wanted to secure that regularization is actually a renormalization. Such conditions will be listed in this Section as they are met, and discussed together in the Section **4**. This conditions is (as the reader will find evident from the sequel), *to within a change of gauge* (see Introduction: gauge properties will be studied in a future work):

$$(18)\qquad C(\mathring{x}\mathring{y}) = C_{0,2}^{(1)} \cdot [xy] + C_{0,2}^{(2)} \cdot \frac{\partial}{\partial m_b^2} [xy] .$$

$C_{0,2}^{(1)}$ and $C_{0,2}^{(2)}$ are (divergent, or ambiguous) functions of λ_1 m_f, m_b. Then Lemmas (I-27) and (I-28) and (I-11) yield, finally:

$$(19)\qquad \left(\frac{\partial K_{N_0P_0}}{\partial \lambda}\right)_{0,2}^{(\xi)} = \frac{1}{2} P_0 C_{0,2}^{(1)} \cdot K_{N_0P_0} + \frac{1}{2} \lambda C_{0,2}^{(1)} \frac{\partial K_{N_0P_0}}{\partial \lambda} + C_{0,2}^{(2)} \frac{\partial}{\partial (m_b^2)} K_{N_0P_0} .$$

3·4. – *Case c*): $s=1,\ \sigma=0$.
We have:

$$(20)\qquad \left(\frac{\partial K_{N_0P_0}}{\partial\lambda}\right)^{(\xi)}_{1,0}=\sum_{M(1)}\frac{\lambda^M}{M!}\int d\xi\sum\gamma^{\xi}\gamma^1\dots\gamma^M\ D^1_{\xi}\dots D^M_{\xi}\cdot$$
$$\cdot[\xi\xi_1\dots\xi_M]\sum_{\sigma_r}(-1)^{p(h,k)}\begin{pmatrix}\xi_{h'_1}\dots\xi_{h'_r}\\ \xi_{k'_1}\dots\xi_{k'_r}\end{pmatrix}\cdot K^{(\xi)}\left(\begin{matrix}\overset{\circ}{\xi}_{h''_1}x_1\dots x_{N_0}\\ \overset{\circ}{\xi}_{k''_1}y_1\dots y_{N_0}\end{matrix}\middle|\, t_1\dots t_{P_0}\right).$$

The discussion is entirely similar to that of case *b*); lemmas (I-29, 30, 31) are now used. One finds that, provided (neglecting questions of gauge: see *b*)):

$$(21)\qquad C\begin{pmatrix}\overset{\circ}{x}\\ \overset{\circ}{y}\end{pmatrix}=C^{(1)}_{1,0}\cdot(xy)+C^{(2)}_{1,0}\frac{\partial(xy)}{\partial m_f}\,;$$

(20) reduces to:

$$(22)\qquad \left(\frac{\partial K_{N_0P_0}}{\partial\lambda}\right)^{(\xi)}_{1,0}=N_0C^{(1)}_{1,0}\cdot K_{N_0P_0}+\lambda C^{(1)}_{1,0}\frac{\partial K_{N_0P_0}}{\partial\lambda}+C^{(2)}_{1,0}\frac{\partial K_{N_0P_0}}{\partial m_f}\,.$$

3·5. – *Case d*): $s=1,\ \sigma=1$.
We have:

$$(23)\qquad \left(\frac{\partial K_{N_0P_0}}{\partial\lambda}\right)^{(\xi)}_{1,1}=\sum_{M(0)>0}\frac{\lambda^N}{M!}\int d\xi\sum\gamma^{\xi}\gamma^1\dots\gamma^M\ D^1_{\xi}\dots D^M_{\xi}\cdot$$
$$\cdot\sum_{\sigma_r}(-1)^{p(h,k)}\begin{pmatrix}\xi_{h'_1}\dots\xi_{h'_r}\\ \xi_{k'_1}\dots\xi_{k'_s}\end{pmatrix}\sum_{\sigma_Q}[\xi l'_1\dots\xi l'_{2Q}]K^{(\xi)}\left(\begin{matrix}\overset{\circ}{\xi}_{h''_1}x_1\dots x_{N_0}\\ \overset{\circ}{\xi}_{k''_0}y_1\dots y_{N_0}\end{matrix}\middle|\begin{matrix}\overset{\circ}{\xi}_{l''_1}t_1\dots t_{P_0}\\ l''\end{matrix}\right).$$

Arguments similar to those already given show that, if:

$$(24)\qquad C\left(\begin{matrix}\overset{\circ}{x}\\ \overset{\circ}{y}\end{matrix}\middle|\,\overset{\circ}{t}\right)=C_{1,1}\int d\xi\sum(x\xi)\gamma^{\xi}(\xi y)[\xi t]\,,$$

then:

$$(25)\qquad \left(\frac{\partial K_{N_0P_0}}{\partial\lambda}\right)^{(\xi)}_{1,1}=C_{1,1}\cdot\frac{\partial K_{N_0P_0}}{\partial\lambda}\,.$$

4. – Renormalization.

4·1. – The results obtained in the preceding Section permit to study the conditions under which use of our $\int$ integrals is equivalent to a consistent infinite renormalization of the standard type. This can be done by means of

the differential equations of the transformation connecting the old to the new parameters, which derive from a comparison between (2) and (26) below (and between the similar equations which originate from the derivatives of the kernels with respect to the other parameters of the theory—of which we shall not need, though, the explicit expressions for our present purposes). Different prescriptions lead to renormalizations which differ by finite amounts; they yield differential equations of the same structure, but with different coefficients: in this sense, more generally, such equations are the Lie equations of the renormalization group. If one studies the transition between different prescriptions $\int$, $\int'$, ..., the Lie equations have finite coefficients; in the transition from $\int$ to $\int$, which is considered here, the coefficients are infinite or indeterminate, and all proofs must be understood as involving suitable auxiliary regularizing devices, as was already stated in I.

Our purpose is not the complete study of any specific theory, but rather a thorough analysis of the means which will permit, in any given instance, such a study; hence the criterion, mentioned in the Introduction, of considering only the significant parts of electrodynamics, without however exhibiting their structure explicitly.

Once one is assured that the Lie equations of the renormalization group (that is, for any given prescription, the differential equations of the renormalizing transformation) are integrable, and that the appropriate reality conditions for the parameters are satisfied, the proof is complete: concrete calculations can be made directly with $\int$ integrals, disregarding all the divergent parts thus suppressed. This part of the investigation offers no special difficulties and gives the conditions which are necessary and sufficient for a theory to be renormalizable. This was beyond the reach of the customary methods: the classical distinction between renormalizable and non-renormalizable theories cannot be accepted any more *a priori* as valid, so that a separate study appears to be necessary for each theory. As an example, the neutral scalar meson theory is shown to be non-renormalizable.

4·2. – We have found that conditions (18), (21) and (24) are *necessary* for our prescription to be a renormalization. The actual calculation of the r.h.s. of those formulae, which we do not report here, shows that (18), (21) *and* (24) *are verified in electrodynamics, to within a gauge transformation.*

A complete study of this question is in progress and will be published soon; it appears already that the ambiguities caused usually by non-gauge invariant terms are eliminated by this formalism.

Another result, the proof of which we postpone to that occasion, is that in electrodynamics, $C_{1,1} = 0$. It is interesting to discuss it here, because it shows some of the implications of the condition (I-46) in electrodynamics.

The thing is at first surprising, because one would traditionally expect non-

vanishing divergent contributions due to vertex parts: the reason is that (I-46) is *not* valid, in general, for non symmetric integrands. It is typical of a vertex part that the first integration is convergent, the second (is logarithmically) divergent:

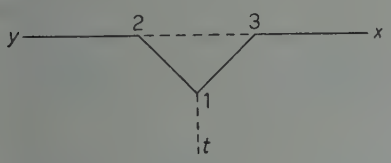

Fig. 1.

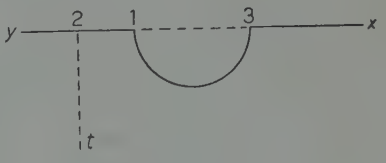

Fig. 2.

e.g., by applying $D_1^2 \int_1 \mathrm{d}3$ to the integrand (see Fig. 1)

$$(x3)\gamma^3(31)\gamma'(12)\gamma^2(2y)[23][1t]\,,$$

one finds first $\int_1 \mathrm{d}3 = \int \mathrm{d}3$, and then the usual divergent contribution, denoted by D_1^2; by applying, instead, $\int \mathrm{d}2\, D_1^3$ one finds zero: (I-46) is not valid, nor should it be in this case. If, however, one considers *all* contributions of that order, the integrand is symmetric and (I-46) is valid; but then, there are also contributions such as

$$(x3)\gamma^3(31)\gamma^1(12)\gamma^2(2y)[31][2t]\,,$$

which are typical electron self-energy terms (Fig. 2).

The validity of (I-46) for our prescriptions, which leads to $C_{1,1} = 0$, implies that with our method *divergent vertex parts need not be introduced at all in electrodynamics*: the cancellation of them against electron self-energy contributions, which is proved to occur, with the standard procedures, *after* their computation, is automatically secured by our requirements *prior* to computation; nor, in our whole treatment, there is any need of considering them.

By splitting our symmetric integrands into graphs, and by applying our arguments in reversed order, one would find, conversely, a rigorous proof of the statement just mentioned that, to all orders, the divergent vertex-part contributions cancel against corresponding electron self-energy parts. In the electron self-energy contributions, as calculated from (21), this cancellation is already taken into account.

This is just one more instance that illustrates the inconvenience of using Feynman graphs (except of course, with due care, as computational tools) in the interpretation of physical processes: the whole is simpler than one of its parts.

3101

We shall continue our discussion under the assumption that (18), (21), (24) are verified, and that we ignore the functional dependence of the coefficients C on the parameters λ, m_f, m_b. We have in mind, doing so, more general cases than electrodynamics; in order not to complicate the language, we speak in the sequel only of m_f and m_b, with the understanding, though, that similar things should hold for what parameters a theory may have, in any number; the extension to other cases will not be difficult, after the pattern set in this work. The conditions (18), (21), (24), and the analogous ones which derive likewise from a study of the derivatives of the kernels with respect to m_f, m_b^2, require careful calculations for their verification. The remaining conditions « of the second type », which are necessary for the integrability of the Lie equations and for the reality of the physical parameters after the renormalization, must be considered specifically for each theory; they require, however, very little computational effort. The discussion of this Section is intended to provide a pattern for analyses of this sort.

4·3. – We proceed now with the study of eq. (5), making use of relations (18), (21) and (24).

Substitution of (13), (19), (22) and (25) in (5) gives:

$$\frac{\partial K_{N_0P_0}}{\partial\lambda} = \left[C_{0,0} + \frac{1}{2}P_0 C^{(1)}_{0,2} + N_0 C^{(1)}_{1,0}\right]\cdot K_{N_0P_0} + \tag{26}$$

$$+ C^{(2)}_{0,2}\frac{\partial}{\partial(m_b^2)}K_{N_0P_0} + C^{(2)}_{1,0}\frac{\partial}{\partial m_f}K_{N_0P_0} + \left[\frac{1}{2}\lambda C^{(1)}_{0,2} + \lambda C^{(1)}_{1,0} + C_{1,1}\right]\frac{\partial}{\partial\lambda}K_{N_0P_0} +$$

$$+ \int \mathrm{d}\xi \sum \gamma^{\xi} K\begin{pmatrix} x_1 \dots x_{N_0}\xi \\ y_1 \dots y_{N_0}\xi \end{pmatrix} \xi t_1 \dots t_{P_0}\Big).$$

The last term of (26) is the same as the first term of (5) because of (I-48) (see discussion in I). This equation is to be compared with (I-23):

$$\frac{\partial K_{N_0P_0}}{\partial\lambda} = \int \mathrm{d}\xi \sum \gamma^{\xi} K\begin{pmatrix} x_1 \dots x_{N_0}\xi \\ y_1 \dots y_{N_0}\xi \end{pmatrix} \xi t_1 \dots t_{P_0}\Big); \tag{27}$$

the discussion made in I is valid also in this case.

Write, for short:

$$C = 1 - \tfrac{1}{2}\lambda C^{(1)}_{0,2} - \lambda C^{(1)}_{1,0} - C_{1,1}\,, \tag{28}$$

and

$$\mathscr{D} = C\frac{\partial}{\partial\lambda} - C^{(2)}_{0,2}\frac{\partial}{\partial(m_b^2)} - C^{(2)}_{1,0}\frac{\partial}{\partial m_f}\,;$$

(26) becomes:

$$\mathscr{D}K_{N_0P_0} = \left[C_{0,0} + \frac{1}{2} P_0 C^{(1)}_{0,2} + N_0 C^{(1)}_{1,0}\right] K_{N_0P_0} + \tag{30}$$
$$+ \int \mathrm{d}\xi \sum \gamma^{\xi} K \left(\begin{matrix} x_1 \dots x_{N_0}\xi \\ y_1 \dots y_{N_0}\xi \end{matrix} \middle| \, \xi t_1 \dots t_{P^0} \right).$$

We can transform the kernels $K_{N_0P_0}$ as follows:

$$K_{N_0P_0}(\lambda, m_f, m_b) = A_{N_0P_0}(\lambda, m_f, m_b) \cdot \tilde{K}_{N_0P_0}(\lambda, m_f, m_b), \tag{31}$$

where $A_{N_0P_0}$ is a coefficient, to be determined, which may depend upon the parameters λ, m_f, m_b. With (31), (30) becomes:

$$[\mathscr{D}(\log A_{N_0P_0})] \cdot K_{N_0P_0} + A_{N_0P_0} \mathscr{D}\tilde{K}_{N_0P_0} = \tag{32}$$
$$= \left[C_{0,0} + \frac{1}{2} P_0 C^{(1)}_{0,2} + N_0 C^{(1)}_{1,0}\right] \cdot K_{N_0P_0} +$$
$$+ A_{N_0+1, P_0+1} \int \mathrm{d}\xi \sum \gamma^{\xi} \tilde{K} \left(\begin{matrix} x_1 \dots x_{N_0}\xi \\ y_1 \dots y_{N_0}\xi \end{matrix} \middle| \, \xi t_1 \dots t_{P_0} \right).$$

The requirement:

$$\mathscr{D}(\log A_{N_0P_0}) = C_{0,0} + \tfrac{1}{2} P_0 C^{(1)}_{0,2} + N_0 C^{(1)}_{1,0} \tag{33}$$

gives, using the standard notation:

$$A_{N_0P_0} = A Z_2^{N_0} Z_3^{P_0/2}, \tag{34}$$

where

$$\mathscr{D}(\log A) = C_{0,0}, \tag{35}$$

$$\mathscr{D}(\log Z_2) = C^{(1)}_{1,0}, \tag{36}$$

$$\mathscr{D}(\log Z_3) = C^{(1)}_{0,2}, \tag{37}$$

and changes (32) into:

$$Z_2^{-1} Z_3^{-\frac{1}{2}} \mathscr{D}\tilde{K}_{N_0P_0} = \int \mathrm{d}\xi \sum \gamma^{\xi} \tilde{K} \left(\begin{matrix} x_1 \dots x_{N_0}\xi \\ y_1 \dots y_{N_0}\xi \end{matrix} \middle| \, \xi t_1 \dots t_{P_0} \right). \tag{38}$$

We notice that, due to the form of (35), (36), (37), passage from a solution of them to another maintains the typical expression of (34).

4·4. – We have thus far only considered eq. (27) (I-(23)); entirely similar considerations should be made, as we have said before, starting from eq.'s (I-24) and (I-25):

$$\frac{\partial K_{N_0P_0}}{\partial m_f} = -i\int \mathrm{d}\xi K\begin{pmatrix}\xi x_1 \dots x_{N_0}\\ \xi y_1 \dots y_{N_0}\end{pmatrix}\begin{matrix} \\ t_1 \dots t_{P_0}\end{matrix}, \tag{39}$$

$$\frac{\partial K_{N_0P_0}}{\partial (m_b^2)} = -\frac{i}{2}\int \mathrm{d}\xi K\begin{pmatrix}x_1 \dots x_{N_0}\\ y_1 \dots y_{N_0}\end{pmatrix}\begin{matrix} \\ \xi\xi t_1 \dots t_{P^0}\end{matrix}; \tag{40}$$

indeed, in (I-23, 24, 25) all the parameters of the theory are treated on the same footing. Working on the r.h.s. of (39) and (40) one would easily obtain other conditions of the type of (18), (21), (24) and results similar to (32) and its consequences: this we shall not do here, because the thing, although straightforward, would not be useful for our present purposes. It suffices to know that equations of the same nature as (35)-(36)-(37) and (44), (45), (46) below, with $\mathscr{D}$ replaced by other operators $\mathscr{D}'$ and $\mathscr{D}''$ and minor obvious changes, can be obtained with our methods when one works on eq.'s (39), (40) as was done to pass from eq. (27) to eq. (26), etc.

A change of parameters:

$$\begin{cases} \lambda = \lambda(\bar{\lambda}, \overline{m}_f, \overline{m}_b^2), \\ m_f = m_f(\bar{\lambda}, \overline{m}_f, \overline{m}_b^2), \\ m_b^2 = m_b^2(\bar{\lambda}, \overline{m}_f, \overline{m}_b^2), \end{cases} \tag{41}$$

gives

$$\tilde{\overline{K}}(\lambda, m_f, m_b^2) = \overline{K}(\bar{\lambda}, \overline{m}_f, \overline{m}_b^2), \tag{42}$$

and (38) becomes:

$$Z_2^{-1}Z_3^{-\frac{1}{2}}\left[\mathscr{D}(\bar{\lambda})\frac{\partial}{\partial\bar{\lambda}} + \mathscr{D}(\overline{m}_f)\frac{\partial}{\partial\overline{m}_f} + \mathscr{D}(\overline{m}_b^2)\frac{\partial}{\partial(\overline{m}_b^2)}\right]\overline{K}_{N_0P_0} = \tag{43}$$

$$= \int \mathrm{d}\xi \sum \gamma^\xi \overline{K}\begin{pmatrix}x_1 \dots x_{N_0}\xi\\ y_1 \dots y_{N_0}\xi\end{pmatrix}\begin{matrix} \\ \xi t_1 \dots t_{P_0}\end{matrix};$$

that is, it is necessary for the renormalizability of the theory that a transformation (41) exists such that its inverse satisfies the equations:

$$\mathscr{D}(\bar{\lambda}) = Z_2 Z_3^{\frac{1}{2}}, \tag{44}$$

$$\mathscr{D}(\overline{m}_f) = 0, \tag{45}$$

$$\mathscr{D}(\overline{m}_b^2) = 0, \tag{46}$$

and the other equations with $\mathscr{D}'$ and $\mathscr{D}''$, here unwritten, which would derive similarly from (39) and (40). (27) becomes thus

$$\frac{\partial \bar{K}_{N_0 P_0}}{\partial \bar{\lambda}} = \int \mathrm{d}\xi \sum \gamma^{\xi} \bar{K} \begin{pmatrix} x_1 \dots x_{N_0} \xi \\ y_1 \dots y_{N_0} \xi \end{pmatrix} \xi t_1 \dots t_{P_0} \Big), \tag{2}$$

and (39), (40) are transformed likewise.

All such equations are, in general, the Lie equations of the renormalization group: the values of the coefficients C which appear in $\mathscr{D}$, $\mathscr{D}'$, $\mathscr{D}''$ vary with the choice of the prescription $\int$. Since we consider here only one special prescription, we shall not be interested in this work in their group-theoretical properties; these may be, though, quite relevant in other connections. Our only concern is with their compatibility; we shall see below that this can be ascertained without actual knowledge of the coefficients C: a pleasing feature, of which we have availed ourselves here to avoid the explicit calculation of $\mathscr{D}'$ and $\mathscr{D}''$.

4·5. – The compatibility of the equations (44) etc., secures the existence of a renormalizing transformation; it appears therefore as an additional requirement for the renormalizability of a theory with a given prescription—or, as we prefer to say, for its self-consistency. The present method permits to give a simple answer to this question, which can be proposed in two different ways:

1) starting from the differential equations: this requires the explicit knowledge of $\mathscr{D}$, $\mathscr{D}'$, $\mathscr{D}''$ and is not of much use if their coefficients are infinite or ambiguous. Such a study would give, though, interesting information on the nature and properties of a theory, if done for finite renormalizations [3];

2) observing that compatibility can only depend upon the definition of the modified integrals $\int$ and upon the structure of the theory: it must be possible, therefore, to prove or disprove it merely with recourse to the properties of the $\int$ integrals, in terms only of finite quantities.

The second approach is the simpler, and is followed here. We begin with the remark that compatibility requires that any iterations among eq. (38) and the other two unwritten similar equations deducible from (39) and (40) should never give rise to new independent equations. The Z factors which appear in (38) etc., are irrelevant in this respect; it is therefore sufficient for

---

[3] N. W. Bogoljubov and D. V. Sirkov: *Nuovo Cimento*, **3**, 845 (1956).

compatibility that

$$\int \mathrm{d}\xi_1 \int \mathrm{d}\xi_2 \sum \gamma^{\xi_1} \overline{K} \left(\begin{matrix} x_1 \dots x_{N_0} \xi_1 \\ y_1 \dots y_{N_0} \xi_1 \end{matrix} \middle| \, \overset{\circ}{\xi}_1 \overset{\circ}{\xi}_2 \overset{\circ}{\xi}_2 t_1 \dots t_{P_0} \right) = \tag{47}$$

$$= \int \mathrm{d}\xi_2 \int \mathrm{d}\xi_1 \sum \gamma^{\xi_1} \overline{K} \left(\begin{matrix} x_1 \dots x_{N_0} \xi_1 \\ y_1 \dots y_{N_0} \xi_1 \end{matrix} \middle| \, \xi_1 \overset{\circ}{\xi}_2 \overset{\circ}{\xi}_2 t_1 \dots t_{P_0} \right),$$

$$\int \mathrm{d}\xi_1 \int \mathrm{d}\xi_2 \sum \gamma^{\xi_1} \overline{K} \left(\begin{matrix} x_1 \dots x_{N_0} \xi_1 \xi_2 \\ y_1 \dots y_{N_0} \xi_1 \xi_2 \end{matrix} \middle| \, \xi_1 t_1 \dots t_{P_0} \right) = \tag{48}$$

$$= \int \mathrm{d}\xi_2 \int \mathrm{d}\xi_1 \sum \gamma^{\xi_1} \overline{K} \left(\begin{matrix} x_1 \dots x_{N_0} \xi_1 \xi_2 \\ y_1 \dots y_{N_0} \xi_1 \xi_2 \end{matrix} \middle| \, \xi_1 t_1 \dots t_{P_0} \right),$$

$$\int \mathrm{d}\xi_1 \int \mathrm{d}\xi_2 \sum \overline{K} \left(\begin{matrix} x_1 \dots x_{N_0} \xi_1 \\ y_1 \dots y_{N_0} \xi_1 \end{matrix} \middle| \, \overset{\circ}{\xi}_2 \overset{\circ}{\xi}_2 t_1 \dots t_{P_0} \right) = \tag{49}$$

$$= \int \mathrm{d}\xi_2 \int \mathrm{d}\xi_1 \sum \overline{K} \left(\begin{matrix} x_1 \dots x_{N_0} \xi_1 \\ y_1 \dots y_{N_0} \xi_1 \end{matrix} \middle| \, \overset{\circ}{\xi}_2 \overset{\circ}{\xi}_2 t_1 \dots t_{P_0} \right).$$

These conditions, which could be somewhat relaxed from a purely mathematical point of view, appear to be also *necessary*, from a physical standpoint, if one accepts the current view that a renormalization is one operation out of a group, in which small changes of the parameters are permissible: all they imply is that

$$\begin{cases} \dfrac{\partial^2}{\partial \bar{\lambda} \partial (\overline{m}_b^2)} \overline{K}_{N_0 P_0} = \dfrac{\partial^2}{\partial (\overline{m}_b^2) \partial \bar{\lambda}} \overline{K}_{N_0 P_0}; \\ \dfrac{\partial^2}{\partial \bar{\lambda} \partial \overline{m}_f} K_{N_0 P_0} = \dfrac{\partial^2}{\partial \overline{m}_f \partial \bar{\lambda}} \overline{K}_{N_0 P_0}; \\ \dfrac{\partial^2}{\partial \overline{m}_f \partial (\overline{m}_b^2)} \overline{K}_{N_0 P_0} = \dfrac{\partial^2}{\partial (\overline{m}_b^2) \partial \overline{m}_f} \overline{K}_{N_0 P_0}, \end{cases} \tag{50}$$

when one imposes that (39), (40) become

$$\frac{\partial \overline{K}_{N_0 P_0}}{\partial \overline{m}_f} = -i \int \mathrm{d}\xi \overline{K} \left(\begin{matrix} \xi x_1 \dots x_{N_0} \\ \xi y_1 \dots y_{N_0} \end{matrix} \middle| \, t_1 \dots t_{P_0} \right), \tag{51}$$

$$\frac{\partial \overline{K}_{N_0 P_0}}{\partial (\overline{m}_b^2)} = -\frac{i}{2} \int \mathrm{d}\xi K \left(\begin{matrix} x_1 \dots x_{N_0} \\ y_1 \dots y_{N_0} \end{matrix} \middle| \, \overset{\circ}{\xi} \overset{\circ}{\xi} t_1 \dots t_{P_0} \right), \tag{52}$$

in agreement with the requirements postulated in I, that substitution of $\int$ with $\overline{\int}$ should change *ipso facto* all unrenormalized expressions into the corresponding renormalized ones.

We have already emphasized that orders of $\overline{\int}$ integration cannot be exchanged if the integrand is not symmetric: conditions (I-46) or (I-55) are very severe in this respect, as was seen in Section 2. We must therefore verify directly whether the compatibility conditions (50), that is (47), (48), (49), are satisfied or not by a given theory, in order to judge its renormalizability.

$\overline{\int} d\xi_1 \overline{\int} d\xi_2$ involves an actual double limiting process, and therefore a possible lack of invertibility, only at confluence of ξ_2 with ξ_1; the inversion is legitimate in all other points, as well as in these parts of the integrands in which this confluence does not alter ordinary integrability. Keeping this in mind, and considering the actual singularities of the free propagators in electro- and mesodynamics, it is not difficult to see that dangerous confluences can occur only in eq. (48), and that they are all contained in the first part of the expansion of the integrand, with the aid of theorem (I-19), by its arguments ξ_1, ξ_2:

$$(53) \qquad \sum \gamma^{\xi_1} \overline{K} \left(\begin{matrix} x_1 \dots x_{N_0} \xi_1 \xi_2 \\ y_1 \dots y_{N_0} \xi_1 \xi_2 \end{matrix} \middle| \, \xi_1 \, t_1 \dots t_{P_0} \right) = \sum \gamma^{\xi_1} \left(\begin{matrix} \overline{\xi_1 \xi_2} \\ \xi_1 \xi_2 \end{matrix} \right) \cdot \overline{K} \left(\begin{matrix} x_1 \dots x_{N_0} \\ y_1 \dots y^{N_0} \end{matrix} \middle| \, \xi_1 t_1 \dots t_{P_0} \right) + \dots .$$

Everything else is either integrable or without confluences.

Non-compatibility can arise, thus, only because of a term

$$(54) \qquad - \operatorname{Tr} \{ (\overline{\xi_2 \xi_1}) \gamma^\mu (\overline{\xi_1 \xi_2}) \} \, \overline{K}_{\mu \dots} \left(\begin{matrix} x_1 \dots x_{N_0} \\ y_1 \dots y_{N_0} \end{matrix} \middle| \, \xi_1 t_1 \dots t_{P_0} \right) .$$

In electrodynamics this vanishes, since, clearly:

$$(55) \qquad \tfrac{1}{4} \operatorname{Tr} \{ [(\gamma \partial_2 - \overline{m}_f) \Delta^f (\xi_2 - \xi_1)] \gamma^\mu [(- \gamma \partial_2 - \overline{m}_f) \Delta^f (\xi_2 - \xi_1)] \} = 0 .$$

To consider scalar and pseudoscalar neutral mesodynamics, we have simply to replace in (55) γ^μ with 1 or γ^5; the term thus obtained vanishes only in the latter instance.

We can conclude that *neutral pseudoscalar mesodynamics may be a consistent* (renormalizable) *theory, but no so neutral scalar mesodynamics.* For the latter, application of the integration criteria given in I gives indeed different results

when the first piece at r.h.s. of (53) is substituted at l.h.s. and r.h.s. of (48), as is easily verified. Neutral scalar mesodynamics, that is, although it has only a finite number of typical ultraviolet divergencies, fails to yield compatible equations for the renormalization group; it can therefore be discarded from the admissible theories on the ground of this finding, if ordinary beliefs are accepted.

The reasons are sufficiently general to lead us to expect that this result is true with all prescriptions. The well-known fact that both mesonic theories require, for their completeness, additional coupling constants cannot affect this finding.

We find, therefore, that the imposition of strict consistency requirements may lead to discard theories accepted before as renormalizable; the opposite may also be true.

4·6. – The compatibility of the Lie equations of the renormalization group may be also viewed in a different light. Suppose that these equations turn out, in some theory, to be *non-compatible*: then it may still happen, as is well known, that they admit nevertheless of *singular integrals*; integrals, that is, which exist only for specific values of the parameters; these would be in this case, in part or wholly, « quantized » to discrete values. We have just proved that such a thing does not happen in electrodynamics; whether this may be a clue, in a more complete theory, toward an explanation of the observed discrete values of some parameters, is beyond our present reach to decide. We just remark that a study of this question can only be made starting from the differential Lie equations, since then the identification of (47), (48), (49) and (50) is not legitimate and the equalities are not meaningful any more.

4·7. – After what we have proved, the actual solution of the differential equations is not necessary for our purposes. It is instructive, though, to exhibit the form that this solution takes, in a theory (which may be only an unrealistic mathematical model) in which the independent equations reduce to (44), (45), (46) and (35), (36), (37). The solutions of (44) and of (45), (46) are then obtained, respectively, from those of the systems:

$$\frac{\mathrm{d}\lambda}{C} = -\frac{\mathrm{d}m_f}{C^{(1)}_{1,0}} = -\frac{\mathrm{d}(m_b^2)}{C^{(1)}_{0,2}} = \frac{\mathrm{d}\bar{\lambda}}{Z_2 Z_3^{\frac{1}{2}}}, \tag{56}$$

and

$$\frac{\mathrm{d}\lambda}{C} = -\frac{\mathrm{d}m_f}{C^{(1)}_{1,0}} = -\frac{\mathrm{d}(m_b^2)}{C^{(1)}_{0,2}}, \tag{57}$$

which are clearly compatible, and give:

$$
(58)\qquad
\begin{cases}
\overline{\lambda} = \int_0^{\lambda} \dfrac{Z_2 Z_3^{\frac{1}{2}}}{C}\, \mathrm{d}\lambda\,, \\
m_f = \overline{m}_f - \int_0^{\lambda} \dfrac{C^{(2)}_{1,0}}{C}\, \mathrm{d}\lambda\,, \\
m_b^2 = \overline{m}_b^2 - \int_0^{\lambda} \dfrac{C^{(2)}_{0,2}}{C}\, \mathrm{d}\lambda\,.
\end{cases}
$$

Unless all functions depend only upon λ, (58) is still a system of equations, the form of which, however, is typical enough to identify the transformation (4), as a renormalization without the need of further considerations. It is completed by the other equations, deduced likewise from (35), (36), (37):

$$
(59)\qquad
\begin{cases}
Z_2 = \exp\left[\int_0^{\lambda} \dfrac{C^{(1)}_{1,0}}{C}\, \mathrm{d}\lambda\right], \\
Z_3 = \exp\left[\int_0^{\lambda} \dfrac{C^{(1)}_{0,2}}{C}\, \mathrm{d}\lambda\right], \\
A = \exp\left[\int_0^{\lambda} \dfrac{C_{0,0}}{C}\, \mathrm{d}\lambda\right].
\end{cases}
$$

The addition of homogeneous solutions would not change the typical form of (58), (59): we see thus that the transformation engendered by the change $\int \to \int\!\!\!\!\!\!\int$ satisfies the differential equations, and exhibits in any case the expected behavior.

5. – Concluding remarks.

5·1. – We have proved that, under the stated conditions, replacement of $\int$ and $\int\!\!\!\!\!\!\int$ changes *ipso facto* the formal unrenormalized perturbative expansions into the corresponding renormalized expansions; the requirement that the indeterminate parameters λ, $\overline{m}_f$, $\overline{m}_b^2$ be adequate to account consistently for any number of data calculated from the theory coincides with the usual requirement of renormalizability. The difficulties of a direct proof were bypassed by demonstrating, equivalently, that the equations (27), the gene-

rators of all unrenormalized expansions, are changed by our procedure into the equations (2), the generators of all renormalized expansions; it was also indicated how similar considerations show that equations (39) and (40) change then into equations (51) and (52), in agreement with the program enunciated in I, that renormalization should amount to changing $\int$ into $\int$ *throughout* in a theory. The deduction of the Lie equations of the renormalization group is a by-product of this analysis.

We have still to prove that the same replacement changes the equations (I-20, 21, 22), or any consequence of them and of the other branching equations obtained by means of arbitrary iterations, into the corresponding renormalized equations. A direct proof would be too complicated, since each integral would require a lengthy treatment (cf. the deduction of eq. (26)); an example of this procedure was given in I-4·3 *b*). It is easy, however, to convince ourself of the truth of this statement without any need of further calculations.

The interplay between branching equations and perturbative expansions has had a significant rôle in our present and past work. Thus, the former were derived initially from the latter (4), and then shown to be valid regardless of the convergence of these (5); to do so was not necessary, but certainly convenient from our point of view. It is evident that the very same arguments suffice also to prove that the branching equations, written with $\int$'s, are identically satisfied by the perturbative expansions similarly written; the only caution which is now required is that of keeping all integrands symmetrized in their integration variables, whenever that is necessary.

If the renormalized expansions are convergent, no more need be said; if not, this still suffices to prove our statement, since we know that the introduction of appropriate cut-offs renders those expansions convergent (6), and our handling of infinite quantities requires in any case the use of such regularizing devices prior to their removal (cfr. Section 4·1). For all finite values of the cut-offs, the fact that the branching equations are correctly renormalized by our procedure is thus proved again, through the (then convergent) perturbative expansions: but this is also the only proof one can offer of the fact that the branching equations are correctly renormalized by our procedure in any case. A direct proof is therefore not necessary; it might prove at most a useful exercise.

We wish to emphasize at this point that we are not making here any statement as to the methods which are appropriate for the rigorous solution of the

---

(4) Cf. ref. (2), Sect. 4, 1, 2, 3.

(5) Ib., Sect. 4·4.

(6) E. R. Caianiello: *Nuovo Cimento*, **3**, 223 (1956); A. Buccafurri and E. R. Caianiello: *Nuovo Cimento*, **8**, 170 (1958)

branching equations written in terms of $\int$ integrals: this task is beyond our present scope, and falls much more in the province of mathematics than in that of physics. We are contented with having given a formulation of the problem and of all equations in a form which may finally permit rigorous quantitative investigations.

In conclusion, we are justified in taking the renormalized branching equations as the axiomatic formulation of a theory, just as we did in the unrenormalized case. The renormalized perturbative expansions follow immediately; all questions of renormalization need never be mentioned in actual computations, after the self-consistency of the theory was proved once for all.

5·2. – It is instructive to recognize how the present formalism compares with the standard procedures. A few trivial remarks may be in order, to begin with.

We observe first that in propagation kernels, whether of free or of interacting fields, variables, whenever they coincide, both in the branching equations and in the perturbative expansions, never do so, in the natural development of the theory, because of some limiting process which takes one into the value of the other: the only thing of interest is the value of the kernel *at* the point of coincidence. To fix things, take, as an example, the simple branching equations:

$$K\begin{pmatrix} x \\ y \end{pmatrix} = K_{00}(xy) - \lambda \int \sum (x\xi)\gamma^{\xi} K\left(\begin{matrix} \xi \\ y \end{matrix}\middle|\, \xi\right) \mathrm{d}\xi \,, \tag{60}$$

$$K\left(\begin{matrix} x \\ y \end{matrix}\middle|\, t\right) = \lambda \int \sum [t\xi]\gamma^{\xi} K\begin{pmatrix} x\ \xi \\ y\ \xi \end{pmatrix} \mathrm{d}\xi \,; \tag{61}$$

it is nowhere required that $K\left(\begin{matrix} x \\ y \end{matrix}\middle|\, x\right)$, which appears in (60), be calculated from (61) by taking the limit $t \to x$; $K\left(\begin{matrix} x \\ y \end{matrix}\middle|\, x\right)$ is given directly by (61), when $t \equiv x$. The requirement

$$\lim_{t \to x} K\left(\begin{matrix} x \\ y \end{matrix}\middle|\, t\right) = K\left(\begin{matrix} x \\ y \end{matrix}\middle|\, x\right), \tag{62}$$

which is currently understood to hold, is in reality an additional condition on the kernels. (60) and (61) originate indeed from the differential equations:

$$(\gamma \partial_x + m_f) K\begin{pmatrix} x \\ y \end{pmatrix} = K_{00} \cdot i\delta(x - y) - i\lambda \sum \gamma^{x} K\left(\begin{matrix} x \\ y \end{matrix}\middle|\, x\right), \tag{63}$$

$$(\Box_t - m_b^2) K\left(\begin{matrix} x \\ y \end{matrix}\middle|\, t\right) = i\lambda \sum \gamma^{t} K\begin{pmatrix} x\ t \\ y\ t \end{pmatrix}; \tag{64}$$

the solution of equations of this nature demands the specification 1) of the boundary (here, causality) conditions, 2) of the *class* to which the functions are required to belong (*e.g.*, in an ordinary Sturm-Liouville system, where the solution is unique if it belongs to the class of functions which are continuous with their first derivatives, the situation changes radically if this class is changed).

Clearly, requirements such as (62), which contribute to specify the class of admissible kernels, are the cause of ultraviolet divergencies; they have, for this very reason, only a formal value.

On the other side, all propagators are vacuum expectation values of time-ordered products of (free or interacting) fields: their values for coincident variables (more generally, for coincident times) are not defined by the theory: a requirement like (62) is an additional, arbitrary imposition. This is best seen in the case of the free fermion propagator (xy); when one uses, correctly, properly symmetrized Lagrangians (*i.e.* Wick products), (xx) is replaced by zero wherever it appears (Heisenberg's prescription): that is, the appropriate definition of (xy), as it stems from the best available formulation of field theory, requires that

$$\lim_{y \to x} (xy) \neq (xx) = 0 \,. \tag{65}$$

If one searches for solutions to the differential branching equations, of which (63), (64) are examples (the thing is absolutely general), such that they satisfy conditions of type (65) rather than of type (62) (the value zero can be replaced equivalently by any finite value - see later) then ultraviolet infinities disappear, $\int$ integrals arise naturally, and the proof that $\int \to \int$ is a « renormalization », made *a posteriori*, serves only to ascertain the self-consistency of the theory. To achieve a better formulation of this statement, we call of class $\mathscr{K}$ all kernels K, solutions to the differential branching equations, which satisfy conditions such as (62); of class $\mathscr{K}$ all kernels $\overline{K}$, solutions to the *same* differential branching equations, such that, if the l.h.s. of (62) is for them infinite, they satisfy instead conditions of the type:

$$\lim_{t \to x} \overline{K}\left(\begin{matrix} x \\ y \end{matrix} \middle| t\right) \neq \overline{K}\left(\begin{matrix} x \\ y \end{matrix} \middle| x\right) = \text{finite} \,, \tag{66}$$

etc. The actual determination of the finite values at r.h.s. is not relevant, and depends upon the choice of the prescription for $\int$. Clearly, if $f(x)$ is of class $\mathscr{K}$ when $x \to 0$,

$$\int f(x)\, \delta(x)\, \mathrm{d}x = \lim_{x \to 0} f(x) \neq f(0) \,; \tag{67}$$

such functions are « unbounded but finite ». Since kernels appear in any easy only as integrands, the use of solutions of class $\overline{\mathscr{K}}$ instead of $\mathscr{K}$ is fully legitimate; passage from class $\mathscr{K}$ to class $\overline{\mathscr{K}}$ is, again, renormalization.

We can see this, quite simply, from eq. (51): for $\overline{\lambda} = 0$, it gives

$$\frac{\partial(\overline{xy})}{\partial \overline{m}_f} = i \int (\overline{x\xi})(\overline{\xi y})\, \mathrm{d}\xi \,; \tag{68}$$

this we may compare with:

$$\frac{\partial(xy)}{\partial m_f} = i \int (x\xi)(\xi y)\, \mathrm{d}\xi \,. \tag{69}$$

The condition (65) gives, at the l.h.s., zero if we take $y = x$; at the r.h.s. we find zero (or a finite value, which amounts to the same) with equation (68), a quadratic infinity with equation (69). This fact is, clearly, absolutely general; it can be proved to all orders and in any case. It shows that the problem of finding solutions to the differential branching equations which belong to the class $\overline{\mathscr{K}}$ is solved by the systematic use of $\overline{\int}$ integrals. A change in the prescription for the evaluation of $\overline{\int}$ (which, among other things, will alter the finite value at r.h.s. of (66)) amounts to a change of the finite quantities $(\lambda, \overline{m}_f, \overline{m}_b^2)$: it is therefore an unobservable effect, which is hidden in the indetermination of the parameters λ, $\overline{m}_f$, $\overline{m}_b^2$ if the theory is self-consistent, *i.e.* renormalizable.

In this way, we reach a definite understanding of the mathematical nature of the ultraviolet divergencies; the reader may see by himself how the replacement, say, of $K\left(\begin{matrix} x \\ y \end{matrix} \middle| x\right)$ in (63), which satisfies (62), with $\overline{K}\left(\begin{matrix} x \\ y \end{matrix} \middle| x\right)$, which satisfies (66), is equivalent to the introduction in (63) of the difference between the r.h.s. of (62) and that of (66), *i.e.* to the addition of the standard counterterms ($m_f \to \overline{m}_f$, etc.). In particular cases this will yield field equations renormalized according to Valatin's prescription [7]; the integral formulation of the problem, which we have adopted consistently, is of course to be preferred.

Again, *what we have proved is not a departure from, but a re-interpretation of, current ideas*; kernels of class $\overline{\mathscr{K}}$ are well defined mathematical entities, and have a clear-cut physical meaning. Ultraviolet infinities have disappeared from the theory, indeterminate parameters have taken their place.

---

[7] J. G. Valatin: *Proc. Roy. Soc.*, A **226**, 254 (1954).

RIASSUNTO

Viene completata l'analisi, iniziata nella parte I, delle condizioni sotto cui la regolarizzazione, ottenuta con l'adozione degli integrali modificati introdotti nella parte I, equivale ad una rinormalizzazione. Le condizioni del secondo tipo annunciate in I sono formulate e discusse; un'analisi quantitativa può fornire risultati differenti dai requisiti usuali per la rinormalizzazione; come ad esempio si mostra che la teoria mesonica scalare neutra non è rinormalizzabile, contrariamente all'opinione corrente. Senza difficoltà si possono dedurre le equazioni di Lie del gruppo di rinormalizzazione e si può indagare sule loro condizioni di integrabilità. Infine si mostra che usare i nostri integrali modificati equivale a risolvere le equazioni differenziali di diramazione per i nuclei con la condizione che le soluzioni appartengano ad una certa classe matematica ben definita $\mathscr{H}$. In questo modo gli infiniti ultravioletti non compaiono più, e la ricerca di condizioni di rinormalizzabilità diventa una ricerca dell'autoconsistenza di una teoria, che deve essere fatta una volta per tutte e non può causare inconvenienti nei calcoli. Il risultato è una formulazione rigorosa della teoria rinormalizzata che evita ogni menzione di « particelle nude », è completamente libera da ambiguità ed è adatta sia per calcoli pratici che per lo studio delle equazioni fondamentali. Viene evitata la suddivisione non fisica dei processi in diagrammi di Feynman; si mostra che le difficotà dovute alle sovrapposizioni hanno un'origine banale e sono completamente eliminate; tutti i contributi dovuti alla parte di vertice si annullano con questo metodo, almeno in elettrodinamica, poichè si verifica l'eliminazione di essi, con i contributi dell'energia propria dell'elettrone, già prima dell'effettivo calcolo. Questi criteri saranno applicati in un prossimo lavoro ad uno studio esauriente dell'elettrodinamica; ci si aspetta che tali criteri giuochino un ruolo rilevante in una ricerca delle teorie consistenti delle particelle elementari.

IL NUOVO CIMENTO Vol. XIV, N. 1 1° Ottobre 1959

Experimental Results on Pion Production Compared with Predictions of the Isobar Model.

V. Alles-Borelli, S. Bergia, E. Perez Ferreira (*) and P. Waloschek

Istituto di Fisica dell'Università - Bologna
Istituto Nazionale di Fisica Nucleare - Sezione di Bologna

(ricevuto il 8 Luglio 1959)

Summary. — The predictions of the model of Lindenbaum and Sternheimer are compared with results obtained from the analysis of the reactions $\pi^- + p \to \pi^- + \pi^+ + n$; $\pi^- + p \to \pi^- + \pi^0 + p$, observed in an H_2 bubble chamber. It was not possible to find any contradiction and all results concerning momentum spectra and branching ratios are sufficiently well described by the model. In the favorable case: $\pi^- + p \to \pi^+ + I^- \to \pi^+ + (\pi^- + n)$, the correct Q-value distribution for the isobar is obtained and angular correlations in its decay are compatible with a $J = \frac{3}{2}$ for the $(\pi^- + n)$-pair.

1. – Introduction.

The relation between pion-proton scattering and photoproduction phenomena observed at low energy (the « $\frac{3}{2}$-$\frac{3}{2}$ » resonance) suggested that it would be of interest to investigate if also at higher energies the observed resonant state would play an important role, in particular, for pion production. During the last few years a phenomenological model for pion production was developed, in which was brought into consideration the possibility of the presence of an excited state of the nucleon in an intermediate step of the process, namely the $\frac{3}{2}$-$\frac{3}{2}$ resonant state. This excited nucleon should be able to decay into a pion and a nucleon and is well known to be also responsible for the low energy pion-proton resonance.

(*) On leave from the Comisión Nacional de Energía Atómica, Rep. Argentina.

The isobar model removes some difficulties appearing when one compares experimental results with earlier models, like Fermi's statistical theory for π-production. Up to now the available experimental material on pion-production in pion-proton and proton-proton collisions was not very extensive [1], but the general agreement with the isobar model was fairly good.

In the present paper we compare the predictions of the detailed isobar model proposed by LINDENBAUM and STERNHEIMER [2] with results obtained from the reactions:

$$\pi^- + \mathrm{p} \to \pi^- + \pi^+ + \mathrm{n} \tag{1}$$

$$\pi^- + \mathrm{p} \to \pi^- + \pi^0 + \mathrm{p} \tag{2}$$

observed in an hydrogen bubble chamber.

2. – Predictions of the isobar model.

We summarize here some conclusions obtained by STERNHEIMER and LINDENBAUM [3] from their detailed model. According to this model, the reaction:

$$\pi + \mathscr{N} \to \pi + \pi + \mathscr{N} \tag{3}$$

should take place in two independent steps:

$$\pi + \mathscr{N} \to \pi + \mathrm{I} \to \pi + \pi_{\mathrm{dec}} + \mathscr{N}\,, \tag{4}$$

where I stands for « isobar », whose decay products should not interact with the « extra-π » of the first step of the reaction.

There are five reactions of type (4), according to the different possibilities of the electric charge of the isobar and the « extra-π » and the different possibilities of decay of the isobar, namely the following:

$$\left\{\begin{array}{ll} (a) & \pi^- + \mathrm{p} \to \pi^- + \mathrm{I}^+ \to \pi^- + \pi^+ + \mathrm{n} \\ (b) & \pi^- + \mathrm{p} \to \pi^- + \mathrm{I}^+ \to \pi^- + \pi^0 + \mathrm{p} \\ (c) & \pi^- + \mathrm{p} \to \pi^+ + \mathrm{I}^- \to \pi^+ + \pi^- + \mathrm{n} \\ (d) & \pi^- + \mathrm{p} \to \pi^0 + \mathrm{I}^0 \to \pi^0 + \pi^- + \mathrm{p} \\ (e) & \pi^- + \mathrm{p} \to \pi^0 + \mathrm{I}^0 \to \pi^0 + \pi^0 + \mathrm{n}\,. \end{array}\right. \tag{5}$$

---

(1) See reference (3).

(2) S. J. LINDENBAUM and R. B. STERNHEIMER: *Phys. Rev.*, **105**, 1874 (1957).

(3) R. B. STERNHEIMER and S. J. LINDENBAUM: *Phys. Rev.*, **109**, 1723 (1958).

Assuming charge independence it is possible to analyse the above listed reactions in terms of two isotopic spin states ($\frac{1}{2}$ and $\frac{3}{2}$) for the initial system. This analysis is perfomed by STERNHEIMER and LINDENBAUM through two suitable parameters ϱ and α, defined as follows:

$$\varrho = \sigma_{\frac{3}{2}}^{\mathrm{in}}/2\cdot\sigma_{\frac{1}{2}}^{\mathrm{in}}\,, \tag{6}$$

where $\sigma_{\frac{1}{2}}^{\mathrm{in}}$ and $\sigma_{\frac{3}{2}}^{\mathrm{in}}$ are the cross sections for single pion production for isotopic spin $\frac{1}{2}$ and $\frac{3}{2}$, respectively, and

$$\alpha = 2\cdot(\varrho/5)^{\frac{1}{2}}\cdot\cos\varphi\,, \tag{7}$$

where φ is the phase difference between the matrix elements of isotopic spin $\frac{1}{2}$ and $\frac{3}{2}$. In terms of these parameters there are several relations between the five reactions (a) to (e); in particular the following will be useful for comparison with the experiment:

$$(c)/(a) = \xi_1 = (45+36\varrho+90\alpha)/(5+16\varrho-20\alpha)\,, \tag{8}$$

$$(b)/(d) = \xi_2 = (5+16\varrho-20\alpha)/(5+\varrho-5\alpha)\,, \tag{9}$$

$$((a)+(c))/((b)+(d)) = R = (10+17\varrho-25\alpha)/(25+26\varrho+35\alpha)\,, \tag{10}$$

$$(e)/((a)+(b)+(c)+(d)+(e)) = S = (10+2\varrho-10\alpha)/45\,(1+\varrho). \tag{11}$$

Now, if the numerical values of ξ_1, ξ_2, R, and S are fixed (from the experiment, for instance) then equations (8) to (11) represent linear relations between ϱ and α; ϱ should simultaneously satisfy (6). This last condition contains the inelastic π^++p cross section through the relations:

$$\sigma_{\pi^+}^{\mathrm{in}} = \sigma_{\frac{3}{2}}^{\mathrm{in}} \qquad \sigma_{\pi^-}^{\mathrm{in}} = \tfrac{2}{3}\,\sigma_{\frac{1}{2}}^{\mathrm{in}} + \tfrac{1}{3}\,\sigma_{\frac{3}{2}}^{\mathrm{in}}\,. \tag{12}$$

Clearly all these equations are superabundant and this situation provides an interesting check of the reliability of the model.

Furthermore the isobar model allows one to calculate the spectra of the emitted particles if several reasonable assumptions are made, for instance, if it is assumed that the probability to form a $\frac{3}{2}$-$\frac{3}{2}$ isobar of a certain mass is related to the π^++p scattering cross section at the corresponding energy ([3]) (phase space factors included). Fig. 1 shows the spectra for the « extra-π » and for the « decay-π » calculated by F. SELLERI ([4]) for an incident pion K.E. of 960 MeV.

([4]) F. SELLERI: *Thesis* (University of Bologna), unpublished.

The peak in the « extra-π » spectrum reproduces, apart from the phase space factors, the peak in the $\pi^+ + p$ cross section.

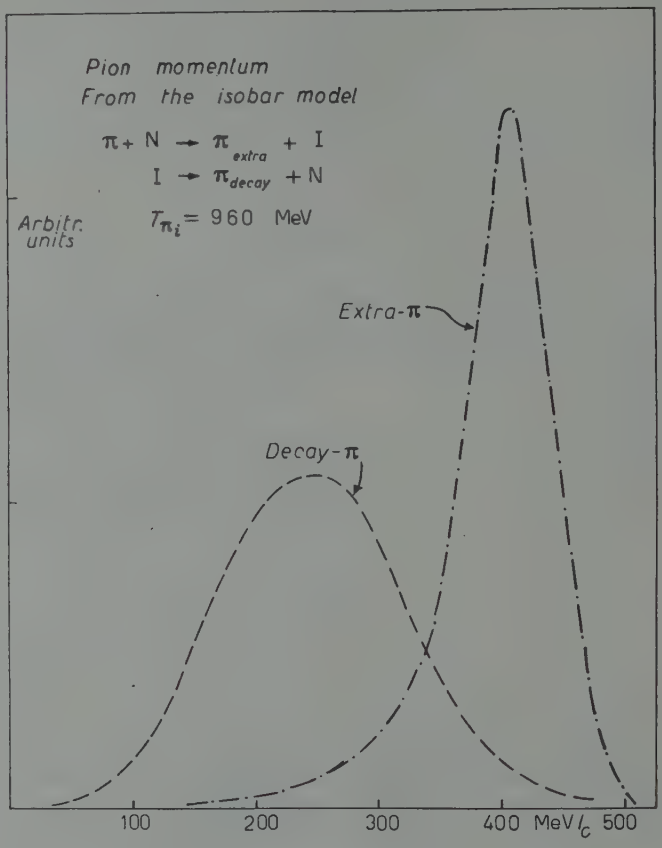

Fig. 1.

The experimentally observed reaction (1) is a superposition of reactions (a) and (c) of (5). In favorable conditions it will be possible to deduce the branching ratio $(c)/(a) = \xi_1$ from the spectrum of the emitted pions. But it is also possible to eliminate ξ_1 lumping together the spectra of the pions of both signs. The resulting spectrum is independent of ϱ and α. In the same way the momentum spectra of the pions from reaction (2) will give information on the parameter ξ_2 and again the spectrum resulting from adding both pions is independent of ϱ and α.

Within the framework of the isobar model the correlation between production and decay angles could give a possibility to determine the spin of

the « isobar » in a similar way as ADAIR (5) proposed for the Λ^0-hyperon in the process $\pi^- + p \to \Lambda^0 + \theta^0$. The spin of the « second » particle emitted is here well known and the argument can be applied as was also observed by MORPURGO (6). One expects a distribution: $1+3\cos^2\theta$ for the decay products of the $\frac{3}{2}$, $\frac{3}{2}$-isobar. The angle of decay must be measured with respect to the line of flight of the incident particles but in the CMS of the decaying isobar (7). In the case in which the isobar is produced not merely in s-waves, only events produced backwards and forwards should be used.

In its present state the isobar model gives no predictions on the absolute values of the cross-sections, except under particular assumptions as those introduced by LINDENBAUM and STERNHEIMER (8). The problem is related to the states of angular momentum involved in the production process. Some arguments in this sense could perhaps be obtained from the analysis of the angular distribution for isobar production.

3. – Experimental results.

The events here reported were obtained in a new scan of pictures of the hydrogen bubble chamber of the Columbia University, exposed to the 960 MeV pion beam of the Brookhaven Cosmotron. The same film was previously used

TABLE I (*).

Clear elastic events	521	(417)	
Stops	222	(190)	
Clear $\pi^0+\pi^-+p$	190		
Clear $\pi^-+\pi^++n$	240		
« n » or « p »	13		
Clear $\pi^-+\pi^++\pi^0+n$	43		(355)
Probable $\pi^-+\pi^0+\pi^0+p(+?)$	8		
Clear $\pi^-+\pi^-+\pi^++p$	23	(21)	
Strange particles	25		
Total	1285	(983)	

(5) R. K. ADAIR: *Phys. Rev.*, **100**, 1540 (1955).

(6) G. MORPURGO: *Nuovo Cimento*, **9**, 564 (1958).

(7) F. EISLER, R. PLANO, A. PRODELL, N. SAMIOS, M. SCHWARTZ, J. STEINBERGER, P. BASSI, V. BORELLI, G. PUPPI, G. TANAKA, P. WALOSCHEK, V. ZOBOLI, M. CONVERSI, P. FRANZINI, I. MANNELLI, R. SANTANGELO, V. SILVESTRINI, G. L. BROWN, D. A. GLASER and C. GRAVES: *Nuovo Cimento*, **7**, 222 (1958).

(8) S. J. LINDENBAUM and R. B. STERNHEIMER: *Phys. Rev.*, **106**, 1107 (1957).

(*) Data between brackets are those obtained by ERWIN and KOPP (9) in a similar experiment. They are in good agreement with our numbers.

(9) A. R. ERWIN and J. K. KOPP: *Phys. Rev.*, **109**, 1364 (1958).

for strange particles experiments ([10]). All events observed in a well defined region of the chamber were analysed. Of a total of 1285 interactions observed, there were found 240 of reaction (1) (neutrons) and 190 of reaction (2) (protons). The classification of all events is shown in Table I. Favorable conditions of the chamber allowed a clear identification of nearly all events. The measured momenta were first adjusted with a least squares fit (in order to balance momentum and energy) and then transformed into the CMS by means of an IBM-650 computer. Details of the measurements and computations as well as some results not included in this paper will be published separately.

Reaction (1) is the most favorable case to observe the isobar. The $(\pi^- + n)$-pair is a pure isotopic spin $\frac{3}{2}$ state, and the isobar model predicts that reaction (1)

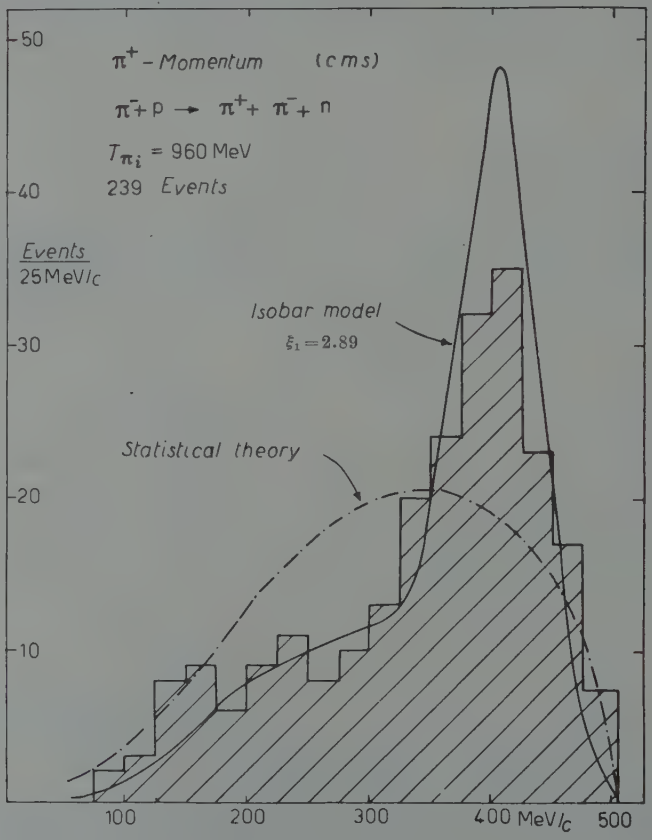

Fig. 2.

([10]) F. EISLER, R. PLANO, A. PRODELL, N. SAMIOS, M. SCHWARTZ, J. STEINBERGER, P. BASSI, V. BORELLI, G. PUPPI, H. TANAKA, P. WALOSCHEK, V. ZOBOLI, M. CONVERSI, P. FRANZINI, I. MANELLI, R. SANTANGELO and V. SILVESTRINI: *Nuovo Cimento*, **10**, 468 (1958).

goes mainly through the channel (*c*). The momentum spectrum of the positive pions is shown in Fig. 2 together with the spectrum obtained from the isobar model. The values of ϱ and α used here will be justified later. The peak at 400 MeV corresponds to the $\frac{3}{2}$, $\frac{3}{2}$ resonance. The π^--spectrum reflects the same situation and shows the small effect of the $(\pi^+ + p)$-isobar (Fig. 3).

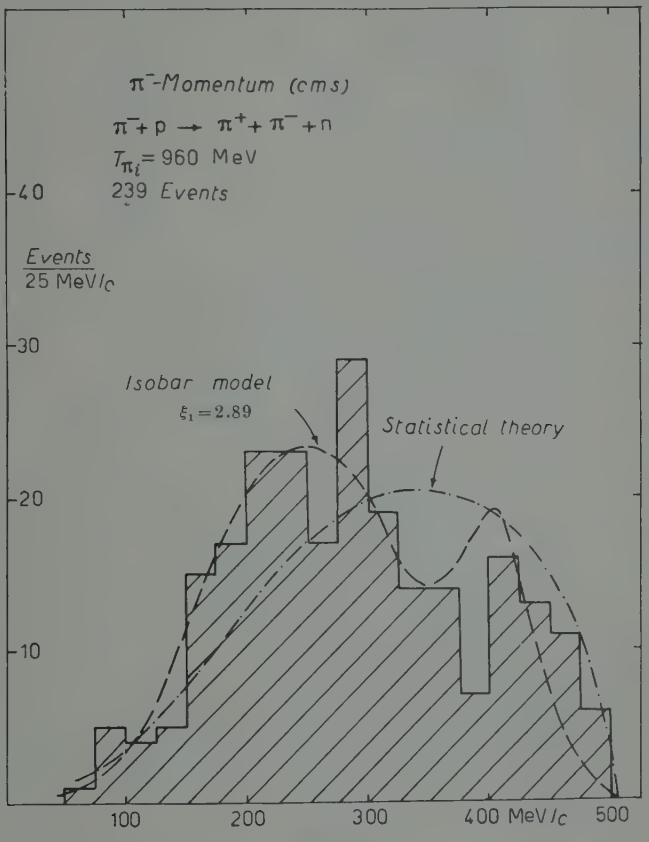

Fig. 3.

Figs. 4 and 5 show the results from reaction (2) and are compared with the spectra obtained from the isobar model, using the same values of ϱ and α as before (full line). The dotted curves, which correspond to values of ξ_2 determined from each spectrum as will be shown later, give a better fit.

As it was remarked before, the superposition of the two spectra of Fig. 2 and 3 is independent of the initial mixture of isotopic spin states. The same holds for Figs. 4 and 5 and also for the sum of all pion spectra. This latter is shown in Fig. 6 and it is in agreement with the spectrum predicted by the isobar model.

In order to get the branching ratios defined in (8) and (9) we first divided each experimental spectrum into two regions: region « A » over 325 MeV/c and region « B » under 325 MeV/c. Region « A » contains 90% of the extra pion

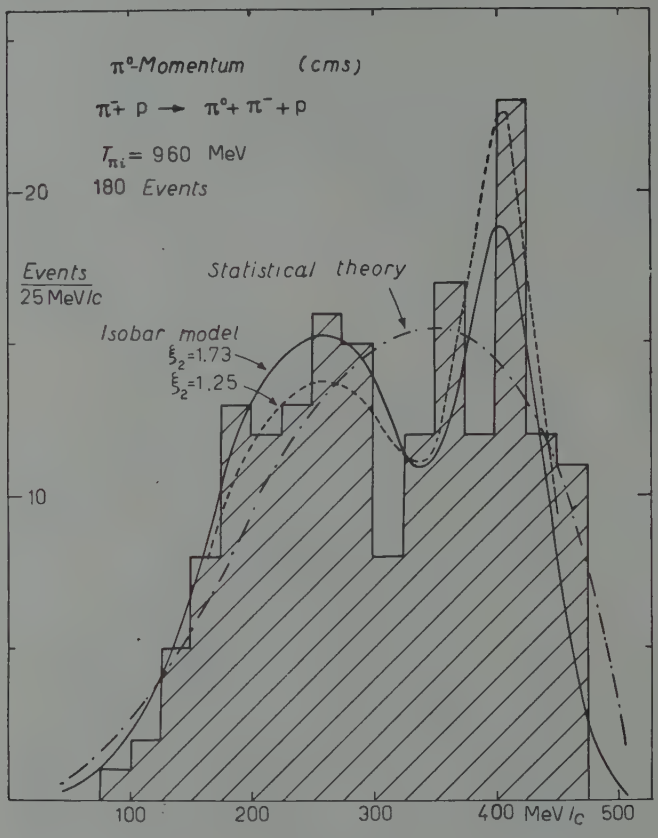

Fig. 4.

spectrum and 15% of the decay pion spectrum, while region « B » contains 85% of the decay pion spectrum and 10% of the extra pion spectrum. These percentages were obtained from the theoretical spectra of Fig. 1. Now, from the number of events observed in « A » and « B » we can deduce the ratio « extra-π »/« decay-π » for every spectrum. This procedure seems more reliable to us than a least squares fit, since small measurement errors could displace some events (in particular from the narrow peak) slightly deforming the spectrum, but the sum of all events contained in « A » and « B » could compensate in part this effect as well as the influence of an eventual anisotropy of the

decay angular distribution of the isobar which would only affect the form of the decay pion part.

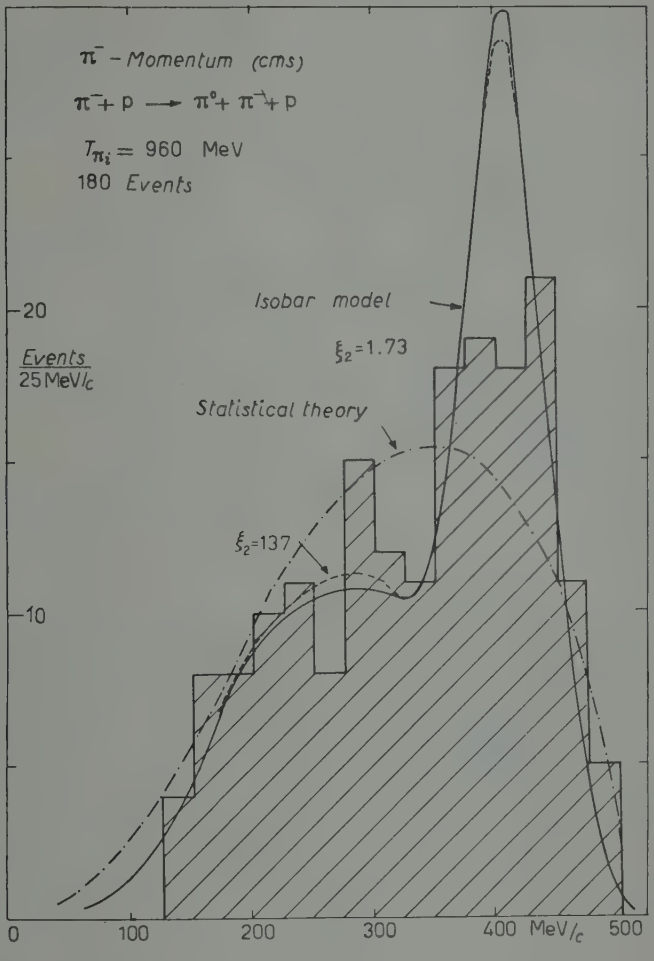

Fig. 5.

All pion spectra were treated in an identical way, and we obtained:

$\xi_1 = 2.25 \pm 0.43$ from the π^+-spectrum (n)

$\xi_1 = 2.98 \pm 0.60$ from the π^--spectrum (n)

$\xi_2 = 1.32 \pm 0.27$ from the π^--spectrum (p)

$\xi_2 = 1.25 \pm 0.25$ from the π^0-spectrum (p).

The branching ratio R is obtained from Table I:

$$R = 0.792 \pm 0.077 = \text{protons/neutrons}\,.$$

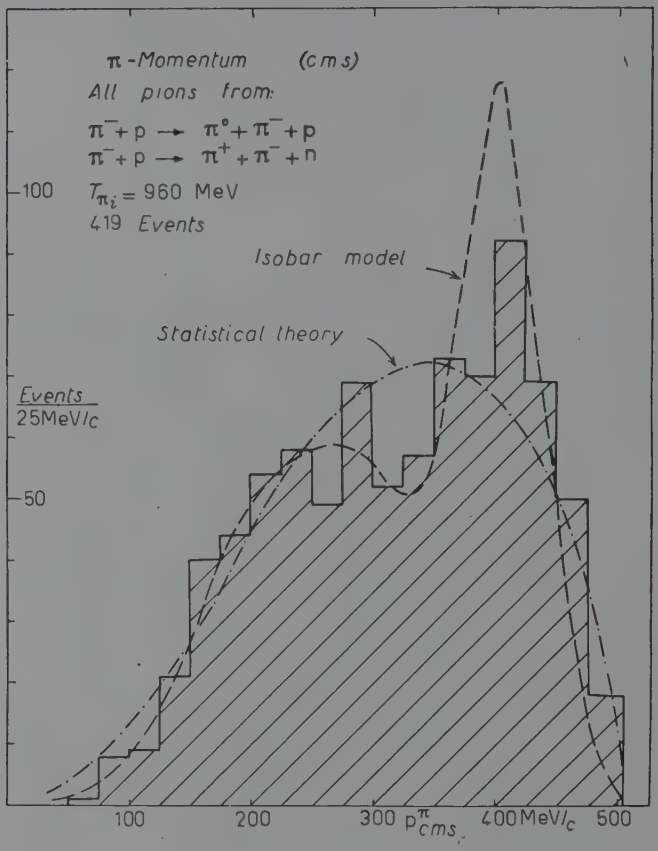

Fig. 6.

The number of « stops » gives an upper limit for the reaction (e) since this number contains also the normal charge exchange events. We obtain:

$$S < 0.334 \pm 0.026 = \text{stops/total}\,.$$

Before discussing the compatibility between all these numbers, we shall show the results of the analysis of the angular correlations.

We first divided all events into four classes, corresponding to reactions (a), (b), (c) and (d). As « extra-π » the more energetic one was always selected. The samples so obtained are contaminated with wrongly classified events in

$\sim 30\%$ for class (*a*), $\sim 10\%$ for class (*b*), $\sim 5\%$ for class (*c*) and $\sim 20\%$ for class (*d*). Figs. 7 to 9 show the angular distribution of the production of the differently charged isobars, without any correction for their mutual contamination. It is clear from these distributions that different waves are involved in each case,

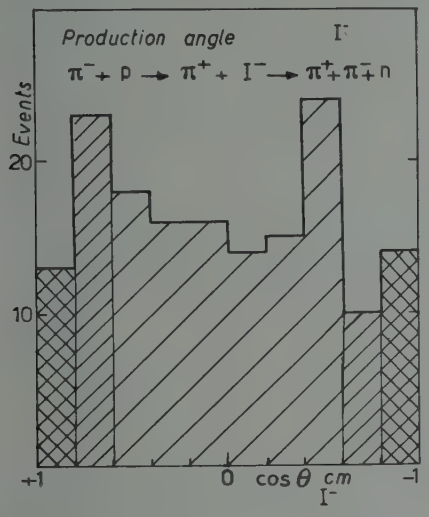

Fig. 7.

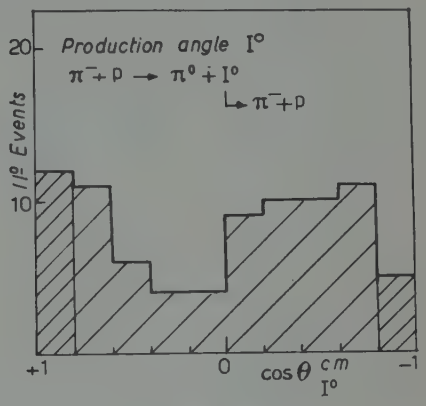

Fig. 8.

For the spin analysis we first considered reaction (*c*). As the production is roughly isotropic, a first attempt would be to assume that the isobar is emitted with $l = 0$. Thus, all events could be used for Adair's analysis, as is shown in Fig. 10. A curve $(1 + 3\cos^2\theta)$ normalized to the total number of events has been superimposed. The agreement is not too good, but it becomes better by selecting events with a small production angle. Corresponding regions are equally shadowed on the decay angle distribution and on the production angle distribution ($|\cos\alpha_{pr}| > 0.6$ and > 0.8). The result is compatible with the assumed $J = \frac{3}{2}$ of the isobar, even though the statistics is not sufficient for a spin determination.

The angular distributions for the production of the other charge states of the isobar are not so simple and it is possible that the limit in the production angle for a successful spin analysis is very small.

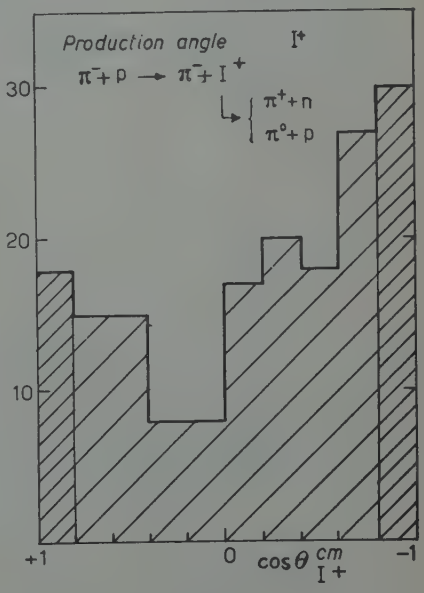

Fig. 9.

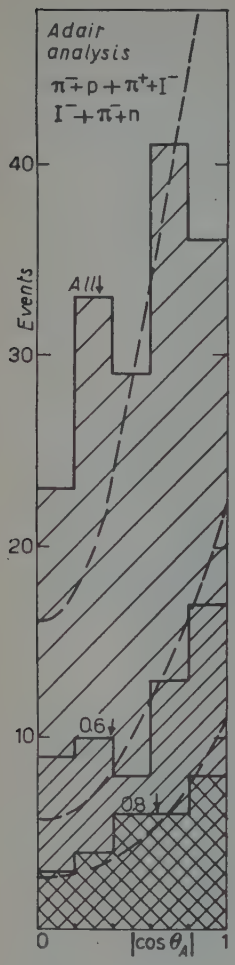

Fig. 10.

Fig. 11 shows the decay distributions for all events and for those produced at $|\cos\alpha_{pr}|>0.8$. With the present statistics it is not possible to reduce any further the limit for the production angle and it remains doubtful if any conclusions could be obtained from this last analysis of reactions (*a*), (*b*) and (*d*).

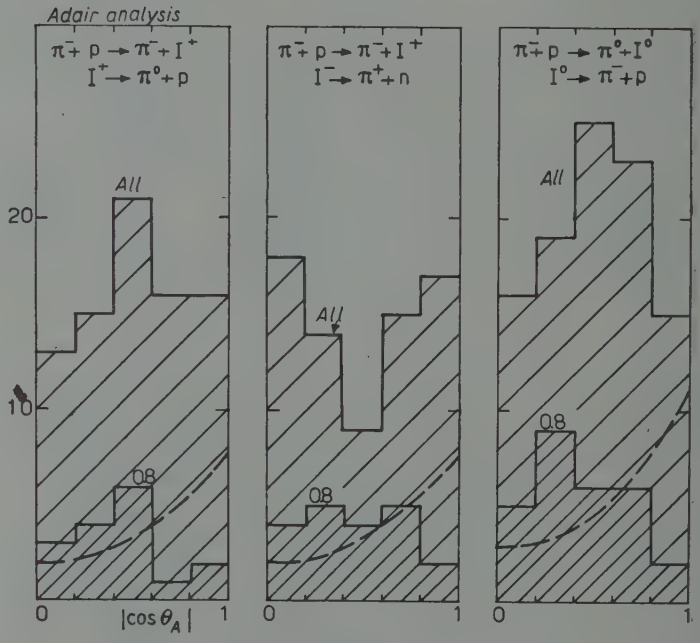

Fig. 11.

4. – Discussion.

As we have shown, momentum spectra and angular correlations seem not to contradict the isobar model. We should now analyse the situation with respect to the branching ratios defined in (8) to (11). As we already said the parameters ϱ and α are related through linear equations containing ξ_1, ξ_2, R S, $\sigma_{\frac{1}{2}}^{in}$ and $\sigma_{\frac{3}{2}}^{in}$. The experimental results on R and ξ_1, define α as very close to -0.2. ϱ could instead vary between 0.02 and 0.2, depending essentially on the value of $\sigma_{\pi^+}^{in}$ (*). We have taken $\sigma_{\pi^+}^{in}=6.3$ mb and consequently

$$\xi_1=2.89, \qquad \xi_2=1.73, \qquad \varrho=0.1\,, \qquad \alpha=-0.2\,,$$

(*) $\sigma_{\pi^+}^{in}$ is understood as referring to production of only one pion.

as convenient values for the isobar model calculations. For this compromise we had to go quite far from the experimentally determined value of ξ_2 but, as it was shown on the pion spectra (Figs. 4 and 5), this does not seem to be in contradiction with the experimental data (*).

The number of « stops » corresponding to the reaction (*e*) obtained from our ϱ and α is 140. Our experimental number of 222 should then contain 82 charge exchange events. Since we have simultaneously fixed $\sigma_{\pi^+}^{el}$ $(=\sigma_{\pi^+}^{tot}-\sigma_{\pi^+}^{in})$ one can verify that there is no contradiction in the « triangular relations » between $\sqrt{\sigma_{\pi^-}^{el}}$, $\sqrt{\sigma_{\pi^+}^{el}}$ and $\sqrt{2\sigma_{ch.ex}}$.

The whole situation does not change very much if we assume any value of $\sigma_{\pi^+}^{in}$ up to about 10 mb (*i.e.* taking $\varrho < 0.18$). Only if $\sigma_{\pi^+}^{in}$ turned out to be higher than this upper limit we would find some trouble in fitting the momentum spectra of the reaction (2) $(\pi^- + \pi^0 + p)$.

5. – Conclusions.

It was not possible for us to find any contradiction between our experimental results and the very precise predictions of the isobar model of Sternheimer and Lindenbaum, since the model describes sufficiently well all the results concerning momentum spectra and branching ratios worked out from the present statistics. With respect to angular correlations, only for reaction (*c*) a reasonable number of events is available; although not statistically significant for a spin determination, it gives distributions which are compatible with the assumed spin $\frac{3}{2}$ for the isobar.

Results from $\pi^+ + p$ reactions will provide a more precise check of the validity of the model.

* * *

We are very grateful to the bubble chamber group of the Columbia University, in particular to Prof. J. Steinberger for allowing us to perform the measurements here presented on photographs of their chamber, obtained at the Cosmotron.

The continuous encouragement and interest as well as the valuable suggestions of Prof. G. Puppi, which made possible this work, are gratefully acknowledged.

In the first stage of the measurements Dr. A. Minguzzi-Ranzi and Dr. V. Zoboli collaborated with us. For many helpful discussions we thank Prof. A. Minguzzi, Dr. F. Selleri and Dr. L. Bertocchi.

(*) To fit ξ_2 within one standard deviation and simultaneously ξ_1 and R, ϱ should be taken near 0.05, $\sigma_{\pi^+}^{in} \approx 3$ mb.

The help of Miss A. Diaz Romero and Mr. C. Alvisi in the computation work is gratefully recognized.

Most of the calculations were performed at the IBM-650 of the Centro Calcoli of the University of Bologna. We are indebted to the members of its staff, in particular to Dr. Ing. F. Pierantoni and Dr. A. Chiarini who gave us helpful advices for the programming work.

One of us (E.P.F.) wishes to thank Prof. G. Puppi and the staff of the « Istituto di Fisica A. Righi » in Bologna, for the kind hospitality extended to her; she is also indebted to the Comisión Nacional de Energía Atómica, Rep. Argentina, for a fellowship.

RIASSUNTO

Si confrontano le previsioni del modello di Lindenbaum e Sternheimer con i risul - tati ottenuti dall'analisi delle reazioni $\pi^- + p \to \pi^- + \pi^+ + n$; $\pi^- + p \to \pi^- + \pi^0 + p$, osservate in una camera a bolle ad idrogeno. I risultati sperimentali non sono in contraddizione con il modello e sono da esso descritti sufficientemente bene. Nel caso favorevole $\pi^- + p \to \pi^+ + I^- \to \pi^+ + (\pi^- + n)$ il modello dà la distribuzione corretta dei valori di Q e le correlazioni angolari nel decadimento sono compatibili con un $J = \frac{3}{2}$ per le coppie $(\pi^- + n)$.

LETTERE ALLA REDAZIONE

(La responsabilità scientifica degli scritti inseriti in questa rubrica è completamente lasciata dalla Direzione del periodico ai singoli autori)

Hypercharge Independence of K Interactions.

N. Dallaporta and V. De Santis

Istituto di Fisica dell'Universi à - Padova
Istituto Nazionale di Fisica Nucleare - Sezione di Padova

(ricevuto il 14 Luglio 1959)

In a recent paper [1], it has been shown that the properties related to the strong interactions of baryons as expressed by the so-called doublet approximation [2-4], may be derived from the consideration of a general Dirac equation satisfied by a 32-component spinor, which is formed by a mixture of the whole of the charge states of baryons known up to now. In the representation in which baryon states corresponding to different hypercharge doublets are already separated, the K interactions may be derived from an interaction Hamiltonian of the form

$$-i\overline{\Psi}(F\omega_K + F'\omega'_K)\times\Gamma^5\varphi_K\Psi\,, \tag{1}$$

where the index K ($K=1, 2, 3, 4$) labels the 4-components of a hypercharge space, independent from the isospin space related to the pion interactions into which the K interactions are entirely displayed, φ_K are the (scalar or pseudoscalar in space time) components of a 4 vector in the hypercharge space representing the K field according to the definitions:

$$\varphi_1 + i\varphi_2 = K_c\,, \qquad \varphi_3 + i\varphi_4 = K_n\,,$$
$$\varphi_1 - i\varphi_2 = K_c^*\,, \qquad \varphi_3 - i\varphi_4 = K_n^*\,,$$

K_c creates K^+ and destroys K^-; K_n creates K^0 and destroys $\overline{K}^0$; K_c^* creates $\overline{K}^-$ and destroys K^+; K_n^* creates $\overline{K}^0$ and destroys K^0; and the $\omega_K\times\Gamma^5$ and $\omega'_K\times\Gamma^5$ are two groups of 32×32 matrices operating on the whole spinor Ψ. As Γ^5 acts on the

(1) N. Dallaporta and T. Toyoda: *Nuovo Cimento*, **14**, 142 (1959).
(2) J. Tiomno: *Nuovo Cimento*, **6**, 69 (1957).
(3) N. Dallaporta: *Proc. Intern. Conf. on Mesons and recently discovered Particles* (Padua-Venice, Sept. 1957 V, 3), *Nuovo Cimento*, **7**, 200 (1958).
(4) A. Pais: *Phys. Rev.*, **110**, 574 (1958).

8-components of every state of given hypercharge, we will be interested in the following only in the 4×4 ω_K and ω'_K operating on the hypercharge indices of the spinor, which are expressed as follows (*):

$$(2)\qquad \left\{\begin{array}{l} \omega_1 = i\begin{vmatrix} & & & 1\\ & & 1 & \\ & -1 & & \\ -1 & & & \end{vmatrix},\quad \omega_2 = \begin{vmatrix} & & & -1\\ & & 1 & \\ & 1 & & \\ -1 & & & \end{vmatrix},\quad \omega_3 = i\begin{vmatrix} & & -1 & \\ & & & 1\\ 1 & & & \\ & -1 & & \end{vmatrix},\quad \omega_4 = \begin{vmatrix} & & 1 & \\ & & & 1\\ 1 & & & \\ & 1 & & \end{vmatrix}.\\[2ex] \omega'_1 = i\begin{vmatrix} & & & 1\\ & & -1 & \\ & 1 & & \\ -1 & & & \end{vmatrix},\quad \omega'_2 = \begin{vmatrix} & & & -1\\ & & -1 & \\ & -1 & & \\ -1 & & & \end{vmatrix},\quad \omega'_3 = i\begin{vmatrix} & & -1 & \\ & & & -1\\ 1 & & & \\ & 1 & & \end{vmatrix},\quad \omega'_4 = \begin{vmatrix} & & 1 & \\ & & & -1\\ 1 & & & \\ & -1 & & \end{vmatrix}. \end{array}\right.$$

The consideration of two different interaction terms with two different coupling constants F and F' allows to introduce the baryon mass differences in a satisfactory way.

In the present note, we wish to investigate the invariance properties of expression (1) for rotations in the hypercharge space which were not analyzed in detail in [1]. Let us first consider the case $F'=0$ so that the Hamiltonian reduces only to the term

$$(3)\qquad -iF\overline{\Psi}\omega_K\times\Gamma^5\varphi_K\Psi\,,$$

this is equivalent to assume all baryons as having the same mass.

We may first build the second order antisymmetric tensor:

$$(4)\qquad M_{ik}=\frac{i}{4}[\omega_i\,\omega_k]\,,$$

and group these components to form two different 3 pseudovectors, as shown by PAIS [5] and TIOMNO [2]:

$$(5)\qquad \left\{\begin{array}{l} Y_1=\dfrac{1}{2}(M_{23}+M_{14})=\dfrac{1}{2}\begin{vmatrix} & -1 & & \\ -1 & & & \\ & & & 0\\ & & 0 & \end{vmatrix},\quad Y_2=\dfrac{1}{2}(M_{31}+M_{24})=\dfrac{1}{2}\begin{vmatrix} & -i & & \\ i & & & \\ & & & 0\\ & & 0 & \end{vmatrix},\\[2ex] Y_3=\dfrac{1}{2}(M_{12}+M_{34})=\dfrac{1}{2}\begin{vmatrix} 1 & & & \\ & -1 & & \\ & & 0 & \\ & & & 0 \end{vmatrix}, \end{array}\right.$$

(*) The present form for these matrices corresponds to the representation through partially separated states Ψ; and is different from the form explicitly given in [1] referring to the completely mixed representation X.

[5] A. PAIS: *Phys. Rev.*, **112**, 624 (1958).

$$(5)\quad \left\{ \begin{array}{l} Z_1 = \dfrac{1}{2}(M_{23} - M_{14}) = \dfrac{1}{2}\begin{vmatrix} 0 & & & \\ & 0 & & \\ & & & -1 \\ & & -1 & \end{vmatrix}, \quad Z_2 = \dfrac{1}{2}(M_{31} - M_{24}) = \dfrac{1}{2}\begin{vmatrix} 0 & & & \\ & 0 & & \\ & & & -i \\ & & i & \end{vmatrix}, \\ \\ Z_3 = \dfrac{1}{2}(M_{12} - M_{34}) = \dfrac{1}{2}\begin{vmatrix} 0 & & & \\ & 0 & & \\ & & 1 & \\ & & & -1 \end{vmatrix}. \end{array} \right.$$

The components of these two 3 vectors satisfy the commutation relations of angular momenta:

$$Y_i Y_k - Y_k Y_i = -iY_l\,, \qquad (i\,k\,l \text{ circularly permuted}),$$

and may be considered as the generators of 3-dimensional rotations in the 4-dimensional hypercharge space ([2,5]). Now, by analogy with the usual isospin of pion interactions, the eigenvalues of Y_3 may be interpreted as representing the hypercharge of the baryon states N_1, N_4, N_2, N_3 respectively (*) (we indicate with these symbols the doublets pn, $\Xi^0\Xi^-$, $\Sigma^+\mathrm{Y}^0$, $\mathrm{Z}^0\Sigma^-$) and the vector $\boldsymbol{Y}$ as an hyperspin operating on the hypercharge states.

Let us now define another set of angular momenta components:

$$(6)\quad U_1 = \frac{1}{2}\begin{vmatrix} & & & 1 \\ & -1 & & \\ & & -1 & \\ 1 & & & \end{vmatrix} \qquad U_2 = \frac{1}{2}\begin{vmatrix} & & & -i \\ & & -i & \\ & i & & \\ i & & & \end{vmatrix} \qquad U_3 = \frac{1}{2}\begin{vmatrix} -1 & & & \\ & +1 & & \\ & & -1 & \\ & & & +1 \end{vmatrix},$$

satisfying also:

$$U_i U_k - U_k U_i = -iU_l\,.$$

This new vector may be interpreted as the hyperspin operating on the K-mesons states and we attribute the 4 hypercharge values of U_3 respectively to

$$\mathrm{K}^-, \mathrm{K}^+, \overline{\mathrm{K}}^0, \mathrm{K}^0\,.$$

Of course, $Y_3 + U_3$ will represent the total hypercharge operator: and it is easy to verify that all three components of $\boldsymbol{Y} + \boldsymbol{U}$ commute with the Hamiltonian (3). Thus the vector $\boldsymbol{Y} + \boldsymbol{U}$ is a constant of the motion which ensures hypercharge independence of K interactions exactly in the same way as does total isospin for charge independence in case of pion interactions.

Equivalent considerations may be obtained when we consider instead the second 3-vector $\boldsymbol{Z}$. Let us define as in the preceding case another 3-vector $\boldsymbol{V}$, related to

(*) These symbols are the same as those used by PAIS in ([4]).

the K-meson, as follows:

$$(7)\qquad V_1=\frac{1}{2}\begin{vmatrix} & & 1 \\ & -1 & \\ 1 & & \\ & -1 & \end{vmatrix}\qquad V_2=\frac{1}{2}\begin{vmatrix} & -i & & \\ i & & & \\ & & & i \\ & & i & \end{vmatrix}\qquad V_3=\frac{1}{2}\begin{vmatrix} -1 & & & \\ & +1 & & \\ & & +1 & \\ & & & -1 \end{vmatrix},$$

for convenience let us term the eigenvalues of the matrices Z_3 and V_3 the hypernumbers related respectively to the baryons and to the K-meson states. Then, one may show that the three components of the total hypernumber vector $\boldsymbol{Z}+\boldsymbol{V}$ all commute with the Hamiltonian (3) so that we have hypernumber independence as we have hypercharge independence.

At this stage it appears in fact that hypercharge or hypernumber conservation and hypercharge or hypernumber independence in strong K reactions are equivalent laws and this is stressed as soon as we try to represent the baryons and K-mesons through 4-dimensional hypercharge vectors and spinors according to a formalism already developed by PAIS (6), but used by him in a different physical interpretation of strong interactions. In a 4-dimensional space eigenstates of the angular momentum operators K, whose components are defined by

$$(8)\qquad K_{LK}=i\left(x_L\frac{\partial}{\partial x_K}-x_K\frac{\partial}{\partial x_L}\right),\qquad L;K=1,2,3,4,$$

are obtained as solutions of the spherical harmonics equation:

$$(9)\qquad [K^2-k(k+1)]Y=0\qquad k=0,\tfrac{1}{2},1,\ldots$$

with

$$(10)\qquad K^2=\sum_3(K_\alpha^+)^2=\sum_3(K_\alpha^-)^2,\qquad K_\alpha^\pm=\tfrac{1}{2}(K_{\beta\gamma}\pm K_{\alpha 4}),$$

$\alpha,\beta,\gamma=1,2,3$ cyclically permuted.

The eigenstates of the equation may then be labelled by 4 indices corresponding to the values of k^+, k^-, k_3^+, k_3^- $(k^+=k^-=k)$ with $-k^+<k_3^+<k^+$, $-k^-<k_3^-<k^-$.

In case of spinors one has to look for the eigenvalues of the operators (total angular momentum)

$$(11)\qquad I_{LK}=K_{LK}+S_{LK},$$

where

$$(12)\qquad S_{LK}=\tfrac{1}{4}[\gamma_L\gamma_K],$$

is the spin $\frac{1}{2}$ tensor expressed by the 4×4 Dirac matrices. In this case

$$(13)\qquad (I^+)^2=\sum_3(I_\alpha^+)^2,\qquad (I^-)^2=\sum_3(I_\alpha^-)^2,$$

with

$$(14)\qquad I_\alpha^\pm=\tfrac{1}{2}[I_{\beta\gamma}\pm I_{\alpha 4}]$$

(6) A. PAIS: *Proc. Nat. Acad. of Sci.*, **40**, 9, 835 (1954).

($\alpha, \beta, \gamma = 1, 2, 3$ cyclically permuted) are now different as shown by the relation

$$(I^{\pm})^2 = 4K^2 + \tfrac{1}{4}(1 \pm \gamma_5)(H + \tfrac{3}{2}),$$

where

$$\gamma_5 = -\gamma_1\gamma_2\gamma_3\gamma_4, \qquad H(H+2) = 4K^2.$$

The labelling of the eigenstates is still given by the eigenvalues of the operators

$$I^+, I^-, I_3^+, I_3^-: \quad I^+ = i^+(i^+ + 1) \quad I^- = i^-(i^- + 1) \quad -i^+ < I_3^+ < i^+ \quad -i^- < I_3^- < i^-.$$

However now, owing to relation (14) only the following choices are possible (for positive eigenvalues of H):

$$(15) \qquad \begin{cases} \gamma_5 = 1 & i^+ = k + \tfrac{1}{2} \quad i^- = k \\ \gamma_5 = -1 & i^+ = k \quad i^- = k + \tfrac{1}{2} \end{cases}$$

Now it is apparent that our baryon and K-meson hypercharge states may well be interpreted as representing the lowest order representation respectively of the spinors and the vector states, by identifying

for baryons: $I^+ = Y \quad I^- = Z \quad I_3^+ = Y_3 \quad I_3^- = Z_3$;

for K-mesons: $I^+ = I^- = K = U = V \quad I_3^+ = K_3^+ = U_3 \quad I_3^- = K_3^- = V_3$.

The following Table expresses the quantum number assignments for the baryons and the K-mesons.

TABLE I.

	N_1	N_4	N_2	N_3	K^+	K^0	$\overline{K^0}$	$\overline{K^-}$
k	0	0	0	0	$\frac{1}{2}$	$\frac{1}{2}$	$\frac{1}{2}$	$\frac{1}{2}$
i^+	$\frac{1}{2}$	$\frac{1}{2}$	0	0	$\frac{1}{2}$	$\frac{1}{2}$	$\frac{1}{2}$	$\frac{1}{2}$
i^-	0	0	$\frac{1}{2}$	$\frac{1}{2}$	$\frac{1}{2}$	$\frac{1}{2}$	$\frac{1}{2}$	$\frac{1}{2}$
I_3^+	$\frac{1}{2}$	$-\frac{1}{2}$	0	0	$\frac{1}{2}$	$\frac{1}{2}$	$-\frac{1}{2}$	$-\frac{1}{2}$
I_3^-	0	0	$\frac{1}{2}$	$-\frac{1}{2}$	$\frac{1}{2}$	$-\frac{1}{2}$	$\frac{1}{2}$	$-\frac{1}{2}$

The assignments are quite consistent with the usual ones as are the selection rules obtained for them. Thus, hypercharge and hypernumber conservation and independence are expressed by the conservation of I^+, I^-, I_3^+, I_3^- in all reactions. Of course, contemporary constance of both hypercharge and hypernumber ensures also that all M_{ik} are constants of the motion.

Let us now consider the F' term

$$(16) \qquad -iF'\overline{\Psi}\omega_K' \times \Gamma^5 \varphi_K' \Psi,$$

of K interactions and let us construct the analogous expressions $\boldsymbol{Y}'$ and $\boldsymbol{Z}'$ as obtained from (4) and (13) when the ω' matrices are substituted to the ω ones

$$M'_{ik} = \frac{i}{4}[\omega'_i \omega'_k], \qquad \left.\begin{matrix} Y'_\alpha \\ Z'_\alpha \end{matrix}\right\} = \frac{1}{2}[M'_{\beta\gamma} \pm M'_{\alpha 4}].$$

One thus obtains

$$(17) \qquad Y'_1 = -Y_1, \quad Y'_2 = -Y_2, \quad Y'_3 = Y_3, \quad Z'_1 = Z_1, \quad Z'_2 = Z_2, \quad Z'_3 = Z_3.$$

Now, in the same way as the preceding case, one may verify that the expressions Y'_1+U_1, Y'_2+U_2, Y'_3+U_3; Z_1+V_1, Z_2+V_2, Z_3+V_3 commute with the Hamiltonian (16) and are therefore also in this case constants of the motion.

However, Y_1+U_1, Y_2+U_2 do not commute with (16) and Y'_1+U_1, Y'_2+U_2 do not commute with (3).

Therefore, when the whole Hamiltonian is considered, while of course hypercharge conservation still holds, this is no more true for the total hypercharge spin, and hypercharge independence is destroyed. This is exactly what was to be expected as the total Hamiltonian (1) includes the baryon mass differences whose consideration, of course, must destroy hypercharge independence.

However, as the hypernumber vector components are the same, whichever set of ω_K or ω'_K matrices is considered, the total hypernumber vector remains still a constant of the motion for the whole Hamiltonian (1), so that hypernumber independence holds even when baryon mass differences are included.

If the preceding approach for K interactions contains any truth, some preliminary consequences of it may be easily deduced concerning different interaction phenomena. In fact, as in the case of isotopic spin, approximate hypercharge independence and exact hypernumber independence should allow to treat all K interaction phenomena through scattering and interaction amplitudes depending only on total hypercharge and hypernumber spin in case of neglect of baryon mass differences, and on total hypernumber spin only when baryon mass differences are considered. Then if we label the scattering amplitudes by $a(I^+I^-)$ in the first case and by $a(I^+I_3^+I^-)$ in the second case, all K interaction phenomena related to different hypermultiplets (we consider pions as labelled by hypercharge and hypernumber spin 0) should be ruled by the amplitudes given in the Table II.

One may remark that K^+ nucleon scattering should occur in a pure $a(1, \frac{1}{2})$ state, while K^- nucleon scattering should be a mixture of $a(1, \frac{1}{2})$ and $a(0, \frac{1}{2})$ state. Moroever, if baryon mass differences are considered, the $a(1, 1, \frac{1}{2})$ amplitude for K^+ scattering is different from the $a(1, 0, \frac{1}{2})$ amplitude of K^- scattering by an order of 25% as indicated by $(m_\Xi - m_N)/m_\Xi \simeq 0.29$.

The two kinds of phenomena should therefore be rather disconnected as in fact seems to be indicated by actual data .

K-captures should occur in a $a(0, \frac{1}{2})$ state only. For associated production only the Y+K states corresponding to a $a(\frac{1}{2}, 0)$ amplitude should be produced in pion nucleon interaction.

At this point, one may observe that the quantum numbers assignment for baryons due to K interactions do not allow to distinguish between the two members of a single doublet (*i.e.* between proton and neutron), which are discriminated only when pion interactions are introduced, to which of course the normal isospin formalism has to

TABLE II.

I^+	I^-	I_3^+	I_3^-	$a(I^+I^-)$ (equal baryon masses)	$a(I^+I_3^+I^-)$ (different baryon masses)	multiplets	related phenomena
0	$\frac{1}{2}$	0	$\frac{1}{2}$ $-\frac{1}{2}$ $\frac{1}{2}$ $-\frac{1}{2}$ $\frac{1}{2}$ $-\frac{1}{2}$	$a(0, \frac{1}{2})$	$a(0, 0, \frac{1}{2})$	$N_2 (+\pi)$ $N_3 (+\pi)$ $N_1\overline{K}^0$ $N_1\overline{K}^-$ N_4K^+ N_4K^0	K^- scattering K^- capture
$\frac{1}{2}$	0	$\frac{1}{2}$	0	$a(\frac{1}{2}, 0)$	$a(\frac{1}{2}, \frac{1}{2}, 0)$	$N_1(+\pi)$ N_2K^0 N_3K^+	associated production
		$-\frac{1}{2}$			$a(\frac{1}{2}, -\frac{1}{2}, 0)$	$N_4(+\pi)$ $N_2\overline{K}^-$ $N_3\overline{K}^0$	
1	$\frac{1}{2}$	1	$\frac{1}{2}$ $-\frac{1}{2}$	$a(1, \frac{1}{2})$	$a(1, 1, \frac{1}{2})$	N_1K^+ N_1K^0	K^+ scattering
		0	$\frac{1}{2}$ $-\frac{1}{2}$ $\frac{1}{2}$ $-\frac{1}{2}$		$a(1, 0, \frac{1}{2})$	$N_1\overline{K}^0$ $N_1\overline{K}^-$ N_4K^+ N_4K^0	$\overline{K}^-$ scattering
		-1	$\frac{1}{2}$ $-\frac{1}{2}$		$a(1, -1, \frac{1}{2})$	$N_4\overline{K}^0$ $N_4\overline{K}^-$	
$\frac{1}{2}$	1	$\frac{1}{2}$	1 0 0 -1	$a(\frac{1}{2}, 1)$	$a(\frac{1}{2}, \frac{1}{2}, 1)$	N_2K^+ N_2K^0 N_3K^+ N_3K^0	associated production
		$-\frac{1}{2}$	1 0 0 -1		$a(\frac{1}{2}, -\frac{1}{2}, 1)$	$N_2\overline{K}^0$ $N_2\overline{K}^-$ $N_3\overline{K}^0$ $N_3\overline{K}^-$	

be applied and extended to all four baryon doublets. If we complete our assumptions of independence between isospin and hypercharge spaces, we should consider all K-mesons as 0 isospin singlets. So all reactions should be ruled by both hypernumber and isospin independence, and interaction probabilities should be obtained by the product of a hypernumber amplitude and an isospin amplitude.

As an example let us consider the K nucleon states; for which the whole set of quantum number values is given in Table III. Their reaction probabilities should be given by the product of the $a(1, \frac{1}{2})$ amplitudes for hypercharge with the b amplitudes for isospin.

TABLE III.

	i^+	i^-	I_3^+	I_3^-	T	T_3	$T_3 + I_3^-$
pK^+	1	$\frac{1}{2}$	1	$\frac{1}{2}$	$\frac{1}{2}$	$\frac{1}{2}$	1
nK^+	1	$\frac{1}{2}$	1	$\frac{1}{2}$	$\frac{1}{2}$	$-\frac{1}{2}$	0
pK^0	1	$\frac{1}{2}$	1	$-\frac{1}{2}$	$\frac{1}{2}$	$\frac{1}{2}$	0
nK^0	1	$\frac{1}{2}$	1	$-\frac{1}{2}$	$\frac{1}{2}$	$-\frac{1}{2}$	-1

Now the complete independence between hypercharge and isospin spaces of the present approach is convalidated by the commutation of isospin operators with the K interaction term and hypercharge and hypernumber operators with the pion interaction term of the Hamiltonian. Then T_3 and I_3^- should be independent quantum numbers separately conserved; and this should forbid in the case we consider the charge-exchange reaction

$$K^+ + n \to p + K^0 ,$$

and in other cases and for similar reasons the reactions

$$K^- + p \to n + K^0 , \qquad \pi^+ + p \to \Sigma^+ + K^+ , \qquad K^- + p \to \Sigma^+ + \pi^- .$$

These same reactions were shown by PAIS to be forbidden in the doublet approximation [4], and it is therefore quite natural, as the present scheme is equivalent to the doublet approximation that the same result is also obtained.

It is well-known, however, that these forbidden reactions exist and are of the same order of magnitude as the not forbidden ones, which fact shows clearly that the doublet approximation in itself is certainly inadequate to explain our present data. We think that the present approach may shed some light on the direction into which the doublet approximation should be modified according to the following considerations. With the present quantum numbers it is evident that T_3, 3rd component of isospin, labels the different substates of the baryon doublets only, while the hypernumber I_3^- labels the different substates of the K-meson. If these substates of baryons and K-mesons were distinguished by some independent physical agents, then probably the complete independence between hypercharge space and isospin space postulated in the scheme should in fact be realized and the reactions now discussed in fact forbidden. It happens, however, that both baryon and K-meson substates are marked by the same physical agent which is electric charge. This degeneration probably establishes a link between hypercharge space and isospin space, whose consequence is that only the sum of T_3 plus I_3^- (which is related to the electric charge) is conserved and not T_3 and I_3^- separately and this would allow reactions such as (17) to occur.

* * *

We wish to express our warmest thanks to Dr. A. SCHRÖDER for many discussions and helpful advices concerning the present subject.

IL NUOVO CIMENTO Vol. XIV, N. 1 1° Ottobre 1959

The Pair Distribution Function of a System of Bose Hard Spheres, Calculated up to the First Order in a/λ (*).

L. Colin (**) and J. Peretti

University of Maryland - College Park, Maryland

(ricevuto il 18 Luglio 1959)

Recently a certain number of papers (1) have appeared, dealing with the Binary Collision Expansion (BCE) method in the many body problem. The method has been used primarily to derive an expression for the grand potential of Kramers for a Fermi or a Bose system of particles interacting via a two body hard sphere potential of radius a. The result is given as a power series expansion in a/λ where λ is the thermal wave length given by $\lambda = h(2\pi mkT)^{-\frac{1}{2}}$. One can get the same result for the boson case to the first order in a/λ, by using the concept of « torons » (2).

In what follows, we have used the BCE method to derive, to the first order in a/λ, the pair distribution function (p.d.f.) of a Bose system of hard spheres.

In general the p.d.f. $\varrho^{(2)}(\boldsymbol{r}_1, \boldsymbol{r}_2)$ can be calculated in the grand canonical ensemble by using the formulae (3):

$$\varrho^{(2)}(\boldsymbol{r}_1, \boldsymbol{r}_2) = F^{(2)}(\boldsymbol{r}_1, \boldsymbol{r}_2) + \varrho_0^2 , \tag{1}$$

$$F^{(2)}(\boldsymbol{r}_1, \boldsymbol{r}_2) = \sum_{p=0}^{\infty} A_p^{(2)}(\boldsymbol{r}_1, \boldsymbol{r}_2) z^{p+2} , \tag{2}$$

$$A_p^{(2)}(\boldsymbol{r}_1, \boldsymbol{r}_2) = \frac{1}{p!} \int U_{p+2}(\boldsymbol{r}_1, \boldsymbol{r}_2, \boldsymbol{t}_1 \dots \boldsymbol{t}_p;\ \boldsymbol{r}_1, \boldsymbol{r}_2, \boldsymbol{t}_1 \dots \boldsymbol{t}_p)\, \mathrm{d}^3 t_1 \dots \mathrm{d}^3 t_p , \tag{3}$$

where ϱ_0 and z are the molecular density and the fugacity of the system respectively and U_n the n-th cluster function defined in ref. (1).

(*) This research was partially supported by the United States Air Force, Office of Scientific Research, Air Research and Development Command under Contracts no. AF 18(600)1315 and no. AF 49(638)399.

(**) On leave from Instituto Nacional de la Investigacion Cientifica, Mexico.

(1) T. D. Lee and C. N. Yang: *Phys. Rev.*, **113**, 1165 (1959), and subsequent papers (to be published). Cfr. also prior work by K. Huang and C. N. Yang: *Phys. Rev.*, **105**, 767 (1956).

(2) E. W. Montroll and J. C. Ward: *Phys. of Fluids*, **1**, 55 (1958). J. Peretti: Technical Report no. 119, University of Maryland.

(3) E. W. Montroll, A. Isihara and S. Fujita: *Bull. of Royal Academy of Science of Belgium*, **44**, 1018 (1958). L. Colin and J. Peretti: *Compt. Rend.*, **248**, 1625 (1959).

Following the BCE method, one can evaluate the Bose U's in terms of the classical U's; if we restrict ourselves to a calculation up to the first order in a/λ, only a knowledge of the classical U_2 function is required. In momentum space U_2 is given by:

$$(4)\quad U_2(\boldsymbol{k}_1'\boldsymbol{k}_2'|\boldsymbol{k}_1\boldsymbol{k}_2) = \partial(\boldsymbol{K}-\boldsymbol{K}')\exp\left[-\frac{\boldsymbol{K}^2}{4\alpha}\right]\left(\frac{-a}{\pi^2}\right)\frac{\exp[-\boldsymbol{k}^2/\alpha]-\exp[-\boldsymbol{k}'^2/\alpha]}{\boldsymbol{k}'^2-\boldsymbol{k}^2},$$

where $\alpha=\hbar^{-2}mkT=2\pi\lambda^{-2}$, and where $(\boldsymbol{K},\boldsymbol{K}')$ and $(\boldsymbol{k},\boldsymbol{k}')$ are the final and initial, total and relative wave vectors for the two interacting particles; the general Bose U_n function is then a sum of products whose factors are free particle propagators U_1 and the binary kernel U_2, the latter one appearing at most once. Integrating over the coordinates of all the particles except 1 and 2, as required by Eq. (3), and using the following shorthand notations:

$$(5)\qquad g_\sigma(z)=\sum_{n=1}^{\infty}\frac{z^n}{n^\sigma}; \qquad g_\sigma(z,s)=\sum_{n=1}^{\infty}\frac{z^n}{n^\sigma}\exp\left[-\frac{s^2}{n}\right],$$

we get [5] (with $r=|\boldsymbol{r}_1-\boldsymbol{r}_2|$):

$$(6)\quad \lambda^6F^{(2)}(\boldsymbol{r}_1,\boldsymbol{r}_2)=\left[g_{\frac{3}{2}}\left(z,\frac{r}{\lambda}\sqrt{\pi}\right)\right]^2-\frac{8a}{\lambda}g_{\frac{3}{2}}(z)g_{\frac{3}{2}}\left(z,\frac{r}{\lambda}\sqrt{\pi}\right)\cdot$$
$$\cdot g_{\frac{1}{2}}\left(z,\frac{r}{\lambda}\sqrt{\pi}\right)-\frac{8a}{\lambda}\frac{\lambda}{r}\left[g_{\frac{3}{2}}\left(z,\frac{r}{\lambda}\sqrt{\pi}\right)\right]^2+0\left(\frac{a^2}{\lambda^2}\right).$$

In this expression the first term corresponds to the ideal Bose gas and is in agreement with the London-Placzek formula [4]; the next two terms represent the corrections, to the first order in a/λ, due to the hard sphere interaction.

---

[4] F. London: *Journ. Chem. Phys.*, **11**, 203 (1943). G. Placzek: *Proc. of the 2nd Berkeley Symposium on Math. Statistics and Probability*, p. 581.

[5] Detailed calculations are available upon request.

IL NUOVO CIMENTO Vol. XIV, N. 1 1° Ottobre 1959

Further Study of Proton-Proton Interactions at 970 MeV.

J. D. Dowell, E. C. Fowler (*), J. G. Hill, G. Martelli (**), B. Musgrave and L. Riddiford

Department of Physics, University of Birmingham

(ricevuto il 26 Luglio 1959)

1. – The analysis of proton-proton interactions at 970 MeV performed by A. P. Batson, B. B. Culwick, J. G. Hill and L. Riddiford [1] has given useful information about the mechanism of the nucleon-nucleon interaction, as deduced from cross-sections and angular and momentum distributions of the secondary particles.

On the other hand it seemed desirable to check

a) the evidence for parity conservation in pion production, and

b) the features of certain angular distributions of the inelastic events, which might give additional information on the preference of the secondary particles for various angular momentum states (as suggested by G. Morpurgo [2]).

With this in mind we have searched for any indication of parity violation in pion production processes. We have also performed a further analysis of the π^+ producing events observed by Batson *et al.* in terms of the crude but simple isobar model.

The data used in the present work were obtained by means of a diffusion cloud chamber placed in a magnetic field of 13 000 gauss [1]. We have studied 565 elastic interactions and 328 π^+ producing interactions, the original data having been used to select and classify each event, as described in [1]. The additional work consisted of collecting the existing data in new ways and in calculating angular distributions and related quantities with respect to directions different from those used previously. To evaluate the possible simulation of such effects by polarization of the primary protons used in this experiment, a check was first made on the right-left asymmetry in the distribution of the secondaries from $p+p \to p+n+\pi^+$ and also $p+p \to p+p$.

2. – Check on possible polarization effects.

If the incident proton beam is polarized, there will exist a right-left asymmetry for the elastically scattered protons. Before proceeding with the ana-

(*) Permanent address: Yale University, U.S.A.

(**) On leave of absence from University of Pisa, Italy.

[1] A. P. Batson, B. B. Culwick, J. G. Hill and L. Riddiford: *Proc. Roy. Soc.*, A 251, 218 (1959).

[2] G. Morpurgo: *Nuovo Cimento*, **9**, 564 (1958).

lysis, the distribution of the azimuthal angle of scattering was examined.

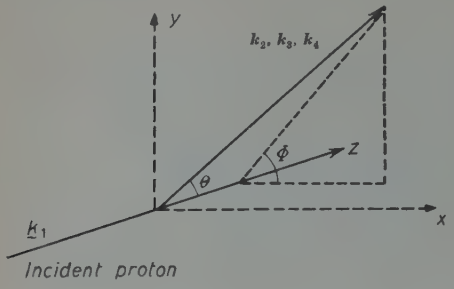

Fig. 1.

In Fig. 1 the meaning of the angles defining the direction of the secondary particle is illustrated. In an elastic scattering, the proton of smaller Θ_L is considered to be the scattered proton and the other the recoil proton.

In Fig. 2*a* and 2*b* histograms of the azimuthal distributions are given for elastic events selected according to the following limits on Θ_L:

(*a*)	$0° \leqslant \Theta_L \leqslant 39°$	552 events.
(*b*)	$7° \leqslant \Theta_L \leqslant 39°$	484 events.

The cut-off at 7° in (*b*) has been introduced to remove the bias due to small angle scanning losses. The 39° limit represents the angle in the laboratory system at which the polarization goes to zero ($\Theta_L = 39°$ corresponds to $\Theta_{c.m.} = 90°$).

In computing $\varepsilon = (R - L)/(R + L)$

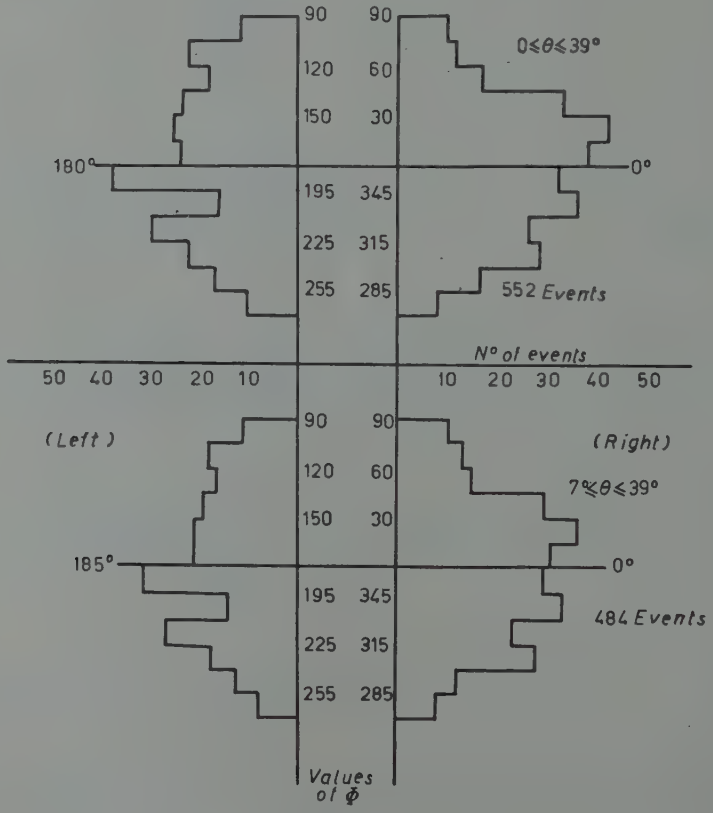

Fig. 2.

only events with $315° \leqslant \varphi \leqslant 45°$ and $135° \leqslant \varphi \leqslant 225°$ were used (*).

In Table I, L and R are the number of protons scattered to the left and to the right, respectively. Δ is the difference between R and L in units of standard deviations, and p is the probability of the given right-left asymmetry occurring by purely statistical fluctuation. Although the statistics are poor, the values of p are sufficiently small to conclude that

TABLE I. – *Elastic asymmetries.*

	L	R	ε	$\Delta = \frac{R-L}{\sqrt{R+L}}$	p
a	154	205	0.142	2.69	0.01
b	131	182	0.163	2.88	0.005

a) the proton beam used in the experiment (1) was polarized,

b) polarized protons are produced in the elastic scattering of protons by protons at 970 MeV.

Moreover, assuming a polarization of about $\frac{1}{3}$ for the incident beam (3) and taking the polarization in the elastic p-p scattering to be also about $\frac{1}{3}$ (**), the computed asymmetry is about 0.11, to be compared with the observed value of 0.15. The above procedure is justified since, although the cross-section for p-p scattering varies considerably from 450 MeV to 635 MeV (4), the average polarization as well as the dependence of the polarization on scattering angle remain practically unchanged.

For the inelastic events, no right-left asymmetries were found in the azimuthal distributions of the secondary particles. It was therefore assumed that the parity check would not be affected by the polarization of the incident beam.

3. – Check on parity conservation.

To test whether parity is conserved in the interaction $p+p \to p+n+\pi^+$, we looked for pseudoscalar quantities in the cross-section. The average value of any such terms should vanish if parity is conserved. Let us call $\boldsymbol{k}_1$, $\boldsymbol{k}_2$ and $\boldsymbol{k}_3$ the unit vectors associated with the directions of the incident proton, the emitted proton and the π^+, respectively. Possible pseudoscalar products which are most obviously suggested are:

$$(a) \qquad \boldsymbol{k}_1 \cdot (\boldsymbol{k}_2 \wedge \boldsymbol{k}_3) ,$$

$$(b) \qquad \boldsymbol{k}_1 \cdot (\boldsymbol{k}_2 \wedge \boldsymbol{k}_3)(\boldsymbol{k}_1 \cdot \boldsymbol{k}_2)$$

$$(c) \qquad \boldsymbol{k}_1 \cdot (\boldsymbol{k}_2 \wedge \boldsymbol{k}_3)(\boldsymbol{k}_1 \cdot \boldsymbol{k}_3)$$

$$(d) \qquad \boldsymbol{k}_1 \cdot (\boldsymbol{k}_2 \wedge \boldsymbol{k}_3)(\boldsymbol{k}_2 \cdot \boldsymbol{k}_3) .$$

In the absence of strong polarization effects, the identity of the two protons requires that, on the average, term (*a*)

(*) No corrections for scanning bias have been employed here, *i.e.* a constant efficiency of scanning was assumed for the regions in which φ was accepted. One attempt to correct the data for possible scanning bias gave a value of ε in good agreement with the quoted value.

(3) M. HUQ: *Ph. D. Thesis* (University of Birmingham, 1958).

(**) This figure is inferred from values obtained, at lower energies (4), by means of an average over the polarization in the angular interval concerned, using the differential cross-section as a weighting factor.

(4) M. G. MEŠERIAKOV, S. B. NURUŠEV and G. STOLITOV: *Žurn. Éksper. Teor. Fiz.*, **33**, 37 (1957).

should vanish. Fig. 3*a* shows this to be the case. If the distribution in any one of the terms (*b*), (*c*) or (*d*) were not now the distributions of these three pseudoscalars. It is seen that they are symmetrical and their contribution to the cross-section is therefore nil.

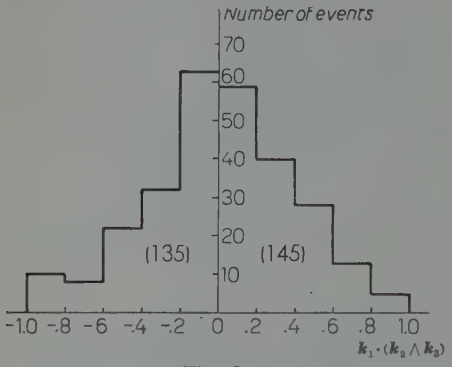

Fig. 3*a*.

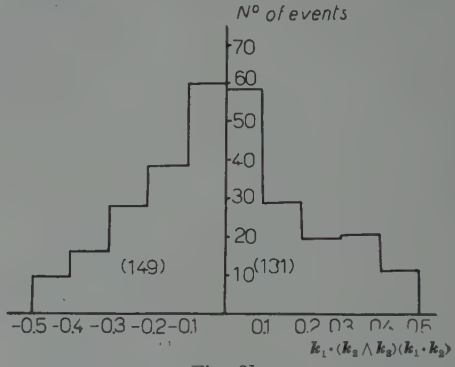

Fig. 3*b*.

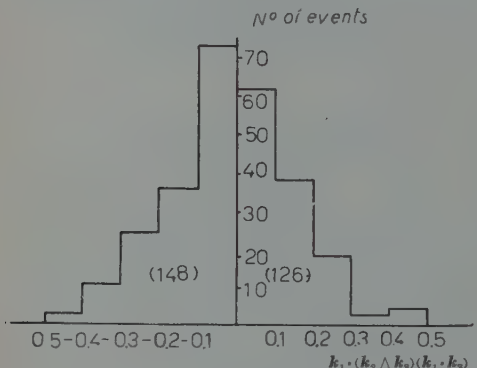

Fig. 3*c*.

4. – Further angular distributions.

An analysis has been attempted in terms of certain angular distributions, assuming the existence of an intermediate isobar state for the pion and the proton (5). The angles which have been calculated are

a) χ, the angle between the pion direction and the line of flight of the isobar in the center of mass frame of the isobar,

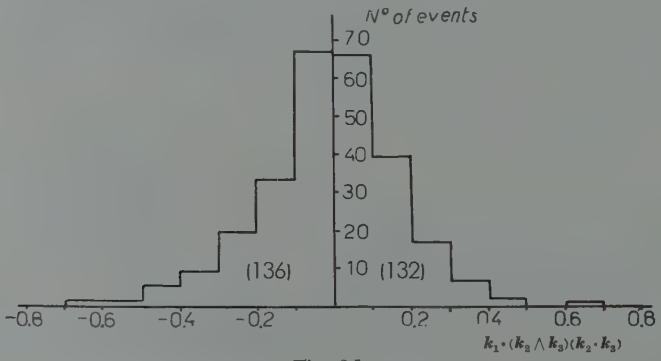

Fig. 3*d*.

symmetrical, one would suspect that parity were violated. In Fig. 3*b*, 3*c* and 3*d* are given the histograms showing

(5) S. J. LINDENBAUM and R. M. STERNHEIMER: *Phys. Rev.*, **105**, 1874 (1957).

b) Φ, the angle between the production plane of the isobar and the decay plane, in the center of mass system of the isobar. If we define the direction of the neutron by a fourth unit vector $\boldsymbol{k}_4$, the angle is given by the following expression

$$\cos \Phi = \frac{(\boldsymbol{k}_1 \wedge \boldsymbol{k}_4) \cdot (\boldsymbol{k}_3 \wedge \boldsymbol{k}_4)}{|\boldsymbol{k}_1 \wedge \boldsymbol{k}_4| \, |\boldsymbol{k}_3 \wedge \boldsymbol{k}_4|} .$$

It has been suggested that these distributions may prove appropriate to establish the prevalence of the $T=J=\frac{3}{2}$ pion-nucleon resonant state.

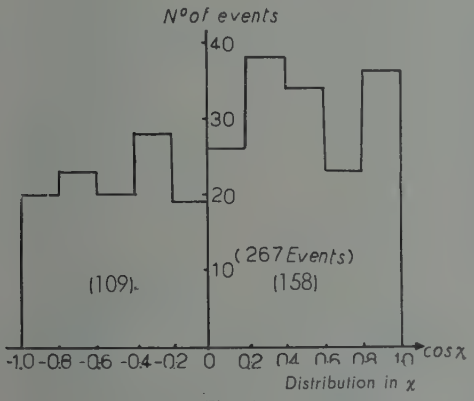

Fig. 4.

The distribution in χ is given in Fig. 4 and shows a forward-backward asymmetry of 2.68 standard deviations. The distribution in Φ is presented in Fig. 5.

The effects on these distributions of a final state interaction in the production process, and of the polarization of the incident proton beam, have been partially investigated, but it is not possible to draw the definite conclusions as suggested by G. MORPURGO [2], without performing detailed calculations similar to these of S. MANDELSTAM [6].

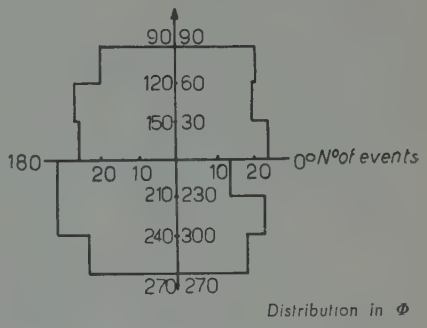

Fig. 5.

It also appears plausible that some asymmetry could arise from a bias introduced by selecting events sufficiently well measured to complete the conversion to the center of mass system.

* * *

Thanks are due to Mr. L. CASTILLEJO and Mr. G. MCCAULEY for very helpful discussions. One of us (E.C.F.) wishes to take this opportunity to acknowledge the support of the U.S. Educational Commission in the United Kingdom.

---

(6) S. MANDELSTAM: *Proc. Roy. Soc.*, A **244**, 491 (1958).

460 MeV Negative Pion Scattering from Neutrons in a Propane Bubble Chamber.

J. Ballam (*) and J. Hang

Department of Physics, Michigan State University - East Lansing, Mich.

J. H. Scandrett and W. D. Walker (**)

Department of Physics, University of Wisconsin - Madison, Wisc.

(ricevuto il 3 Agosto 1959)

The purpose of this note is to describe an experiment which compares the angular distribution in (π^+-p) scattering with that from (π^--n) scattering at roughly the same energy The (π^+-p) data were obtained from Willis [1] at 500 MeV, Erwin and Kopp [2] at 950 MeV and Glaser *et al.* [3] at 1.1 GeV. The first two groups used a hydrogen bubble chamber and the third a propane chamber. The (π^--n) data were obtained in a propane chamber operated at the Cosmotron of the Brookhaven National Laboratory and the apparatus has been briefly described elsewhere [4].

Since the (π^--n) data were obtained from scattering of (460 ± 50) MeV pions from neutrons bound in a carbon nucleus, two main corrections have to be made before a direct comparison can be made with the (π^+-p) data which were obtained from free protons. These are (1) corrections for the motion of the neutron and (2) corrections for the diffraction scattering of the pions by the carbon nuclei. The raw data consisted of some 900 « deflections » of a beam of negative pion of energy (460 ± 50) MeV sent into the chamber. A deflection was characterized by an abrupt change of direction of the beam pion unaccompanied by any charged particle. All deflections with

(*) Supported in part by a grant from the National Science Foundation.

(**) Supported in part by the U.S. Atomic Energy Commission.

(1) W. J. Willis: *Proc. of the CERN High Energy Physics Conference* (1958), p. 68.

(2) A. Erwin and J. Kopp: private communication.

(3) D. Glaser and A. Rollig: *Proc. of the CERN High Energy Physics Conf.* (1958), p. 68.

(4) Crittenden, J. H. Scandrett, Shephard, W. D. Walker and J. Ballam: *Phys. Rev. Lett.*, **2**, 121 (1959).

angles greater than 6 degrees were counted. The total cross-section for all deflection events with angles $> 6°$ was computed to be (106 ± 5) mb based on a carbon cross-section for all events of (316 ± 16) mb [5]. The angular distribution for deflections is shown by the histograms in Figs. 1 and 2.

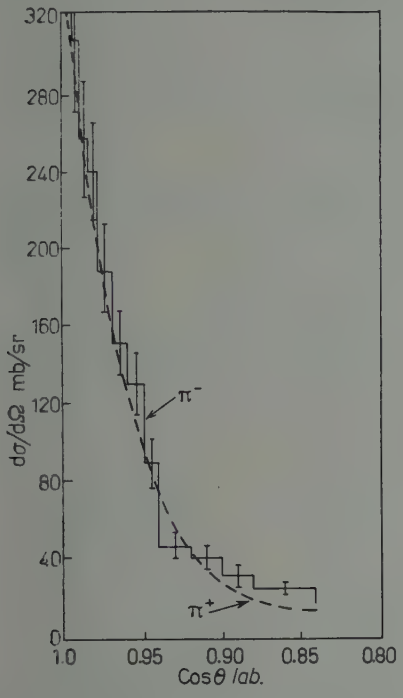

Fig. 1. – Histogram of the π^- deflection events in the propane chamber for $\theta < 32°$ in the laboratory. These are considered as a mixture of diffraction and scattering. The dotted curve is the modified 500 MeV (π^+-p) distribution.

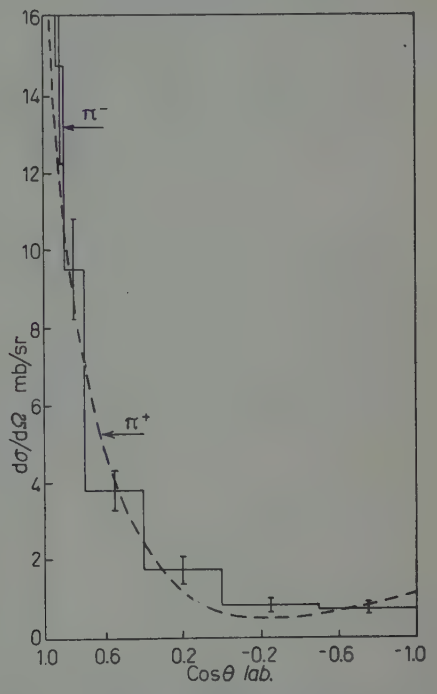

Fig. 2. – Histogram of π^- deflections for $\theta > 32°$ in the laboratory. These are considered mainly (π^--n) scatterings. The dotted curve is the modified 500 MeV (π^+-p) distribution.

The corrections were made by modifying the distributions given for the (π^+-p) data by using a Serber model [6,7] and giving the proton a Gaussian momentum distribution, isotropic in direction and with a mean value of 190 MeV/c. The suppression of small energy transfers (< 25 MeV) by the Pauli principle has been neglected [8]. The laboratory angular distribution is then completely determined by p^* (the momentum of the pion in the center of mass) and β, the velocity of the center of mass. Each collision is then treated as the scattering of pion from a stationary proton. However, the pions now are given a whole range of momenta and directions differing somewhat from the actual beam direction. In each case β is constant.

([5]) J. W. CRONIN: private communication. Total cross-sections for carbon at somewhat higher energies have been made by J. W. CRONIN, R. COOL and A. ABASHIAN: *Phys. Rev.*, **107**, 1121 (1957).

([6]) R. SERBER: *Phys. Rev.*, **72**, 1114 (1947).

([7]) J. CLADIS: *Thesis* (University of California, 1952).

([8]) T. K. FOWLER: *Phys. Rev.*, **112**, 1325 (1958).

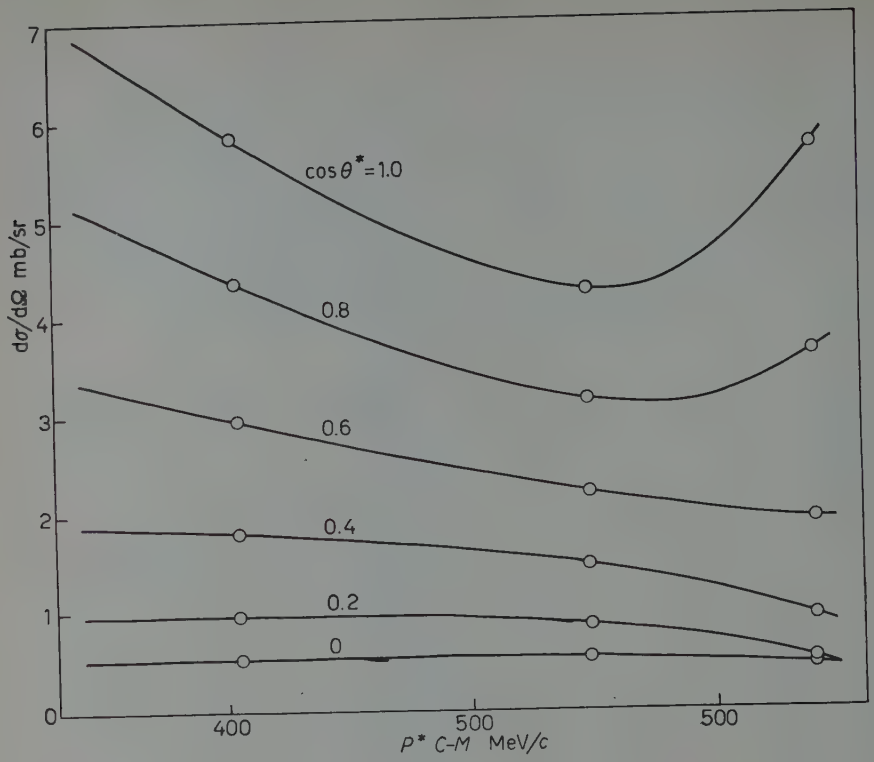

Fig. 3.

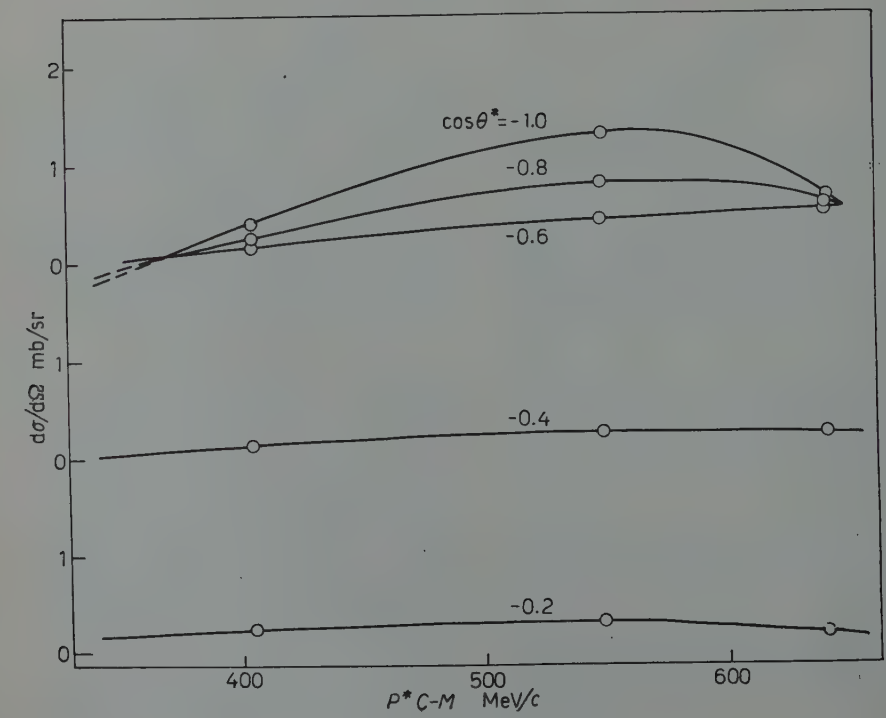

Fig. 4.

Figs. 3-4. – The differential cross-section for (π^+-p) scattering in the energy range (350 ÷ 650) MeV for various C.M. scattering angles.

The differential cross-sections at a given center-of-mass angle as a function of energy have been measured [1-3] and are shown in Figs. 3 and 4. Thus the effect of using a band of momenta for the incoming pion can be calculated. The effect of varying the direction has been averaged out by a stepwise numerical integration. The result of this entire calculation is shown in Fig. 5, from which it can be seen that the effect of the moving nucleon is not very large at these energies. An experimental verification of this calculation was made by comparing the angular distribution of (π^--p) scatterings from protons in carbon (quasi-elastic events) with (π^--p) scatterings from free hydrogen in our propane chamber and is shown in Fig. 6. The results check quite satisfactorily.

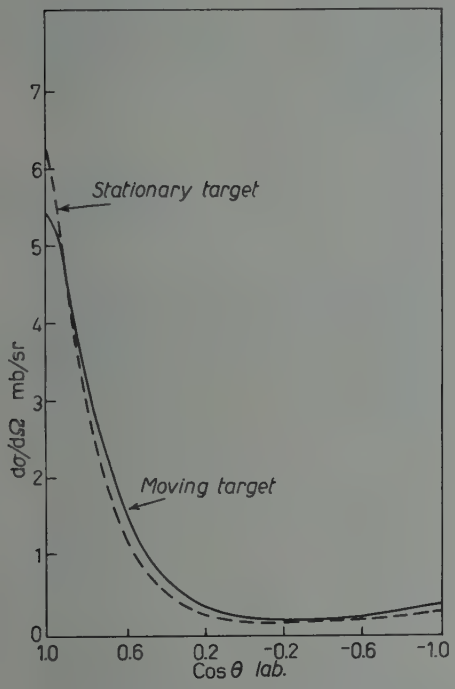

Fig. 5. – Comparison of the differential elastic (π^+-p) cross-section at 500 MeV for a stationary proton and one bound in a carbon nucleus. The stationary data are derived from WILLIS [3].

There remains the diffraction scattering. For this purpose we assumed a black sphere model in which

$$(1) \qquad \frac{d\sigma_{(diff.)}}{d\Omega} = \frac{\sigma_{(diff.)}}{\pi}\left[\frac{J_1(k^*R\sin\theta^*)}{\sin\theta^*}\right],$$

where $k^* = \hbar/p^*$ and $R = r_0 A^{\frac{1}{3}}$ are the wave number of the incident pion and the radius of the nucleus respectively and r_0 and $\sigma_{(diff.)}$ are parameters to be determined from the data. It was assumed that the laboratory and center of mass systems were the same for a diffraction event.

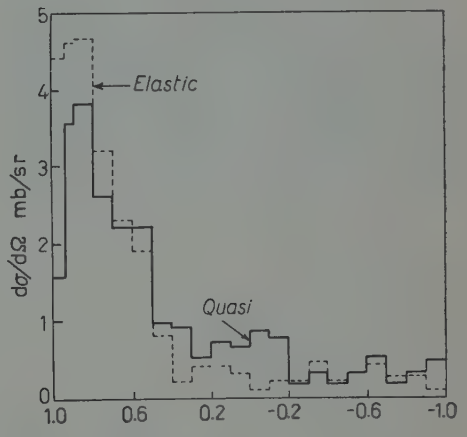

Fig. 6. – Comparison of experimentally obtained differential cross-sections for (π^--p) scatterings at 460 MeV for a stationary proton and for a proton bound in a carbon nucleus.

In this analysis we have assumed that the deflection events are due to two main causes; diffraction and pion-neutron scattering. There is also the possibility that some of the deflections were 1 π^--2 n stars with the π's having a large kinetic energy. To check on this background we looked for 1 π^--1 p stars with fast π's. We assumed that most of these were really 1 π^--1 p-1 n stars and that the number of π^--2 n stars would not exceed this number. The number of

1 π^--1 p-? n stars was 28, as compared with 900 deflections and is considered negligible. Events corresponding to π^0 production on neutrons ($\pi^- + n \to \pi^- + \pi^0 + n$) were eliminated because the resulting π^- had low kinetic energy.

The best fit to the forward peak gave $\sigma_{(\text{diff.})} = 78$ mb and $r_0 = 1.1 \cdot 10^{-13}$ cm. The calculation was carried out to the first minimum only. We can then write:

$$(2) \qquad \frac{d\sigma_{(\text{defl.})}}{d\Omega} = \frac{d\sigma_{(\text{diff.})}}{d\Omega} + n_{\text{eff.}} \frac{d\sigma_{(\pi^- - n)}}{d\Omega},$$

where $n_{\text{eff.}}$ is the effective number of neutrons in the carbon nucleus taking part in the scattering. To find $n_{\text{eff.}}$ we compare the number of quasi-elastic (π^--p) scatterings with those from free hydrogen in the propane and assume this ratio applies to π^+ mesons in propane. We find $n_{\text{eff.}} = 3.3$. If charge symmetry is to hold we must have

$$(3) \qquad \frac{d\sigma_{(\text{defl.})}}{d\Omega} = 3.3 \frac{d\sigma_{(\pi^+ - p)}}{d\Omega} + \frac{d\sigma_{(\text{diff.})}}{d\Omega}.$$

The fit of equation (3) to the histogram of deflections is shown in Figs. 1 and 2 with a χ^2 test giving an $\varepsilon = 0.05$ for the forward angles in Fig. 1 and $\varepsilon = 0.2$ for the larger angles in Fig. 2. The large angle events are relatively free of the inherent difficulties in making the diffraction corrections under simple assumptions.

* * *

We wish to thank Drs. G. B. COLLINS and W. MOORE of the Brookhaven Staff for their co-operation during the experiments and Drs. ERWIN and KOPP for advance information on the π^+-p data at 950 MeV. Two of us (J. BALLAM and J. HUANG) wish to acknowledge helpful discussions with Drs. D. LICHTENBERG and J. KOVACS.

IL NUOVO CIMENTO Vol. XIV, N. 1 1° Ottobre 1959

Paramagnetic Resonance in the Free Hydroxyl Radical(*).

H. E. Radford

National Bureau of Standards - Washington, D.C.

(ricevuto il 3 Agosto 1959)

Microwave measurements [1] of Λ-doubling in OH have given detailed information on the structure of the ground $^2\pi$ electronic term, including a partial measurement of its hyperfine structure (hfs). The Λ-doubling also permits the observation of electric dipole (ED) Zeeman spectra at microwave frequencies. These Zeeman spectra can complement the zero-field work by providing new Λ-doubling and hfs data, and are of separate interest as a test of the molecular Zeeman theory in a mathematically tractable case. Detection of ED Zeeman spectra by standard paramagnetic resonance methods is feasible if the microwave electric field at the gaseous absorption sample is arranged to have a component normal to the dc magnetic field [2].

We have observed paramagnetic resonance in electrically discharged water vapor. Products of the discharge, which was excited by a 2450 MHz diathermy generator, were continuously pumped through a pillbox-shaped quartz absorption cell that filled the cylindrical TE_{011} cavity of an X-band spectrometer. A slow field sweep over the range $(0 \div 12\,000)$ G disclosed three well defined groups of lines, centered at 5520, 8065 and 9965 G; derivative recordings are shown in Fig. 1. Under similar ob-

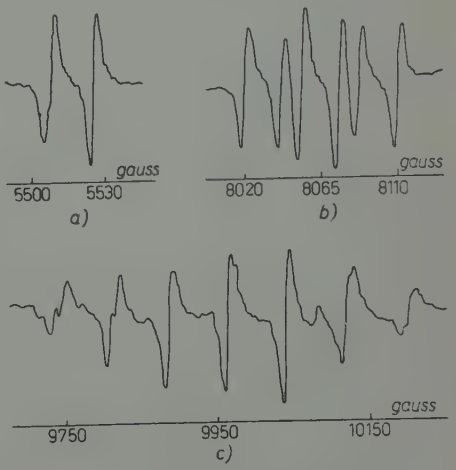

Fig. 1. – Paramagnetic resonance spectrum of electrically discharged water vapor (derivative recordings). The three line groups were recorded at different vapor pressures. Microwave frequency: 8894 MHz.

(*) This research was performed under the National Bureau of Standards Free Radicals Research Program, supported by the Department of the Army.

(1) G. C. Dousmanis, T. M. Sanders and C. H. Townes: *Phys. Rev.*, **100**, 1735 (1955).

(2) R. Beringer and E. B. Rawson: *Phys. Rev.*, **94**, 343 (1954).

serving conditions the relative intensities of lines in Fig. 1 (*a*), (*b*) and (*c*) were about 15, 5 and 1, respectively. At a vapor pressure of roughly 1 mm Hg a typical line width was 5 G; pressure broadening was apparent. The spectra of Fig. 1 were assigned to the OH radical on the basis of calculations sketched below. Experimental support for this assignment was provided by corresponding OD spectra observed in discharged D_2O.

Fine structure and rotational energies are both large in the $^2\pi$ term of OH and, except for a complete decoupling of the proton spin, a field of several thousand gauss has little effect on the vector coupling scheme; this allows a calculation of the molecular Zeeman effect within a few parts in 10^4 by second order perturbation theory. To this precision, sufficient here, the hfs need be computed only to first order. For a given J the energy sublevels calculated in this way can be written as

$$(1)\quad W^{\pm}(M_J, M_I) = g_J^{\pm}\mu_0 M_J H \pm \tfrac{1}{2}h\nu_\Lambda + f(M_J^2)(\mu_0 H)^2/hc + hA^{\pm}M_J M_I + g_I\mu_0 M_I H,$$

where $f(M_J^2)$ measures the net magnetic perturbation from nearby levels. The plus and minus signs refer to the upper and lower Λ-doubling level, respectively; ν_Λ is the doubling frequency. The interactions responsible for Λ-doubling alter the ideal $^2\pi$ g-factors by admixing excited molecular terms; these effects differ for the two doublet components and hence the notation $g_J^{\pm}$. «Hyperfine doubling» [1] is represented by $A^{\pm}$.

Fairly accurate paramagnetic resonance spectra ($\Delta M_J = \pm 1$, $\Delta M_I = 0$) can be calculated from (1) on the basis of the previously measured microwave properties of OH. Spectra corresponding to ED transitions between the two components of the Λ-doublet have the general form of two compact groups of $2J(J+1)$ lines; their separation is a measure of the doubling frequency. Midway between the ED groups is a magnetic dipole (MD) spectrum, the type usually encountered in paramagnetic resonance. This spectrum is produced by transitions within each Λ-doubling level, and may show $4J(2I+1)$ resolved lines; it should be much weaker than the ED spectrum.

From such calculations spectra (*a*) and (*b*) are identified with ED transitions in the $\pi_{\frac{3}{2}}$, $J=\frac{3}{2}$ level. Their dissimilarity is accountable by the g-factor difference $g_J^- - g_J^+ \sim 10^{-3}$; in (*a*) this compensates for the quadratic Zeeman splitting and condenses the spectrum to three nearly superposed hfs doublets; in (*b*) the reverse occurs and splittings are enhanced. Hyperfine doubling is expected to be small for this level, and indeed was undetectable. Absolute measurements give [3]

$$g_J = 0.935 \pm 0.001,$$
$$\nu_\Lambda = (1667 \pm 2)\ \text{MHz} \quad (\pi_{\frac{3}{2}}, J=\tfrac{3}{2}),$$
$$A = (26 \pm 2)\ \text{MHz}.$$

Spectrum (*c*) can be assigned to ED transitions in the $\pi_{\frac{3}{2}}$, $J=\frac{7}{2}$ level. Here ν_Λ is above X-band, and only half the spectrum is observable. Pressure broadening washes out the hfs of the central lines, but hyperfine doubling is clearly demonstrated by the greater widths and incipient structure of the outside lines. The total spread of the spectrum is some 6 times that expected from quadratic Zeeman splittings—presumably because of the g-factor perturbations mentioned above.

The ED spectrum of the $\pi_{\frac{3}{2}}$, $J=\frac{5}{2}$ level should also be observable; one group should lie at 4 200 G, the other

---

[3] Direct measurements of the $\pi_{\frac{3}{2}}$, $J=\frac{3}{2}$; Λ-doubling absorption have been reported recently [EHRENSTEIN, TOWNES and STEVENSON: *Phys. Rev. Lett.*, **3**, 40 (1959)]. These results, which came to our attention during preparation of this report, agree with the less accurate value of ν_Λ given here.

at a field above our instrumental limit of 12 000 G. Investigation of the field interval below 5 000 G was limited by an extremely broad and intense electron cyclotron resonance absorption. Although complicated structure was observed on this electron resonance line near the expected location of the $J=\frac{5}{2}$ spectrum, a definite identification could not be made. Other $\pi_{\frac{3}{2}}$ spectra all lie above 12 000 G at X-band frequencies. Two $\pi_{\frac{1}{2}}$ spectra are pushed to low fields by Λ-doubling, but their expected intensities are low. In a search for the $\pi_{\frac{1}{2}}$, $J=\frac{3}{2}$ MD spectrum the pillbox-shaped absorption cell was replaced by a straight tube passing axially through the cavity. The Q of this arrangement is particularly high, and the spectra of ground state hydrogen and oxygen atoms, absent in work with the larger cell, were easily detected in the discharged water vapor. No OH spectra were found, of either the magnetic or electric dipole type, the latter because there was essentially no electric field to excite them.

IL NUOVO CIMENTO Vol. XIV, N. 1 1° Ottobre 1959

Interaction between Electron Beam and Magnet.

S. Yamaguchi

The Institute of Physical and Chemical Research - Tokyo

(ricevuto il 3 Agosto 1959)

The purpose of this work is to elucidate a singular interaction taking place between an electron beam and a magnet body. A camera for electron diffraction was utilized for the experiment. An electron beam grazed a sharp edge (thickness, about 2000 Å) of a permanent magnet (remanence, about 10^4 G). A typical diffraction pattern obtained is shown in Fig. 1. The central spot found in Fig. 1 is optically enlarged 35 times in Fig. 2. In this figure we see that the incident beam is splitted into the several beams. The intact beam here used is shown in Fig. 3.

Fig. 1. – Diffraction pattern obtained from the magnet edge. Wavelength: 0.0286 Å. Camera length: 495 mm. Positive enlarged 2.3 times.

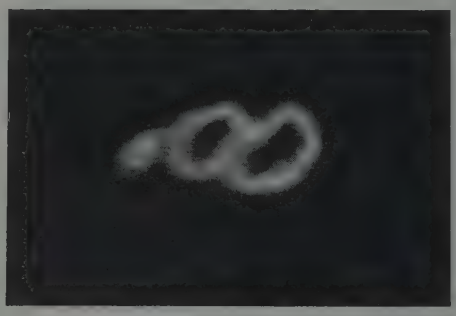

Fig. 2. – The central spot in Fig. 1 is enlarged 35 times. Splitting of the incident beam is recognizable.

The splitting as seen in Fig. 2 was observed as a semi-permanent or stationary state under the given conditions. This stationary state was not attained immediately after the incident beam had touched the specimen. A time lag or retardation (about one second) had always been witnessed before the final semi-permanent splitting was attained. The appearance of this retardation was quite similar to the lapse of charging-up frequently observable in electron diffraction at an insulator.

There are the positive holes in the d-band of iron [1]. These holes could be filled up with the incident electrons as the result of a quantum mechanical resonance which tunnel through the specimen. This resonance could take place

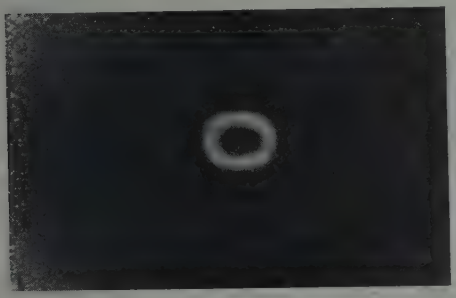

Fig. 3. – The intact electron beam here used. 35 times enlarged.

between the electrons of the parallel spin found in the d-band of the magnet body and those of the anti-parallel spin included in the incident beam. The above-mentioned retardation means the time necessary for filling up the half-vacant d-band with the scanty antiparallel electrons found among the incident electrons.

A localized area in the magnet body remains negative-charged in a stationary state, so long as it is continuously and steadily illuminated with the incident electrons. This negative charge can not escape to the earth, although the conductive specimen is connected to the earth. Only the s-electrons can remove to the earth through the metallic specimen. The circumstance of the stationary state realized in the present experiment is illustrated in Fig. 4. The arrows drawn in the magnet body show the parallel and the anti-parallel spins of the electrons which are paired in the d-band.

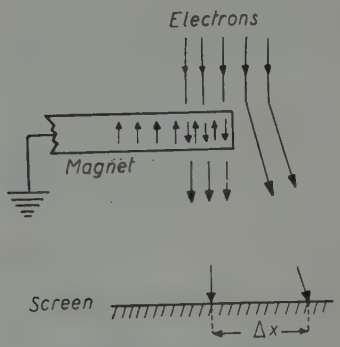

Fig. 4. – Experimental arrangement. The small arrows in the magnet body show the parallel and the anti-parallel spin of the electrons.

The author has tried to calculate the splitting ΔX in Fig. 2 from the interaction between the incident beam and the electrostatic field given by the « negative-charged » d-band of the specimen. This splitting depended upon the shape of the specimen. We have, however, a relation between ΔX and the electric field E for the simplest arrangement:

$$\Delta X = eEm\left(\frac{\lambda}{h}\right)^2 Ll\,, \tag{1}$$

where e means the electron charge ($4.8 \cdot 10^{-10}$ esu), m means the electron mass ($9.1 \cdot 10^{-28}$ g), λ means the wavelength of the electrons (0.0286 Å), h means Planck's constant ($6.6 \cdot 10^{-27}$ erg/s), L means the camera constant (495 mm), and l means the electrostatic path travelled by the electrons. We measure $\Delta X = 0.03$ cm in Fig. 2. Therefore, we obtain $E \simeq 10^5$ V according to Eq. (1) if $l \simeq 10$ μm is assumed here. This value is reasonable as an electrostatic potential obtainable.

---

[1] N. F. Mott and H. Jones: *The Theory of Properties of Metals and Alloys* (Oxford, 1936), p. 222.

IL NUOVO CIMENTO Vol. XIV, N. 1 1° Ottobre 1959

A Search for (Σ^+ p) Hypernuclei.

R. C. Kumar and F. R. Stannard

Physics Department, University College - London

(ricevuto il 7 Agosto 1959)

Several authors [1] have discussed the possibility that Σ^+ hyperons might bind with one or more protons and Σ^- hyperons with neutrons. Such hypernuclei could decay according to the following schemes:

(1) $(\Sigma^+ p) \to p + \pi^0 + p + (116 - B_{\Sigma^+})$ MeV

(2) $\to n + \pi^+ + p + (110 - B_{\Sigma^+})$ MeV

(3) $\to d + \pi^+ + (112 - B_{\Sigma^+})$ MeV

(4) $\to p + p + (251 - B_{\Sigma^+})$ MeV

(5) $(\Sigma^- n) \to n + \pi^- + n + (117 - B_{\Sigma^-})$ MeV

where B_{Σ^+} and B_{Σ^-} are the binding energies.

To date only one event has been put forward as a (Σ-nucleon) compound and, as the authors [2] point out, there is some doubt concerning its interpretation.

K^- capture stars are a copious source of hyperons; 9% emit Σ^+ and 8% Σ^--particles [3]. However, no (Σ-nucleon) fragments have been reported from the extensive studies made of these stars, and the question arises as to whether or not events are being misinterpreted. For example, a decay according to reaction (1) could be mistaken for a 2-prong Σ^- capture star or the decay of a Λ^0-hypernucleus. Also, if the π-meson has not been followed to rest to determine its sign, reaction (2) could be taken as a mesonic decay of a Λ^0-hypernucleus.

A sample of 1 200 K^- capture stars which had been used previously for the European K^- Stack Collaboration [3], have been re-examined specifically for (Σ^+p) hypernuclei.

Due to the great difficulty of distinguishing between reaction (5) and ordinary $\Sigma^\pm$ decays in flight, no attempt has been made to find (Σ^-n) hypernuclei in the investigation reported here.

Any 2-body decays according to reactions (3) and (4) would be readily identified owing to the colinearity and unique ranges of the decay products. However, none were found.

---

[1] D. Holladay: quoted by R. G. Sachs: *Phys. Rev.*, **99**, 1573 (1955); R. H. Dalitz: *Nucl. Phys.*, **1**, 372 (1956); F. Ferrari and L. Fonda: *Nuovo Cimento*, **6**, 1027 (1957); A. Pais and S. Treiman: *Phys. Rev.*, **107**, 1396 (1957); D. B. Lichtenberg and M. H. Ross: *Phys. Rev.*, **107**, 1714 (1957); G. A. Snow: *Phys. Rev.*, **110**, 1192 (1958); A. Pais: *Phys. Rev.*, **112**, 624 (1958); T. B. Day and G. A. Snow: *Phys. Rev. Lett.*, **2**, 59 (1959); R. C. Kumar: to be published in the *Ind. Journ. Phys.*

[2] M. Baldo-Ceolin, W. F. Fry, W. D. B. Greening, H. Huzita and S. Limentani: *Nuovo Cimento*, **6**, 144 (1957).

[3] European K^--Stack Collaboration, Part I: *Nuovo Cimento*, **13**, 690 (1959).

With regard to decays occurring through reaction (1), all tracks emitted from K^- stars and coming to rest to produce two heavy prongs were examined on the assumption that they were (Σ^-p) fragments. From the momentum unbalance of the 2 prongs, the energy of the π^0-meson, supposedly emitted, was found and hence the Q value. If an appreciable number of (Σ^+p) hypernuclei were present one would expect a peak in the distribution of Q values at an energy a little less than 116 MeV. As can be seen from Fig. I, no peak was found and, in fact, only two events merited further investigation. Details of these are given in Table I.

The errors on the calculated binding energies derive mainly from the uncertainties in the range and dip angle measurements on the shorter proton tracks.

Integrated gap measurements were made on the primary of event 3 859 and also on samples of protons, Σ, and α-particles of the same dip. The results are given in Table II, the errors quoted being the experimentally found standard errors of the samples. No α-particles

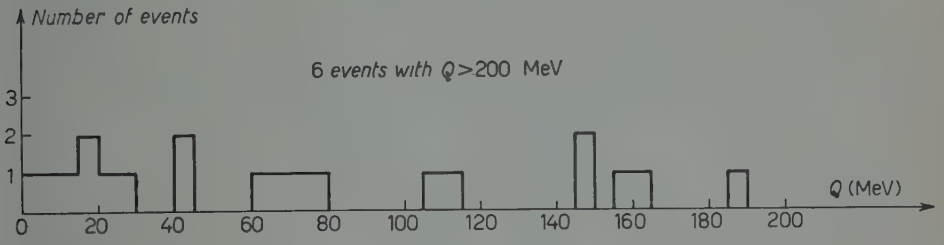

Fig. 1. – Distribution of Q-values on the assumption that all events giving rise to 2 prongs are (Σ^+p) compounds.

TABLE I.

Event number	Range of primary (μm)	Dip of primary	Ranges of protons (μm)		Energy of π^0 (MeV)	Q (MeV)	B_{Σ^+} (MeV)
3 859	3 870	11°	1 559	3.3	91	109.5	6.5^{+2}_{-4}
2 806	5	50°	1 810	1.7	90	110	$6^{+3}_{-7.5}$

TABLE II.

Residual range (μm)	Integrated gap-length (μm)			
	p	B	α	3 859
200	8.0 ± 2	6.7 ± 2	3.8 ± 1	6.7
800	54 ± 5	37 ± 4	—	40.5

were available of 800 μm residual range.

These measurements indicate that the primary of event 3 859 is almost certainly a Σ-particle, and it is concluded that the event itself is a 2-prong Σ^--capture star.

A similar investigation on the primary of event 2 806 could not be made owing to its short range and large dip angle. It is impossible to determine directly from measurements of mass and charge whether or not it is a (Σ^+p) hypernucleus. It only remains to be seen what inferences, if any, can be drawn from the energies of the decay products. It will be seen from Table I that one of the two decay protons has a very short range. However, A. K. COMMON [4] in an approximate calculation has shown that the proton in a (Σ^+p) fragment would, in fact, generally take comparatively little energy when the Σ^+-hyperon decays. Much depends upon the assumed value of B_{Σ^+}, but if, for example it is taken to be as small as 0.25 MeV, the proton would receive less than 0.5 MeV in 40% of cases. Finally, it should be noted that the original K^--star was a large one, emitting 8 heavy prongs. Summing up it appears impossible to arrive at any definite interpretation for this event.

With regard to decays according to reaction (2), there are 9 particles from K^--stars which on coming to rest give rise to 1 heavy prong and a lightly ionising track. 7 of these tracks have been followed to rest and all proved to be negatively charged π-mesons. These events are therefore, certainly not examples of reaction (2). The other 2 light tracks have dip angles $> 70°$ and could not be followed to rest.

The conclusion of the investigation is that in a sample of 1 200 K^--stars from which 110 Σ^+ hyperons were emitted, only one event was found which could be interpreted as a (Σ^+p) hypernucleus, and the identification of this event is uncertain. It would, therefore, appear desirable to extend this re-examination of K^--stars to a considerably larger sample.

[4] A. K. COMMON: private communication.

IL NUOVO CIMENTO Vol. XIV, N. 1 1° Ottobre 1959

On μ-Meson Electron Scattering.

B. De Tollis

Istituto di Fisica dell'Università - Roma
Istituto Nazionale di Fisica Nucleare - Sezione di Roma

(ricevuto il 12 Agosto 1959)

Assuming a possible coupling of μ-meson with a spinless boson neutral field (σ-meson) [1-5], we shall attempt in this note an evaluation of the form factors in μ^+-meson electron scattering (knock-on processes) [6]. We consider both cases of scalar and pseudoscalar σ with non-derivative couplings.

The interaction hamiltonians are:

$$H_1 = -ie\bar{\psi}^{(\mu)}\gamma_\alpha\psi^{(\mu)}A_\alpha\,; \qquad H_2 = ie\bar{\psi}^{(e)}\gamma_\alpha\psi^{(e)}A_\alpha$$

$$H_3^S = g\bar{\psi}^{(\mu)}\psi^{(\mu)}\varphi^{(\sigma)} - \delta M\,\bar{\psi}^{(\mu)}\psi^{(\mu)}\,; \qquad H_3^P = ig\bar{\psi}^{(\mu)}\gamma_5\psi^{(\mu)}\varphi^{(\sigma)} - \delta M\,\bar{\psi}^{(\mu)}\psi^{(\mu)}$$

in obvious notations. In perturbative approximation the lowest order diagrams contributing to the process are:

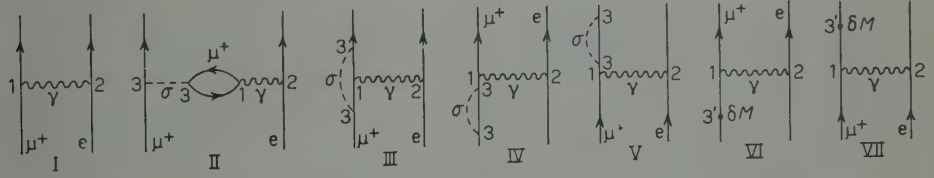

The contribution from diagram II is zero for both scalar and pseudoscalar σ. It is sufficient to evaluate the first of the following five diagrams. By subtracting from the resulting expression its value at $q^2=0$, one automatically includes the self-energy contributions of the diagrams IV-VII.

---

(1) J. Schwinger: *Ann. Phys.*, **2**, 407 (1957).
(2) W. S. Cowland: *Nucl. Phys.*, **8**, 397 (1958).
(3) I. R. Gatland: *Nucl. Phys.*, **9**, 267 (1958-59).
(4) I. Saavedra: *Nucl. Phys.*, **11**, 569 (1959).
(5) S. N. Gupta: *Phys. Rev.*, **111**, 1436, 1698 (1958).
(6) Processes of this kind have already been observed with cosmic ray μ-mesons, see for example references in *Progress in Elementary Particle and Cosmic Ray Physics*, **4**, 107 (1958).

The resulting finite matrix element is:

$$(1)\quad M=ie^2(2\pi)^4\,\delta_4(P'+p'-P-p)(\bar{u}_{p'}\gamma'_\mu u_p)\,\frac{1}{q^2M^2}\left(\bar{u}_{P'}\left[F_1(q^2)\gamma'_\mu+\frac{1}{2}\varkappa F_2(q^2)\sigma_{\nu\mu}\,q_\nu\right]u_P\right),$$

where: $p\equiv(\boldsymbol{p},i\varepsilon)$ the is electron 4-momentum before scattering,;
$P\equiv(\boldsymbol{P},iE)$ the is μ^+-meson 4-momentum before scattering;
p' and P' are the 4-momenta after scattering; $q=P'-P=p-p'$; $\hbar=c=1$;
$\varkappa$ is the μ-anomalous magnetic moment (units $e/2M$); $\sigma_{\nu\mu}=[\gamma_\nu\gamma_\mu-\gamma_\mu\gamma_\nu]/2i$.

Moreover here and in the following:

M is the μ^+-meson mass,

m is the electron mass,

μ is the σ-meson mass,

$\eta=\mu^2/M^2$; $\quad\lambda=m/M\sim 0.5\cdot10^{-2}$.

All energies and momenta are divided by M and are therefore pure numbers. F_1 and F_2 are electric and magnetic form factors and for the two cases (S and P) are given by:

$$(2)\quad\begin{cases}F_1^S(q^2)=1-\dfrac{G^2}{4\pi}\displaystyle\int_0^1\mathrm{d}x\int_0^1\mathrm{d}y\,x\left[\frac{q^2x^2y^2+8xy-2x^2y-4}{x^2-\eta x+\eta+q^2x^2y(1-y)}+\frac{(2-x)^2}{x^2-\eta x+\eta}\right],\\ \varkappa^S F_2^S(q^2)=\dfrac{G^2}{\pi}\displaystyle\int_0^1\mathrm{d}x\int_0^1\mathrm{d}y\,\frac{x^2y(2-x)}{x^2-\eta x+\eta+q^2x^2y(1-y)},\end{cases}$$

$$(3)\quad\begin{cases}F_1^P(q^2)=1-\dfrac{G^2}{4\pi}\displaystyle\int_0^1\mathrm{d}x\int_0^1\mathrm{d}y\,x^3\left|\frac{q^2y^2-2y}{x^2-\eta x+\eta+q^2x^2y(1-y)}+\frac{1}{x^2-\eta x+\eta}\right],\\ \varkappa^P F_2^P(q^2)=-\dfrac{G^2}{\pi}\displaystyle\int_0^1\mathrm{d}x\int_0^1\mathrm{d}y\,\frac{x^3y}{x^2-\eta x+\eta+q^2x^2y(1-y)}.\end{cases}$$

$$(G^2=g^2/4\pi).$$

The cross-section (valid in any reference system (*)), evaluated from (1), is

$$(4)\qquad \mathrm{d}\sigma=r_0^2\frac{X}{q^4}\,\frac{\lambda^2\beta'E'}{\sqrt{(pP)^2-\lambda^2}}\,\frac{\mathrm{d}\Omega'}{\beta'(E+\varepsilon)-|\boldsymbol{p}+\boldsymbol{P}|\cos\theta'},$$

(*) See for example Jauch and Rohrlich: *Theory of Photon and Electrons* (Cambridge Mass., (1955)) p. 254.

$$\beta' = |\boldsymbol{P}'|/E' \; ; \qquad r_0 = e^2/4\pi m \sim 2.8 \cdot 10^{-13} \text{ cm} \, ,$$

$$X = F_1^2[4(pP)(pP') - q^2] + (F_1 + \varkappa F_2)^2[q^2 - 2\lambda^2]\frac{q^2}{2} + \varkappa^2 F_2^2[4(pP)(pP') - q^2]\frac{q^2}{4} \, .$$

Round brackets denote 4-vector products. Quantities with apex are related to scattered μ^+. The eq. (4), in the limit, reduces, of course, to the well known Rosenbluth formula (7).

Considering, now, that $q^2_{\max}$ (max for a determined energy of the incident μ^+) given by

$$q^2_{\max} = 4|\boldsymbol{P}_{\text{C.M.}}|^2 = \frac{4|\boldsymbol{P}_L|^2 \lambda^2}{1 + \lambda^2 + 2\lambda E_L}$$

is only of the order of unity when the energy of the incident μ^+ (in the laboratory system) is as high as 15 GeV, it is convenient to retain terms proportional to q^2 in the expansion in powers of q^2 of the electric form factors, and to substitute the magnetic form factors by one. That is:

$$\begin{cases} F_1^S \to 1 - \dfrac{G^2}{12\pi} f^S(\eta) q^2 \\ \varkappa^S F_2^S \to \varkappa^S = \dfrac{G^2}{2\pi} g^S(\eta) \end{cases} \qquad \begin{cases} F_1^P \to 1 - \dfrac{G^2}{12\pi} f^P(\eta) q^2 \\ \varkappa^P F_2^P \to \varkappa^P = -\dfrac{G^2}{2\pi} g^P(\eta) \, , \end{cases}$$

$$g^S(\eta) = \int_0^1 \mathrm{d}x \, \frac{x^2(2-x)}{x^2 - \eta x + \eta} \; ; \qquad g^P(\eta) = \int_0^1 \mathrm{d}x \, \frac{x^3}{x^2 - \eta x + \eta} \, ,$$

$$f^S(\eta) = g^P(\eta) + \frac{1}{2}\int_0^1 \mathrm{d}x \, \frac{x^3(2-x)^2}{(x^2 - \eta x + \eta)^2} \; ; \quad f^P(\eta) = g^P(\eta) + \frac{1}{2}\int_0^1 \mathrm{d}x \, \frac{x^5}{(x^2 - \eta x + \eta)^2} \, .$$

With these approximations, keeping terms in G^2 and neglecting λ^2 with respect to one, the cross-section, in the center of mass system, becomes:

$$\mathrm{d}\sigma_{\text{C.M.}} = r_0^2 \frac{\lambda^2}{q^4(E+\varepsilon)^2} \{2(pP)^2 + 2(pP')^2 - q^2\}(1+\delta)\,\mathrm{d}\Omega' \, . \tag{5}$$

Now:

$$q^2 = 4|\boldsymbol{P}|^2 \sin^2\frac{\theta}{2} \; ; \qquad (pP) = -|\boldsymbol{P}|^2 - E\varepsilon \; ; \qquad (pP') = -|\boldsymbol{P}|^2 \cos\theta - E\varepsilon \; ;$$

$$E^2 = |\boldsymbol{P}|^2 + 1 \; ; \qquad \varepsilon^2 = |\boldsymbol{P}|^2 + \lambda^2 \, .$$

(7) M. N. ROSENBLUTH: *Phys. Rev.*, **79**, 615 (1950).

with all quantities referred to the C.M. system. δ is the correction due to the form factors and it is written:

$$\delta^{S,P} = \frac{G^2}{6\pi} q^2 \left[-f^{S,P}(\eta) \pm g^{S,P}(\eta) \frac{3(q^2 - 2\lambda^2)}{2(pP)^2 + 2(pP')^2 - q^2} \right] \tag{6}$$

or, with no approximations:

$$\delta^{S,P} = 2(F_1^{S,P} - 1) + \varkappa^{S,P} F_2^{S,P} \frac{q^2(q^2 - 2\lambda^2)}{2(pP)^2 + (2pP')^2 - q^2} . \tag{6'}$$

Coming back to eq. (6) we shall try to evaluate the magnitude of δ. We take $\theta_{\text{C.M.}} = \pi$ (where δ is max) and we choose, for example, $E_L \sim 15$ GeV. Then, as we have seen before, $q^2(\theta_{\text{C.M.}} = \pi) = q^2_{\max}$ is of the order of unity. It is easy to see that the contribution of the second term in (6) is negligible because (see also (6')) $\varkappa$ can at most be ~ 0.001 (according to the recent experiments (8)) and the other factor is ~ 3. We have now to evaluate the contribution of the first term. In order to do that, we shall have in mind that G and η are correlated since $\varkappa \approx 0.001$. The limits of G are approximatively 0.005 when $\eta = 0$, and 2 when $\eta = 10^3$, and they do not differ greatly for scalar and pseudoscalar σ. From this and by an examination of the functions $f^{S,P}$ (which are monotonic decreasing *vs.* η) it can be immediately seen that an appreciable contribution to the cross-section (for ex. $\sim 50\%$) is obtained only when η is very small, and only for scalar σ, because f^P is 0.5 when $\eta = 0$, while f^S goes to ∞ when $\eta \to 0$ as $2 \ln (1/\sqrt{\eta})$. However, also in this case, a contribution of 50% can only be obtained for $\ln (1/\sqrt{\eta}) \sim 100$, that is for unreasonably small values of η.

We can conclude that for energies (in the electron rest system) of the incident μ^+-meson up to ~ 15 GeV (which will probably become available at the CERN proto-synchrotron), there should be no essential corrections to the usual expression for the cross-section due to a possible structure of the μ-meson like the one that has been considered here. This conclusion cannot be extended to higer energies for which it is necessary to consider the general form factors as written in (2), (3), keeping in mind that in (5), δ must be expressed through (6').

One should finally note that, avoiding particular hypotheses on the μ-meson structure, an appreciable contribution to the cross-section can only be given by the electric form factor F_1, because of the present strong limitation on the magnetic form factor.

* * *

Thanks are due to the Prof. R. GATTO for having suggested the problem and for helpful discussions.

(8) R. L. GARWIN, D. P. HUTCHINSON, S. PENMAN and G. SHAPIRO: *Phys. Rev. Lett.*, **2**, 213 (1959).

IL NUOVO CIMENTO Vol. XIV, N. 1 1° Ottobre 1959

Observations on the Photodisintegration of ^{16}O through the Inverse Process $^{15}N(p, \gamma)^{16}O$.

N. W. Tanner and G. C. Thomas
Clarendon Laboratory - Oxford

W. E. Meyerhof (*)
Stanford University - Cal.

(ricevuto il 20 Agosto 1959)

Nuclei which are reached by (p, γ) reactions having large Q-values will permit observation of the giant resonances observed in photodisintegration at energies near 20 MeV excitation. ^{16}O is the most interesting of the nuclei that can be studied, as it has been the subject of considerable theoretical (1) and experimental (2) investigation. The interest arises because ^{16}O is doubly magic, which offers simplicities to the theoretician and some practical advantage to the experimenter as none of ^{16}O, or ^{15}O and ^{15}N (the final nuclei from $^{16}O(\gamma, n)$ and $^{16}O(\gamma. p)$) have excited states below 5 MeV.

The high energy γ-rays from $^{15}N(p, \gamma)^{16}O$, $(E_\gamma\ (\mathrm{MeV}) = 12.11 + 0.93\, E_p)$, were analysed using a 6 in. long by 5 in. diameter NaI crystal scintillation counter, which had been calibrated with pure γ-rays of up to 20 MeV. Some preliminary measurements on $^{27}Al(p, \gamma)^{28}Si$ ($Q = 11.6$ MeV) at $E_p = 6$ MeV demonstrated that this reaction could be used to provide an energy calibration for the NaI counter as γ-rays to the ground state and first two excited states of ^{28}Si (at 1.78 and 4.61 MeV) could be comfortably resolved.

Targets of effective thickness 10 and 400 keV for protons of 7 MeV were used. With the NaI crystal some 6 in. from the target, proton beams of the order of 0.5 μA gave as high a count rate as could be safely handled without risk of pile-up or gain shift. Most of these counts were of small pulse height relative to the capture γ-rays and arose from $^{15}N(p, \alpha\gamma)^{12}C$ and unidentified (p, n) and (p, p′) reactions. While these reactions merely limited the rate of recording data at the lower bombarding energies, they seriously interfered with the interesting part of the spectrum at higher energies, and made the experiment impracticable with tantalum nitride targets above 8 MeV.

(*) Supported by the Alfred P. Sloan Foundation, New York, N. Y., while on leave at the Clarendon Laboratory, Oxford.

(1) J. P. Elliott and B. H. Flowers: *Proc. Roy. Soc.*, A **242**, 57 (1957).

(2) F. Ajzenberg and T. Lauritsen: *Nucl. Phys.*, **11**, 1 (1959).

The excitation curve shown in Fig. 1 taken at 90° to the proton beam was derived from the analysis of spectra taken at each of the bombarding energies indicated. The absolute cross-section scale was obtained by examining the $^{15}N(p, \alpha\gamma)^{12}C$ resonance at $E_p = 3.00$ MeV. In the region below 4 MeV the absolute cross-section agrees quite satisfactorily with the work of WILKINSON and BLOOM [3]. their (γ, p) cross-section to a (p, γ) cross-section by the detailed balance relation. The agreement is good except for the magnitude of the $E_p = 5.5$ MeV resonance. This is partly explained by our failure to allow for the rather strong angular distribution of $1 + 3.5 \sin^2 \theta$, observed by JOHANSSON and FORKMAN, in comparing our 90° measurement with their total cross-section. The correction factor is 1.35 which still leaves nearly a factor of

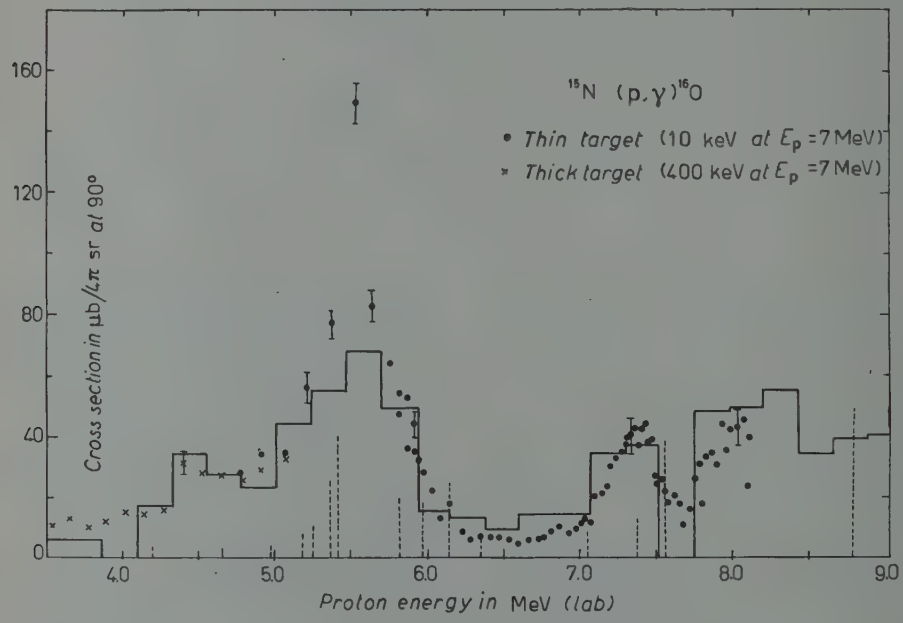

Fig. 1. – Excitation function for $^{15}N(p, \gamma)^{16}O$. The points are the experimental results for this reaction. The histogram is the excitation function for $^{15}N(p, \gamma)^{16}O$ derived by detailed balance from the excitation function [4] for $^{16}O(\gamma, p)^{15}N$. The dotted lines indicate the position of resonances that might be expected in $^{15}N(p, \gamma)^{16}O$ from the fine structure [5] in $^{16}O(\gamma, n)^{15}O$.

The histogram in Fig. 1 is the $^{15}N(p, \gamma)^{16}O$ excitation function obtained from the $^{16}O(\gamma, p)^{15}N$ excitation function of JOHANSSON and FORKMAN [4] by a conversion of their γ-ray energy to equivalent proton bombarding energy and of two unexplained. (The lonely point at 5.5 MeV was confirmed by thick target measurements which are not plotted in Fig. 1.)

MILONE *et al.* [5] have also obtained an excitation function for $^{16}O(\gamma, p)^{15}N$

[3] D. H. WILKINSON and S. D. BLOOM: *Phys. Rev.*, **105**, 683 (1957).

[4] S. A. E. JOHANSSON and B. FORKMAN: *Ark. f. Fys.*, **12**, 359 (1957).

[5] C. MILONE, S. MILONE-TAMBURINO, R. RINZIVILLO, A. RUBBINO and C. TRIBUNO: *Nuovo Cimento*, **7**, 729 (1958).

and while this is qualitatively similar the agreement is not quite as good.

ELLIOTT and FLOWERS [1] have calculated the excited states of ^{16}O of $J^\pi = 1^-$ and $T = 1$ arising from the configuration $1p^{-1}(2s, 1d)$ which should be important for the $^{15}N(p, \gamma)^{16}O$ reaction. In particular they predict a strong resonance at $E_p = 5.55$ MeV which is in such good agreement with the observed resonance at $E_p = 5.52$ MeV that it can only be regarded as partly fortuituous. It was noted that the $^{15}N(p, \alpha\gamma)^{12}C$ reaction (observed through the 4.43 MeV γ-ray) is not strongly resonant at $E_p = 5.5$ MeV which is consistent with the $T = 1$ assignment.

The vertical dotted lines in Fig. 1 indicate the position of the resonances (in terms of proton bombarding energy) deduced by PENFOLD and SPICER [6] from breaks in the $^{16}O(\gamma, n)^{15}O$ activation curve. The length of each of the dotted lines is proportional to the integral over each resonance. A careful search was made in the region between 5.97 MeV and 6.60 MeV using a 10 keV thick tantalum nitride target and steps of 5 keV in proton energy. (These points are not plotted in Fig. 1.) Within this energy region two strong (γ, n) resonances are supposed to occur having widths of the order of 25 keV. In addition a strong $^{15}N(p, n)^{15}O$ resonance of 40 keV width has been observed by JONES *et al.* [7]. None of these sharp effects appeared in $^{15}N(p, \gamma)^{16}O$. While the (p, n) resonances may have high spin and therefore small radiation widths, it is not at all easy to understand how the supposed fine structure in $^{16}O(\gamma, n)^{15}O$ can fail to have any effect in $^{15}N(p, \gamma)^{16}O$.

The only consolation that can be drawn from the (γ, n) resonances is that they do tend to group about the region of $E_p = 5.5$ MeV. If we take the extreme view that the (γ, n) fine structure is false but that the grouping is meaningful, *i.e.* the (γ, n) reaction is subject to the same resonance as the (p, γ) reaction, then we can compare the ratio of the integrated cross-sections of (γ, n) and (γ, p) in the region of the resonance. JOHANSSON and FORKMAN [3] give the ratio as 2.2 and this is equal to Γ_p/Γ_n. Assuming $\Gamma_{\alpha_0} \sim \Gamma_{\alpha_1} \sim 0$ from our failure to observe a $^{15}N(p, \alpha\gamma)^{12}C$ resonance and the predicted [1] $T = 1$ character of the state, then $\Gamma = \Gamma_p + \Gamma_n = 280$ keV from Fig. 1, $\Gamma_p = 190$ keV and $\Gamma_n = 90$ keV. Making due allowance for the angular distribution we find the peak cross-section to be 110 μb and assuming $J = 1$ we get $\Gamma_\gamma = 145$ eV. ELLIOT and FLOWERS [1] predict $\Gamma_\gamma = 140$ eV.

This paper represents the first yield from a programme of proton capture reactions using the tandem electrostatic generator at A.E.R.E., Harwell.

* * *

The tandem electrostatic generator used in this experiment was constructed by Dr. W. D. ALLEN of the Accelerator Division, A.E.R.E., Harwell. We are grateful to the Director of A.E.R.E., Harwell and to Dr. E. BRETSCHER for the experimental facilities placed at our disposal.

We are also indebted to Dr. D. E. ALBURGER of Brookhaven and to the Isotope Division, A.E.R.E., Harwell for the supply of target materials, to Dr. P. F. D. SHAW for assistance in making targets, and to Dr. W. D. ALLEN and Dr. E. B. PAUL for considerable help in the course of the experiment.

The investigation of the inverse photodisintegration process was suggested to us by Professor D. H. WILKINSON and we have profited greatly by his interest and advice.

(6) A. S. PENFOLD and B. M. SPICER: *Phys. Rev.*, **100**, 1377 (1955).

(7) K. W. JONES, L. J. LIDOFSKY and J. L. WEIL: *Phys. Rev.*, **112**, 1252 (1958).

IL NUOVO CIMENTO Vol. XIV, N. 1 1° Ottobre 1959

On the Ergodic Methods in Statistical Mechanics.

P. Caldirola

Istituto di Scienze Fisiche dell'Università - Milano
Istituto Nazionale di Fisica Nucleare - Sezione di Milano

(ricevuto il 25 Agosto 1959)

1. – This letter has two aims:

i) to stress that the ergodic approach to statistical mechanics (in the single system version or in the version of the ensemble theory) is conceptually the most satisfactory one;

ii) to discuss from a methodological point of view some recent developments of the classical and quantal ergodic theories.

As far as the first point is concerned, we remark that the ergodic method has not always been considered in the right light [1,2] or even it has been misunderstood [3]. This fact seems to us rather strange, since the soundness of a purely dynamical foundation of the statistical mechanics has been definitely established a long time ago in a famous discussion between Boltzmann and Zermelo. The ergodic point of view has been successively adopted by the most distinguished physicists of our time as Einstein, von Neumann, Pauli.

The objections raised against the ergodic method are essentially the following:

a) to consider a physical system as isolated is evidently only an abstraction, because of the unavoidable occurrence of small, practically uncontrollable interactions with the surrounding medium, due for instance to the presence of radiation fields. Thus the ergodic approach, making an essential use of the concept of isolated conservative system, would be founded on a schematization of doubtful physical meaning.

---

[1] D. ter Haar: *Rev. Mod. Phys.*, **27**, 289 (1955); A. Münster: *Prinzipien der statistischen Mechanik*, in *Handb. d. Phys.*, III/2 (Berlin, 1959), p. 207.

[2] A purely subjective form of statistical mechanics has been recently developed by E. T. Jaynes (*Phys. Rev.*, **108**, 171 (1957)), following information theory methods, in particular identifying Shannon's entropy with statistical entropy. In this way the central problem of deducing from microscopic laws the macroscopic behaviour of a system with many degrees of freedom is completely eluded. According to this method, statistical mechanics is no longer a real physical theory, but only a statistical inference technique.

[3] R. C. Tolman: *The Principles of Statistical Mechanics* (Oxford, 1938), § 25; L. D. Landau and E. M. Lifšitz: *Statistical Physics* (London, 1958).

b) The quantities averaged over an infinite time interval having no operational meaning, the connection of the results of the ergodic theory with the experimental data would be problematic. In fact, the physically significant quantities of the macroscopic experience are time averages of phase functions in the classical case and of expectation values in the quantal case, taken on time intervals of the same order of magnitude of the actual measurement times.

These objections can be easily confuted. Against the first, one can remark that the interactions with the environment have a negligible effect on a system *with a large number* of degrees of freedom (and such are the systems studied by statistical mechanics), since in this case the effects of the above interactions reduce to mere surface effects (4).

With respect to the second objection, we notice that in the ergodic method the time averages represent only a useful mathematical tool, by which the theory can be built up in a consistent manner. Let us consider for example the classical case (5). The time averages over an infinite time interval of phase functions which are physically significant for the macroscopic description of the system (sum-functions), coincide in the overwhelming majority of the time instants with the corresponding instantaneous values. This is a consequence of the representativity of the microcanonical ensemble, following from mere geometrical considerations, in virtue of the large number of the degrees of freedom (6).

It follows that the averages over an infinite time interval of physically significant phase functions coincide actually with the measured equilibrium values.

The application of the classical ergodic theory (founded on Birkhoff's (7)

(4) Some authors have suggested (see for instance LANDAU and LIFŠITZ (3), p. 31) that in the quantal case the unavoidable and uncontrollable interaction between system and measuring apparatus would make physically meaningless the study of an isolated system, since the tendency towards equilibrium could be essentially influenced by the disturbances created by the external observations. But, as was remarked by PAULI (*Suppl. Nuovo Cimento*, **6**, 169 (1949)), « the otherwise so important difference between classical and quantum mechanics is not relevant in principle for thermodynamical questions. Indeed the disturbance by observations defined as macroscopic can be made small and a single macroscopic observation is sufficient in principle for controlling whether or not the system has reached its thermal equilibrium ».

(5) In this connection see also: P. CALDIROLA and A. LOINGER: *The Developments of the Ergodic Approach to Statistical Mechanics*, in *Max-Planck-Festschrift* (1958), p. 225, § 2.

(6) To make this point clearer we recall that it can be *rigorously* proved (A. I. KHINCHIN: *Mathematical Foundations of Statistical Mechanics* (New York, 1949)) that to the Maxwell-Boltzmann distribution law of the molecular positions and velocities corresponds a set of points of Γ space, whose microcanonical measure coincides practically with the microcanonical measure of the whole energy surface. From this fact it can be inferred in particular the justification of the irreversible behaviour of a system with many degrees of freedom. Assuming for instance that the conditions required for the validity of the Birkhoff's theorem are verified, the ratio between the permanence time of the phase-point P_t in the non-equilibrium region and the permanence time in the equilibrium region approaches the ratio of the corresponding microcanonical measures. Then, in the ovewhelming majority of the time instants, the system will be in the equilibrium region. Obviously, it can leave this region for relatively short times (fluctuations). Therefore it is clear that the irreversible behaviour of a system with many degrees of freedom can be explained by means of pure dynamics without introducing the « information degree » of the observer.

(7) The identity between time average (over an infinite time interval) and microcanonical average of a phase-function, stated by Birkhoff's theorem, is valid with the exception of a set of phase trajectories such that their initial points form a set of zero Lebesgue measure. The frequency with which a fixed initial condition occurs in practice evidently cannot be foreseen by mechanics. Consequently, to link Birkhoff's theorem with physical reality it is necessary to make some assumption on the occurrence probability of the exceptional initial conditions;

and Hopf's theorems) to statistical mechanics met an obstacle in the fact that it is not known — strictly speaking — which are the metrically transitive systems. This difficulty has recently been overcome by KHINCHIN ([8]) in the framework of the single system formulation of the classical ergodic theory. His procedure has been developed in detail by TRUESDELL and MORGENSTERN ([9]). These authors have given an ergodic theorem based only on the canonicity of the time evolution and on the large number of degrees of freedom (macroscopic condition of ergodicity). This theorem, which implies no microscopic ergodicity condition (like metric transitivity), is from the mathematical point of view restricted to the case of systems described by separable Hamiltonians (for instance a system of weakly interacting particles): it gives practically the same consequences of Birkhoff's theorem, but the set of the exceptional initial phases, instead of zero measure has a small measure μ and the ratio between μ and the microcanonical measure of the energy surface vanishes when the number of degrees of freedom goes to infinity. The enlargement of the class of the exceptional initial conditions is the price one has to pay in order to get rid of the microscopic condition of ergodicity.

Considering now quantum theory, we wish to point out that the original approach by VON NEUMANN ([10,12]), who made essential use of the concept of average over the macro-observers, has turned out to be definitely unsatisfactory ([13]). A new approach to the quantum ergodic theory has been recently proposed by BOCCHIERI and LOINGER ([14]). This approach replaces von Neumann's averages over the macro-observers by an average over the initial state-vectors, all considered as *a priori* equiprobable. From the methodological point of view, this approach represents the exact quantum counterpart of the K-T-M theorem; further, its validity is not restricted to systems characterized by separable Hamiltonians. As in the corresponding classical case, there is no need of microscopic ergodicity conditions. The theorem rests only on the following assumptions:

a) the system has a large number of degrees of freedom;

b) the time evolution operator is unitary.

The ratio between the measure of the set of the exceptional initial states *corresponding to a given subdivision in « cells » of the quantum « energy shell »* and the measure of the set of all the possible initial states vanishes as the number of the degrees of freedom goes to infinity.

---

the most natural assumption consists obviously in attributing a zero *a priori* probability to the set of the exceptional initial conditions. Such a statistical element, however, has a completely different nature from the statistical postulates adopted in Tolman's « utilitarian » approach.

We remark finally that in the ensemble theory version of the ergodic approach (based on Hopf's theorem) a zero statistical weight is automatically attributed to the set of the exceptional initial conditions of Birkhoff's theorem.

([8]) See the book by KHINCHIN quoted in ([6]), § 13, p. 62.

([9]) C. TRUESDELL and D. MORGENSTERN: *Erg. ex. Naturwiss.*, **13**, 286 (1958). See also the interesting qualitative considerations of D. BOHM and W. SCHÜTZER: *Suppl. Nuovo Cimento*, **2**, 1004 (1955), § 6.

([10]) J. VON NEUMANN: *Zeits. Phys.*, **57**, 30 (1929).

([11]) W. PAULI and M. FIERZ: *Zeits. Phys.*, **106**, 572 (1937).

([12]) L. ROSENFELD: *Acta Phys. Polon.*, **14**, 3 (1955).

([13]) P. BOCCHIERI and A. LOINGER: *Phys. Rev.*, **111**, 668 (1958). For previous criticisms see: M. FIERZ: *Helv. Phys. Acta*, **28**, 705 (1955); I. E. FARQUHAR and P. T. LANDSBERG: *Proc. Roy. Soc.*, A **239**, 134 (1957).

([14]) P. BOCCHIERI and A. LOINGER: *Phys. Rev.*, **114**, 948 (1959); for further results obtained following this line of thought see: G. M. PROSPERI and A. SCOTTI: *Nuovo Cimento* **13**, 1007 (1959).

2. – We should like to remark that in the classical theory the theorems of Birkhoff and of K-T-M occupy, in a certain sense, two extreme positions. Birkhoff's theorem has a «maximum content of dynamics» because the assumption of metric transitivity determines, in some way, the form of the Hamiltonian, while the number of degrees of freedom of the system does not play any explicit rôle [15]. On the contrary the K-T-M theorem has a « minimum content of dynamics » and is not, strictly speaking, a theorem of pure general dynamics, since the assumption of a large number of degrees of freedom is required for its validity.

It is also clear that a whole class of ergodic theorems, occupying intermediate positions between the extreme ones mentioned above, is in principle conceivable. Also in the quantum theory it seems possible to establish ergodic theorems having a larger dynamical « content » than the theorem of Bocchieri and Loinger [16]. Attemps in this direction have been made by LUDWIG [17] and along another line of thought by PROSPERI and SCOTTI [18].

These latter authors employ an averaging procedure on the initial states weaker than Bocchieri and Loinger's; more precisely, for a given probability distribution relative to a fixed set of cells (macrostates) of the energy shell, they perform an average on the initial states only in the interior of the various cells. Thus, they obtain ergodic relations only assuming suitable microscopic ergodicity conditions. The usefulness of such an approach rests mainly on the circumstance that it characterizes in a clear-cut way the systems exhibiting tendency toward equilibrium.

Finally, we observe that in order to reach a classical result having the same mathematical validity as the result of Bocchieri and Loinger, a more sophisticated mathematical apparatus would be required and it would be necessary to introduce microscopic ergodicity conditions. To get a clear idea of the origin of this dissimmetry, one may observe that the classical analogue of the quantum proposition; A « small » system $C^{(1)}$, weakly interacting with a « large » system $C^{(2)}$, is canonically distributed in the time average — would be as follows: « The phase-point P_t remains in each of the cells of a suitably given set during a time proportional to the microcanonical measure of the cells themselves ». This result evidently requires a « larger amount of dynamics » than the corresponding quantum one.

From a general viewpoint, one may perhaps observe that the classical and quantum pure cases are not completely comparable, because — as also VAN KAMPEN [19] and VAN HOVE [20] have recently emphasized in different contexts — the quantum pure case has many properties analogous to the classical mixture (ensemble). In this respect we could also point out that — as it has been particularly stressed by ROSENFELD [12] — the ergodic theorem that VON NEUMANN tried to prove would have been the quantum analogue of Hopf's classical theorem, which holds

---

[15] However, it does play a decisive rôle in proving the representativity of the microcanonical ensemble.

[16] The foundation of the quantum statistical mechanics recently given by KHINCHIN (*Mathematische Grundlagen der Quantenstatistik*, Berlin, 1956) eludes completely the ergodic question, because it is restricted to the consideration of systems in stationary and highly degenerate states. According to this method, for the foundation of the quantum statistical mechanics it is sufficient to prove the representativity of the quantum microcanonical ensemble corresponding to the considered stationary state.

[17] G. LUDWIG: *Zeits. Phys.*, **150**, 346 (1958); **152**, 98 (1958).

[18] G. M. PROSPERI and A. SCOTTI: in prepar.

[19] N. G. VAN KAMPEN: *Proc. Int. Symp. on Transp. Proc. in Stat. Mech.* (Brussels, 1956), p. 239.

[20] L. VAN HOVE: *Physica*, **25**, 268 (1959), § 3.

true for *all* the initial Liouville distributions $\varrho(0)$.

Vice-versa, we could try to prove a theorem of the classical ensemble theory corresponding to the quantum theorem of Bocchieri and Loinger; *i.e.* a theorem valid for the « overwhelming majority » of the $\varrho(0)$ and requiring no microscopic condition of ergodicity ([21]).

([21]) An attempt in this direction has been made by BOCCHIERI and LOINGER (private communication).

* * *

This letter originates from a series of discussions on the foundations of statistical mechanics which took place recently (June 1959) among the members of the theoretical group of the Sezione di Milano dell'INFN.

The writer wishes to thank particularly Prof. LÉON ROSENFELD, who participated in these discussions with stimulating criticisms and useful suggestions.

IL NUOVO CIMENTO Vol. XIV, N. 1 1° Ottobre 1959

The Inelastic Scattering of Σ^+ Hyperons with Emulsion Nuclei.

D. H. Davis
University College - London

B. D. Jones and J. Zakrzewski (*)
H. H. Wills Physical Laboratory - Bristol

(ricevuto il 28 Agosto 1959)

1. – Introduction.

It is to be expected that charged Σ hyperons may interact with nucleons in the following ways:

(1) $\Sigma^+ + p \to \Sigma^+ + p$,

(2) $\Sigma^+ + n \to \Sigma^+ + n$,

(3) $\Sigma^0 + p$,

(4) $\Lambda^0 + p$,

(5) $\Sigma^- + p \to \Sigma^- + p$,

(6) $\Sigma^0 + n$,

(7) $\Lambda^0 + n$,

(8) $\Sigma^- + n \to \Sigma^- + n$.

During a systematic study of fast baryons resulting from the capture of K^--mesons at rest by emulsion nuclei, the following two events have been found. In each, a fast baryon interacted in flight with an emulsion nucleus and a Σ^+ hyperon was emitted as one of the secondaries. Since no strange particle production is possible by « non-strange » particles emitted from K^- captures at rest, it can be concluded that the interacting particle was in each case a Σ^+ hyperon. Two similar interactions of Σ^+ hyperons with complex nuclei and one with hydrogen have previously been reported [1-3].

2. – Results.

2·1. *Event* 1. - A K^--meson comes to rest to form a 4 pronged capture star (Photograph 1). 3 of the particles emitted are of low energy and are due to evaporation, the fourth is seen to interact in flight after a path length of 970 μm. The interaction gives rise to two charged

(*) On leave from the University of Warsaw.

(1) W. F. Fry, J. Schneps, G. A. Snow and M. S. Swami: *Phys. Rev.*, **100**, 939 (1955).

(2) R. G. Glasser, N. Seeman and G. A. Snow: *Phys. Rev.*, **107**, 277 (1957).

(3) F. C. Gilbert and R. S. White: *Phys. Rev.*, **107**, 1685 (1957).

secondaries, one of which is most probably a proton of 22 MeV (possibly deuteron) and the other a Σ^+ hyperon of (78^{+4}_{-3}) MeV. The Σ^+ hyperon has been identified by a protonic decay in flight after a path length of 11.00 mm from the interaction. The energy at decay has been determined by a blob and hole count (4) as (42.8^{+7}_{-5}) MeV whereas the energy calculated from decay dynamics is 40.7 MeV. The normalized grain density of the original Σ^+ hyperon track as determined by a blob and hole count is 2.78 ± 0.28. This corresponds to a Σ^+ energy of (191^{+30}_{-22}) MeV. The results of the measurements at the interaction are summarized in Table I.

Table I.

Track	Identity	Dip angle	Plane angle	Range (μm)	Energy (MeV)
4	Σ^+	$-4\frac{1}{2}°$	0°	$\Delta R = 970$	191^{+30}_{-22}
5	p (d)	$+20\frac{1}{2}°$	84°	2 200	22 (29)
6	Σ^+	$-5\frac{1}{2}°$	339°	$\Delta R = 11\,000$	78^{+4}_{-3}

At decay the space angle in the laboratory system between Σ^+ and proton is 49° and the range of the proton is 2 330 μm.

2·2. *Event* 2. - A K^--meson is captured at rest giving rise to a two pronged star (Photograph 2). One of the prongs is a 6 μm long recoil, the other is seen to interact in flight after traversing 3 920 μm. The interaction star consists of three prongs, one of length 7 870 μm due to a proton, the second of 9 μm, the third of 53 μm due to a Σ^+ hyperon. The Σ^+ hyperon has been identified from its decay at rest into a proton of range 1 648 μm. The energy of the incident particle, assumed to be a Σ^+ hyperon, has been estimated as (69^{+9}_{-7}) MeV from a blob and hole count at interaction, and hence (80^{+9}_{-7}) MeV at emission. The measurements at the interaction are listed in Table II.

Table II.

Track	Identity	Dip angle	Plane angle	Range (μm)	Energy (MeV)
2	Σ^+	$-17\frac{1}{2}$	0°	$\Delta R = 3\,920$	69^{-7}_{+6}
3	p	$-61°$	332°	7 870	45.5
4	—	$+33\frac{1}{2}°$	9°	9	—
5	Σ^+	$-56°$	151°	53	2.6

Coplanarity and momentum tests have been performed on the interaction products. The three tracks are found to be non-coplanar by 15° and assuming that the stable particle is a proton, the momentum unaccounted for by the re-

It is found that the residual momentum of particles 2, 3 and 5 is

(4) P. H. FOWLER and D. H. PERKINS: *Phil. Mag.*, **46**, 587 (1955).

Event 1.

Event 2.

(367^{+20}_{-14}) MeV/c, and lies, within measurements error, in the direction of track 4. This would indicate that all products of the interaction are observed and that track 4 should be due to a light nuclear recoil, as no heavy nucleus with the required momentum would have the observed range of 9 μm. Moreover, the observation of two low energy positive particles emitted from the interaction and the fact that most of the incident energy is carried away by the observed secondary particles, support the interpretation of an interaction with a light nucleus.

The following schemes are suggested for the interaction:

$$\Sigma^+ + ({}^{12}\mathrm{C}, {}^{14}\mathrm{N}, \mathrm{O}^{16}) \rightarrow$$
$$\rightarrow \Sigma^+ + \mathrm{p} + ({}^{11}\mathrm{B}, {}^{13}\mathrm{C}, {}^{15}\mathrm{N}) .$$

3. – Conclusion.

It can be concluded that two inelastic scatterings of Σ^+ hyperons have been observed, one (event 2) according to the reaction:

$$(1) \qquad \Sigma^+ + \mathrm{p} \rightarrow \Sigma^+ + \mathrm{p} ,$$

the other (event 1) according to either the above or:

$$(2) \qquad \Sigma^+ + \mathrm{n} \rightarrow \Sigma^+ + \mathrm{n} .$$

A track length of 79 cm of charged Σ hyperons of energy greater than 50 MeV has been observed by the K^- European Collaboration [5] and in the present work.

* * *

The authors wish to express their thanks to Dr. Levi Setti for exposing the stack to the Bevatron and to Prof. G. P. S. Occhialini and the Brussels group for processing it. We also wish to thank the other members of the K^- European Collaboration with whom this work has been done. One of us (J.Z.) wishes to express his gratitude to Prof. C. F. Powell for the hospitality shown to him at Bristol University. Two of us (D.H.D. and B.D.J.) are indebted to the Department of Scientific and Industrial Research and the other (J.Z.) to the Institute for Nuclear Research, Warsaw for financial support.

---

[5] K^- European Collaboration: *Nuovo Cimento*, part III to be published.

IL NUOVO CIMENTO Vol. XIV, N. 2 1° Ottobre 1959

Search for New Neutral Mesons (the ρ^0-Mesons).

C. Bernardini, R. Querzoli, G. Salvini, A. Silverman (*) and G. Stoppini

Comitato Nazionale per le Ricerche Nucleari - Laboratori di Frascati

(ricevuto il 7 Settembre 1959)

We describe here an experiment we performed with the aim of detecting the new neutral meson frequently quoted in the recent literature as the ρ^0-meson (1). We did not find any evidence for a strong production in H_2 of such a particle.

The method is based on the following line: suppose a neutral particle is photoproduced according to

$$\gamma + p \to p + X . \tag{1}$$

By measuring energy and angle of the recoil proton, all other kinematical parameters are fixed, including the γ-ray energy, for each mass of X. Since the γ-ray source gives a bremsstrahlung spectrum, the excitation curve (that is the number of protons/equivalent quanta as a function of the maximum energy of the spectrum) should appear as a step starting when the energy of the head of the spectrum is the right one to produce a proton at the given angle and momentum. The mass of particle X, if unknown, can be determined by this threshold energy. The situation is sketched in Fig. 1, where the π^0 step and the hypothetical ρ^0 step are shown.

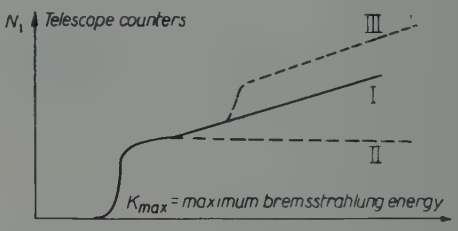

Fig. 1.

The π^0 photoproduction is an example of process (1) and it gave indeed to us a step of the just described type. If a ρ^0 particle exists, a further step should add to the π^0's one, starting at a different energy corresponding to the ρ^0 mass.

The two pion production has to be taken into account in the interpretation of the data. In fact, from a certain energy corresponding to the threshold, in our geometry, of the processes

$$\gamma + p \to p + \begin{cases} \pi^+ + \pi^- \\ \pi^0 + \pi^0 \end{cases}, \tag{2}$$

(*) On leave from Laboratory for Nuclear Studies, Cornell University, Ithaca, N.Y.

(1) Y. Nambu: *Phys. Rev.*, **106**, 1366 (1957); S. N. Gupta: *Phys. Rev.*, **111**, 1436 (1958). For a complete bibliography: A. Alberigi, C. Bernardini and G. Stoppini: Report CNF 2, Lab. Naz. di Frascati, July 1959 (unpublished).

protons of the right energy arising from processes (2) begin to reach the counting apparatus. The number of these protons is generally a slowly increasing function of the maximum energy of the γ-rays because of the three body nature of the final state of the reaction.

A further remark on the method: any step-like behaviour in the curve (Fig. 1) could indicate not only the existence of a new meson of definite mass, but also some particular correlation among the pions ($\pi\pi$ interaction) in processes (2).

Because of the negative result this experimental method allowed us to give only an upper limit for the cross section of process (1), the size of this limit being due to the statistical errors and to the energy and angle resolution of the proton telescope.

In conclusion, the excitation curve should roughly appear as sketched in Fig. 1 where

1) is the sum of π^0 plus two pions contributions;

2) is the π^0 contribution alone;

3) includes the ϱ^0 contribution, if any.

We obtained an excitation curve using the scintillation counter apparatus described in Fig. 2. The proton telescope detected particles of energy $T_p = (150 \pm 10)$ MeV at an angle $\theta_p = 42° \pm 1.5°$

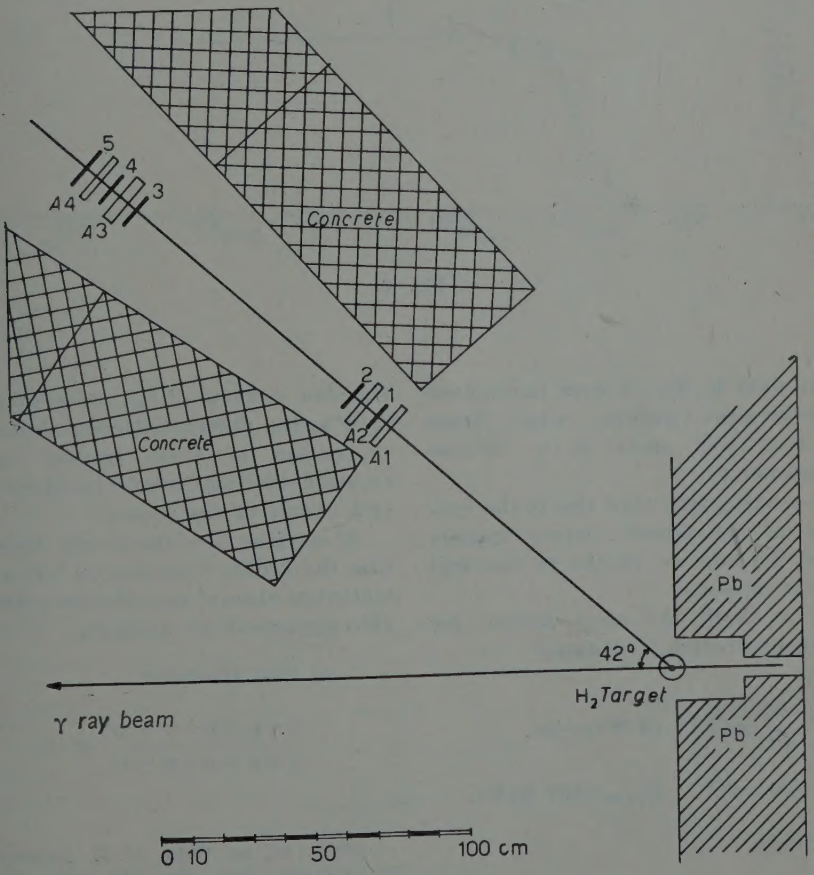

Fig. 2.

(lab. syst.) with the γ-ray beam from the 1.1 GeV Frascati Electronsynchrotron.

An event was detected as a coincidence

$$(1+2)+(2+3+4-5)\,.$$

Discrimination against pions in the telescope was made by pulse height analysis in counters 2+3.

and it is in good agreement with the known value ([3,4]).

The dotted line in Fig. 3 is the calculated single π^0 contribution, taking into account the angular and momentum spread of our telescope. Its agreement with the experimental results gives confidence to the method.

Because of the two pions contribution we can only say that if a part of

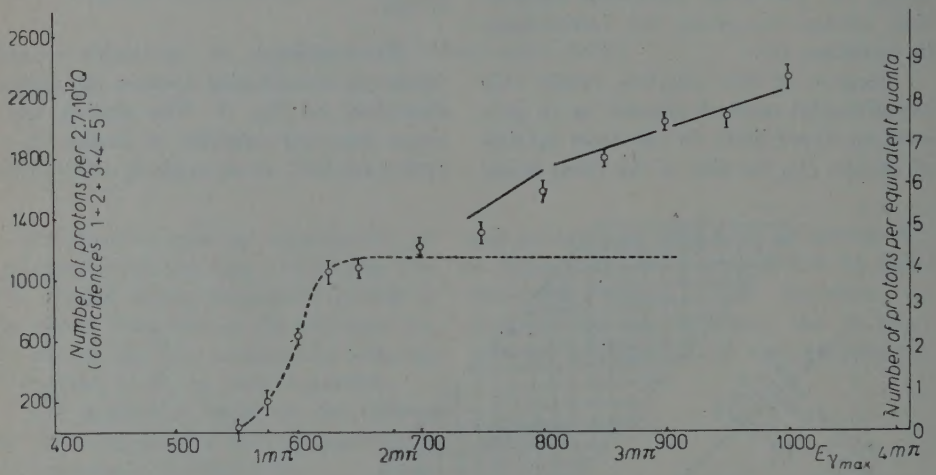

Fig. 3.

The data in Fig. 3 were normalized per equivalent quanta; γ-ray beam monitoring was made by a Wilson quantameter ([2]).

No evident step (and this is the contribute of the present paper) appears besides the one we ascribe to the well known π^0-mesons.

As a check the cross section for π^0 photoproduction is deduced

$$\frac{d\sigma}{d\Omega} = 3.11\cdot 10^{-30}\ \mathrm{cm^2/sr}\,,$$

$$(\theta_{\pi^0}\ \mathrm{c.m.}=90^\circ\,,\quad E_{\gamma\,\mathrm{Lab}}=580\ \mathrm{MeV})\,,$$

the slow increase of the curve were due to ρ^0's, the differential cross section for production of these particle cannot exceed $6\cdot 10^{-31}\ \mathrm{cm^2/ster}$ (at the given angle and energy of the proton).

If one tries to fit the data by assuming that the double π production follows the statistical theory, one obtains a reasonable agreement by assuming

a) that the ratio

$$\frac{\gamma+\mathrm{p}\to\mathrm{p}+\pi^0+\pi^0}{\gamma+\mathrm{p}\to\mathrm{p}+\pi^+ +\pi^-}\ll 1\,;$$

([2]) R. Wilson: *Nucl. Instr.*, **1**, 101 (1957).

([3]) J. W. de Wire, H. E. Jackson and R. Littauer: *Phys. Rev.*, **110**, 1208 (1958).

([4]) J. I. Vette: *Phys. Rev.*, **111**, 622 (1958).

b) that the cross section for production of two charged pions decreases smoothly (in the interval (700÷1000) MeV γ-ray energy) by a factor of 3. This is not inconsistent with the results of SELLEN *et al.* [5].

The solid line in Fig. 3 summarizes these calculations; of course, this is only an order of magnitude estimate. Nevertheless, this estimate allows a further reduction of the upper limit on the differential cross section for ρ^0 photoproduction to the value

$$\left(\frac{\mathrm{d}\sigma}{\mathrm{d}\Omega}\right)_{\substack{T_p=105\,\mathrm{MeV}\\ \theta_p=42^\circ}} = (2\div 3)\cdot 10^{-31}\ \mathrm{cm}^2\ .$$

* * *

We want to thank doctor A. ALBERIGI for helpful assistance during the development of this work.

(5) J. M. SELLEN, G. COCCONI, T. V. COCCONI and E. L. HART: *Phys. Rev.*, **113**, 1323 (1959).

Direttore responsabile: G. POLVANI

Tipografia Compositori - Bologna

Questo fascicolo è stato licenziato dai torchi il 23-X-1959

3176